Focus on the axon:

from neuronal development to dynamic synapses

ISBN: 978-90-393-6856-5

The studies described in this thesis were performed at the division of Cell Biology at the Faculty of Science of the Utrecht University in Utrecht, the Netherlands.

This thesis was partially supported by the People Programme (Marie Curie Actions; MC-ITN) of the European Union's Seventh Framework Programme FP7/2007-2013/ under REA grant agreement 289581. The printing of the thesis was kindly supported by Vereniging van Huntington and Alzheimer Nederland.

Cover: Neuron Tangram

Cover design by Cátia P. Frias and Reinier Damman.
Layout by Cátia P. Frias.
Printed by Gildeprint.

Focus on the axon:
from neuronal development to dynamic synapses

Het axon centraal: van ontwikkelende hersencellen tot dynamische synapsen
(met een samenvatting in het Nederlands)

Foco no axónio: do desenvolvimento neuronal às sinapses dinâmicas
(com um sumário em Português)

Proefschrift

ter verkrijging van de graad van doctor aan de Universiteit Utrecht op gezag van de rector magnificus, prof.dr. G.J. van der Zwaan, ingevolge het besluit van het college voor promoties in het openbaar te verdedigen op woensdag 8 november 2017 des middags te 2.30 uur

door

Cátia Sofia Pereira Frias

geboren op 15 januari 1989 te Funchal, Portugal

Promotor: Prof. dr. C. C. Hoogenraad

Copromotor: Dr. C. J. Wierenga

Para os meus pais

TABLE OF CONTENTS

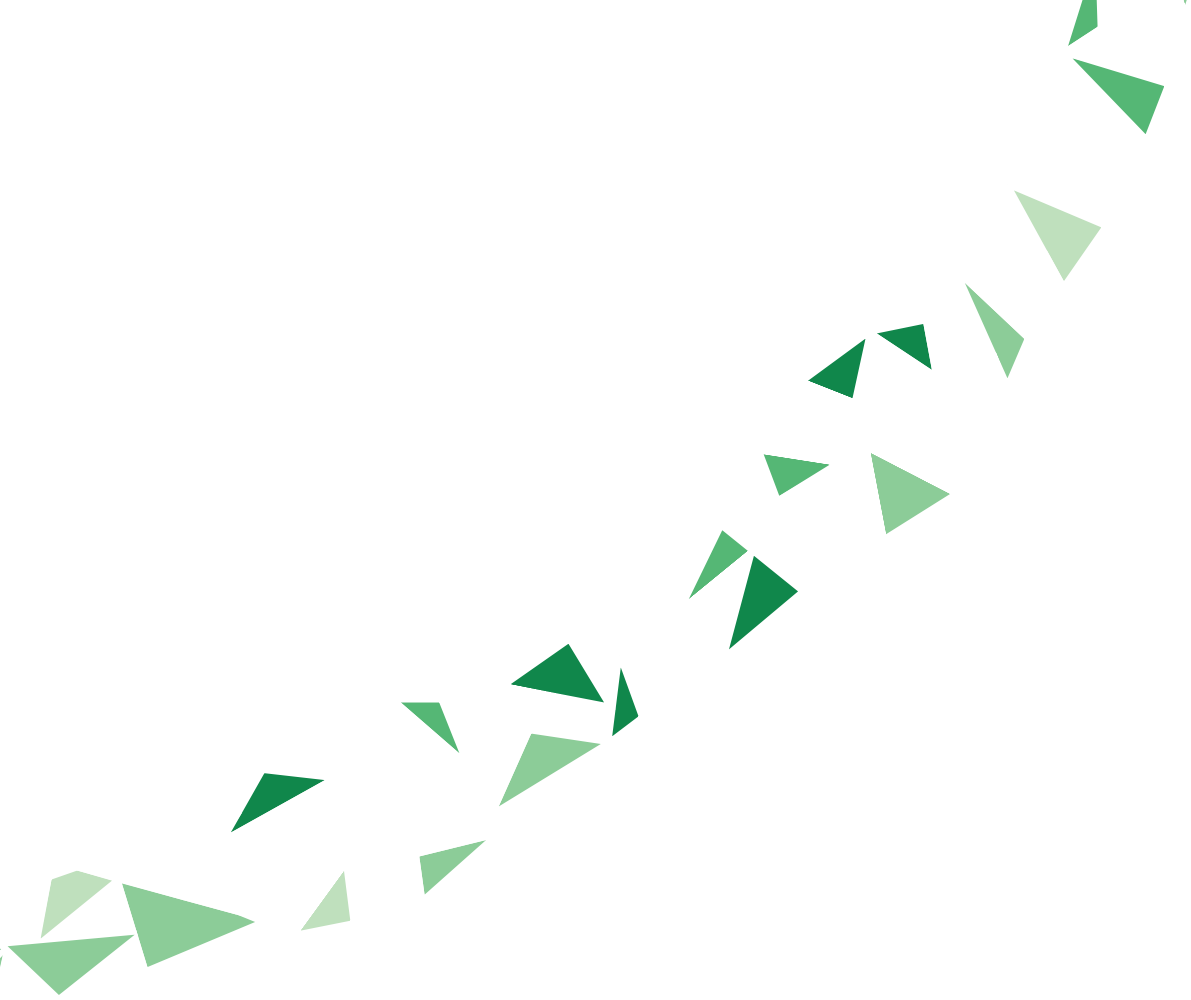

Cell Biology, Department Biology, Faculty of Science, Utrecht University, Utrecht, the Netherlands

Chapter 1

General Introduction

Cátia P. Frias

THE MAKING OF A NERVOUS SYSTEM

The nervous system is central in the coordination of an animal body, promoting the translation of sensory inputs into coordinated actions. The primitive nervous systems are thought to have been simple coupling of sensory systems to effectors, important for food and mates location and for avoidance of unsuitable habitats (Wray, 2015). All animals more evolutionarily advanced than sponges have a nervous system, and their brains have a common evolutionary origin in a primitive brain-like structure that existed 570 million years ago (Sprecher and Reichert, 2003) (Figure 1). In this way, even though morphological and functionally different, the nervous systems of a fly or of a human share a common ancestry. The complexity of the nervous system continued to increase, in order for animals to perform tasks more complex and intricate than the ones allowed by the primordial one. In fact, the nervous system has allowed for the animal body to develop perception capabilities as vision and smell, to promote active movement, to coordinate the different organs in the body, or to perform complex social interactions. At a cellular level, the nervous system is composed by two types of cells: the neurons, which are responsible for the translation of inputs into outputs, and the glia, which are responsible for supporting the neuronal network.

Neurons, also known as nerve cells, contain long protrusions arising from the cell body or soma, which are essential for the communication with other cells. These protrusions require a high degree of neuronal polarization, which lead to morphological and functional differences. The axon is a long protrusion responsible for the transmission of electrochemical signals, whereas the dendrites are normally shorter and highly ramified protrusions that receive signals. The directional transfer of signals from the axon of one neuron to the dendrite of another happens at a specialized contact site called the synapse. Typically, the synapse is composed by the axonal presynapse, the dendritic postsynapse, and the synaptic cleft in between, and the majority of the synapses are chemical in the vertebrate nervous

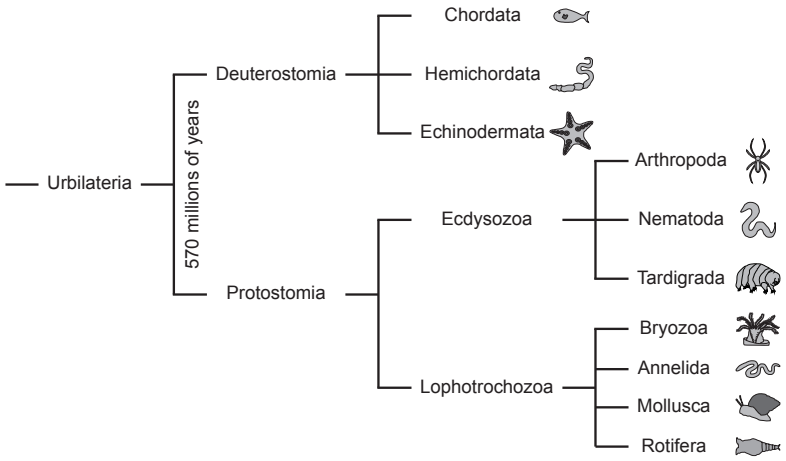

Figure 1. Evolution of the nervous system.

Phylogenetic tree based on molecular data, mainly based on ribosomal and Hox gene sequence analysis. None of the phyla present today represent a truly ancestral state, and the molecular resemblance between phyla suggests a monophyletic origin of the nervous system. For simplification, not all phyla are represented. Based on (Sprecher, 2008; Sprecher and Reichert, 2003).

system. Electrical signals travel along the axon in the form of an action potential and, when they reach the presynaptic terminal, they can induce the fusion of synaptic vesicles with the plasma membrane, releasing neurotransmitters to the synaptic cleft. These neurotransmitters can bind to receptors present at the membrane of the postsynaptic cell, inducing signaling cascades that are processed in the soma. The cycle of neurotransmission is completed by the generation of an output signal at a specialized region preceding the axon. This region is called the axon initial segment (AIS), and is characterized by a high density of voltage-gated sodium channels, which are required for the generation of action potentials required for neuronal transmission (Kole et al., 2008). Besides from the role on action potentials, the AIS separates the somatodendritic and the axonal compartments, which is important for the maintenance of neuronal polarity. More precisely, the AIS acts as a membrane diffusion barrier for membrane proteins and ion channels, and as a cytoplasmic gate that allows the entrance of axonal cargoes into the axon (Zhang and Rasband, 2016).

STUDY OF NEURODEVELOPMENTAL PROCESSES

Unravelling the molecular mechanisms underlying brain development and functionality has been an ambitious aim of past and nowadays neuroscientists. The establishment of in vitro systems became instrumental to investigate intracellular mechanisms during neuronal polarization, growth and connectivity. One of the most popular *in vitro* systems relies on the dissociation of rodent hippocampal neurons from embryos upon completion of pyramidal neuron formation (Tahirovic and Bradke, 2009). Pioneer studies from the Banker lab have shown that upon dissociation, rodent hippocampal neurons can re-start their developmental program to develop two distinct cellular compartments: a single axon and multiple dendrites (Dotti et al., 1988). This program comprises five stages that induce morphological changes and culminate in the establishment of a functional neuronal network (Figure 2A). In more detail, shortly after plating, round neuronal cells start to spread a lamellipodium around the cell body, and attach to the substrate (stage 1). Development proceeds with the acquisition of several extensions called neurites (stage 2), which exhibit dynamic growth cones at their tips and undergo alternated periods of growth and retraction. Next, cell symmetry is broken and neuronal polarization is triggered, with the rapid growth of one neurite that becomes the axon (stage 3). The remaining neurites will further grow and develop into dendrites (stage 4), and neurons become functionally connected with the formation of synapses (stage 5). This system allows cell manipulation and biochemical studies, but several systems have been developed to study neuronal function within the tissue architecture. One of these systems relies on the culture of hippocampal slices, normally prepared from postnatal rodents (Figure 2B). Even though afferent fibers are cut and degenerate upon the preparation of slice cultures, the intra-hippocampal connections are maintained, allowing for the study of a structured network with specific connections. Cultured slices also contain different glia cell types in the tissue, which may help to better understand the mechanisms underlying brain function. The electrophysiological properties of cultured slices seem to be similar to those of acute slice preparations (De Simoni and Yu, 2006). Organotypic slice cultures are well suitable for live-imaging of neuronal processes, such as synapse formation, for which the development of transgenic mice has contributed enormously (Figure 2B).

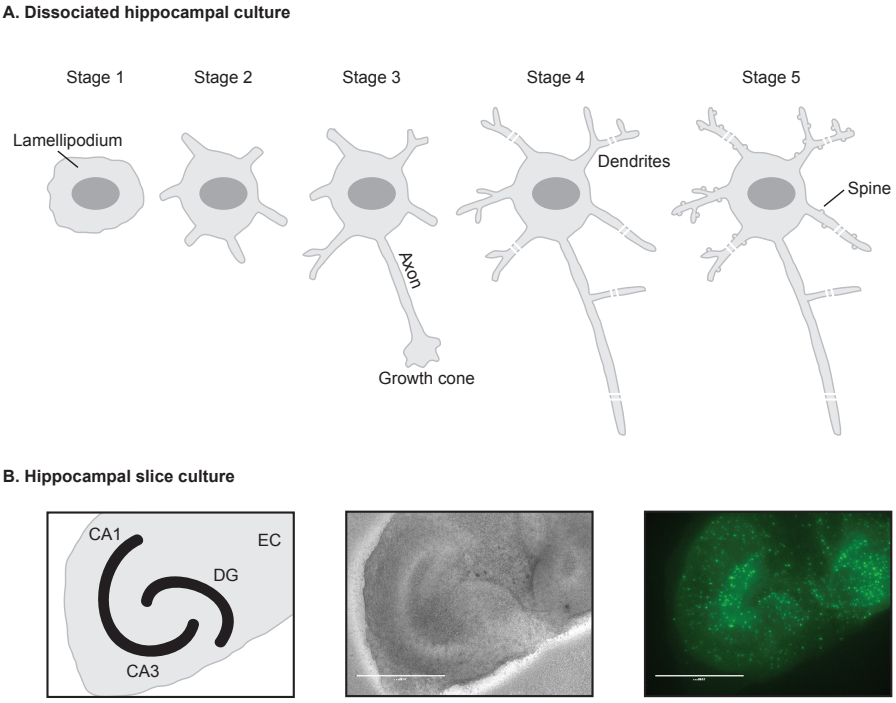

Figure 2. Different systems for the study of neuronal development.
(A) Developmental stages of dissociated hippocampal neurons. Initially, neurons are non-polarized cells that extend lamellipodia (stage 1) and develop processes of similar length called neurites (stage 2). One of these neurites starts to grow more rapidly and becomes the axon (stage 3), while the remaining neurites develop as dendrites (stage 4). Finally, neurons mature and develop synaptic contacts and dendritic spines (stage 5). (B) Scheme (left), widefield (middle) and fluorescent (right) images of organotypic hippocampal cultures from transgenic mice. CA1/CA3: *cornu ammonis* 1/3; DG: dentate gyrus; EC: entorhinal cortex. Scale bar 1000 µm.

THE CYTOSKELETON

Cellular morphogenesis and function highly rely on the underlying cytoskeleton, which provides structure for the organization of the cell. However, the cytoskeleton is far from being a rigid structure, as several dynamic processes at the cytoskeleton allow the cells to rapidly adapt in response to environmental or molecular signals. Cytoskeletal rearrangements contribute to a multitude of cellular processes, ranging from mitosis, cell migration, neuronal development and outgrowth, and synapse formation and plasticity. Moreover, the cytoskeleton provides highways for molecular motors to move cargo, establishing directionality in intracellular transport. In eukaryotic cells, the cytoskeleton is composed by three organized types of filaments: microtubules, intermediate filaments and microfilaments.

Microtubules

Microtubules are hollow polymers of α- and β-tubulin heterodimers, with a fast-growing plus-end with exposed β-tubulin and a slow-growing minus-end with exposed α-tubulin. These polymers are highly dynamic structures that can undergo periods of polymerization (growth) and depolymerization (shrinkage), a process called dynamic instability (Mitchison and Kirschner, 1984). The control of microtubule dynamics is achieved by a variety of factors that include microtubule-associated proteins (MAPs), plus-end binding proteins, molecular motors and post-translational tubulin modifications. Microtubule dynamics is important for different aspects of neuronal development, including neuronal polarization and synaptic plasticity (Hoogenraad and Bradke, 2009). For example, absence of MAP2, a protein that decorates somatodendritic microtubules, inhibits the initial growth of minor neurites, whereas axon-specific MAP Tau is required for axonal extension (Caceres et al., 1992). In neurons, microtubules are the main longitudinal cytoskeletal filament in axons and dendrites (together with neurofilaments), and they exhibit compartment-specific orientations. In axons, microtubules are uniformly distributed with their-plus ends towards the axonal tip (Baas et al., 1988), while dendrites exhibit mixed microtubule orientations (Baas et al., 1988; Yau et al., 2016) (Figure 3A,B). These specific orientations contribute to the polarized transport of cargo to axons and dendrites (Kapitein and Hoogenraad, 2011).

Actin microfilaments

Microfilaments are composed of two helical and intertwined strands of filamentous actin (F-actin), and each strand is a polymer of globular actin monomers (G-actin). Like microtubules, actin filaments are intrinsically dynamic and polarized, with a polymerizing barbed end and a depolymerizing pointed end. The simultaneous gain of monomers at the barbed end and loss of monomers from the pointed end creates a phenomenon known as treadmilling that contributes to a dynamic turnover of actin filaments without changing their length (Brandt, 1998). Due to the weak interactions between actin monomers, actin filaments can undergo cycles of rapid assembly and disassembly (Cingolani and Goda, 2008), but the dynamics and organization of the actin cytoskeleton is ultimately regulated by a multitude of actin-binding proteins (ABPs). ABPs can promote the nucleation of filaments, bind to filaments ends to modify filament turnover, induce the severing or growth of actin filaments, or establish different actin networks by crosslinking (Letourneau, 2009). Actin dynamics contribute to several neurodevelopmental processes, including axon initiation and branching (Pacheco and Gallo, 2016). In neurons, actin filaments are highly enriched at growth cones, where they regulate the formation of dynamic filopodia and lamellipodia structures (Figure 3E), as well as in mature synapses (Hotulainen and Hoogenraad, 2010; Pacheco and Gallo, 2016). Moreover, visualization of actin by super-resolution and live-imaging techniques allowed the observation that actin is intricately organized along the axon shaft. Recently, axonal actin has been shown to be assembled into rings (D'Este et al., 2015; Xu et al., 2013) (Figure 3C) and trails (Ganguly et al., 2015), but the overall function of such structures remains poorly understood. Along the axon, actin is highly enriched at presynaptic sites (Wilhelm et al., 2014) (Figure 3D), and modulation of actin dynamics underlies adaptations to changes in synaptic activity (Cingolani and Goda, 2008).

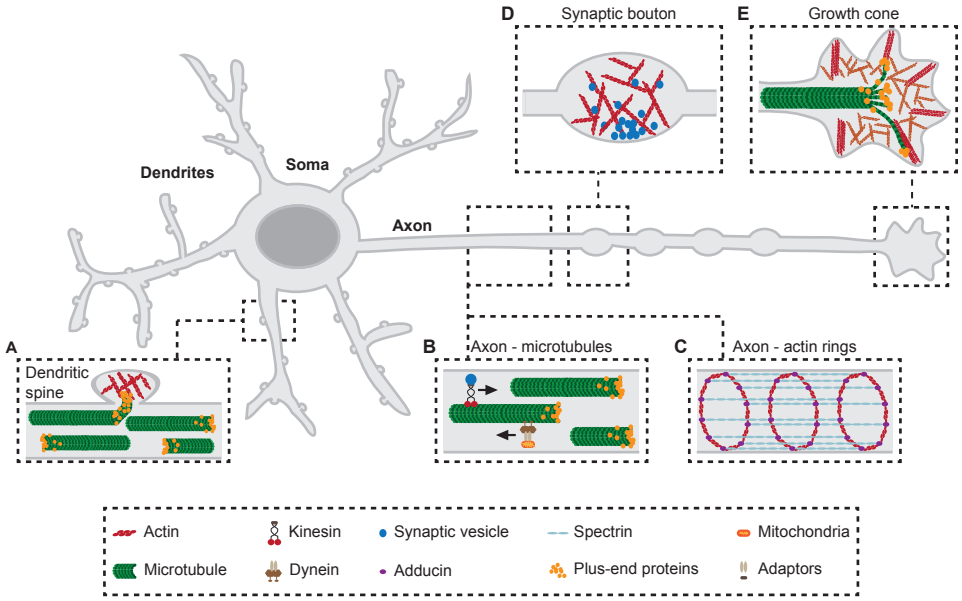

Figure 3. The cytoskeleton in different neuronal compartments.
(A) In dendrites, microtubules have mixed orientations and, occasionally, they can invade dendritic spines, which are enriched in actin filaments. (B) In the axon, microtubules exhibit uniform orientations, with their plus-end towards the end of the axon. Hence, cargo is moved anterogradely by plus-end directed kinesins and retrogradely by dynein. (C) Within the axon, the actin cytoskeleton is organized in periodically spaced rings below the plasma membrane. This organization is maintained by spectrin and adducin proteins, and provides support to the axon. (D) At presynaptic boutons, actin is thought to exist in a branched network, which may be important for the positioning of neurotransmitter-filled synaptic vesicles and for the organization of the active zone. (E) In the growth cone, microtubules emerge from the axon and splay out in the central domain, while the peripheral domain is enriched in actin filaments. Microtubules can invade the actin-rich regions to promote directional growth.

Motor proteins

Besides regulating different cellular processes, the cytoskeletal filaments provide roads for the movement of cargoes carried out by molecular motors. These proteins are from three different superfamilies (kinesin, dynein and myosin), and they generate movement by hydrolyzing ATP. Generally, motor proteins contain a relatively highly conserved motor domain that binds the cytoskeleton, and a more diverse tail domain, which interacts with different adaptor proteins and discriminates the transport of specific cargoes (Hirokawa et al., 2010; Schlager and Hoogenraad, 2009). Myosins bind to actin filaments, being involved in cargo transport along these filaments and in the generation of contractile forces (Kneussel and Wagner, 2013). In neuronal cells, the actin-enriched growth cones, presynaptic terminals and dendritic spines rely on myosin activity for cargo delivery, with motor myosin V (MyoV) and myosin VI (MyoVI) moving in opposite directions of actin filaments. Kinesin (KIF) and dynein motors promote long-range transport along microtubules, moving in opposite directions: the majority of kinesin proteins move towards the plus-end of microtubules, whereas dynein moves towards their minus-end. In mammals, 45 KIF genes have been identified and divided

into 14 families (Hirokawa et al., 2009). Besides the role in microtubule-based transport, KIFs can also affect microtubule dynamics (Walczak et al., 2013). Cytoplasmic dynein is a large protein complex composed of heavy chains, intermediate chains, intermediate light chains and light chains, which can further associate with the dynactin complex and accessory factors to promote transport of cargo (van den Berg and Hoogenraad, 2012). Mutations in motor protein encoding genes from the three superfamilies are linked to several neurodevelopmental and neurological disorders, such as hereditary spastic paraplegia (Franker and Hoogenraad, 2013; Hirokawa et al., 2010; Kneussel and Wagner, 2013; Lipka et al., 2013).

NEURONAL POLARIZATION: THE GROWTH OF THE AXON

Axon initiation and outgrowth

Rearrangements of the actin and microtubule cytoskeletons are crucial for the initial establishment of polarity. Immature neurites (prior to polarization) contain bundled microtubules and are tipped with an actin-rich growth cone (Conde and Caceres, 2009). The actin cytoskeleton present at the growth cone is important for axon formation, and pharmacological actin depolymerization in one individual growth cones induces this neurite to become the axon (Bradke and Dotti, 1999). At the growth cone of the future axon, the actin filaments are more dynamic and permissive, allowing the intrusion of microtubules that support axonal differentiation and outgrowth (Hoogenraad and Bradke, 2009). By using a photoactivable analog of microtubule-stabilizing drug Taxol, Witte and colleagues showed that local stabilization of microtubules is sufficient to promote axon formation in unpolarized neurons (Witte et al., 2008). Furthermore, treatment with low doses of taxol triggers the formation of multiple axons in hippocampal neurons (Witte et al., 2008). Overall, axon formation seems to rely on the cross-talk between actin and microtubules, and a permissive actin cytoskeleton and increased microtubule stability are important during this process. The increased microtubule stability may dictate cargo trafficking into the future axon. In fact, the motor domain of KIF5 accumulates in the future axon (Jacobson et al., 2006; Nakata and Hirokawa, 2003). Furthermore, KIF3A is required for the axonal localization of polarity protein complexes, promoting the establishment of neuronal polarity (Nishimura et al., 2004; Shi et al., 2004). However, we understand very little about the role of motor proteins in early phases of neuronal development. New insights into the role of myosin and kinesin motors in axon development and outgrowth are discussed in *chapters 3* and *4*.

Actin and microtubule dynamics are regulated by a plethora of signaling pathways, which influence axon growth (Coles and Bradke, 2015; Schelski and Bradke, 2017). These pathways are normally triggered by the binding of secreted or cell-surface guidance cues to receptors found on the surface navigating growth cones. Hence, besides the involvement on neuronal polarization, growth cones are involved in axon guidance and pathfinding by promoting axon growth towards (attraction) or away (repulsion) of the source of the guidance cues.

Axon initial segment organization and function

The AIS is a specialized region between the somatodendritic and axonal compartments with two main functions. Firstly, due to the accumulation of ion channels, the AIS is able to generate action potentials upon integration of synaptic inputs. Secondly, it is crucial for

the maintenance of neuronal polarity, by acting as a membrane diffusion barrier and as a selective filter for the transport of organelles and proteins between the somatodendritic and axonal compartments (Zhang and Rasband, 2016). In order to perform such functions, there is an accumulation of specific proteins at the AIS that provide a connection between the extracellular matrix and the intracellular cytoskeleton, such as Ankyrin-G (AnkG), β-IV-spectrin, neurofascin and voltage-gated ion channels. AnkG is considered the master regulator of the AIS, as it not only recruits almost all proteins to the AIS, but also interacts with proteins at both the plasma membrane and the cytoplasm (Jones and Svitkina, 2016). In fact, depletion of AnkG leads to a loss of other AIS proteins at the proximal axon (Hedstrom et al., 2008; Zhou et al., 1998).

The earliest observed characteristic of the AIS was the presence of microtubule bundles linked by cross bridges (Palay et al., 1968). It has been recently shown that tripartite motif containing protein 46 (TRIM46) is enriched in the proximal axon, where it promotes microtubule bundling (van Beuningen et al., 2015). Other proteins that bind microtubules have been shown to be important for AIS functionality, including the microtubule plus-end proteins (Fréal et al., 2016). The dynein regulator NUDEL (NDEL1) was shown to bind AnkG and to be required for keeping dendritic cargoes away from the axon (Kuijpers et al., 2016). Recent findings have found a periodic actin cytoskeletal arrangement in axons, including the AIS (D'Este et al., 2015; Leterrier et al., 2015; Xu et al., 2013), and this is conserved from Caenorhabditis elegans to Homo sapiens (He et al., 2016). The actin rings are observed at every ~190 nm, separated by spectrin tetramers (Leterrier et al., 2015; Xu et al., 2013). The periodical arrangement of actin within the AIS is observed early in development, and it is important for the precise distribution and location of proteins in axons (Albrecht et al., 2016; Zhong et al., 2014). Besides actin rings, patches and short stable actin filaments have been observed at the AIS (Jones et al., 2014; Watanabe et al., 2012). Interestingly, actin depolymerization disrupts filter capabilities of the AIS, as large proteins move freely towards the distal tip of the axon (Song et al., 2009). Altogether, the cytoskeleton is important for the establishment and function of the AIS.

ESTABLISHMENT OF NEURONAL NETWORKS

After extensive growth and navigation, the axon can reach the appropriate target within the brain with the ultimate aim of forming synaptic connections. In vertebrates, synapse formation begins during embryonic development and extends into adulthood, involving a myriad of ligand-receptor interactions, signaling cascades and cytoskeleton remodeling (Shen and Cowan, 2010; Waites et al., 2005). In mature networks, synapses are dynamic and constantly shaped in order to adapt to changes in the circuitry, in a process called synaptic plasticity. This process can promote changes in the composition of synapses, in the efficiency of synapse communication, and in determining if the synapse is kept or eliminated (Rudenko, 2017). Synaptic plasticity is critically involved in brain processes that promote memory formation and learning, and it is therefore not surprising that mutations in genes encoding synaptic proteins are associated with several neurological disorders, such as schizophrenia and autism spectrum disorder. As the mutations lead to synaptic impairments, the term "synaptopathies" is now commonly used to describe neurodevelopmental, neurodegenerative, and neuropsychiatric disorders (Rudenko, 2017). Consequently, it is important to understand the mechanisms that underlie synapse formation, maturation, plasticity and elimination, as

this may bring us closer to understand the etiology of different brain diseases.

It is still not fully understood how neurons assemble into specific circuits, and how correct synaptic connections are established and maintained over time. In general, after the axon is guided towards a target, secreted factors act to promote the formation of presynaptic specializations at the proper place. Afterwards, dynamic and actin-rich dendritic filopodia extend from the dendritic shaft and seem to inspect the surrounding area for a presynaptic axon (Shen and Cowan, 2010). Once a positive contact is achieved, cell-adhesion proteins are thought to stabilize the contact and to promote the activation of intracellular signaling cascades that promote the maturation of pre- and postsynaptic sites (Shen and Cowan, 2010). Several adhesion proteins have been discovered and implicated in synapse formation and stabilization, including the postsynaptic neuroligins and their presynaptic partner neurexins (de Wit and Ghosh, 2016; Siddiqui and Craig, 2011). Interestingly, in hetereologous systems, the overexpression of postsynaptic cell-adhesion proteins is sufficient to promote the development of presynaptic sites in the contacting axon region (Scheiffele et al., 2000; Siddiqui and Craig, 2011). This suggests that postsynaptic adhesion may trigger the development of the presynaptic site. Interestingly, synaptic vesicles can pause at specific sites along the axon in the absence of neuronal contacts (Sabo et al., 2006), and these sites are then stabilized by trans-synaptic adhesion signals (Bury and Sabo, 2014).

In the brain, there are two main types of synapses, determined by the neurotransmitter released from the presynaptic terminal: glutamatergic (release of glutamate) and GABAergic (release of γ-aminobutyric acid – GABA). Glutamatergic synapses are excitatory and depolarize the postsynaptic neuron, while GABAergic synapses are inhibitory and induce hyperpolarization of the postsynaptic neuron. Even though both types of synapses show similar organizing principles (e.g. postsynaptic scaffolding proteins or neurotransmitter receptors, the molecular processes underlying the formation and maturation of excitatory and inhibitory synapses are distinct (Sheng and Kim, 2011).

Organization of excitatory postsynapses

The majority of excitatory synapses are formed at tiny dendritic protrusions called dendritic spines (Bourne and Harris, 2008). Dendritic spines consist of three distinct areas: a delta-shaped base linked to the dendritic shaft, followed by a constricted neck and a bulbous head that contacts the axon (Hotulainen and Hoogenraad, 2010). They can be found in different shapes, and dendritic spines are very dynamic structures that can change their morphology in response to changes in neuronal activity (Holtmaat et al., 2006; Roberts et al., 2010). The postsynaptic density (PSD), an electron-dense thickening of the postsynaptic membrane opposed to the presynaptic terminal, is usually found at the tip of the dendritic spine. Due to the difference in electron density between the pre- and postsynaptic sites in electron microscopy studies, excitatory synapses are often named asymmetric synapses. The PSD contains a meshwork of proteins crucial for neuronal transmission, such as glutamate receptors, signaling proteins and adhesion molecules (Figure 4A). Therefore, the PSD is essential in mediating the apposition of pre- and postsynaptic sites, and in regulating signaling cascades that are prompted by the activation of glutamate receptors in the postsynaptic cell. During postnatal development, the expression and synaptic localization of PSD proteins increases, correlating with the period of intense synapse formation and maturation in the brain (Sheng and Kim, 2011). Within the PSD, several scaffolding proteins, such as PSD-95, stabilize or tether membrane or signaling proteins in the PSD via protein-protein interactions.

For example, PSD-95 can directly interact with N-methyl-D-aspartate receptors (NMDARs), recruit α-amino-3-hydroxy-5-methyl-4-isoxazolepropionic acid receptors (AMPARs) via association with accessory subunits or organize synaptic adhesion by binding to adhesion molecules (Sheng and Kim, 2011; Siddiqui and Craig, 2011). The PSD is not a uniform and static structure, with recent single molecule localization studies showing it is organized into dynamic nanodomains enriched for glutamate receptors that are important for excitatory transmission (MacGillavry et al., 2013; Nair et al., 2013). The mechanisms underlying this organization are not understood, but it is possible that the nanodomains are determined by transsynaptic contacts between the pre- and postsynaptic membrane.

For proper synaptic transmission and plasticity, PSD proteins need to be transported towards the dendritic spine after being synthesized in the cell body. Therefore, synaptic function highly relies on the activity of motor proteins, and several have been implicated in the transport of PSD proteins. For instance, kinesins KIF5 and KIF17 are involved in the transport of AMPAR and NMDAR subunits, as well as of voltage-gated potassium channels along dendrites (Chu et al., 2006; Heisler et al., 2014; Setou et al., 2000; Setou et al., 2002). Besides a role on trafficking, motor proteins have also been shown to regulate the development of dendritic spines (Muhia et al., 2016; Ryu et al., 2006) and synaptic plasticity (Rex et al., 2010). In *chapter 5*, we further investigate the role of motor proteins in the maintenance of excitatory synapses by performing a targeted knockdown screen of kinesins, myosins and dynein-interacting proteins.

Overall, the molecular organization of excitatory synapses is intricate and has intrigued scientists throughout the years (Sheng and Kim, 2011), but recent studies continue to identify new candidate proteins at excitatory synaptic clefts (Loh et al., 2016). Therefore, there is still much to unveil on excitatory synapse formation and transmission, and future studies will help us to decipher the complex function of neuronal circuits in the brain.

Molecular composition of inhibitory postsynapses

The knowledge we have on synapse formation and plasticity is mainly based on studies performed on excitatory synapses, but recent efforts have uncovered many aspects of inhibitory synapse formation and function (Flores and Mendez, 2014; Frias and Wierenga, 2013; Kuzirian and Paradis, 2011; Wierenga, 2017). Inhibitory synapses are often termed symmetric synapses, as the pre- and postsynaptic terminals have similar electron densities when visualized by electron microscopy, and they are located along the dendritic shaft or around the neuronal cell body. Similarly to excitatory postsynapses, inhibitory postsynapses develop a specialization that accumulates a myriad of proteins essential for inhibitory neurotransmission (Figure 4B). Interestingly, recent studies have revealed that inhibitory postsynapses are also organized into nanodomains, which rearrange in response to synaptic activity (Pennacchietti et al., 2017; Specht et al., 2013). A prominent component of inhibitory postsynapses is a protein called gephryin, which is exclusively found at inhibitory synapses (Sassoe-Pognetto et al., 1995). Gephyrin is expressed throughout the nervous system and is regarded as the scaffolding protein of inhibitory synapses (Tyagarajan and Fritschy, 2014). It undergoes different post-translational modifications that can influence its function and localization to inhibitory synapses, which may promote changes on inhibitory neurotransmission (Dejanovic and Schwarz, 2014; Dejanovic et al., 2014; Flores et al., 2015; Ghosh et al., 2016; Tyagarajan et al., 2011). Gephyrin interacts with many proteins at inhibitory synapses, including ionotropic $GABA_A$ receptors ($GABA_A$Rs). The stabilization of $GABA_A$Rs

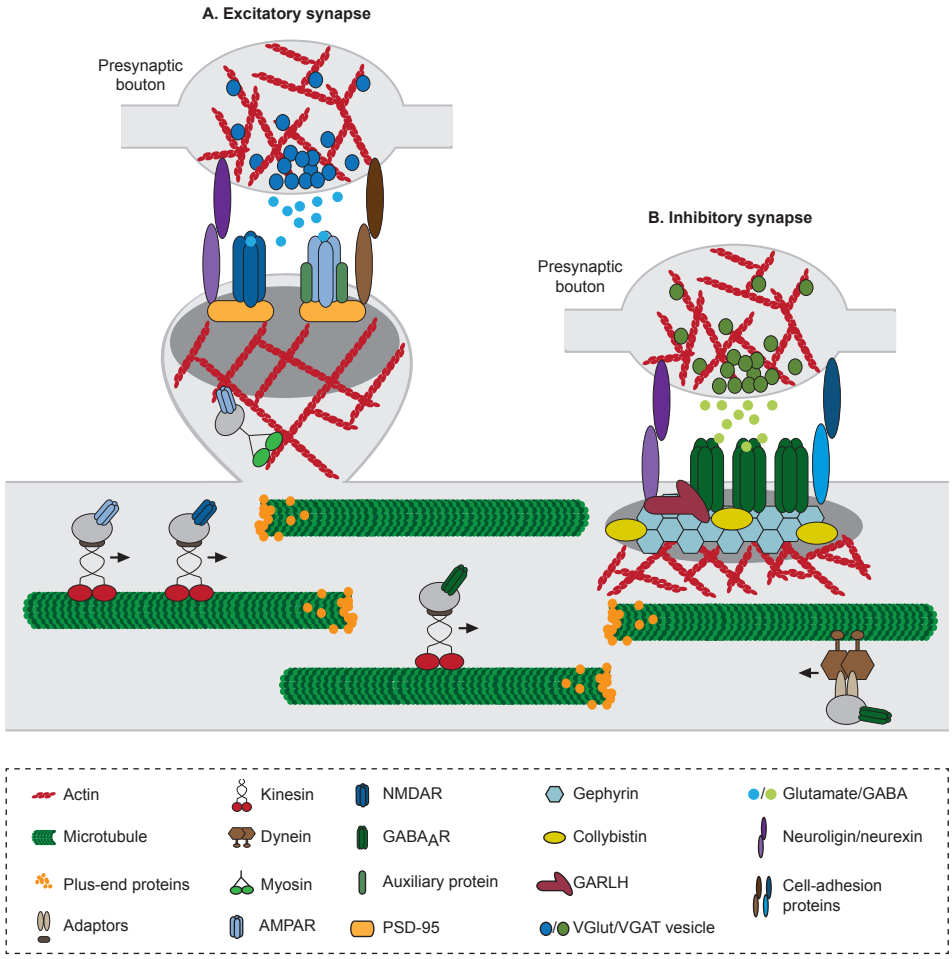

Figure 4. Excitatory and inhibitory synapses architecture.
Along dendrites, kinesins and dynein promote the transport of cargo, including vesicles containing neurotransmitter receptors, along microtubules, while myosins are important for actin-based transport in postsynaptic sites. The apposition of pre- and postsynaptic sites is maintained by different cell-adhesion proteins, including neuroligin-neurexin proteins. (A) Excitatory synapses are generally formed onto actin-rich dendritic spines. Glutamate-filled synaptic vesicles are found at the presynaptic site and they can fuse with the presynaptic membrane. The released glutamate can bind to glutamate receptors (N-methyl-D-aspartate receptors – NMDARs, and α-amino-3-hydroxy-5-methyl-4-isoxazolepropionic acid receptors – AMPARs), which interact with postsynaptic density p rotein PSD-95. (B) Inhibitory synapses can be found along the dendritic shaft. Gephyrin is the inhibitory postsynaptic scaffolding protein, and interacts with several proteins, including γ-aminobutyric acid receptors ($GABA_AR$s) and collybistin. The apposed presynaptic sites contain vesicles filled with γ-aminobutyric acid (GABA), which can bind to postsynaptic $GABA_AR$s. $GABA_AR$s are stabilized at postsynaptic sites by different proteins, including $GABA_AR$ regulatory Lhfpl (GARLH).

at synapses is at least partly due to gephyrin (Jacob et al., 2005; Levi et al., 2004), but other proteins, including giant Ankyrin-G and $GABA_AR$ regulatory Lhfpl (GARLH), have been shown to be involved in the process (Tseng et al., 2015; Yamasaki et al., 2017). As many other proteins, $GABA_ARs$ are assembled in the soma, and need to be transported to the dendrites and inserted at the appropriate location of the membrane. Some kinesin proteins have been implicated in the transport of $GABA_ARs$ receptors to synaptic and extrasynaptic sites (Labonté et al., 2014; Nakajima et al., 2012; Twelvetrees et al., 2010), but the understanding of the transport of inhibitory PSD proteins seems to lack behind when compared to the one of excitatory synapses. Therefore, we have performed a targeted knockdown screen to unravel the contribution of each individual motor protein in the maintenance of inhibitory synapses (*chapter 5*).

Mature inhibitory synapses in dendrites are formed at pre-existing axon-dendrite crossings in hippocampal neurons (Wierenga et al., 2008), where interactions between the pre- and postsynaptic inhibitory terminals occur. These interactions may be regulated by transsynaptic cell-adhesion proteins or secreted factors. The most studied pair of transsynaptic proteins in inhibitory synapses is postsynaptic neuroligin-2 and presynaptic neurexins, and both proteins are sufficient to promote inhibitory synapse formation in co-culture assays (Graf et al., 2004; Kang et al., 2008). Even though mice lacking neuroligin-2 have defects in inhibitory neurotransmission, only perisomatic synapses were affected in these mice (Chubykin et al., 2007; Poulopoulos et al., 2009), suggesting the existence of other inhibitory synaptic organizing proteins. In recent years, many proteins have been identified in inhibitory synaptogenesis, including the guidance protein semaphorin 4D (Sema4D) (Kuzirian et al., 2013; Paradis et al., 2007) or the transsynaptic pair Slit and NTRK-like family member 3 (Slitrk3)/PTPδ (Takahashi et al., 2012). These proteins may act to stabilize the synaptic contact, promote the clustering and stabilization of scaffolding proteins and receptors at pre- and postsynaptic sites, or regulate intracellular signaling pathways. New insights into a signaling pathway triggered by Sema4D at inhibitory presynaptic sites are discussed in *chapter 6*. Not much is known about signaling cascades promoting the disassembly of inhibitory synapses, but the protein MDGA1 has been shown to abolish the interaction between neuroligin-2 and neurexins (Lee et al., 2013; Pettem et al., 2013). Secreted factors, such as neuregulin or fibroblast growth factor 7 (FGF7), can also instruct inhibitory synapse formation by promoting the development and organization of presynaptic terminals (Fazzari et al., 2010; Terauchi et al., 2010).

Mature inhibitory synapses are not static, but rather dynamic structures that can adapt to changes on synaptic activity *in vitro* and *in vivo* (Flores and Mendez, 2014; Frias and Wierenga, 2013). This structural plasticity contributes to neuronal circuitry remodeling and is thought to be important for experience-dependent circuit adaptations.

AXON DYNAMICS: A FOCUS ON INHIBITORY BOUTONS

Prolonged changes in network activity trigger homeostatic mechanisms that adjust both excitatory and inhibitory synapses to restore a proper balance within the neuronal circuitry. Live-imaging studies have shown that axons and their presynaptic terminals (often called as boutons) are highly dynamic structures that can rapidly adapt to changes in neuronal activity. Presynaptic boutons can appear, disappear and reappear in the course of minutes to hours (Fu et al., 2012; Schuemann et al., 2013; Wierenga et al., 2008), and this behavior may reflect

different stages of synapse formation and elimination. Recent in vivo studies have shown that inhibitory synapses rapidly change upon sensory deprivation (Keck et al., 2011; Marik et al., 2010; Villa et al., 2016). More precisely, inhibitory axons and their boutons undergo significant remodeling, which may represent an adaptive mechanism to decreased levels of synaptic activity. In other words, by modifying their axons, inhibitory neurons can modify the contacts they make with postsynaptic cells, which suggest the involvement of mechanisms that coordinate structural changes at pre- and postsynaptic sites during synaptic plasticity and sensory experience. These mechanisms are further discussed in *chapter 2*.

SCOPE OF THE THESIS

Proper synapse formation and plasticity are instrumental for information transmission to other neurons. This thesis focuses on the axon, responsible for transmitting signals to postsynaptic cells. The axon develops a unique cytoskeletal organization and specialized structures required for its task, including the AIS and presynaptic boutons. This thesis aims to increase our understanding on the mechanisms that support axon development and outgrowth and that underlie the dynamics of its presynaptic boutons. Moreover, this thesis also provides new insights into how molecular motors affect different neurobiological processes, from axon initiation to synaptic maintenance.

In *chapter 2* we present an overview of mechanisms important for the regulation of inhibitory presynaptic dynamics, and discuss some signaling pathways involved in this process.

Chapters 3 to *5* use targeted knockdown-screen approaches to study motor protein roles in the development and maturation of dissociated hippocampal neurons. In *chapter 3,* we studied the role of myosin proteins in the regulation of axon formation. We show that Myosin IIb, an actin cross-linking protein, is important for neuronal polarization and the establishment of the AIS. In *chapter 4*, we found that kinesin motor proteins are important for proper axon outgrowth, and that KIF19, a microtubule depolymerizing protein, is a regulator of neuronal polarity and axon growth in hippocampal neurons. In *chapter 5*, we assessed the role of the three motor protein superfamilies in the maintenance of excitatory and inhibitory synapses within the same neuron. We found that dynein-interacting proteins are required to support both types of synapses, and we suggest that they may do so by different mechanisms.

Chapter 6 focuses on inhibitory axon dynamics, important for activity-dependent inhibitory plasticity during circuit adaptation. We studied the molecular mechanisms underlying inhibitory bouton dynamics in organotypic hippocampal slices, and found a new regulatory pathway of inhibitory synapse formation. This pathway is triggered by the guidance protein Sema4D, is activity-dependent and involves the receptor tyrosine kinase MET, an autism-linked gene.

In *chapter 7*, we give a summary and a general discussion on how some of the results described in this thesis contribute to the research fields, and highlight some future research directions.

REFERENCES

Albrecht, D., Winterflood, C.M., Sadeghi, M., Tschager, T., Noe, F., and Ewers, H. (2016). Nanoscopic compartmentalization of membrane protein motion at the axon initial segment. J. Cell Biol. 215, 37-46.

Baas, P.W., Deitch, J.S., Black, M.M., and Banker, G.A. (1988). Polarity orientation of microtubules in hippocampal neurons: uniformity in the axon and nonuniformity in the dendrite. Proc. Natl. Acad. Sci. USA 85, 8335-8339.

Bourne, J.N., and Harris, K.M. (2008). Balancing structure and function at hippocampal dendritic spines. Annu. Rev. Neurosci. 31, 47-67.

Bradke, F., and Dotti, C.G. (1999). The role of local actin instability in axon formation. Science 283, 1931-1934.

Brandt, R. (1998). Cytoskeletal mechanisms of axon outgrowth and pathfinding. Cell Tissue Res. 292, 181-189.

Bury, L.A., and Sabo, S.L. (2014). Dynamic mechanisms of neuroligin-dependent presynaptic terminal assembly in living cortical neurons. Neural Dev. 9, 13.

Caceres, A., Mautino, J., and Kosik, K.S. (1992). Suppression of MAP2 in cultured cerebellar macroneurons inhibits minor neurite formation. Neuron 9, 607-618.

Chu, P.J., Rivera, J.F., and Arnold, D.B. (2006). A role for Kif17 in transport of Kv4.2. J. Biol. Chem. 281, 365-373.

Chubykin, A.A., Atasoy, D., Etherton, M.R., Brose, N., Kavalali, E.T., Gibson, J.R., and Sudhof, T.C. (2007). Activity-dependent validation of excitatory versus inhibitory synapses by neuroligin-1 versus neuroligin-2. Neuron 54, 919-931.

Cingolani, L.A., and Goda, Y. (2008). Actin in action: the interplay between the actin cytoskeleton and synaptic efficacy. Nat. Rev. Neurosci. 9, 344-356.

Coles, C.H., and Bradke, F. (2015). Coordinating neuronal actin-microtubule dynamics. Cur. Biol. 25, R677-691.

Conde, C., and Caceres, A. (2009). Microtubule assembly, organization and dynamics in axons and dendrites. Nat. Rev. Neurosci. 10, 319-332.

D'Este, E., Kamin, D., Gottfert, F., El-Hady, A., and Hell, S.W. (2015). STED nanoscopy reveals the ubiquity of subcortical cytoskeleton periodicity in living neurons. Cell Rep. 10, 1246-1251.

De Simoni, A., and Yu, L.M. (2006). Preparation of organotypic hippocampal slice cultures: interface method. Nat. Protoc. 1, 1439-1445.

de Wit, J., and Ghosh, A. (2016). Specification of synaptic connectivity by cell surface interactions. Nat. Rev. Neurosci. 17, 22-35.

Dejanovic, B., and Schwarz, G. (2014). Neuronal nitric oxide synthase-dependent S-nitrosylation of gephyrin regulates gephyrin clustering at GABAergic synapses. J. Neurosci. 34, 7763-7768.

Dejanovic, B., Semtner, M., Ebert, S., Lamkemeyer, T., Neuser, F., Luscher, B., Meier, J.C., and Schwarz, G. (2014). Palmitoylation of gephyrin controls receptor clustering and plasticity of GABAergic synapses. PLoS Biol. 12, e1001908.

Dotti, C.G., Sullivan, C.A., and Banker, G.A. (1988). The establishment of polarity by hippocampal neurons in culture. J. Neurosci. 8, 1454-1468.

Fazzari, P., Paternain, A.V., Valiente, M., Pla, R., Lujan, R., Lloyd, K., Lerma, J., Marin, O., and Rico, B. (2010). Control of cortical GABA circuitry development by Nrg1 and ErbB4 signalling. Nature 464, 1376-1380.

Flores, C.E., and Mendez, P. (2014). Shaping inhibition: activity dependent structural plasticity of GABAergic synapses. Front. Cell. Neurosci. 8, 327.

Flores, C.E., Nikonenko, I., Mendez, P., Fritschy, J.M., Tyagarajan, S.K., and Muller, D. (2015). Activity-dependent inhibitory synapse remodeling through gephyrin phosphorylation. Proc. Natl. Acad. Sci. USA 112, E65-72.

Franker, M.A., and Hoogenraad, C.C. (2013). Microtubule-based transport - basic mechanisms, traffic rules and role in neurological pathogenesis. J. Cell Sci. 126, 2319-2329.

Fréal, A., Fassier, C., Le Bras, B., Bullier, E., De Gois, S., Hazan, J., Hoogenraad, C.C., and Couraud, F. (2016). Cooperative Interactions between 480 kDa Ankyrin-G and EB Proteins Assemble the Axon Initial Segment. J. Neurosci. 36, 4421-4433.

Frias, C.P., and Wierenga, C.J. (2013). Activity-dependent adaptations in inhibitory axons. Front. Cell. Neurosci. 7, 219.

Fu, Y., Wu, X., Lu, J., and Huang, Z.J. (2012). Presynaptic

GABA(B) Receptor Regulates Activity-Dependent Maturation and Patterning of Inhibitory Synapses through Dynamic Allocation of Synaptic Vesicles. Front. Cell. Neurosci. 6, 57.

Ganguly, A., Tang, Y., Wang, L., Ladt, K., Loi, J., Dargent, B., Leterrier, C., and Roy, S. (2015). A dynamic formin-dependent deep F-actin network in axons. J. Cell Biol. 210, 401-417.

Ghosh, H., Auguadri, L., Battaglia, S., Simone Thirouin, Z., Zemoura, K., Messner, S., Acuna, M.A., Wildner, H., Yevenes, G.E., Dieter, A., et al. (2016). Several posttranslational modifications act in concert to regulate gephyrin scaffolding and GABAergic transmission. Nat. Commun. 7, 13365.

Graf, E.R., Zhang, X., Jin, S.X., Linhoff, M.W., and Craig, A.M. (2004). Neurexins induce differentiation of GABA and glutamate postsynaptic specializations via neuroligins. Cell 119, 1013-1026.

He, J., Zhou, R., Wu, Z., Carrasco, M.A., Kurshan, P.T., Farley, J.E., Simon, D.J., Wang, G., Han, B., Hao, J., et al. (2016). Prevalent presence of periodic actin-spectrin-based membrane skeleton in a broad range of neuronal cell types and animal species. Proc. Natl. Acad. Sci. USA 113, 6029-6034.

Hedstrom, K.L., Ogawa, Y., and Rasband, M.N. (2008). AnkyrinG is required for maintenance of the axon initial segment and neuronal polarity. J. Cell Biol. 183, 635-640.

Heisler, F.F., Lee, H.K., Gromova, K.V., Pechmann, Y., Schurek, B., Ruschkies, L., Schroeder, M., Schweizer, M., and Kneussel, M. (2014). GRIP1 interlinks N-cadherin and AMPA receptors at vesicles to promote combined cargo transport into dendrites. Proc. Natl. Acad. Sci. USA 111, 5030-5035.

Hirokawa, N., Niwa, S., and Tanaka, Y. (2010). Molecular motors in neurons: transport mechanisms and roles in brain function, development, and disease. Neuron 68, 610-638.

Hirokawa, N., Noda, Y., Tanaka, Y., and Niwa, S. (2009). Kinesin superfamily motor proteins and intracellular transport. Nat. Rev. Mol. Cell Biol. 10, 682-696.

Holtmaat, A., Wilbrecht, L., Knott, G.W., Welker, E., and Svoboda, K. (2006). Experience-dependent and cell-type-specific spine growth in the neocortex. Nature 441, 979-983.

Hoogenraad, C.C., and Bradke, F. (2009). Control of neuronal polarity and plasticity--a renaissance for microtubules? Trends Cell Biol. 19, 669-676.

Hotulainen, P., and Hoogenraad, C.C. (2010). Actin in dendritic spines: connecting dynamics to function. J. Cell Biol. 189, 619-629.

Jacob, T.C., Bogdanov, Y.D., Magnus, C., Saliba, R.S., Kittler, J.T., Haydon, P.G., and Moss, S.J. (2005). Gephyrin regulates the cell surface dynamics of synaptic GABAA receptors. J. Neurosci. 25, 10469-10478.

Jacobson, C., Schnapp, B., and Banker, G.A. (2006). A change in the selective translocation of the Kinesin-1 motor domain marks the initial specification of the axon. Neuron 49, 797-804.

Jones, S.L., Korobova, F., and Svitkina, T. (2014). Axon initial segment cytoskeleton comprises a multiprotein submembranous coat containing sparse actin filaments. J Cell Biol. 205, 67-81.

Jones, S.L., and Svitkina, T.M. (2016). Axon Initial Segment Cytoskeleton: Architecture, Development, and Role in Neuron Polarity. Neural Plast. 2016, 6808293.

Kang, Y., Zhang, X., Dobie, F., Wu, H., and Craig, A.M. (2008). Induction of GABAergic postsynaptic differentiation by alpha-neurexins. J. Biol. Chem. 283, 2323-2334.

Kapitein, L.C., and Hoogenraad, C.C. (2011). Which way to go? Cytoskeletal organization and polarized transport in neurons. Mol. Cell. Neurosci. 46, 9-20.

Keck, T., Scheuss, V., Jacobsen, R.I., Wierenga, C.J., Eysel, U.T., Bonhoeffer, T., and Hubener, M. (2011). Loss of sensory input causes rapid structural changes of inhibitory neurons in adult mouse visual cortex. Neuron 71, 869-882.

Kneussel, M., and Wagner, W. (2013). Myosin motors at neuronal synapses: drivers of membrane transport and actin dynamics. Nat. Rev. Neurosci. 14, 233-247.

Kole, M.H., Ilschner, S.U., Kampa, B.M., Williams, S.R., Ruben, P.C., and Stuart, G.J. (2008). Action potential generation requires a high sodium channel density in the axon initial segment. Nat. Neurosci. 11, 178-186.

Kuijpers, M., van de Willige, D., Freal, A., Chazeau, A., Franker, M.A., Hofenk, J., Rodrigues, R.J., Kapitein, L.C., Akhmanova, A., Jaarsma, D., et al. (2016). Dynein Regulator NDEL1 Controls Polarized Cargo Transport at the Axon Initial Segment. Neuron 89, 461-471.

Kuzirian, M.S., Moore, A.R., Staudenmaier, E.K., Friedel,

R.H., and Paradis, S. (2013). The class 4 semaphorin Sema4D promotes the rapid assembly of GABAergic synapses in rodent hippocampus. J. Neurosci. 33, 8961-8973.

Kuzirian, M.S., and Paradis, S. (2011). Emerging themes in GABAergic synapse development. Prog. Neurobiol. 95, 68-87.

Labonté, D., Thies, E., and Kneussel, M. (2014). The kinesin KIF21B participates in the cell surface delivery of gamma2 subunit-containing GABAA receptors. Eur. J. Cell Biol. 93, 338-346.

Lee, K., Kim, Y., Lee, S.J., Qiang, Y., Lee, D., Lee, H.W., Kim, H., Je, H.S., Sudhof, T.C., and Ko, J. (2013). MDGAs interact selectively with neuroligin-2 but not other neuroligins to regulate inhibitory synapse development. Proc. Natl. Acad. Sci. USA 110, 336-341.

Leterrier, C., Potier, J., Caillol, G., Debarnot, C., Rueda Boroni, F., and Dargent, B. (2015). Nanoscale Architecture of the Axon Initial Segment Reveals an Organized and Robust Scaffold. Cell Rep. 13, 2781-2793.

Letourneau, P.C. (2009). Actin in axons: stable scaffolds and dynamic filaments. Results Probl. Cell Differ. 48, 65-90.

Levi, S., Logan, S.M., Tovar, K.R., and Craig, A.M. (2004). Gephyrin is critical for glycine receptor clustering but not for the formation of functional GABAergic synapses in hippocampal neurons. J. Neurosci. 24, 207-217.

Lipka, J., Kuijpers, M., Jaworski, J., and Hoogenraad, C.C. (2013). Mutations in cytoplasmic dynein and its regulators cause malformations of cortical development and neurodegenerative diseases. Biochem. Soc. Trans. 41, 1605-1612.

Loh, K.H., Stawski, P.S., Draycott, A.S., Udeshi, N.D., Lehrman, E.K., Wilton, D.K., Svinkina, T., Deerinck, T.J., Ellisman, M.H., Stevens, B., et al. (2016). Proteomic Analysis of Unbounded Cellular Compartments: Synaptic Clefts. Cell 166, 1295-1307 e1221.

MacGillavry, H.D., Song, Y., Raghavachari, S., and Blanpied, T.A. (2013). Nanoscale scaffolding domains within the postsynaptic density concentrate synaptic AMPA receptors. Neuron 78, 615-622.

Marik, S.A., Yamahachi, H., McManus, J.N., Szabo, G., and Gilbert, C.D. (2010). Axonal dynamics of excitatory and inhibitory neurons in somatosensory cortex. PLoS Biol. 8, e1000395.

Mitchison, T., and Kirschner, M. (1984). Dynamic instability of microtubule growth. Nature 312, 237-242.

Muhia, M., Thies, E., Labonte, D., Ghiretti, A.E., Gromova, K.V., Xompero, F., Lappe-Siefke, C., Hermans-Borgmeyer, I., Kuhl, D., Schweizer, M., et al. (2016). The Kinesin KIF21B Regulates Microtubule Dynamics and Is Essential for Neuronal Morphology, Synapse Function, and Learning and Memory. Cell Rep. 15, 968-977.

Nair, D., Hosy, E., Petersen, J.D., Constals, A., Giannone, G., Choquet, D., and Sibarita, J.B. (2013). Super-resolution imaging reveals that AMPA receptors inside synapses are dynamically organized in nanodomains regulated by PSD95. J. Neurosci. 33, 13204-13224.

Nakajima, K., Yin, X., Takei, Y., Seog, D.H., Homma, N., and Hirokawa, N. (2012). Molecular motor KIF5A is essential for GABA(A) receptor transport, and KIF5A deletion causes epilepsy. Neuron 76, 945-961.

Nakata, T., and Hirokawa, N. (2003). Microtubules provide directional cues for polarized axonal transport through interaction with kinesin motor head. J. Cell Biol. 162, 1045-1055.

Nishimura, T., Kato, K., Yamaguchi, T., Fukata, Y., Ohno, S., and Kaibuchi, K. (2004). Role of the PAR-3-KIF3 complex in the establishment of neuronal polarity. Nat. Cell Biol. 6, 328-334.

Pacheco, A., and Gallo, G. (2016). Actin filament-microtubule interactions in axon initiation and branching. Brain Res. Bull. 126, 300-310.

Palay, S.L., Sotelo, C., Peters, A., and Orkand, P.M. (1968). The axon hillock and the initial segment. J. Cell Biol. 38, 193-201.

Paradis, S., Harrar, D.B., Lin, Y., Koon, A.C., Hauser, J.L., Griffith, E.C., Zhu, L., Brass, L.F., Chen, C., and Greenberg, M.E. (2007). An RNAi-based approach identifies molecules required for glutamatergic and GABAergic synapse development. Neuron 53, 217-232.

Pennacchietti, F., Vascon, S., Nieus, T., Rosillo, C., Das, S., Tyagarajan, S.K., Diaspro, A., Del Bue, A., Petrini, E.M., Barberis, A., et al. (2017). Nanoscale Molecular Reorganization of the Inhibitory Postsynaptic Density Is a Determinant of GABAergic Synaptic Potentiation. J. Neurosci. 37, 1747-1756.

Pettem, K.L., Yokomaku, D., Takahashi, H., Ge, Y., and Craig, A.M. (2013). Interaction between autism-linked MDGAs and neuroligins suppresses inhibitory synapse development. J. Cell Biol. 200, 321-336.

Poulopoulos, A., Aramuni, G., Meyer, G., Soykan, T., Hoon, M., Papadopoulos, T., Zhang, M., Paarmann, I., Fuchs, C., Harvey, K., et al. (2009). Neuroligin 2 drives postsynaptic assembly at perisomatic inhibitory synapses through gephyrin and collybistin. Neuron 63, 628-642.

Rex, C.S., Gavin, C.F., Rubio, M.D., Kramar, E.A., Chen, L.Y., Jia, Y., Huganir, R.L., Muzyczka, N., Gall, C.M., Miller, C.A., et al. (2010). Myosin IIb regulates actin dynamics during synaptic plasticity and memory formation. Neuron 67, 603-617.

Roberts, T.F., Tschida, K.A., Klein, M.E., and Mooney, R. (2010). Rapid spine stabilization and synaptic enhancement at the onset of behavioural learning. Nature 463, 948-952.

Rudenko, G. (2017). Dynamic Control of Synaptic Adhesion and Organizing Molecules in Synaptic Plasticity. Neural Plast. 2017, 6526151.

Ryu, J., Liu, L., Wong, T.P., Wu, D.C., Burette, A., Weinberg, R., Wang, Y.T., and Sheng, M. (2006). A critical role for myosin IIb in dendritic spine morphology and synaptic function. Neuron 49, 175-182.

Sabo, S.L., Gomes, R.A., and McAllister, A.K. (2006). Formation of presynaptic terminals at predefined sites along axons. J. Neurosci. 26, 10813-10825.

Sassoe-Pognetto, M., Kirsch, J., Grunert, U., Greferath, U., Fritschy, J.M., Mohler, H., Betz, H., and Wassle, H. (1995). Colocalization of gephyrin and GABAA-receptor subunits in the rat retina. J. Comp. Neurol. 357, 1-14.

Scheiffele, P., Fan, J., Choih, J., Fetter, R., and Serafini, T. (2000). Neuroligin expressed in nonneuronal cells triggers presynaptic development in contacting axons. Cell 101, 657-669.

Schelski, M., and Bradke, F. (2017). Neuronal polarization: From spatiotemporal signaling to cytoskeletal dynamics. Mol. Cell. Neurosci.

Schlager, M.A., and Hoogenraad, C.C. (2009). Basic mechanisms for recognition and transport of synaptic cargos. Mol. Brain 2, 25.

Schuemann, A., Klawiter, A., Bonhoeffer, T., and Wierenga, C.J. (2013). Structural plasticity of GABAergic axons is regulated by network activity and GABAA receptor activation. Front. Neural Circuits 7, 113.

Setou, M., Nakagawa, T., Seog, D.H., and Hirokawa, N. (2000). Kinesin superfamily motor protein KIF17 and mLin-10 in NMDA receptor-containing vesicle transport. Science 288, 1796-1802.

Setou, M., Seog, D.H., Tanaka, Y., Kanai, Y., Takei, Y., Kawagishi, M., and Hirokawa, N. (2002). Glutamate-receptor-interacting protein GRIP1 directly steers kinesin to dendrites. Nature 417, 83-87.

Shen, K., and Cowan, C.W. (2010). Guidance molecules in synapse formation and plasticity. Cold Spring Harb. Perspect. Biol. 2, a001842.

Sheng, M., and Kim, E. (2011). The postsynaptic organization of synapses. Cold Spring Harb. Perspect. Biol. 3.

Shi, S.H., Cheng, T., Jan, L.Y., and Jan, Y.N. (2004). APC and GSK-3beta are involved in mPar3 targeting to the nascent axon and establishment of neuronal polarity. Curr. Biol. 14, 2025-2032.

Siddiqui, T.J., and Craig, A.M. (2011). Synaptic organizing complexes. Curr. Opin. Neurobiol. 21, 132-143.

Song, A.H., Wang, D., Chen, G., Li, Y., Luo, J., Duan, S., and Poo, M.M. (2009). A selective filter for cytoplasmic transport at the axon initial segment. Cell 136, 1148-1160.

Specht, C.G., Izeddin, I., Rodriguez, P.C., El Beheiry, M., Rostaing, P., Darzacq, X., Dahan, M., and Triller, A. (2013). Quantitative nanoscopy of inhibitory synapses: counting gephyrin molecules and receptor binding sites. Neuron 79, 308-321.

Sprecher, S.G. (2008). Evolution of the brain in Urbilateria. Essay in: "Encyclopedic Reference of Neuroscience", Springer, 1339-1342.

Sprecher, S.G., and Reichert, H. (2003). The urbilaterian brain: developmental insights into the evolutionary origin of the brain in insects and vertebrates. Arthropod Struct. Dev. 32, 141-156.

Tahirovic, S., and Bradke, F. (2009). Neuronal polarity. Cold Spring Harb. Perspect. Biol. 1, a001644.

Takahashi, H., Katayama, K., Sohya, K., Miyamoto, H., Prasad, T., Matsumoto, Y., Ota, M., Yasuda, H., Tsumoto, T., Aruga, J., et al. (2012). Selective control of inhibitory synapse development by Slitrk3-PTPdelta trans-synaptic interaction. Nat. Neurosci. 15, 389-398, S381-382.

Terauchi, A., Johnson-Venkatesh, E.M., Toth, A.B., Javed, D., Sutton, M.A., and Umemori, H. (2010). Distinct FGFs promote differentiation of excitatory and inhibitory synapses. Nature 465, 783-787.

Tseng, W.C., Jenkins, P.M., Tanaka, M., Mooney, R., and Bennett, V. (2015). Giant ankyrin-G stabilizes somatodendritic GABAergic synapses through opposing endocytosis of GABAA receptors. Proc. Natl. Acad. Sci. USA 112, 1214-1219.

Twelvetrees, A.E., Yuen, E.Y., Arancibia-Carcamo, I.L., MacAskill, A.F., Rostaing, P., Lumb, M.J., Humbert, S., Triller, A., Saudou, F., Yan, Z., et al. (2010). Delivery of GABAARs to synapses is mediated by HAP1-KIF5 and disrupted by mutant huntingtin. Neuron 65, 53-65.

Tyagarajan, S.K., and Fritschy, J.M. (2014). Gephyrin: a master regulator of neuronal function? Nat. Rev. Neurosci. 15, 141-156.

Tyagarajan, S.K., Ghosh, H., Yevenes, G.E., Nikonenko, I., Ebeling, C., Schwerdel, C., Sidler, C., Zeilhofer, H.U., Gerrits, B., Muller, D., et al. (2011). Regulation of GABAergic synapse formation and plasticity by GSK3beta-dependent phosphorylation of gephyrin. Proc. Natl. Acad. Sci. USA 108, 379-384.

van Beuningen, S.F., Will, L., Harterink, M., Chazeau, A., van Battum, E.Y., Frias, C.P., Franker, M.A., Katrukha, E.A., Stucchi, R., Vocking, K., et al. (2015). TRIM46 Controls Neuronal Polarity and Axon Specification by Driving the Formation of Parallel Microtubule Arrays. Neuron 88, 1208-1226.

van den Berg, R., and Hoogenraad, C.C. (2012). Molecular motors in cargo trafficking and synapse assembly. Adv. Exp. Med. Biol. 970, 173-196.

Villa, K.L., Berry, K.P., Subramanian, J., Cha, J.W., Oh, W.C., Kwon, H.B., Kubota, Y., So, P.T., and Nedivi, E. (2016). Inhibitory Synapses Are Repeatedly Assembled and Removed at Persistent Sites In Vivo. Neuron 89, 756-769.

Waites, C.L., Craig, A.M., and Garner, C.C. (2005). Mechanisms of vertebrate synaptogenesis. Annu. Rev. Neurosci. 28, 251-274.

Walczak, C.E., Gayek, S., and Ohi, R. (2013). Microtubule-depolymerizing kinesins. Annu. Rev. Cell Dev. Biol. 29, 417-441.

Watanabe, K., Al-Bassam, S., Miyazaki, Y., Wandless, T.J., Webster, P., and Arnold, D.B. (2012). Networks of polarized actin filaments in the axon initial segment provide a mechanism for sorting axonal and dendritic proteins. Cell Rep. 2, 1546-1553.

Wierenga, C.J. (2017). Live imaging of inhibitory axons: Synapse formation as a dynamic trial-and-error process. Brain Res. Bull. 129, 43-49.

Wierenga, C.J., Becker, N., and Bonhoeffer, T. (2008). GABAergic synapses are formed without the involvement of dendritic protrusions. Nat. Neurosci. 11, 1044-1052.

Wilhelm, B.G., Mandad, S., Truckenbrodt, S., Krohnert, K., Schafer, C., Rammner, B., Koo, S.J., Classen, G.A., Krauss, M., Haucke, V., et al. (2014). Composition of isolated synaptic boutons reveals the amounts of vesicle trafficking proteins. Science 344, 1023-1028.

Witte, H., Neukirchen, D., and Bradke, F. (2008). Microtubule stabilization specifies initial neuronal polarization. J. Cell Biol. 180, 619-632.

Wray, G.A. (2015). Molecular clocks and the early evolution of metazoan nervous systems. Philos. Trans. R. Soc. Lond., B, Biol. Sci. 370.

Xu, K., Zhong, G., and Zhuang, X. (2013). Actin, spectrin, and associated proteins form a periodic cytoskeletal structure in axons. Science 339, 452-456.

Yamasaki, T., Hoyos-Ramirez, E., Martenson, J.S., Morimoto-Tomita, M., and Tomita, S. (2017). GARLH Family Proteins Stabilize GABAA Receptors at Synapses. Neuron 93, 1138-1152 e1136.

Yau, K.W., Schatzle, P., Tortosa, E., Pages, S., Holtmaat, A., Kapitein, L.C., and Hoogenraad, C.C. (2016). Dendrites In Vitro and In Vivo Contain Microtubules of Opposite Polarity and Axon Formation Correlates with Uniform Plus-End-Out Microtubule Orientation. J. Neurosci. 36, 1071-1085.

Zhang, C., and Rasband, M.N. (2016). Cytoskeletal control of axon domain assembly and function. Curr. Opin. Neurobiol. 39, 116-121.

Zhong, G., He, J., Zhou, R., Lorenzo, D., Babcock, H.P., Bennett, V., and Zhuang, X. (2014). Developmental mechanism of the periodic membrane skeleton in axons. eLife 3.

Zhou, D., Lambert, S., Malen, P.L., Carpenter, S., Boland, L.M., and Bennett, V. (1998). AnkyrinG is required for clustering of voltage-gated Na channels at axon initial segments and for normal action potential firing. J. Cell Biology 143, 1295-1304.

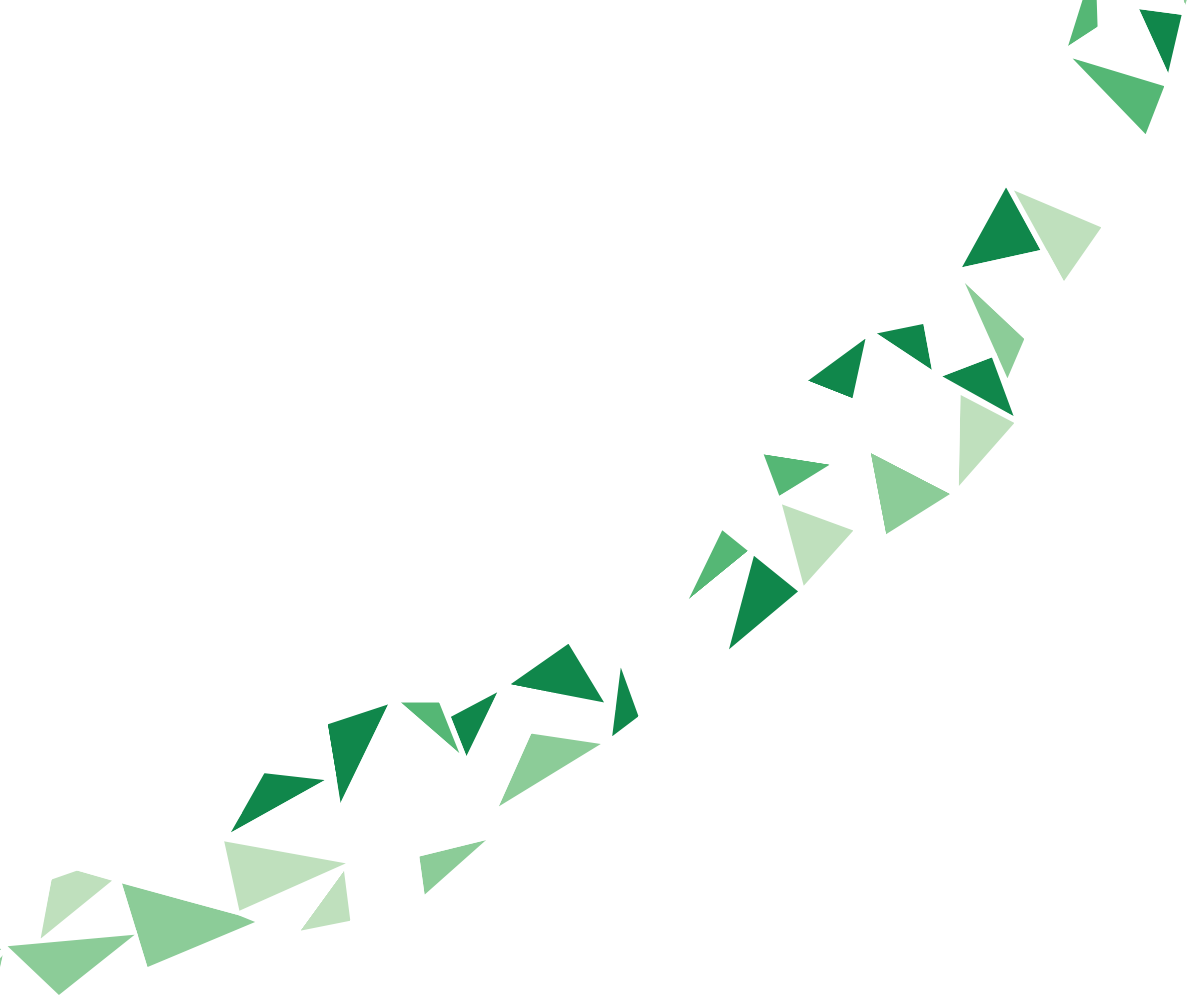

Cell Biology, Department Biology, Faculty of Science, Utrecht University, Utrecht, the Netherlands

Chapter 2

Activity-dependent adaptations in inhibitory axons

Cátia P. Frias and Corette J. Wierenga

Front. Cell Neurosci., November 2013, 7: 1-16

ABSTRACT

Synaptic connections in our brains change continuously and throughout our lifetime. Despite ongoing synaptic changes, a healthy balance between excitation and inhibition is maintained by various forms of homeostatic and activity-dependent adaptations, ensuring stable functioning of neuronal networks. In this review we summarize experimental evidence for activity-dependent changes occurring in inhibitory axons, in cultures as well as *in vivo*. Axons form many presynaptic terminals, which are dynamic structures sharing presynaptic material along the axonal shaft. We discuss how internal (e.g. vesicle sharing) and external factors (e.g. binding of cell adhesion molecules or secreted factors) may affect the formation and plasticity of inhibitory synapses.

INTRODUCTION

Our brain is a complex organ with tremendous self-organizing abilities. Its computational power is based in the adjustable synaptic connections between neurons. When new experiences and memories are established, specific synapses in specific brain regions are changed, both in strength and in number. To ensure proper global functioning despite changes in local connectivity, these synaptic changes must be coordinated within neurons, as well as within neuronal circuits. An important aspect is the coordination between changes in excitatory and inhibitory synapses to regulate and maintain an overall balance between excitation and inhibition. When this balance is disturbed, neurological diseases such as autism or schizophrenia can develop (Bateup et al., 2013; Han et al., 2012; Yizhar et al., 2011; Palop et al., 2007).

Homeostatic plasticity is a term that is used for plasticity mechanisms which ensure that overall neuronal spiking activity is maintained within neuronal networks. Many forms of homeostatic plasticity have been described in excitatory and inhibitory neurons (Turrigiano, 2008; Wenner, 2011; Pozo and Goda, 2010; Tyagarajan and Fritschy, 2010). In neuronal circuits in the brain, inhibitory neurons serve multiple functions, making connections to excitatory as well as inhibitory neurons, and providing feedforward inhibition to some neurons, while supplying feedback input to others. In such complicated networks, there are multiple ways to compensate for changes in network activity, which makes it hard, if not impossible, to classify synaptic changes in inhibitory axons as truly homeostatic. Therefore, we will discuss activity-dependent feedback signals in inhibitory axons in a more general context in this review. We will discuss experimental evidence showing that synaptic activity can affect the formation and plasticity of inhibitory synapses and we will speculate on possible mechanisms.

ACTIVITY-DEPENDENT ADAPTATIONS OF INHIBITORY SYNAPSES

When prolonged changes occur in network activity, homeostatic mechanisms come into play which adjust excitatory and inhibitory synapses to compensate and restore the activity level in the network (Turrigiano, 2011, 1999; Pozo and Goda, 2010; Wenner, 2011; Burrone and Murthy, 2003). Generally speaking, when the activity is too high, excitation must be downregulated and inhibition should be increased to bring activity levels back to baseline. And opposite changes should occur during activity blockade. Homeostatic plasticity has been studied extensively in cultures, where neurons are randomly connected. Dissociated cultures provide superb access for experimental manipulations and therefor form an excellent system to study the cell biological mechanisms underlying homeostatic plasticity. However, in our brain neurons are embedded in multiple neuronal networks and make specific synaptic connections. Recurrent connections between neurons or groups of neurons are very common and different types of GABAergic interneurons are known to have high specificity, making inhibitory synapses onto specific target neurons, including inhibitory neurons (Pfeffer et al., 2013; Jiang et al., 2013). In such complex networks, it is not easy to determine rules of homeostatic plasticity. Adaptation to changes in the activity of the network will be strongly synapse-specific and likely depends on the precise function and location of the synapse in the network (Chen et al., 2011; Maffei et al., 2004; Maffei and Turrigiano, 2008). Here we briefly describe the experimental evidence for activity-dependent plasticity of inhibitory synapses from *in vitro* (i.e. in dissociated and organotypic cultures) and *in vivo* studies.

Primary cell cultures

Activity manipulations in cultures of dissociated hippocampal or neocortical neurons generally affect excitatory and inhibitory synapses in opposite directions. After a prolonged period of activity blockade, excitatory synapses get strengthened and inhibitory synapses are weakened, and synaptic changes are in opposite directions when activity is enhanced (Turrigiano et al., 1998; Hartman et al., 2006; Swanwick et al., 2006; Kilman et al., 2002). Therefore, changes in excitation and inhibition cooperate to compensate for the change in activity level. For inhibitory synapses, changes in mIPSC amplitude are most commonly reported, reflecting changes in synaptic strength. Sometimes they are accompanied by changes in mIPSC frequency, which could either reflect a change in the number of synapses or a change in release properties. Dissociated cultures provide excellent experimental access and are therefore well-suited for studying underlying mechanisms of homeostatic plasticity. However, the artificial environment in which neurons grow in culture may affect synaptic maturation (Wierenga et al., 2006; Rose et al., 2013) and consequently cellular or synaptic mechanisms of plasticity. Cellular mechanisms that were identified to mediate the changes in inhibitory synapses after activity manipulations include: changes in number of postsynaptic receptors (Kilman et al., 2002; Rannals and Kapur, 2011; Peng et al., 2010; Swanwick et al., 2006; Saliba et al., 2007) or scaffolding proteins (Vlachos et al., 2012; study in slice cultures) on the postsynaptic side, and changes in presynaptic release probability (Kim and Alger, 2010), presynaptic vesicle loading (De Gois et al., 2005; Hartman et al., 2006; Lau and Murthy, 2012), or GABA-producing enzymes (Peng et al., 2010; Rannals and Kapur, 2011) on the presynaptic side. Only in a few cases, changes in the number of inhibitory synapses were reported (Peng et al., 2010; Hartman et al., 2006). Homeostatic changes of inhibitory synapses could be induced in a cell autonomous fashion (Peng et al., 2010), or required a change in activity of the entire neuronal network (Hartman et al., 2006), emphasizing that there are multiple mechanisms of homeostatic plasticity at inhibitory synapses. In particular, distinct mechanisms could exist for activity-dependent downregulation and upregulation of inhibitory synapses.

Organotypic cultures

In contrast to dissociated cultures neurons in more intact tissue, such as acute slices or organotypic cultures, make more specific connections and form structured networks. This network configuration makes the interpretation of synaptic changes more complex. In slices that were submitted to activity manipulations, changes in inhibition have been observed opposite to (Karmarkar and Buonomano, 2006; Kim and Alger, 2010; Marty et al., 2004) as well as in conjunction with (Echegoyen et al., 2007; Buckby et al., 2006) changes in excitation. It was also shown that different types of homeostatic mechanisms have different time courses (Karmarkar and Buonomano, 2006) and that different subsets of inhibitory synapses can respond differently. For instance, the presence of cannabinoid receptors in a subset of inhibitory synapses renders them selectively receptive to changes in endocannabinoid levels induced by inactivity (Kim and Alger, 2010). In another example, inactivity differentially affected somatic and dendritic inhibitory inputs on CA1 pyramidal cells. Interestingly, both types of synapses showed reduction in the number of presynaptic boutons and upregulation of release probability, but the functional end-effect on inhibitory input to the postsynaptic cells was different (Bartley et al., 2008; Chattopadhyaya et al., 2004). This emphasizes that simple *in vitro* homeostatic rules for scaling inhibitory synapses get complicated in more

complex networks. In addition, other factors such as different cell (glia) types or the extracellular environment in more intact tissue potentially influence homeostatic plasticity compared to dissociated cultured cells.

In vivo studies

Typically, when studying activity-dependent or homeostatic changes *in vivo*, sensory deprivation is used as experimental paradigm to lower activity levels in the primary sensory cortex (e.g. whisker trimming, monocular deprivation, or retinal lesion). While *in vitro* activity manipulations by pharmacological means affect the activity of all neurons in equal amounts, sensory deprivation *in vivo* will affect different neurons in the circuitry differentially. Therefore, *in vivo* responses of inhibitory synapses to changes in activity vary widely and strongly depend on the specific cell types, cortical layer and specific circuitry (Chen et al., 2011; Maffei et al., 2004; Maffei and Turrigiano, 2008). Furthermore, it is well-known that inhibition in sensory cortex areas undergoes important developmental changes (Hensch, 2005), which means that the same deprivation paradigm can have different effects on inhibitory synapses depending on the postnatal period that is considered (Maffei et al., 2010; Chattopadhyaya et al., 2004; Maffei et al., 2006). An emerging theme from the *in vivo* studies is that inhibitory synapses can respond rapidly to sensory deprivation. It was shown that inhibitory axons in cortical layer 2/3 reduce the number of boutons within the first 24 hours after a retinal lesion or monocular deprivation (Keck et al., 2011; Chen et al., 2011). Over longer periods, inhibitory axons in the barrel cortex were shown to sprout and form new axonal branches after whisker plucking (Marik et al., 2010). Interestingly, the reduction of inhibition was often found to precede adaptive changes of the excitatory circuitry (Keck et al., 2011; Marik et al., 2010). The rapid downregulation of inhibition might serve to render the local circuit more permissive for excitatory plasticity to occur (Gambino and Holtmaat, 2012; Ormond and Woodin, 2011). In two recent studies it was shown that inhibitory synapses that are located on spines (presumably next to an excitatory synapse) showed much higher turnover rates compared to inhibitory synapses on shaft after visual deprivation (van Versendaal et al., 2012; Chen et al., 2012). It will be interesting to see whether direct cross talk of the two types of synapses exists.

In conclusion, there is a large amount of compelling evidence for activity-dependent adaptations in inhibitory synapses *in vitro* as well as *in vivo*. The precise expression mechanisms significantly vary between different preparations and experimental paradigms.

AXONS

In this review we focus on possible feedback signals that occur in inhibitory axons in response to changes in network or synaptic activity and that induce changes in the number or properties of presynaptic terminals along the axon. The axon of a single neuron forms several thousands of presynaptic terminals (i.e. 'boutons') along its shaft and contacts many different postsynaptic neurons. Presynaptic boutons along an axon show a large variety in their volumes, in the number of synaptic vesicles and in the presence or absence of mitochondria (Shepherd and Harris, 1998). It is now well-established that neighboring boutons are not independent entities, but they continuously share and exchange molecular components of the release machinery and synaptic vesicles (Darcy et al., 2006; Staras, 2007; Sabo et al., 2006; Krueger et al., 2003; Yamada et al., 2013). Synaptic vesicles may not belong

to a specific presynaptic terminal, but form a superpool of vesicles in the axonal shaft and are shared by multiple release sites (Staras et al., 2010).

The exchange of presynaptic proteins means that the exact composition of presynaptic terminals is continuously changing. These changes can occur in a correlated fashion with the postsynaptic site in some synapses, but can be uncoordinated in others (Fisher-Lavie et al., 2011; Fisher-Lavie and Ziv, 2013). Release properties and synaptic strength are highly variable between individual boutons along the same axon (Zhao et al., 2011; Branco et al., 2008; Rose et al., 2013). Therefore the demand for synaptic vesicles or other presynaptic proteins will vary between presynaptic boutons and neighboring boutons compete for available resources. Indeed, reduced availability of synaptic proteins within the axon has been shown to enhance competition between boutons (Yamada et al., 2013). In addition, vesicle exchange is regulated by neuronal activity through changes in axonal calcium levels (Kim and Ryan, 2013, 2010).
Synaptic vesicles are kept at the presynaptic terminal by interacting with a scaffolding meshwork of actin, β-catenin, synapsin and many other proteins (Peng et al., 2012; Takamori et al., 2006; Cingolani and Goda, 2008; Fernández-Busnadiego et al., 2010; Taylor et al., 2013; Bamji et al., 2003). Synaptic vesicles can escape from the presynaptic terminal into the axon, while other vesicles that were traveling along the axonal shaft can be captured. Although the loss of a strict presynaptic compartmentalization may seem disadvantageous at first, the main advantage of sharing presynaptic material between boutons is flexibility. When presynaptic material is continuously being lost and gained at synapses, synapses can rapidly change their strength by adjusting the ratio of vesicle capture and release (Wu et al., 2013). In addition, synapses can be formed or disassembled within a few hours. It was shown that presynaptic proteins can be transported together in small packages in axons (Zhai et al., 2001; Friedman et al., 2000; Wu et al., 2013). Such multi-protein packages can be recruited to locations where new synapses are being formed and a few of these ready-to-go packages are enough to rapidly build a functional active zone and release site (Jin and Garner, 2008; Owald and Sigrist, 2009).

Live imaging of axons have shown that transient and mobile release sites exist (Krueger et al., 2003) and that transient boutons occur at predefined locations along the axon (Sabo et al., 2006; Bury and Sabo, 2011; Ou and Shen, 2010), presumably reflecting contact sites with potential postsynaptic targets (Schuemann et al., 2013; Wierenga et al., 2008). The transient nature of boutons in such locations suggest that presynaptic structures are immature or incomplete and may serve a role in 'testing' a new synaptic location (Schuemann et al., 2013; Wierenga et al., 2008; Dobie and Craig, 2011; Fu et al., 2012). Transient boutons might therefore reflect failed attempts or intermediate stages of building new synapses, but they could also have a physiological function. Transient boutons, or orphan release sites, are likely capable of neurotransmitter release (Krueger et al., 2003; Ratnayaka et al., 2011; Coggan et al., 2005) and besides having a role in synapse formation, ectopic release of neurotransmitter by transient boutons could also serve to signal to nearby astrocytes or to regulate ambient neurotransmitter levels.

Synapse assembly is a complicated process involving interactions of multiple proteins. It does not necessarily need to be a linear process, where one component necessarily recruits the next, but some of the interactions could occur in parallel and the sequence of protein recruitment may vary. Rapid self-assembly of presynaptic components may be an important element during synaptogenesis. This would mean that the formation of a presynaptic terminal merely needs an initial trigger to ascertain a specific axonal location

or postsynaptic partner, but then the new presynaptic terminal 'unfolds' automatically by spontaneous clustering of its components. It is likely that multiple triggers can induce self-assembly. Indeed, it was recently reported that synaptic material is actively prevented from aggregating and assembling new synapses during transport (Wu et al., 2013), supporting the self-assembly hypothesis. Without prevention of aggregation, presynaptic terminals were formed at locations where no postsynaptic targets were present and no postsynaptic specializations were recruited. Furthermore, the ectopic formation of presynaptic terminals on nonneuronal cells can be induced when these cells express 'synaptogenic' cell adhesion molecules (Takahashi et al., 2012; Scheiffele et al., 2000; Graf et al., 2004), indicating that a single transsynaptic trigger is enough to start the presynaptic cascade to assemble functional release sites.

A dynamic control of the strength and number of presynaptic terminals in axons implies that control of transport, capture and release of synaptic material are essential processes regulating the formation, maintenance and strength of presynaptic terminals. In a dynamic axon with competing presynaptic terminals, a general change in synaptic strength is expected to also have an effect on ongoing synapse formation within the same axon and vice versa (Figure 1). For instance, enhancement of synaptic strength by increasing vesicle capture or anchoring at presynaptic terminals would also result in lower amounts of 'free' vesicles in the axonal shaft thereby reducing the chance that new synapses are formed at nascent sites (Yamada et al., 2013). However, a similar increase in synaptic strength could also be achieved by increasing vesicle clustering (Wu et al., 2013), but such a mechanism would actually promote synapse formation (Figure 1). This illustrates that synaptic plasticity and synapse formation should be considered mutually dependent processes when neighboring presynaptic terminals are sharing synaptic proteins and vesicles.

Inhibitory axons

Most of the studies that were mentioned above were performed in excitatory axons and it is not entirely clear to what extent the results are also valid for inhibitory axons. Important observations have been made in live imaging studies of inhibitory axons. Presynaptic terminals in inhibitory axons were shown to be dynamic structures *in vitro* and *in vivo*. Inhibitory boutons can appear, disappear, and reappear over the course of several minutes to hours (Schuemann et al., 2013; Keck et al., 2011; Kuhlman and Huang, 2008; Fu et al., 2012; Marik et al., 2010), and the same has been shown for clusters of pre- or postsynaptic proteins at inhibitory synapses (van Versendaal et al., 2012; Kuriu et al., 2012; Dobie and Craig, 2011; Chen et al., 2012). Bouton dynamics are comparable *in vitro* and *in vivo* and likely reflect physiological processes. Interestingly, these dynamic changes were shown to be affected by network activity and mediated, at least in part, by activation of GABA receptors (Fu et al., 2012; Schuemann et al., 2013; Kuriu et al., 2012). This could represent a mechanism by which the synaptic activity of inhibitory synapses may regulate their own stability using GABA as a feedback signal.

New inhibitory synapses can form rapidly by the appearance of a bouton at locations where the inhibitory axon is in close contact with a dendrite, without the involvement of dendritic protrusions (Wierenga et al., 2008; Dobie and Craig, 2011). This finding indicates an important contrast with the formation of excitatory synapses, in which new synapses are usually formed by the outgrowth of dendritic protrusions. It also emphasizes the important role of crosstalk between neighboring boutons within inhibitory axons for synapse formation.

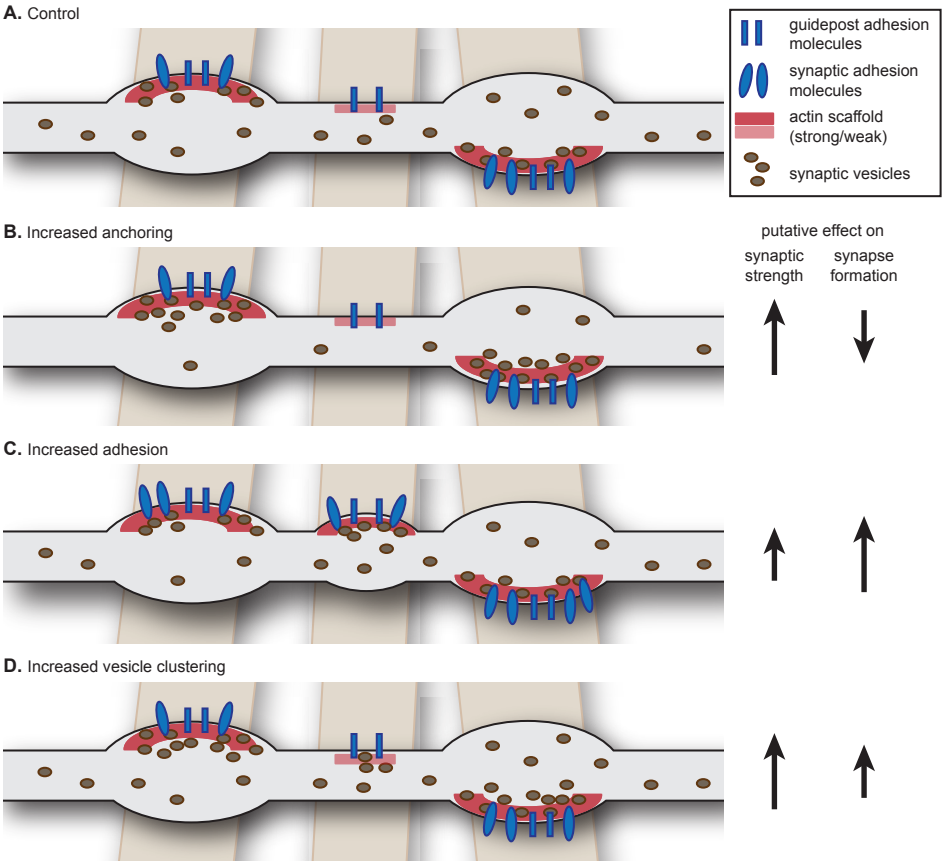

Figure 1. Intrinsic factors: axon-wide increase in synaptic strength or release properties may also affect synapse formation.

A. Schematic drawing of an axon (grey) forming two mature and one nascent bouton on crossing dendrites (brown). We hypothesize that axon-dendrite crossings are marked at potential synaptic locations and contain guidepost adhesion molecules (Shen et al., 2004; Shen and Bargmann, 2003) and weak actin scaffold (Chia et al., 2012). **B.** Increasing anchoring of vesicles at presynaptic terminals could decrease the pool of 'free' vesicles, thereby reducing the probability of forming new synapses (Yamada et al., 2013). **C.** Increasing synaptic adhesion increases the number of synapses (Kuzirian et al., 2013; Takahashi et al., 2012; Scheiffele et al., 2000) and may also affect properties of existing synapses (Varoqueaux et al., 2006; Wittenmayer et al., 2009). **D.** Overexpression of vesicle clustering factors induce changes in release properties, but may also promote synapse formation (Wentzel et al., 2013; Wu et al., 2013).

Nascent inhibitory synapses recruit release machinery proteins and synaptic vesicles on the presynaptic side and receptors and scaffolding molecules on the postsynaptic side within a few hours (Wierenga et al., 2008; Dobie and Craig, 2011; Kuriu et al., 2012; Schuemann et al., 2013). Interestingly, simultaneous translocations of pre- and postsynaptic proteins over several micrometers were observed in cultures and it will be interesting to see if such movement of inhibitory synapses can also occur in slices or *in vivo*. Together, these

observations reveal the dynamic nature of inhibitory axons and strongly suggest that the exchange of presynaptic material between existing and emerging boutons within the axonal shaft plays an essential role in the activity-dependent formation, maintenance and plasticity of inhibitory synapses.

In general, it is not clear if molecular differences exist between excitatory and inhibitory axons, other than the neurotransmitter that is produced and loaded into synaptic vesicles. For instance, the extent or regulation of dynamic exchange between boutons could be different in these two types of axons. The protein composition of the release machinery at excitatory and inhibitory presynaptic terminals is surprisingly similar, although small difference have been reported (Boyken et al., 2013; Bragina et al., 2013; Gitler et al., 2004; Grønborg et al., 2010; Kerr et al., 2008; Kaeser et al., 2009; Zander et al., 2010). It is currently not known if some of these differences have consequences for plasticity or presynaptic dynamics within axons. Furthermore, it is not known if there are differences between axons of the various inhibitory cell types (Ascoli et al., 2008; Klausberger and Somogyi, 2008). However, there is a clear difference between excitatory and inhibitory axons in the expression of specific cell adhesion molecules at excitatory and inhibitory synapses.

Role of cell-adhesion molecules in synaptic plasticity

The observation that inhibitory boutons appear at specific, predefined locations along the axon (Wierenga et al., 2008; Schuemann et al., 2013; Sabo et al., 2006), strongly suggests that something is marking these locations prior to bouton formation (Shen et al., 2004; Shen and Bargmann, 2003). Inhibitory axons are characterized by their tortuous and highly branched morphology and they are in close contacts with many nearby dendrites. In fact, it was shown that inhibitory axons have substantially larger overlap with the dendritic trees of their potential target neurons than expected from chance, whereas this is not the case for excitatory axons (Stepanyants et al., 2004). This suggests that inhibitory axons possibly search for or are attracted by dendrites during development. Contacts between dendrites and inhibitory axons could be maintained by guidepost cell-adhesion molecules, even without inhibitory synapses present (Shen et al., 2004; Shen and Bargmann, 2003). Their presence would mark the location of a postsynaptic dendrite and therefore a potential spot for an inhibitory synapse.

Cell adhesion molecules are transmembrane proteins, which play a role in recognition of synaptic partners during the initial contact and provide specificity of synaptic connections (Wojtowicz et al., 2007; Meijers et al., 2007). In addition, cell adhesion molecules have been shown to play a role in the process of synaptic maturation following the initial contact, in the recruitment of synaptic proteins as well as in maintaining proper synaptic function throughout the lifetime of the synapse (Dalva et al., 2007; Thalhammer and Cingolani, 2013; Krueger et al., 2012). Cell adhesion molecules can also play an active role in the process of synapse disassembly (O'Connor et al., 2009). In conclusion, cell adhesion molecules are an essential part of synapses and synaptic plasticity most likely involves regulation of cell-adhesion molecules. Here we discuss how synaptic adhesion could be regulated in an activity-dependent manner (Figure 2) and we summarize current knowledge of cell adhesion molecules that are specific for inhibitory synapses.

Activity-dependent regulation of protein expression levels

Cell adhesion molecules often serve as recognition or identity signals to specify neuronal

connectivity, in which they can either promote or prevent synapse formation (Dalva et al., 2007; Bukalo and Dityatev, 2012). Neurons presumably express a combination of cell adhesion molecules and the specific combination (both the variety as well as relative levels) likely regulate the specificity and number of their synaptic contacts (Sassoè-Pognetto et al., 2011). Different cell adhesion molecules can cooperate to promote synapse formation, but the opposite is also possible: cis-interactions between different cell adhesion molecules within a neuron can preclude trans-interactions with cell adhesion molecules on neighboring neurons and thereby inhibit or prevent synapse formation (Taniguchi et al., 2007; Lee et al., 2013). Most importantly, the combination of cell adhesion molecules that a neuron expresses might not be static (Figure 2A). Indeed, for a number of cell adhesion molecules, activity-dependent changes in expression level have been observed (Cingolani et al., 2008; Pinkstaff et al., 1998; Pregno et al., 2013). Changes in expression level may be regulated by the activity level of the neuron itself or by extracellular signals from the environment, such as secreted factors from neighboring cells. For instance, TNFα, a glia-derived factor, which is secreted in an activity-dependent manner, regulates expression levels of β3 integrin and N-cadherin (Kubota et al., 2009; Thalhammer and Cingolani, 2013). In theory, local protein synthesis in the axon could also contribute to changes in expression level of cell adhesion proteins (Taylor et al., 2013, 2009; Zivraj et al., 2010), but direct experimental evidence is currently lacking.

Activity-dependent regulation of splicing

For many adhesion molecules different splice forms have been identified. Different splice variants often have different affinities for their binding partners and thereby differentially affect synapse formation or plasticity (Aoto et al., 2013; Missler and Südhof, 1998; Hattori et al., 2008). For instance, alternative splicing of neuroligins and neurexins affects specificity for excitatory or inhibitory synapses (Chih et al., 2006; Graf et al., 2006). Therefore, alternative splicing might be a way to enlarge the available set of adhesion molecules within a neuron and to enhance the range of molecular specificity of synaptic connections.

Activity-dependent regulation of cell surface distribution

To have their effect specifically at synapses, cell adhesion molecules should be enriched at synaptic membranes. There is experimental evidence that the distribution of cell adhesion molecules over the cellular surface can be regulated (Tai et al., 2007; Fu and Huang, 2010). For instance, while neurexin1α shows a diffuse pattern along the axonal membrane in inhibitory axons, neurexin1β is specifically enriched in the membrane at presynaptic terminals. Anchoring of neurexin1β at presynaptic boutons is regulated by presynaptic GABA release and subsequent $GABA_B$ receptor activation (Fu and Huang, 2010). Further investigation is needed to understand how such local changes are regulated by protein modifications or localized endo- or exocytosis and how they affect local synapse formation (Figure 2B).

Activity-dependent regulation of protein cleavage

Synaptic adhesion molecules execute their function by binding to a trans-synaptic partner at their extracellular domain. In some cases, the extracellular domain can be cleaved, with strong effects on local synaptic adhesion. For instance, activity-dependent cleavage of agrin was shown to mediate the formation of dendritic filopodia (Matsumoto-Miyai et al., 2009; Frischknecht et al., 2008) and cleavage of neuroligin-1 was shown to regulate synaptic

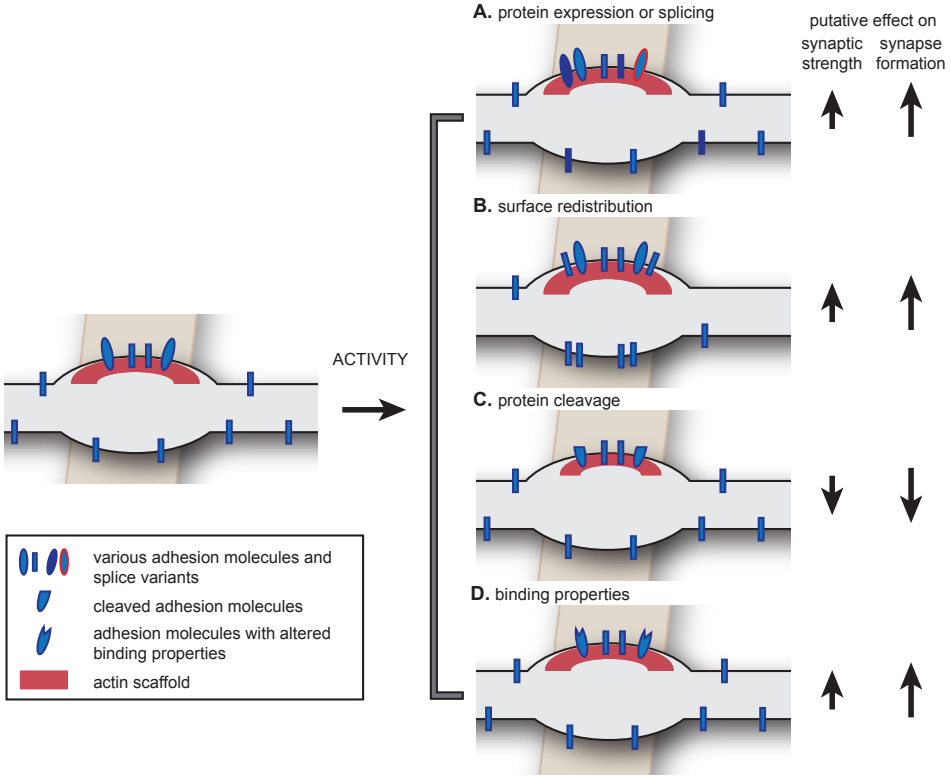

Figure 2. Extrinsic factors: possible activity-dependent changes in cell adhesion molecules.
Neural activity may induce a number of changes in adhesion molecules. **A.** The expression level of cell adhesion molecules (Cingolani et al., 2008), or their splice variants (Chih et al., 2006; Graf et al., 2006), can be regulated in an activity-dependent manner, potentially affecting synapse formation and synapse specificity. **B.** Activity-dependent redistribution of adhesion molecules over the axonal membrane can facilitate synapse formation (Fu and Huang, 2010). **C.** Activity-dependent cleavage of synaptic adhesion molecules could induce synapse disassembly or plasticity (Suzuki et al., 2012; Peixoto et al., 2012; Matsumoto-Miyai et al., 2009; O'Connor et al., 2009). **D.** Activity-dependent changes in binding properties of adhesion molecules (Kim et al., 2011b, 2011a) could affect synaptic properties. In addition, the intracellular signaling pathways (not depicted) may also be regulated in an activity-dependent manner, affecting all of these processes.

strength of individual excitatory synapses in an activity-dependent manner (Peixoto et al., 2012; Suzuki et al., 2012). Many other adhesion molecules have known cleavage sites and it will be interesting to see whether this mechanism for activity-dependent regulation is also present at inhibitory synapses (Figure 2C).

Activity-dependent regulation of binding

For some cell adhesion molecules activity can regulate the binding properties of the proteins. For instance, interactions between cadherins are affected by extracellular calcium concentrations (Kim et al., 2011b) and integrins can switch between an active or inactive configuration by extra- or intracellular factors (Hynes, 2002). In this way, synaptic adhesion

can be modulated in an activity-dependent manner without a change in synaptic composition (Figure 2D).

Activity-dependent regulation of interacting proteins

Upon binding to other cell adhesion molecules, cell adhesion molecules cluster at the cell membrane and signal through interactions with many intracellular proteins, whose levels may be regulated in an activity-dependent manner. Ultimately, signaling through synaptic adhesion molecules in the presynaptic terminal result in direct or indirect alterations of the actin cytoskeleton and vesicle recycling, affecting the number, function and/or stability of synapses (Swiercz et al., 2008; Sun and Bamji, 2011; Tabuchi et al., 2002; Zhang et al., 2001; Takahashi and Craig, 2013). It will be crucial to identify the precise molecular pathways that are involved to fully understand how activity-dependent changes at inhibitory synapses occur.

CELL ADHESION MOLECULES AT INHIBITORY SYNAPSES

The list of known synaptic adhesion molecules is rapidly growing, but our knowledge on the precise function of most of these proteins remains incomplete. Interestingly, several synaptic cell-adhesion molecules have been reported to be specifically involved in inhibitory, and not excitatory, synapses. These include sema4D (Paradis et al., 2007; Kuzirian et al., 2013), slitrk3 (Takahashi et al., 2012) and neuroligin2 (Poulopoulos et al., 2009; Patrizi et al., 2008; Varoqueaux et al., 2004), and it is to be expected that new discoveries will be made in the near future. Here we briefly summarize what is known on the role of various cell adhesion molecules at inhibitory synapses.

Neuroligin-2

Postsynaptic neuroligins and their presynaptic partners neurexins are transmembrane cell adhesion molecules that have been established as important synaptic regulators (Südhof, 2008; Siddiqui and Craig, 2011; Krueger et al., 2012). When expressed in non-neuronal cells, neurexins as well as neuroligins can induce the formation of synapses in co-cultured neurons (Kang et al., 2008; Graf et al., 2004). This suggests that neurexins and neuroligins function in the initial assembly of synaptic connections. However, knock out studies showed that they are not strictly required for synaptogenesis, but they play a crucial role in the proper assembly and functional maturation of synapses (Varoqueaux et al., 2006). Neuroligin-2 localizes specifically to the postsynaptic membrane of inhibitory synapses (Chubykin et al., 2007; Varoqueaux et al., 2004) and has been shown to be a regulator of inhibitory synapse formation and function (Poulopoulos et al., 2009; Chubykin et al., 2007; Varoqueaux et al., 2006). Interestingly, a recent report suggested that the preferential localization of neuroligin-2 at inhibitory synapses can be contributed to the low abundance of β-neurexin1 in inhibitory axons (Futai et al., 2013), suggesting that the presynaptic axon determines specificity of cell adhesion molecules at inhibitory synapses. Mice lacking neuroligin-2 show impairments in inhibitory synaptic transmission and exhibit anxiety-like behavior and increased excitability (Gibson et al., 2009; Jedlicka et al., 2011; Blundell et al., 2009). Interestingly, although neuroligin-2 is present at all inhibitory synapses, only perisomatic synapses were affected in the absence of neuroligin-2 (Gibson et al., 2009). Recently, two adhesion molecules were found to show specific interactions with neuroligin-2 at inhibitory synapses. MDGA1 inhibits the interaction between neuroligin-2 and neurexins and therefore specifically suppresses

the inhibitory synaptogenic activity of neuroligin-2 (Pettem et al., 2013; Lee et al., 2013). IgSF9 specifically localizes at inhibitory synapses on inhibitory neurons, where it binds to neuroligin-2 via the scaffolding protein S-SCAM (Woo et al., 2013). These findings raises the possibility that neuroligin-2 serves different functions at different inhibitory synapses, depending on its interactions with other cell adhesion molecules.

Slitrk3

Leucine-rich repeat (LRR) proteins have received considerable research attention recently. The members of the subfamily of Slitrk (Slit and Trk-like) proteins is involved in synapse formation and has been linked to several neurological disorders (Takahashi and Craig, 2013; Aruga and Mikoshiba, 2003). Slitrk3 has been shown to be present at the postsynaptic side of inhibitory synapses and it can induce the formation of inhibitory synapses through its interaction with the presynaptic tyrosine phosphatase receptor PTPδ (Takahashi et al., 2012; Yim et al., 2013). Here, the specificity for inhibitory synapses is dictated by the postsynaptic slitrk3, as it was shown that presynaptic PTPδ can interfere with other synaptic organizing molecules to promote formation of excitatory synapses (Yoshida et al., 2011, 2012). The slitrk3 knock out mouse has no gross defect in brain morphology, but shows decreased expression of inhibitory markers (Takahashi et al., 2012). Accordingly, these mice have an increased susceptibility for seizures and sometimes display spontaneous seizures. Interestingly, not all inhibitory synapses were equally affected by the loss of slitrk3. In the hippocampal CA1 region, specifically inhibitory synapses in the middle of the pyramidal layer were lost (Takahashi et al., 2012). It will be interesting to examine whether specificity of inhibitory synapses correlates with different subsets of pre- or postsynaptic neurons types or function.

Members of the closely related subfamily of leucine-rich transmembrane proteins (LRRTMs) have also been implicated in excitatory synapse formation and plasticity (Linhoff et al., 2009; Ko et al., 2011; de Wit et al., 2013; Siddiqui et al., 2013), but so far no LRRTM that is specific for inhibitory synapses has been identified.

Semaphorin4D

Semaphorins are well-known as (repulsive) axon guidance molecules acting through rearrangements of the cytoskeleton in the growth cone. They play an important role in the early development of the brain (Pasterkamp, 2012). Some semaphorins are also expressed later in development and have been implicated in the formation and plasticity of neuronal connections (Sahay et al., 2005; Ding et al., 2012; O'Connor et al., 2009; Morita et al., 2006; Paradis et al., 2007; Mizumoto and Shen, 2013)(Pasterkamp, 2012). Knocking down the membrane-bound semaphorin Sema4D was shown to specifically reduce the number of inhibitory synapses, while excitatory synapses were not affected (Paradis et al., 2007). Furthermore, application of soluble Sema4D was able to increase the density of GABAergic synapses within 30 minutes in rat hippocampal neurons (Kuzirian et al., 2013). These new inhibitory synapses became functional within two hours and could restore normal levels of activity in an *in vitro* model for epilepsy (Kuzirian et al., 2013). The effect of sema4D on inhibitory synapses depends on the plexinB1 receptor (Kuzirian et al., 2013). It was earlier shown that activation of plexinB1 by sema4D can induce opposing responses on the cytoskeleton, depending on different interacting proteins (Swiercz et al., 2008; Tasaka et al., 2012; Basile et al., 2004) , but the intracellular pathway used for inhibitory synapse

formation is not known. Sema4D is a membrane-bound protein, but the protein can also be cleaved (Zhu et al., 2007; Basile et al., 2007). It was recently shown that extracellular cleavage of sema4D occurs in neurons, but does not interfere with its synaptogenic properties at inhibitory synapses (Raissi et al., 2013).

Other cell adhesion molecules

There are many other cell adhesion molecule proteins and with continued research on inhibitory synapses, it is expected that more of them will be found to play a role at inhibitory synapses. Here we just mention a few that have been reported at inhibitory synapses.

Neural cell adhesion molecule (NCAM) has been reported to be important for the maturation of perisomatic inhibitory synapses in the cortex (Chattopadhyaya et al., 2013; Brennaman and Maness, 2008; Pillai-Nair et al., 2005). NCAM acts through activation of Fyn kinases and possibly recruits other adhesion molecules (Chattopadhyaya et al., 2013). Interestingly, it was recently reported that also members of the ephrin family, ephrinA5 and EphA3, can affect inhibitory synapses and they require NCAM for their action (Brennaman et al., 2013). *In vivo*, NCAM is polysialyated (NCAM-PSA) in an experience-dependent manner and developmental downregulation of NCAM-PSA was shown to coordinate maturation of perisomatic inhibitory synapses in the visual cortex (Di Cristo et al., 2007).

Several components of the dystrophin-associated glycoprotein complex (DGC), such as dystroglycan, dystrophin and dystrobrevin, are also specifically located at a subset of inhibitory synapses (Lévi et al., 2002; Knuesel et al., 1999; Brünig et al., 2002; Grady et al., 2006), but the function of this complex at inhibitory synapses is not well understood. The DGC could be linked to postsynaptic neuroligin-2 via the scaffolding protein S-SCAM (Sumita et al., 2007) and to presynaptic neurexins (Sugita, 2001). Interestingly, a synaptic guanine exchange factor SynArfGEF has been identified that specifically co-localizes at inhibitory synapses, which could be involved in the downstream signaling pathway of the DGC (Fukaya et al., 2011), but its exact function remains to determined.

Integrins are receptors for extracellular matrix proteins, soluble factors and counter-receptors on adjacent cells and they have an intracellular link to actin filaments via adaptor proteins (Hynes, 2002; Harburger and Calderwood, 2009). Integrins have been implicated in activity-dependent synaptic changes (Chavis and Westbrook, 2001; Chan et al., 2003) and in homeostatic scaling of excitatory synapses (Cingolani et al., 2008). At glycinergic inhibitory synapses in the spinal cord, postsynaptic β1 and β3 integrins have been reported to regulate glycine receptor stabilization at the postsynaptic membrane, with the two integrins acting in opposing directions (Charrier et al., 2010).

Finally, the cell adhesion molecule neurofascin has been shown to regulate the formation of a specific subset of inhibitory synapses on the axon initial segment of principal neurons (Ango et al., 2004; Kriebel et al., 2011; Burkarth et al., 2007).

ROLE OF SECRETED FACTORS AND RETROGRADE MESSENGERS AT INHIBITORY SYNAPSES

Above we have described how cell adhesion molecules may provide signals to inhibitory axons from direct cell-cell contacts. However, inhibitory synapses may also be affected by signals from more distal origin. Nearby dendrites or surrounding cells can secrete trophic (or anti-trophic) factors, which may affect inhibitory synapse function and/or formation.

Indeed, retrograde signals from the postsynaptic dendrite, such as endocannabinoids, NO or BDNF, or glutamate spillover from nearby excitatory synapses are known to regulate synaptic release at inhibitory synapses during many forms of short-term and long-term plasticity (Castillo et al., 2011; Heifets and Castillo, 2009; Regehr et al., 2009). Here we discuss secreted factors that have been linked to the formation of inhibitory synapses and that might play a role in activity-dependent regulation of the number of presynaptic terminals made by inhibitory axons.

Brain-derived neurotrophic factor (BDNF)

BDNF is a secreted neurotrophin that has been shown in many different preparations to promote the formation and maturation of inhibitory synapses by presynaptic modifications (Gottmann et al., 2009; Huang et al., 1999; Yamada et al., 2002; Marty et al., 2000; Vicario-Abejón et al., 1998). Only excitatory neurons produce BDNF (Gottmann et al., 2009; Park and Poo, 2013) and BDNF is released from principal neurons in an activity-dependent manner (Matsuda et al., 2009; Kuczewski et al., 2008; Kolarow et al., 2007), which makes BDNF an attractive candidate molecule to regulate activity-dependent inhibitory synapse formation (Liu et al., 2007). Interestingly, the availability of postsynaptic BDNF signaling in individual neurons was shown to affect the number and strength of inhibitory synapses specifically onto the affected neurons (Ohba et al., 2005; Kohara et al., 2007; Peng et al., 2010). These cell-autonomous effects indicate the potential for BDNF in mediating changes in inhibitory synapses with high synaptic specificity. In excitatory axons, BDNF was shown to reduce the anchoring of synaptic vesicles at presynaptic terminals and thereby increase the exchange of vesicles between boutons (Bamji et al., 2006). It is currently not known if BDNF has a similar effect in inhibitory axons.

Neuregulin1

Neuregulin1 is a neurotrophic factor, which exist in various membrane-bound and diffusible isoforms. Mutations (both loss-of-functions and gain-of-function) in neuregulin1 have been linked to schizophrenia (Mei and Xiong, 2008). The main receptor for neuregulin1, ErbB4, is specifically expressed in interneurons (Fazzari et al., 2010; Vullhorst et al., 2009) and is located at postsynaptic densities of excitatory synapses in interneuron dendrites as well as at inhibitory axon terminals. An important role for neuregulin1 is the regulation of excitatory input onto interneurons through postsynaptic ErbB4 (Ting et al., 2011; Fazzari et al., 2010; Wen et al., 2010). Presynaptic ErbB4 can enhance GABA release from inhibitory synapses (Fazzari et al., 2010; Woo et al., 2007) and may affect the number of synapses made by inhibitory axons (del Pino et al., 2013). In addition to ErbB4, neuregulin1 isoforms can also activate other receptors resulting in downregulation of postsynaptic $GABA_A$ receptors (Yin et al., 2013). This suggests that neuregulin1 has multiple actions on inhibitory synapses depending on the isoform and activated receptors.

FGF7

Fibroblast growth factors (FGFs) are secreted signaling glycoproteins, which exert their effect by binding to FGF receptor tyrosine kinases (FGFR). In the brain, FGF signaling is important for several developmental processes, including patterning of different brain structures(Reuss and von Bohlen und Halbach, 2003) and neurogenesis(Turner et al., 2006) (Dono, 2003; Reuss and von Bohlen und Halbach, 2003)(Butt and Berry, 2000). In addition, they have

been implicated as target-derived presynaptic organizers (Umemori et al., 2004). FGF7 is of particular interest, as it localizes specifically to inhibitory synapses in the hippocampal CA3 region, where it is secreted from the postsynaptic membrane and organizes presynaptic release properties (Terauchi et al., 2010). Remarkably, FGF receptors have been shown to directly interact with adenosine A2A receptors (Flajolet et al., 2008), which are important for GABA release (Cunha and Ribeiro, 2000) as well as for GABA uptake from the synaptic cleft (Cristóvão-Ferreira et al., 2009). In this way, FGFR and A2A receptors may act together to regulate GABAergic transmission in the hippocampus.

Factors from glia cells

Studies with neuronal and astrocyte co-cultures and astrocyte-conditioned medium have shown that astrocyte-released factors are crucial for synapse formation and plasticity (Elmariah et al., 2005; Hughes et al., 2010; Crawford et al., 2012; Christopherson et al., 2005a). For instance, thrombospondins, oligomeric proteins of the extracellular matrix produced by astrocytes (Christopherson et al., 2005b; Eroglu et al., 2009) are involved in the formation of glutamatergic synapses and the pro-inflammatory cytokine TNFα, coming from glia, (Stellwagen and Malenka, 2006) plays a role in homeostatic plasticity of these synapses(Crawford et al., 2012). In addition, a different and so far unidentified, protein is secreted by astrocytes, which has been found to increase the density of inhibitory synapses in cultured neurons (Hughes et al., 2010; Elmariah et al., 2005).

GABA

A special secreted factor is the inhibitory neurotransmitter GABA itself. It is well-established that synapse formation does not depend on neurotransmitter release (Harms and Craig, 2005; Verhage, 2000; Schubert et al., 2013). However, the development and maturation of inhibitory synapses are influenced by their neurotransmitter GABA (Lau and Murthy, 2012; Huang, 2009; Li et al., 2005; Huang and Scheiffele, 2008). It was shown that individual axons of parvalbumin-positive basket cells are sensitive to their own GABA release (Chattopadhyaya et al., 2007; Wu et al., 2012) and that the amount of GABA release per vesicle can be regulated by activity (Lau and Murthy, 2012; Hartman et al., 2006). Inhibitory boutons are less dynamic in axons in which GABA release is impaired (Wu et al., 2012) or when GABA receptors are blocked (Schuemann et al., 2013), strongly suggesting that GABA is used as an important activity sensor for regulating activity-dependent presynaptic changes at inhibitory synapses. Both $GABA_A$ and $GABA_B$ receptors have been implicated in mediating this regulation (Schuemann et al., 2013; Fu et al., 2012), but the precise molecular mechanisms remain unknown.

OTHER FACTORS

In addition to cell adhesion molecules and secreted factors, there are many other factors that may affect activity-dependent plasticity of inhibitory axons. For instance, it is well-established that extracellular matrix molecules can play a role in the development and maturation of synapses in the central nervous system and specific interactions between cell adhesion molecules and the extracellular matrix have been revealed (Di Cristo et al., 2007; de Wit et al., 2013; Siddiqui et al., 2013). There are a few studies in which the absence or overexpression of extracellular matrix proteins affected inhibitory synapses specifically

(Brenneke et al., 2004; Pavlov et al., 2006; Nikonenko et al., 2003; Saghatelyan et al., 2001; Su et al., 2010), but the underlying mechanisms remain largely unknown.

And finally, while it is clear that presynaptic components are continuously shared and exchanged between inhibitory boutons along the axons, it is not clear how exactly these proteins are dispersed along the axonal shaft. Presumably sharing occurs through passive diffusion of presynaptic proteins through the axonal shaft, but intracellular transport of synaptic cargo could also play a role. Axons contain extensive microtubule and actin networks and there are various motor proteins that deliver and ship transport vesicles, potentially affecting the amount of proteins available for exchange and synapse formation at boutons. For instance, it was shown that intra-axonal movement of mitochondria is enhanced when activity is blocked (Obashi and Okabe, 2013; Cai and Sheng, 2009; Goldstein et al., 2008), but it is not clear if this is due to enhanced motor protein activity or decreased anchoring at synapses. Further research on the possible activity-dependent regulation of intracellular transport of synaptic cargo (Maas et al., 2009; MacAskill et al., 2009; Guillaud et al., 2008) will be needed to address this issue in the future.

IN CONCLUSION

Research on activity-dependent adaptations in inhibitory axons continues to generate novel insight in the cellular processes of synapse formation and plasticity. Many open questions remain to be answered in the future and we listed a few of these in a small scheme (Figure 3). In this review we have painted a picture of the inhibitory axon as a dynamic structure that can quickly adjust to a changing environment, by responding to local signals from postsynaptic cells via adhesion molecules and to global signals from the local neuronal network. A highly dynamic inhibitory system might serve to quickly respond to changes to allow circuit rearrangements by excitatory connections. For a healthy brain changes at inhibitory and excitatory synapses need to be well-coordinated at all times as subtle defects in this coordination can cause defects in circuitry and may underlie psychiatric disorders.

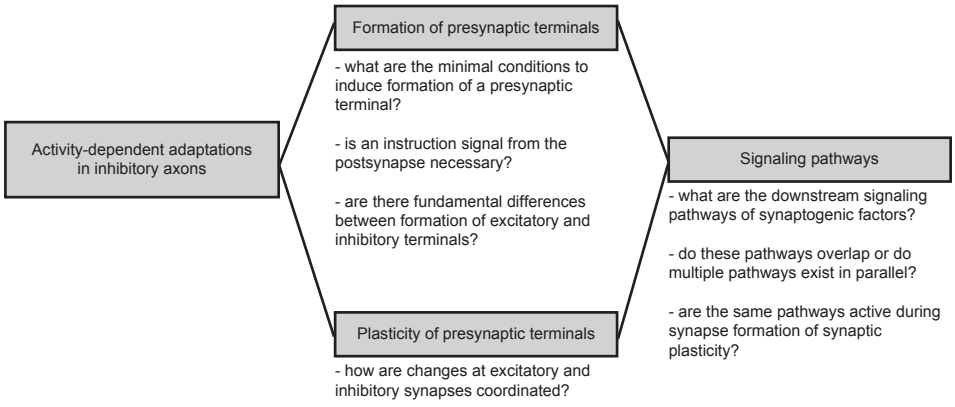

Figure 3. Outstanding research questions.
Schematic overview of open research questions on activity-dependent adaptations in inhibitory axons.

This means that the interplay between plasticity of excitatory and inhibitory synapses is an important factor for the stability of neuronal circuits. The precise response of the inhibitory axon will be determined by the combination of internal and external factors, such as the availability of synaptic proteins within the axon, or the combination of the extracellular factors and cell adhesion molecules that are present at the membrane. It will be an important challenge for future research to unravel the precise molecular and cellular mechanisms and to further uncover pathways that affect synapse formation and plasticity of inhibitory synapses.

ACKNOWLEDGMENTS

The authors like to thank Anne Schuemann, Tara Keck and Casper Hoogenraad for critical reading of the manuscript and helpful comments. Our research was supported by the People Programme (Marie Curie Actions) of the European Union's Seventh Framework Programme FP7/2007-2013/ under REA grant agreement n° 289581 (CPF), and a Marie Curie Reintegration Grant 256284 and Dutch NWO-VIDI grant (CJW).

REFERENCES

Ango, F., di Cristo, G., Higashiyama, H., Bennett, V., Wu, P., and Huang, Z. J. (2004). Ankyrin-based subcellular gradient of neurofascin, an immunoglobulin family protein, directs GABAergic innervation at purkinje axon initial segment. Cell 119, 257–72.

Aoto, J., Martinelli, D. C., Malenka, R. C., Tabuchi, K., and Südhof, T. C. (2013). Presynaptic Neurexin-3 Alternative Splicing trans-Synaptically Controls Postsynaptic AMPA Receptor Trafficking. Cell 154, 75–88.

Aruga, J., and Mikoshiba, K. (2003). Identification and characterization of Slitrk, a novel neuronal transmembrane protein family controlling neurite outgrowth. Mol. Cell. Neurosci. 24, 117–129.

Ascoli, G. A., Alonso-Nanclares, L., Anderson, S. A., Barrionuevo, G., Benavides-Piccione, R., Burkhalter, A., Buzsáki, G., Cauli, B., Defelipe, J., Fairén, A., et al. (2008). Petilla terminology: nomenclature of features of GABAergic interneurons of the cerebral cortex. Nat. Rev. Neurosci. 9, 557–568.

Bamji, S. X., Rico, B., Kimes, N., and Reichardt, L. F. (2006). BDNF mobilizes synaptic vesicles and enhances synapse formation by disrupting cadherin-beta-catenin interactions. J. Cell Biol. 174, 289–299.

Bamji, S. X., Shimazu, K., Kimes, N., Huelsken, J., Birchmeier, W., Lu, B., Reichardt, L. F., and Francisco, S. (2003). Role of Beta-Catenin in Synaptic Vesicle Localization and Presynaptic Assembly. Neuron 40, 719–731.

Bartley, A. F., Huang, Z. J., Huber, K. M., and Gibson, J. R. (2008). Differential Activity-Dependent, Homeostatic Plasticity of Two Neocortical Inhibitory Circuits. J. Neurophysiol. 100, 1983–1994.

Basile, J. R., Barac, A., Zhu, T., Guan, K.-L., and Gutkind, J. S. (2004). Class IV semaphorins promote angiogenesis by stimulating Rho-initiated pathways through plexin-B. Cancer Res. 64, 5212–24.

Basile, J. R., Holmbeck, K., Bugge, T. H., and Gutkind, J. S. (2007). MT1-MMP controls tumor-induced angiogenesis through the release of semaphorin 4D. J. Biol. Chem. 282, 6899–905.

Bateup, H. S., Johnson, C. a, Denefrio, C. L., Saulnier, J. L., Kornacker, K., and Sabatini, B. L. (2013). Excitatory/Inhibitory synaptic imbalance leads to hippocampal hyperexcitability in mouse models of tuberous sclerosis. Neuron 78, 510–22.

Blundell, J., Tabuchi, K., Bolliger, M. F., Blaiss, C. A., Brose, N., Liu, X., Südhof, T. C., and Powell, C. M. (2009). Increased anxiety-like behavior in mice lacking the inhibitory synapse cell adhesion molecule neuroligin 2. Genes. Brain. Behav. 8, 114–126.

Boyken, J., Grønborg, M., Riedel, D., Urlaub, H., Jahn, R., and Chua, J. J. E. (2013). Molecular Profiling of Synaptic Vesicle Docking Sites Reveals Novel Proteins but Few Differences between Glutamatergic and GABAergic Synapses. Neuron 78, 285–297.

Bragina, L., Fattorini, G., Giovedì, S., Bosco, F., Benfenati, F., and Conti, F. (2013). Heterogeneity of presynaptic proteins: do not forget isoforms. Front. Cell. Neurosci. 7, 8.

Branco, T., Staras, K., Darcy, K. J., and Goda, Y. (2008). Local dendritic activity sets release probability at hippocampal synapses. Neuron 59, 475–485.

Brennaman, L. H., and Maness, P. F. (2008). Developmental regulation of GABAergic interneuron branching and synaptic development in the prefrontal cortex by soluble neural cell adhesion molecule. Mol. Cell. Neurosci. 37, 781–793.

Brennaman, L. H., Zhang, X., Guan, H., Triplett, J. W., Brown, A., Demyanenko, G. P., Manis, P. B., Landmesser, L., and Maness, P. F. (2013). Polysialylated NCAM and ephrinA/EphA regulate synaptic development of GABAergic interneurons in prefrontal cortex. Cereb. Cortex 23, 162–177.

Brenneke, F., Bukalo, O., Dityatev, A., and Lie, A. A. (2004). Mice deficient for the extracellular matrix glycoprotein tenascin-r show physiological and structural hallmarks of increased hippocampal excitability, but no increased susceptibility to seizures in the pilocarpine model of epilepsy. Neuroscience 124, 841–55.

Brünig, I., Suter, A., Knuesel, I., Lüscher, B., and Fritschy, J.-M. (2002). GABAergic terminals are required for postsynaptic clustering of dystrophin but not of GABA(A) receptors and gephyrin. J. Neurosci. 22, 4805–4813.

Buckby, L. E., Jensen, T. P., Smith, P. J. E., and Empson, R. M. (2006). Network stability through homeostatic scaling of excitatory and inhibitory synapses following inactivity in CA3 of rat organotypic hippocampal

slice cultures. Mol. Cell. Neurosci. 31, 805–816..

Bukalo, O., and Dityatev, A. (2012). Synaptic cell adhesion molecules. Adv. Exp. Med. Biol. 970, 97–128.

Burkarth, N., Kriebel, M., Kranz, E. U., and Volkmer, H. (2007). Neurofascin regulates the formation of gephyrin clusters and their subsequent translocation to the axon hillock of hippocampal neurons. Mol. Cell. Neurosci. 36, 59–70

Burrone, J., and Murthy, V. N. (2003). Synaptic gain control and homeostasis. Curr. Opin. Neurobiol. 13, 560–7.

Bury, L. A., and Sabo, S. L. (2011). Coordinated trafficking of synaptic vesicle and active zone proteins prior to synapse formation. Neural Dev. 6, 24.

Cai, Q., and Sheng, Z.-H. (2009). Mitochondrial transport and docking in axons. Exp. Neurol. 218, 257–267.

Castillo, P. E., Chiu, C. Q., and Carroll, R. C. (2011). Long-term plasticity at inhibitory synapses. Curr. Opin. Neurobiol. 21, 1–11.

Chan, C.-S., Weeber, E. J., Kurup, S., Sweatt, J. D., and Davis, R. L. (2003). Integrin requirement for hippocampal synaptic plasticity and spatial memory. J. Neurosci. 23, 7107–7116.

Charrier, C., Machado, P., Tweedie-Cullen, R. Y., Rutishauser, D., Mansuy, I. M., and Triller, A. (2010). A crosstalk between β1 and β3 integrins controls glycine receptor and gephyrin trafficking at synapses. Nat. Neurosci. 13, 1388–1395.

Chattopadhyaya, B., Baho, E., Huang, Z. J., Schachner, M., and Di Cristo, G. (2013). Neural cell adhesion molecule-mediated Fyn activation promotes GABAergic synapse maturation in postnatal mouse cortex. J. Neurosci. 33, 5957–5968.

Chattopadhyaya, B., Cristo, G. Di, Higashiyama, H., Knott, G. W., Kuhlman, S. J., Welker, E., Huang, Z. J., and Di Cristo, G. (2004). Experience and activity-dependent maturation of perisomatic GABAergic innervation in primary visual cortex during a postnatal critical period. J. Neurosci. 24, 9598–9611.

Chattopadhyaya, B., Di Cristo, G., Wu, C. Z., Knott, G., Kuhlman, S., Fu, Y., Palmiter, R. D., Huang, Z. J., Cristo, G. Di, Cristo, D., et al. (2007). GAD67-mediated GABA synthesis and signaling regulate inhibitory synaptic innervation in the visual cortex. Neuron 54, 889–903.

Chavis, P., and Westbrook, G. (2001). Integrins mediate functional pre- and postsynaptic maturation at a hippocampal synapse. Nature 411, 317–21.

Chen, J. L., Lin, W. C., Cha, J. W., So, P. T., Kubota, Y., and Nedivi, E. (2011). Structural basis for the role of inhibition in facilitating adult brain plasticity. Nat. Neurosci. 14, 587–594.

Chen, J. L., Villa, K. L., Cha, J. W., So, P. T. C., Kubota, Y., and Nedivi, E. (2012). Clustered Dynamics of Inhibitory Synapses and Dendritic Spines in the Adult Neocortex. Neuron 74, 361–373.

Chia, P. H., Patel, M. R., and Shen, K. (2012). NAB-1 instructs synapse assembly by linking adhesion molecules and F-actin to active zone proteins. Nat. Neurosci. 15, 234–242.

Chih, B., Gollan, L., and Scheiffele, P. (2006). Alternative Splicing Controls Selective Trans-Synaptic Interactions of the Neuroligin-Neurexin Complex. Neuron 51, 171–178.

Christopherson, K. S., Stokes, C. C. A., Barres, B. A., Ullian, E. M., Mullowney, C. E., Hell, J. W., Agah, A., Lawler, J., Mosher, D. F., and Bornstein, P. (2005a). Thrombospondins are astrocyte-secreted proteins that promote CNS synaptogenesis. Cell 120, 421–433.

Christopherson, K. S., Ullian, E. M., Stokes, C. C. A., Mullowney, C. E., Hell, J. W., Agah, A., Lawler, J., Mosher, D. F., Bornstein, P., and Barres, B. A. (2005b). Thrombospondins Are Astrocyte-Secreted Proteins that Promote CNS Synaptogenesis. Cell 120, 421–433.

Chubykin, A. A., Atasoy, D., Etherton, M. R., Brose, N., Kavalali, E. T., Gibson, J. R., and Su, T. C. (2007). Activity-Dependent Validation of Excitatory versus Inhibitory Synapses by Neuroligin-1 versus Neuroligin-2. Neuron 54, 919–931.

Cingolani, L. A., and Goda, Y. (2008). Actin in action: the interplay between the actin cytoskeleton and synaptic efficacy. Nat. Rev. Neurosci. 9, 344–356.

Cingolani, L. A., Thalhammer, A., Yu, L. M. Y., Catalano, M., Ramos, T., Colicos, M. A., and Goda, Y. (2008). Activity-dependent regulation of synaptic AMPA receptor composition and abundance by beta3 integrins. Neuron 58, 749–762.

Coggan, J. S., Bartol, T. M., Esquenazi, E., Stiles, J. R., Lamont, S., Martone, M. E., Berg, D. K., Ellisman, M. H., and Sejnowski, T. J. (2005). Evidence for ectopic

neurotransmission at a neuronal synapse. Science (80-.). 309, 446–451.

Crawford, D. C., Jiang, X., Taylor, A., and Mennerick, S. (2012). Astrocyte-Derived Thrombospondins Mediate the Development of Hippocampal Presynaptic Plasticity In Vitro. J. Neurosci. 32, 13100–13110.

Di Cristo, G., Chattopadhyaya, B., Kuhlman, S. J., Fu, Y., Bélanger, M.-C., Wu, C. Z., Rutishauser, U., Maffei, L., and Huang, Z. J. (2007). Activity-dependent PSA expression regulates inhibitory maturation and onset of critical period plasticity. Nat. Neurosci. 10, 1569–1577.

Cristóvão-Ferreira, S., Vaz, S. H., Ribeiro, J. a, and Sebastião, A. M. (2009). Adenosine A2A receptors enhance GABA transport into nerve terminals by restraining PKC inhibition of GAT-1. J. Neurochem. 109, 336–47.

Cunha, R. a, and Ribeiro, J. a (2000). Purinergic modulation of [(3)H]GABA release from rat hippocampal nerve terminals. Neuropharmacology 39, 1156–67.

Dalva, M. B., McClelland, A. C., and Kayser, M. S. (2007). Cell adhesion molecules: signalling functions at the synapse. Nat. Rev. Neurosci. 8, 206–20.

Darcy, K. J., Staras, K., Collinson, L. M., and Goda, Y. (2006). Constitutive sharing of recycling synaptic vesicles between presynaptic boutons. Nat. Neurosci. 9, 315–321.

del Pino, I., García-Frigola, C., Dehorter, N., Brotons-Mas, J. R., Alvarez-Salvado, E., Martínez de Lagrán, M., Ciceri, G., Gabaldón, M. V., Moratal, D., Dierssen, M., et al. (2013). Erbb4 Deletion from Fast-Spiking Interneurons Causes Schizophrenia-like Phenotypes. Neuron 79, 1152–1168.

Ding, J. B., Oh, W.-J., Sabatini, B. L., and Gu, C. (2012). Semaphorin 3E-Plexin-D1 signaling controls pathway-specific synapse formation in the striatum. Nat. Neurosci. 15, 215–23.

Dobie, F. A., and Craig, A. M. (2011). Inhibitory Synapse Dynamics: Coordinated Presynaptic and Postsynaptic Mobility and the Major Contribution of Recycled Vesicles to New Synapse Formation. J. Neurosci. 31, 10481–10493.

Dono, R. (2003). Fibroblast growth factors as regulators of central nervous system development and function. Am. J. Physiol. Regul. Integr. Comp. Physiol. 284, R867–881.

Echegoyen, J., Neu, A., Graber, K. D., and Soltesz, I. (2007). Homeostatic plasticity studied using in vivo hippocampal activity-blockade: synaptic scaling, intrinsic plasticity and age-dependence. PLoS One 2, e700.

Elmariah, S. B., Oh, E. J., Hughes, E. G., and Balice-Gordon, R. J. (2005). Astrocytes regulate inhibitory synapse formation via Trk-mediated modulation of postsynaptic GABAA receptors. J. Neurosci. 25, 3638–36350.

Eroglu, C., O'Rourke, N. A., Barres, B. A., Allen, N. J., Susman, M. W., Park, C. Y., Ozkan, E., Chakraborty, C., Mulinyawe, S. B., Annis, D. S., et al. (2009). Gabapentin receptor alpha2delta-1 is a neuronal thrombospondin receptor responsible for excitatory CNS synaptogenesis. Cell 139, 380–392.

Fazzari, P., Paternain, A. V, Valiente, M., Pla, R., Luján, R., Lloyd, K., Lerma, J., Marín, O., and Rico, B. (2010). Control of cortical GABA circuitry development by Nrg1 and ErbB4 signalling. Nature 464, 1376–1380.

Fernández-Busnadiego, R., Zuber, B., Maurer, U. E., Cyrklaff, M., Baumeister, W., and Lucic, V. (2010). Quantitative analysis of the native presynaptic cytomatrix by cryoelectron tomography. J. Cell Biol. 188, 145–156.

Fisher-Lavie, A., Zeidan, A., Stern, M., Garner, C. C., and Ziv, N. E. (2011). Use dependence of presynaptic tenacity. J. Neurosci. 31, 16770–16780.

Fisher-Lavie, A., and Ziv, N. E. (2013). Matching Dynamics of Presynaptic and Postsynaptic Scaffolds. J. Neurosci. 33, 13094–13100.

Flajolet, M., Wang, Z., Futter, M., Shen, W., Nuangchamnong, N., Bendor, J., Wallach, I., Nairn, A. C., Surmeier, D. J., and Greengard, P. (2008). FGF acts as a co-transmitter through adenosine A(2A) receptor to regulate synaptic plasticity. Nat. Neurosci. 11, 1402–9.

Friedman, H. V, Bresler, T., Garner, C. C., and Ziv, N. E. (2000). Assembly of new individual excitatory synapses: time course and temporal order of synaptic molecule recruitment. Neuron 27, 57–69.

Frischknecht, R., Fejtova, A., Viesti, M., Stephan, A., and Sonderegger, P. (2008). Activity-Induced Synaptic Capture and Exocytosis of the Neuronal Serine Protease Neurotrypsin. Cultures 28, 1568 –1579.

Fu, Y., and Huang, Z. J. (2010). Differential dynamics and

activity-dependent regulation of α- and β-neurexins at developing GABAergic synapses. Proc. Natl. Acad. Sci. U. S. A. 107, 22699–22704.

Fu, Y., Wu, X., Lu, J., and Huang, Z. J. (2012). Presynaptic GABAB Receptor Regulates Activity-Dependent Maturation and Patterning of Inhibitory Synapses through Dynamic Allocation of Synaptic Vesicles. Front. Cell. Neurosci. 6, 1–20.

Fukaya, M., Kamata, A., Hara, Y., Tamaki, H., Katsumata, O., Ito, N., Takeda, S., Hata, Y., Suzuki, T., Watanabe, M., et al. (2011). SynArfGEF is a guanine nucleotide exchange factor for Arf6 and localizes preferentially at post-synaptic specializations of inhibitory synapses. J. Neurochem. 116, 1122–37.

Futai, K., Doty, C. D., Baek, B., Ryu, J., and Sheng, M. (2013). Specific trans-synaptic interaction with inhibitory interneuronal neurexin underlies differential ability of neuroligins to induce functional inhibitory synapses. J. Neurosci. 33, 3612–3623.

Gambino, F., and Holtmaat, A. (2012). Spike-timing-dependent potentiation of sensory surround in the somatosensory cortex is facilitated by deprivation-mediated disinhibition. Neuron 75, 490–502.

Gibson, J. R., Huber, K. M., and Südhof, T. C. (2009). Neuroligin-2 deletion selectively decreases inhibitory synaptic transmission originating from fast-spiking but not from somatostatin-positive interneurons. Cell 29, 13883–13897.

Gitler, D., Takagishi, Y., Feng, J., Ren, Y., Rodriguiz, R. M., Wetsel, W. C., Greengard, P., and Augustine, G. J. (2004). Different presynaptic roles of synapsins at excitatory and inhibitory synapses. J. Neurosci. 24, 11368–11380.

De Gois, S., Schäfer, M. K.-H., Defamie, N., Chen, C., Ricci, A., Weihe, E., Varoqui, H., and Erickson, J. D. (2005). Homeostatic scaling of vesicular glutamate and GABA transporter expression in rat neocortical circuits. J. Neurosci. 25, 7121–7133.

Goldstein, A. Y. N., Wang, X., and Schwarz, T. L. (2008). Axonal transport and the delivery of pre-synaptic components. Curr. Opin. Neurobiol. 18, 495–503.

Gottmann, K., Lessmann, V., and Mittmann, T. (2009). BDNF signaling in the formation, maturation and plasticity of glutamatergic and GABAergic synapses. Exp. Brain Res. 199, 203–234.

Grady, R. M., Wozniak, D. F., Ohlemiller, K. K., and Sanes, J. R. (2006). Cerebellar synaptic defects and abnormal motor behavior in mice lacking alpha- and beta-dystrobrevin. J. Neurosci. 26, 2841–2851.

Graf, E. R., Kang, Y., Hauner, A. M., and Craig, A. M. (2006). Structure function and splice site analysis of the synaptogenic activity of the neurexin-1 beta LNS domain. J. Neurosci. 26, 4256–4265.

Graf, E. R., Zhang, X., Jin, S. X., Linhoff, M. W., and Craig, A. M. (2004). Neurexins induce differentiation of GABA and glutamate postsynaptic specializations via neuroligins. Cell 119, 1013–1026.

Grønborg, M., Pavlos, N. J., Brunk, I., Chua, J. J. E., Münster-Wandowski, A., Riedel, D., Ahnert-Hilger, G., Urlaub, H., and Jahn, R. (2010). Quantitative comparison of glutamatergic and GABAergic synaptic vesicles unveils selectivity for few proteins including MAL2, a novel synaptic vesicle protein. J. Neurosci. 30, 2–12.

Guillaud, L., Wong, R., and Hirokawa, N. (2008). Disruption of KIF17-Mint1 interaction by CaMKII-dependent phosphorylation: a molecular model of kinesin-cargo release. Nat. Cell Biol. 10, 19–29.

Han, S., Tai, C., Westenbroek, R. E., Yu, F. H., Cheah, C. S., Potter, G. B., Rubenstein, J. L., Scheuer, T., de la Iglesia, H. O., and Catterall, W. a. (2012). Autistic-like behaviour in Scn1a±mice and rescue by enhanced GABA-mediated neurotransmission. Nature 489, 385–390.

Harburger, D. S., and Calderwood, D. A. (2009). Integrin signalling at a glance. J. Cell Sci. 122, 159–63.

Harms, K. J., and Craig, A. M. (2005). Synapse composition and organization following chronic activity blockade in cultured hippocampal neurons. J. Comp. Neurol. 490, 72–84.

Hartman, K. N., Pal, S. K., Burrone, J., and Murthy, V. N. (2006). Activity-dependent regulation of inhibitory synaptic transmission in hippocampal neurons. Nat. Neurosci. 9, 642–649.

Hattori, D., Millard, S. S., Wojtowicz, W. M., and Zipursky, S. L. (2008). Dscam-mediated cell recognition regulates neural circuit formation. Annu. Rev. Cell Dev. Biol. 24, 597–620.

Heifets, B. D., and Castillo, P. E. (2009). Endocannabinoid signaling and long-term synaptic plasticity. Annu. Rev. Physiol. 71, 283–306.

Hensch, T. K. (2005). Critical period plasticity in local cortical circuits. Nat. Rev. Neurosci. 6, 877–888.

Huang, Z. J. (2009). Activity-dependent development of inhibitory synapses and innervation pattern: role of GABA signalling and beyond. J. Physiol. 587, 1881–1888.

Huang, Z. J., Kirkwood, A., Pizzorusso, T., Porciatti, V., Morales, B., Bear, M. F., Maffei, L., and Tonegawa, S. (1999). BDNF regulates the maturation of inhibition and the critical period of plasticity in mouse visual cortex. Cell 98, 739–755.

Huang, Z. J., and Scheiffele, P. (2008). GABA and neuroligin signaling: linking synaptic activity and adhesion in inhibitory synapse development. Curr. Opin. Neurobiol. 18, 77–83.

Hughes, E. G., Elmariah, S. B., and Balice-Gordon, R. J. (2010). Astrocyte secreted proteins selectively increase hippocampal GABAergic axon length, branching, and synaptogenesis. Mol. Cell. Neurosci. 43, 136–45.

Hynes, R. O. (2002). Integrins : Bidirectional , Allosteric Signaling Machines. Cell 110, 673–687.

Jedlicka, P., Hoon, M., Papadopoulos, T., Vlachos, A., Winkels, R., Poulopoulos, A., Betz, H., Deller, T., Brose, N., Varoqueaux, F., et al. (2011). Increased dentate gyrus excitability in neuroligin-2-deficient mice in vivo. Cereb. Cortex 21, 357–67.

Jiang, X., Wang, G., Lee, A. J., Stornetta, R. L., and Zhu, J. J. (2013). The organization of two new cortical interneuronal circuits. Nat. Neurosci. 16, 210–220.

Jin, Y., and Garner, C. C. (2008). Molecular mechanisms of presynaptic differentiation. Annu. Rev. Cell Dev. Biol. 24, 237–262.

Kaeser, P. S., Deng, L., Chávez, A. E., Liu, X., Castillo, P. E., and Südhof, T. C. (2009). ELKS2alpha/CAST deletion selectively increases neurotransmitter release at inhibitory synapses. Neuron 64, 227–239.

Kang, Y., Zhang, X., Dobie, F., Wu, H., and Craig, A. M. (2008). Induction of GABAergic postsynaptic differentiation by alpha-neurexins. J. Biol. Chem. 283, 2323–2334.

Karmarkar, U. R., and Buonomano, D.V (2006). Different forms of homeostatic plasticity are engaged with distinct temporal profiles. Eur. J. Neurosci. 23, 1575–1584.

Keck, T., Scheuss, V., Jacobsen, R. I. I., Wierenga, C. J. J., Eysel, U. T. T., Bonhoeffer, T., and Hübener, M. (2011). Loss of Sensory Input Causes Rapid Structural Changes of Inhibitory Neurons in Adult Mouse Visual Cortex. Neuron 71, 869–882.

Kerr, A. M., Reisinger, E., and Jonas, P. (2008). Differential dependence of phasic transmitter release on synaptotagmin 1 at GABAergic and glutamatergic hippocampal synapses. Proc. Natl. Acad. Sci. U. S. A. 105, 15581–15586.

Kilman, V., Rossum, M. C. W. Van, and Turrigiano, G. G. (2002). Activity deprivation reduces miniature IPSC amplitude by decreasing the number of postsynaptic GABA. J. Neurosci. 22, 1328–1337.

Kim, C., Ye, F., and Ginsberg, M. H. (2011a). Regulation of integrin activation. Annu. Rev. Cell Dev. Biol. 27, 321–45.

Kim, J., and Alger, B. E. (2010). Reduction in endocannabinoid tone is a homeostatic mechanism for specific inhibitory synapses. Nat. Neurosci. 13, 592–600.

Kim, S. A., Tai, C.-Y., Mok, L.-P., Mosser, E. A., and Schuman, E. M. (2011b). Calcium-dependent dynamics of cadherin interactions at cell-cell junctions. Proc. Natl. Acad. Sci. U. S. A. 108, 9857–9862.

Kim, S. H., and Ryan, T. A. (2013). Balance of Calcineurin A and CDK5 Activities Sets Release Probability at Nerve Terminals. J. Neurosci. 33, 8937–8950.

Kim, S. H., and Ryan, T. A. (2010). CDK5 serves as a major control point in neurotransmitter release. Neuron 67, 797–809.

Klausberger, T., and Somogyi, P. (2008). Neuronal diversity and temporal dynamics: the unity of hippocampal circuit operations. Science (80-.). 321, 53–57.

Knuesel, I., Mastrocola, M., Zuellig, R. A., Bornhauser, B., Schaub, M. C., and Fritschy, J. (1999). Altered synaptic clustering of GABA A receptors in mice lacking dystrophin (mdx mice). Eur. J. Neurosci. 11, 4457–4462.

Ko, J., Soler-Llavina, G. J., Fuccillo, M. V, Malenka, R. C., and Südhof, T. C. (2011). Neuroligins/LRRTMs prevent activity- and Ca2+/calmodulin-dependent synapse elimination in cultured neurons. J. Cell Biol. 194, 323–334.

Kohara, K., Yasuda, H., Huang, Y., Adachi, N., Sohya, K., and Tsumoto, T. (2007). A local reduction in cortical GABAergic synapses after a loss of endogenous brain-derived neurotrophic factor, as revealed by

single-cell gene knock-out method. J. Neurosci. 27, 7234–7244.

Kolarow, R., Brigadski, T., and Lessmann, V. (2007). Postsynaptic secretion of BDNF and NT-3 from hippocampal neurons depends on calcium calmodulin kinase II signaling and proceeds via delayed fusion pore opening. J. Neurosci. 27, 10350–10364.

Kriebel, M., Metzger, J., Trinks, S., Chugh, D., Harvey, R. J., Harvey, K., and Volkmer, H. (2011). The cell adhesion molecule neurofascin stabilizes axo-axonic GABAergic terminals at the axon initial segment. J. Biol. Chem. 286, 24385–24393.

Krueger, D. D., Tuffy, L. P., Papadopoulos, T., and Brose, N. (2012). The role of neurexins and neuroligins in the formation, maturation, and function of vertebrate synapses. Curr. Opin. Neurobiol. 22, 412–422.

Krueger, S. R., Kolar, A., and Fitzsimonds, R. M. (2003). The presynaptic release apparatus is functional in the absence of dendritic contact and highly mobile within isolated axons. Neuron 40, 945–57.

Kubota, K., Inoue, K., Hashimoto, R., Kumamoto, N., Kosuga, A., Tatsumi, M., Kamijima, K., Kunugi, H., Iwata, N., Ozaki, N., et al. (2009). Tumor necrosis factor receptor-associated protein 1 regulates cell adhesion and synaptic morphology via modulation of N-cadherin expression. J. Neurochem. 110, 496–508.

Kuczewski, N., Porcher, C., Ferrand, N., Pellegrino, C., Kolarow, R., Lessmann, V., Medina, I., Gaiarsa, J.-L., and Fiorentino, H. (2008). Backpropagating action potentials trigger dendritic release of BDNF during spontaneous network activity. J. Neurosci. 28, 7013–7023.

Kuhlman, S. J., and Huang, Z. J. (2008). High-resolution labeling and functional manipulation of specific neuron types in mouse brain by Cre-activated viral gene expression. PLoS One 3, e2005.

Kuriu, T., Yanagawa, Y., and Konishi, S. (2012). Activity-dependent coordinated mobility of hippocampal inhibitory synapses visualized with presynaptic and postsynaptic tagged-molecular markers. Mol. Cell. Neurosci. 49, 184–195.

Kuzirian, M. S., Moore, a. R., Staudenmaier, E. K., Friedel, R. H., and Paradis, S. (2013). The Class 4 Semaphorin Sema4D Promotes the Rapid Assembly of GABAergic Synapses in Rodent Hippocampus. J. Neurosci. 33, 8961–8973.

Lau, C. G., and Murthy, V. N. (2012). Activity-Dependent Regulation of Inhibition via GAD67. J. Neurosci. 32, 8521–8531.

Lee, K., Kim, Y., Lee, S.-J., Qiang, Y., Lee, D., Lee, H. W., Kim, H., Je, H. S., Südhof, T. C., and Ko, J. (2013). MDGAs interact selectively with neuroligin-2 but not other neuroligins to regulate inhibitory synapse development. Proc. Natl. Acad. Sci. U. S. A. 110, 336–341.

Lévi, S., Grady, R. M., Henry, M. D., Campbell, K. P., Sanes, J. R., and Craig, A. M. (2002). Dystroglycan is selectively associated with inhibitory GABAergic synapses but is dispensable for their differentiation. J. Neurosci. 22, 4274–85.

Li, R.-W., Yu, W., Christie, S., Miralles, C. P., Bai, J., Loturco, J. J., and De Blas, A. L. (2005). Disruption of postsynaptic GABA receptor clusters leads to decreased GABAergic innervation of pyramidal neurons. J. Neurochem. 95, 756–770.

Linhoff, M. W., Laurén, J., Cassidy, R. M., Dobie, F. A., Takahashi, H., Nygaard, H. B., Airaksinen, M. S., Strittmatter, S. M., and Craig, A. M. (2009). An unbiased expression screen for synaptogenic proteins identifies the LRRTM protein family as synaptic organizers. Neuron 61, 734–749.

Liu, Y., Zhang, L. I., and Tao, H. W. (2007). Heterosynaptic scaling of developing GABAergic synapses: dependence on glutamatergic input and developmental stage. J. Neurosci. 27, 5301–5312.

Maas, C., Belgardt, D., Lee, H. K., Heisler, F. F., Lappe-Siefke, C., Magiera, M. M., van Dijk, J., Hausrat, T. J., Janke, C., and Kneussel, M. (2009). Synaptic activation modifies microtubules underlying transport of postsynaptic cargo. Proc. Natl. Acad. Sci. U. S. A. 106, 8731–6.

MacAskill, A. F., Rinholm, J. E., Twelvetrees, A. E., Arancibia-Carcamo, I. L., Muir, J., Fransson, A., Aspenstrom, P., Attwell, D., and Kittler, J. T. (2009). Miro1 is a calcium sensor for glutamate receptor-dependent localization of mitochondria at synapses. Neuron 61, 541–55.

Maffei, A., Lambo, M. E., and Turrigiano, G. G. (2010). Critical period for inhibitory plasticity in rodent binocular V1. J. Neurosci. 30, 3304–3309.

Maffei, A., Nataraj, K., Nelson, S. B., and Turrigiano, G. G. (2006). Potentiation of cortical inhibition by visual deprivation. Nature 443, 81–84.

Maffei, A., Nelson, S. B., and Turrigiano, G. G. (2004). Selective reconfiguration of layer 4 visual cortical circuitry by visual deprivation. Nat. Neurosci. 7, 1353–9.

Maffei, A., and Turrigiano, G. G. (2008). Multiple modes of network homeostasis in visual cortical layer 2/3. J. Neurosci. 28, 4377–4384.

Marik, S. a, Yamahachi, H., McManus, J. N. J., Szabo, G., and Gilbert, C. D. (2010). Axonal dynamics of excitatory and inhibitory neurons in somatosensory cortex. PLoS Biol. 8, e1000395.

Marty, S., Wehrlé, R., Fritschy, J., and Sotelo, C. (2004). Quantitative effects produced by modifications of neuronal activity on the size of GABA A receptor clusters in hippocampal slice cultures. Eur. J. Neurosci. 20, 427–440.

Marty, S., Wehrle, R., and Sotelo, C. (2000). Neuronal activity and brain-derived neurotrophic factor regulate the density of inhibitory synapses in organotypic slice cultures of postnatal hippocampus. J. Neurosci. 20, 8087–8095.

Matsuda, N., Lu, H., Fukata, Y., Noritake, J., Gao, H., Mukherjee, S., Nemoto, T., Fukata, M., and Poo, M.-M. (2009). Differential activity-dependent secretion of brain-derived neurotrophic factor from axon and dendrite. J. Neurosci. 29, 14185–14198.

Matsumoto-Miyai, K., Sokolowska, E., Zurlinden, A., Gee, C. E., Lüscher, D., Hettwer, S., Wölfel, J., Ladner, A. P., Ster, J., Gerber, U., et al. (2009). Coincident pre- and postsynaptic activation induces dendritic filopodia via neurotrypsin-dependent agrin cleavage. Cell 136, 1161–1171.

Mei, L., and Xiong, W.-C. (2008). Neuregulin 1 in neural development, synaptic plasticity and schizophrenia. Nat. Rev. Neurosci. 9, 437–452.

Meijers, R., Puettmann-Holgado, R., Skiniotis, G., Liu, J., Walz, T., Wang, J., and Schmucker, D. (2007). Structural basis of Dscam isoform specificity. Nature 449, 487–91.

Missler, M., and Südhof, T. C. (1998). Neurexins: three genes and 1001 products. Trends Genet. 14, 20–6.

Mizumoto, K., and Shen, K. (2013). Interaxonal interaction defines tiled presynaptic innervation in C. elegans. Neuron 77, 655–66.

Morita, A., Yamashita, N., Sasaki, Y., Uchida, Y., Nakajima, O., Nakamura, F., Yagi, T., Taniguchi, M., Usui, H., Katoh-Semba, R., et al. (2006). Regulation of dendritic branching and spine maturation by semaphorin3A-Fyn signaling. J. Neurosci. 26, 2971–2980.

Nikonenko, A., Schmidt, S., Skibo, G., Brückner, G., and Schachner, M. (2003). Tenascin-R-deficient mice show structural alterations of symmetric perisomatic synapses in the CA1 region of the hippocampus. J. Comp. Neurol. 456, 338–349.

O'Connor, T. P., Cockburn, K., Wang, W., Tapia, L., Currie, E., and Bamji, S. X. (2009). Semaphorin 5B mediates synapse elimination in hippocampal neurons. Neural Dev. 4, 18.

Obashi, K., and Okabe, S. (2013). Regulation of mitochondrial dynamics and distribution by synapse position and neuronal activity in the axon. Eur. J. Neurosci. 38, 2350–2363.

Ohba, S., Ikeda, T., Ikegaya, Y., Nishiyama, N., Matsuki, N., and Yamada, M. K. (2005). BDNF locally potentiates GABAergic presynaptic machineries: target-selective circuit inhibition. Cereb. Cortex 15, 291–298.

Ormond, J., and Woodin, M. a. (2011). Disinhibition-Mediated LTP in the Hippocampus is Synapse Specific. Front. Cell. Neurosci. 5, 1–11.

Ou, C.-Y., and Shen, K. (2010). Setting up presynaptic structures at specific positions. Curr. Opin. Neurobiol. 20, 489–493.

Owald, D., and Sigrist, S. J. (2009). Assembling the presynaptic active zone. Curr. Opin. Neurobiol. 19, 311–8.

Palop, J. J., Chin, J., Roberson, E. D., Wang, J., Thwin, M. T., Bien-Ly, N., Yoo, J., Ho, K. O., Yu, G.-Q., Kreitzer, A., et al. (2007). Aberrant excitatory neuronal activity and compensatory remodeling of inhibitory hippocampal circuits in mouse models of Alzheimer's disease. Neuron 55, 697–711.

Paradis, S., Harrar, D. B., Lin, Y., Koon, A. C., Hauser, J. L., Griffith, E. C., Zhu, L., Brass, L. F., Chen, C., and Greenberg, M. E. (2007). An RNAi-based approach identifies molecules required for glutamatergic and GABAergic synapse development. Neuron 53, 217–232.

Park, H., and Poo, M. (2013). Neurotrophin regulation of neural circuit development and function. Nat. Rev. Neurosci. 14, 7–23.

Pasterkamp, R. J. (2012). Getting neural circuits into shape with semaphorins. Nat. Rev. Neurosci. 13,

605–618.

Patrizi, A., Scelfo, B., Viltono, L., Briatore, F., Fukaya, M., Watanabe, M., Strata, P., Varoqueaux, F., Brose, N., Fritschy, J., et al. (2008). Synapse formation and clustering of neuroligin-2 in the absence of GABAA receptors. Proc. Natl. Acad. Sci. U. S. A. 105, 13151–13156.

Pavlov, I., Rauvala, H., and Taira, T. (2006). Enhanced hippocampal GABAergic inhibition in mice overexpressing heparin-binding growth-associated molecule. Neuroscience 139, 505–11.

Peixoto, R. T., Kunz, P. A., Kwon, H., Mabb, A. M., Sabatini, B. L., Philpot, B. D., and Ehlers, M. D. (2012). Transsynaptic Signaling by Activity-Dependent Cleavage of Neuroligin-1. Neuron 76, 396–409.

Peng, A., Rotman, Z., Deng, P.-Y., and Klyachko, V. a (2012). Differential motion dynamics of synaptic vesicles undergoing spontaneous and activity-evoked endocytosis. Neuron 73, 1108–15.

Peng, Y.-R., Zeng, S.-Y., Song, H.-L., Li, M.-Y., Yamada, M. K., and Yu, X. (2010). Postsynaptic Spiking Homeostatically Induces Cell-Autonomous Regulation of Inhibitory Inputs via Retrograde Signaling. J. Neurosci. 30, 16220–16231.

Pettem, K. L., Yokomaku, D., Takahashi, H., Ge, Y., and Craig, A. M. (2013). Interaction between autism-linked MDGAs and neuroligins suppresses inhibitory synapse development. J. Cell Biol. 200, 321–326.

Pfeffer, C. K., Xue, M., He, M., Huang, Z. J., and Scanziani, M. (2013). Inhibition of inhibition in visual cortex: the logic of connections between molecularly distinct interneurons. Nat. Neurosci. 16, 1068–1076.

Pillai-Nair, N., Panicker, A. K., Rodriguiz, R. M., Gilmore, K. L., Demyanenko, G. P., Huang, J. Z., Wetsel, W. C., and Maness, P. F. (2005). Neural cell adhesion molecule-secreting transgenic mice display abnormalities in GABAergic interneurons and alterations in behavior. J. Neurosci. 25, 4659–46571.

Pinkstaff, J. K., Lynch, G., and Gall, C. M. (1998). Localization and seizure-regulation of integrin beta 1 mRNA in adult rat brain. Brain Res. Mol. Brain Res. 55, 265–76.

Poulopoulos, A., Aramuni, G., Meyer, G., Soykan, T., Hoon, M., Harvey, K., Jedlicka, P., Zhang, M., Paarmann, I., Schwarzacher, S. W., et al. (2009). Neuroligin 2 drives postsynaptic assembly at perisomatic inhibitory synapses through gephyrin and collybistin. Neuron 63, 628–642.

Pozo, K., and Goda, Y. (2010). Unraveling mechanisms of homeostatic synaptic plasticity. Neuron 66, 337–351.

Pregno, G., Frola, E., Graziano, S., Patrizi, A., Bussolino, F., Arese, M., and Sassoè-Pognetto, M. (2013). Differential regulation of neurexin at glutamatergic and GABAergic synapses. Front. Cell. Neurosci. 7, 35.

Raissi, A. J., Staudenmaier, E. K., David, S., Hu, L., and Paradis, S. (2013). Sema4D localizes to synapses and regulates GABAergic synapse development as a membrane-bound molecule in the mammalian hippocampus. Mol. Cell. Neurosci., doi: 10.1016/j.mcn.2013.08.004.

Rannals, M. D., and Kapur, J. (2011). Homeostatic Strengthening of Inhibitory Synapses Is Mediated by the Accumulation of GABAA Receptors. J. Neurosci. 31, 17701–17712.

Ratnayaka, A., Marra, V., Branco, T., and Staras, K. (2011). Extrasynaptic vesicle recycling in mature hippocampal neurons. Nat. Commun. 2, 531.

Regehr, W. G., Carey, M. R., and Best, A. R. (2009). Activity-dependent regulation of synapses by retrograde messengers. Neuron 63, 154–70.

Reuss, B., and von Bohlen und Halbach, O. (2003). Fibroblast growth factors and their receptors in the central nervous system. Cell Tissue Res. 313, 139–157.

Rose, T., Schoenenberger, P., Jezek, K., and Oertner, T. G. (2013). Developmental refinement of vesicle cycling at Schaffer collateral synapses. Neuron 77, 1109–21.

Sabo, S. L., Gomes, R. A., and McAllister, A. K. (2006). Formation of presynaptic terminals at predefined sites along axons. J. Neurosci. 26, 10813–10825.

Saghatelyan, A. K., Dityatev, A., Schmidt, S., Schuster, T., Bartsch, U., and Schachner, M. (2001). Reduced perisomatic inhibition, increased excitatory transmission, and impaired long-term potentiation in mice deficient for the extracellular matrix glycoprotein tenascin-R. Mol. Cell. Neurosci. 17, 226–40.

Sahay, A., Kim, C.-H., Sepkuty, J. P., Cho, E., Huganir, R. L., Ginty, D. D., and Kolodkin, A. L. (2005). Secreted semaphorins modulate synaptic transmission in the adult hippocampus. J. Neurosci. 25, 3613–3620.

Saliba, R. S., Michels, G., Jacob, T. C., Pangalos, M. N., and

Moss, S. J. (2007). Activity-dependent ubiquitination of GABA(A) receptors regulates their accumulation at synaptic sites. J. Neurosci. 27, 13341–13351.

Sassoè-Pognetto, M., Frola, E., Pregno, G., Briatore, F., and Patrizi, A. (2011). Understanding the molecular diversity of GABAergic synapses. Front. Cell. Neurosci. 5, 4.

Scheiffele, P., Fan, J., Choih, J., Fetter, R., and Serafini, T. (2000). Neuroligin expressed in nonneuronal cells triggers presynaptic development in contacting axons. Cell 101, 657–669.

Schubert, T., Hoon, M., Euler, T., Lukasiewicz, P. D., and Wong, R. O. L. (2013). Developmental regulation and activity-dependent maintenance of GABAergic presynaptic inhibition onto rod bipolar cell axonal terminals. Neuron 78, 124–37.

Schuemann, A., Klawiter, A., Bonhoeffer, T., Wierenga, C. J., Huang, J., and Harbor, C. S. (2013). Structural plasticity of GABAergic axons is regulated by network activity and GABA A receptor activation. Front. Neural Circuits 7, 113.

Shen, K., and Bargmann, C. I. (2003). The immunoglobulin superfamily protein SYG-1 determines the location of specific synapses in C. elegans. Cell 112, 619–630.

Shen, K., Fetter, R. D., and Bargmann, C. I. (2004). Synaptic Specificity is Generated by the Synaptic Guidepost Protein SYG-2 and Its Receptor , SYG-1. Cell 116, 869–881.

Shepherd, G. M., and Harris, K. M. (1998). Three-dimensional structure and composition of CA3-->CA1 axons in rat hippocampal slices: implications for presynaptic connectivity and compartmentalization. J. Neurosci. 18, 8300–8310.

Siddiqui, T. J., and Craig, A. M. (2011). Synaptic organizing complexes. Curr. Opin. Neurobiol. 21, 132–43.

Siddiqui, T. J., Tari, P. K., Connor, S. A., Zhang, P., Dobie, F. A., She, K., Kawabe, H., Wang, Y. T., Brose, N., and Craig, A. M. (2013). An LRRTM4-HSPG Complex Mediates Excitatory Synapse Development on Dentate Gyrus Granule Cells. Neuron.

Staras, K. (2007). Share and share alike: trading of presynaptic elements between central synapses. Trends Neurosci. 30, 292–298.

Staras, K., Branco, T., Burden, J. J., Pozo, K., Darcy, K., Marra, V., Ratnayaka, A., and Goda, Y. (2010). A vesicle superpool spans multiple presynaptic terminals in hippocampal neurons. Neuron 66, 37–44.

Stellwagen, D., and Malenka, R. C. (2006). Synaptic scaling mediated by glial TNF-alpha. Nature 440, 1054–9.

Stepanyants, A., Tamás, G., and Chklovskii, D. B. (2004). Class-specific features of neuronal wiring. Neuron 43, 251–259.

Su, J., Gorse, K., Ramirez, F., and Fox, M. A. (2010). Collagen XIX Is Expressed by Interneurons and Contributes to the Formation of Hippocampal Synapses. J. Comp. Neurol. 518, 229–253.

Südhof, T. C. (2008). Neuroligins and neurexins link synaptic function to cognitive disease. Nature 455, 903–911.

Sugita, S. (2001). A stoichiometric complex of neurexins and dystroglycan in brain. J. Cell Biol. 154, 435–446.

Sumita, K., Sato, Y., Iida, J., Kawata, A., Hamano, M., Hirabayashi, S., Ohno, K., Peles, E., and Hata, Y. (2007). Synaptic scaffolding molecule (S-SCAM) membrane-associated guanylate kinase with inverted organization (MAGI)-2 is associated with cell adhesion molecules at inhibitory synapses in rat hippocampal neurons. J. Neurochem. 100, 154–166.

Sun, Y., and Bamji, S. X. (2011). β-Pix modulates actin-mediated recruitment of synaptic vesicles to synapses. J. Neurosci. 31, 17123–17133.

Suzuki, K., Hayashi, Y., Nakahara, S., Kumazaki, H., Prox, J., Horiuchi, K., Zeng, M., Tanimura, S., Nishiyama, Y., Osawa, S., et al. (2012). Activity-dependent proteolytic cleavage of neuroligin-1. Neuron 76, 410–22.

Swanwick, C. C., Murthy, N. R., and Kapur, J. (2006). Activity-dependent scaling of GABAergic synapse strength is regulated by brain-derived neurotrophic factor. Mol. Cell. Neurosci. 31, 481 – 492.

Swiercz, J. M., Worzfeld, T., and Offermanns, S. (2008). ErbB-2 and met reciprocally regulate cellular signaling via plexin-B1. J. Biol. Chem. 283, 1893–1901.

Tabuchi, K., Biederer, T., Butz, S., and Sudhof, T. C. (2002). CASK participates in alternative tripartite complexes in which Mint 1 competes for binding with caskin 1, a novel CASK-binding protein. J. Neurosci. 22, 4264–4273.

Tai, C.-Y., Mysore, S. P., Chiu, C., and Schuman, E. M. (2007). Activity-regulated N-cadherin endocytosis. Neuron 54, 771–85.

Takahashi, H., and Craig, A. M. (2013). Protein tyrosine phosphatases PTPδ, PTPσ and LAR: presynaptic hubs

for synapse organization. Trends Neurosci., 1–13.

Takahashi, H., Katayama, K., Sohya, K., Miyamoto, H., Prasad, T., Matsumoto, Y., Ota, M., Yasuda, H., Tsumoto, T., Aruga, J., et al. (2012). Selective control of inhibitory synapse development by Slitrk3-PTPδ trans-synaptic interaction. Nat. Neurosci. 15, 389–398.

Takamori, S., Holt, M., Stenius, K., Lemke, E. a, Grønborg, M., Riedel, D., Urlaub, H., Schenck, S., Brügger, B., Ringler, P., et al. (2006). Molecular anatomy of a trafficking organelle. Cell 127, 831–46.

Taniguchi, H., Gollan, L., Scholl, F. G., Mahadomrongkul, V., Dobler, E., Limthong, N., Peck, M., Aoki, C., and Scheiffele, P. (2007). Silencing of neuroligin function by postsynaptic neurexins. J. Neurosci. 27, 2815–2824.

Tasaka, G.-I., Negishi, M., and Oinuma, I. (2012). Semaphorin 4D/Plexin-B1-mediated M-Ras GAP activity regulates actin-based dendrite remodeling through Lamellipodin. J. Neurosci. 32, 8293–8305.

Taylor, A. M., Berchtold, N. C., Perreau, V. M., Tu, C. H., Li Jeon, N., and Cotman, C. W. (2009). Axonal mRNA in uninjured and regenerating cortical mammalian axons. J. Neurosci. 29, 4697–4707.

Taylor, A. M., Wu, J., Tai, H.-C., and Schuman, E. M. (2013). Axonal translation of β-catenin regulates synaptic vesicle dynamics. J. Neurosci. 33, 5584–5589.

Terauchi, A., Johnson-Venkatesh, E. M., Toth, A. B., Javed, D., Sutton, M. a., and Umemori, H. (2010). Distinct FGFs promote differentiation of excitatory and inhibitory synapses. Nature 465, 783–787.

Thalhammer, A., and Cingolani, L. a (2013). Cell adhesion and homeostatic synaptic plasticity. Neuropharmacology, 1–8.

Ting, A. K., Chen, Y., Wen, L., Yin, D.-M., Shen, C., Tao, Y., Liu, X., Xiong, W.-C., and Mei, L. (2011). Neuregulin 1 Promotes Excitatory Synapse Development and Function in GABAergic Interneurons. J. Neurosci. 31, 15–25.

Turrigiano, G. (2011). Too Many Cooks? Intrinsic and Synaptic Homeostatic Mechanisms in Cortical Circuit Refinement. Annu. Rev. Neurosci., 89–103.

Turrigiano, G. G. (1999). Homeostatic plasticity in neuronal networks: the more things change, the more they stay the same. Trends Neurosci. 22, 221–227.

Turrigiano, G. G. (2008). The self-tuning neuron: synaptic scaling of excitatory synapses. Cell 135, 422–435.

Turrigiano, G. G., Leslie, K. R., Desai, N. S., Rutherford, L. C., and Nelson, S. B. (1998). Activity-dependent scaling of quantal amplitude in neocortical neurons. Nature 391, 892–6.

Tyagarajan, S. K., and Fritschy, J.-M. (2010). GABA(A) receptors, gephyrin and homeostatic synaptic plasticity. J. Physiol. 588, 101–106.

Umemori, H., Linhoff, M.W., Ornitz, D. M., and Sanes, J. R. (2004). FGF22 and its close relatives are presynaptic organizing molecules in the mammalian brain. Cell 118, 257–270.

van Versendaal, D., Rajendran, R., Saiepour, M. H., Klooster, J., Smit-Rigter, L., Sommeijer, J.-P., De Zeeuw, C. I., Hofer, S. B., Heimel, J. A., and Levelt, C. N. (2012). Elimination of Inhibitory Synapses Is a Major Component of Adult Ocular Dominance Plasticity. Neuron 74, 374–383.

Varoqueaux, F., Aramuni, G., Rawson, R. L., Mohrmann, R., Missler, M., Gottmann, K., Zhang, W., Südhof, T. C., and Brose, N. (2006). Neuroligins determine synapse maturation and function. Neuron 51, 741–754.

Varoqueaux, F., Jamain, S., and Brose, N. (2004). Neuroligin 2 is exclusively localized to inhibitory synapses. Eur. J. Cell Biol. 83, 449–456.

Verhage, M. (2000). Synaptic Assembly of the Brain in the Absence of Neurotransmitter Secretion. Science (80-.). 287, 864–869.

Vicario-Abejón, C., Collin, C., Mckay, R. D. G., and Segal, M. (1998). Neurotrophins induce formation of functional excitatory and inhibitory synapses between cultured hippocampal neurons. J. Neurosci. 18, 7256–7271.

Vlachos, A., Reddy-Alla, S., Papadopoulos, T., Deller, T., and Betz, H. (2012). Homeostatic Regulation of Gephyrin Scaffolds and Synaptic Strength at Mature Hippocampal GABAergic Postsynapses. Cereb. Cortex.

Vullhorst, D., Neddens, J., Karavanova, I., Tricoire, L., Petralia, R. S., McBain, C. J., and Buonanno, A. (2009). Selective expression of ErbB4 in interneurons, but not pyramidal cells, of the rodent hippocampus. J. Neurosci. 29, 12255–12264.

Wen, L., Lu, Y.-S., Zhu, X.-H., Li, X.-M., Woo, R.-S., Chen, Y.-J., Yin, D.-M., Lai, C., Terry, A. V, Vazdarjanova, A., et al. (2010). Neuregulin 1 regulates pyramidal neuron activity via ErbB4 in parvalbumin-positive interneurons. Proc. Natl. Acad. Sci. U. S. A. 107, 1211–6.

Wenner, P. (2011). Mechanisms of GABAergic homeostatic plasticity. Neural Plast. 2011, 489470.

Wentzel, C., Sommer, J. E., Nair, R., Stiefvater, A., Sibarita, J.-B., and Scheiffele, P. (2013). mSYD1A, a mammalian synapse-defective-1 protein, regulates synaptogenic signaling and vesicle docking. Neuron 78, 1012–23.

Wierenga, C. J., Becker, N., and Bonhoeffer, T. (2008). GABAergic synapses are formed without the involvement of dendritic protrusions. Nat. Neurosci. 11, 1044–1052.

Wierenga, C. J., Walsh, M. F., and Turrigiano, G. G. (2006). Temporal regulation of the expression locus of homeostatic plasticity. J. Neurophysiol. 96, 2127–33.

De Wit, J., O'Sullivan, M. L., Savas, J. N., Condomitti, G., Caccese, M. C., Vennekens, K. M., Yates, J. R., and Ghosh, A. (2013). Unbiased Discovery of Glypican as a Receptor for LRRTM4 in Regulating Excitatory Synapse Development. Neuron.

Wittenmayer, N., Körber, C., Liu, H., Kremer, T., Varoqueaux, F., Chapman, E. R., Brose, N., Kuner, T., and Dresbach, T. (2009). Postsynaptic Neuroligin1 regulates presynaptic maturation. Proc. Natl. Acad. Sci. U. S. A. 106, 13564–9.

Wojtowicz, W. M., Wu, W., Andre, I., Qian, B., Baker, D., and Zipursky, S. L. (2007). A vast repertoire of Dscam binding specificities arises from modular interactions of variable Ig domains. Cell 130, 1134–45.

Woo, J., Kwon, S.-K., Nam, J., Choi, S., Takahashi, H., Krueger, D., Park, J., Lee, Y., Bae, J. Y., Lee, D., et al. (2013). The adhesion protein IgSF9b is coupled to neuroligin 2 via S-SCAM to promote inhibitory synapse development. J. Cell Biol. 201, 929–944.

Woo, R.-S., Li, X.-M., Tao, Y., Carpenter-Hyland, E., Huang, Y. Z., Weber, J., Neiswender, H., Dong, X.-P., Wu, J., Gassmann, M., et al. (2007). Neuregulin-1 enhances depolarization-induced GABA release. Neuron 54, 599–610.

Wu, X., Fu, Y., Knott, G., Lu, J., Cristo, G. Di, and Huang, J. (2012). GABA signaling promotes synapse elimination and axon pruning in developing cortical inhibitory interneurons. J. Neurosci. 32, 331–343.

Wu, Y. E., Huo, L., Maeder, C. I., Feng, W., and Shen, K. (2013). The balance between capture and dissociation of presynaptic proteins controls the spatial distribution of synapses. Neuron 78, 994–1011.

Yamada, M. K., Nakanishi, K., Ohba, S., Nakamura, T., Ikegaya, Y., Nishiyama, N., and Matsuki, N. (2002). Brain-derived neurotrophic factor promotes the maturation of GABAergic mechanisms in cultured hippocampal neurons. J. Neurosci. 22, 7580–7585.

Yamada, T., Yang, Y., Huang, J., Coppola, G., Geschwind, D. H., and Bonni, A. (2013). Sumoylated MEF2A coordinately eliminates orphan presynaptic sites and promotes maturation of presynaptic boutons. J. Neurosci. 33, 4726–4740.

Yim, Y. S., Kwon, Y., Nam, J., In, H., Lee, K., Goo, D., and Kim, E. (2013). Slitrks control excitatory and inhibitory synapse formation with LAR receptor protein tyrosine phosphatases. Proc. Natl. Acad. Sci. U. S. A. 110, 4057–4062.

Yin, D.-M., Chen, Y.-J., Lu, Y.-S., Bean, J. C., Sathyamurthy, A., Shen, C., Liu, X., Lin, T. W., Smith, C. a., Xiong, W.-C., et al. (2013). Reversal of Behavioral Deficits and Synaptic Dysfunction in Mice Overexpressing Neuregulin 1. Neuron 78, 644–657.

Yizhar, O., Fenno, L. E., Prigge, M., Schneider, F., Davidson, T. J., O'Shea, D. J., Sohal, V. S., Goshen, I., Finkelstein, J., Paz, J. T., et al. (2011). Neocortical excitation/inhibition balance in information processing and social dysfunction. Nature 477, 171–178.

Yoshida, T., Shiroshima, T., Lee, S.-J., Yasumura, M., Uemura, T., Chen, X., Iwakura, Y., and Mishina, M. (2012). Interleukin-1 receptor accessory protein organizes neuronal synaptogenesis as a cell adhesion molecule. J. Neurosci. 32, 2588–2600.

Yoshida, T., Yasumura, M., Uemura, T., Lee, S.-J., Ra, M., Taguchi, R., Iwakura, Y., and Mishina, M. (2011). IL-1 receptor accessory protein-like 1 associated with mental retardation and autism mediates synapse formation by trans-synaptic interaction with protein tyrosine phosphatase δ. J. Neurosci. 31, 13485–13499.

Zander, J.-F., Münster-Wandowski, A., Brunk, I., Pahner, I., Gómez-Lira, G., Heinemann, U., Gutiérrez, R., Laube, G., and Ahnert-Hilger, G. (2010). Synaptic and Vesicular Coexistence of VGLUT and VGAT in Selected Excitatory and Inhibitory Synapses. J. Neurosci. 30, 7634–7645.

Zhai, R. G., Vardinon-Friedman, H., Cases-Langhoff, C., Becker, B., Gundelfinger, E. D., Ziv, N. E., and Garner, C. C. (2001). Assembling the presynaptic active zone: a characterization of an active zone precursor vesicle. Neuron 29, 131–143.

Zhang, Y., Luan, Z., Liu, A., and Hu, G. (2001). The scaffolding protein CASK mediates the interaction between rabphilin3a and beta-neurexins. FEBS Lett. 497, 99–102.

Zhao, C., Dreosti, E., and Lagnado, L. (2011). Homeostatic synaptic plasticity through changes in presynaptic calcium influx. J. Neurosci. 31, 7492–7496.

Zhu, L., Bergmeier, W., Wu, J., Jiang, H., Stalker, T. J., Cieslak, M., Fan, R., Boumsell, L., Kumanogoh, A., Kikutani, H., et al. (2007). Regulated surface expression and shedding support a dual role for semaphorin 4D in platelet responses to vascular injury. Proc. Natl. Acad. Sci. U. S. A. 104, 1621–1626.

Zivraj, K. H., Tung, Y. C. L., Piper, M., Gumy, L., Fawcett, J. W., Yeo, G. S. H., and Holt, C. E. (2010). Subcellular profiling reveals distinct and developmentally regulated repertoire of growth cone mRNAs. J. Neurosci. 30, 15464–15478.

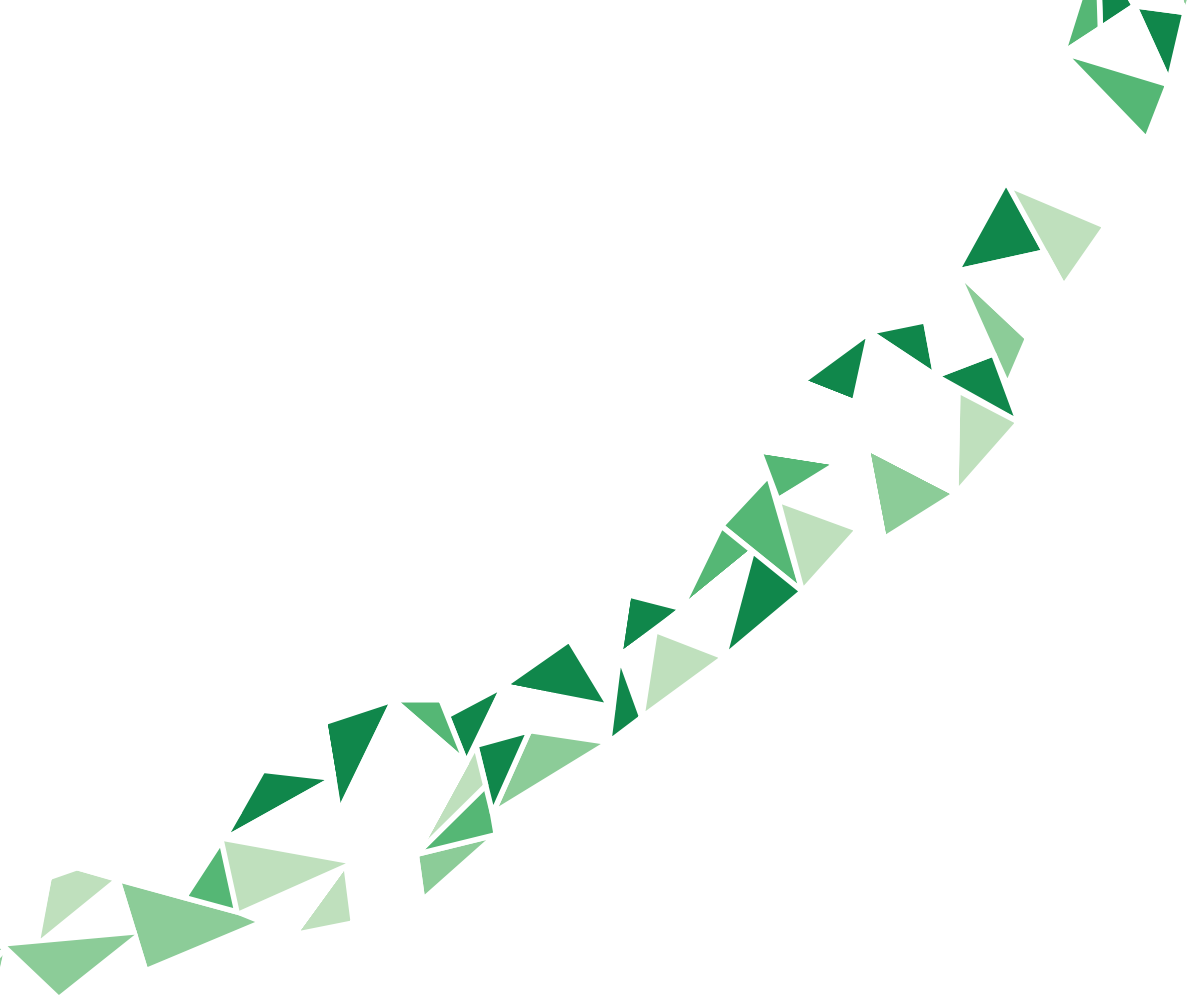

[1] Cell Biology, Department of Biology, Faculty of Science, Utrecht University, Utrecht, the Netherlands
[2] Biomolecular Mass Spectrometry and Proteomics, Bijvoet Center for Biomolecular Research, Utrecht Institute for Pharmaceutical Sciences and The Netherlands Proteomics Centre, Utrecht University, the Netherlands

Chapter 3

Non-muscle MyosinIIb is a regulator of axon formation in hippocampal neurons

Cátia P. Frias[1], Elena Tortosa[1], Riccardo Stucchi[1,2], A. F. Maarten Altelaar[2], Corette J. Wierenga[1], Casper C. Hoogenraad[1]

ABSTRACT

Actin is one of the most abundant proteins in neurons, and is fundamental for several neuronal developmental processes, including axon formation and elongation. However, the contribution of actin-binding proteins to such processes remains unknown. Here, we performed a targeted knockdown screen to determine the role of myosin and tropomyosin proteins in the development of hippocampal neurons. While tropomyosins are dispensable for the establishment of the axonal arborization, we found that different myosin proteins regulate the development of axonal and dendritic processes. We show that non-muscle Myosin II proteins are required for the induction of multiple axons upon treatment with taxol, a microtubule-stabilizing drug. Depletion of MyoIIb leads to changes in growth cone morphology and in the microtubule cytoskeleton at the proximal axon. Altogether, our data highlights a role for MyoIIb in the formation of the axon in hippocampal neurons. Our results suggest that MyoIIb may promote interactions between the actin and microtubule cytoskeletons at the growth cone and/or at the proximal axon during the early stages of axon development.

INTRODUCTION

The development of the nervous system requires the outgrowth of axons towards their targets, to establish the neuronal circuits of the brain. The formation and growth of a single axon for transmission of information characterizes the polarized morphology of mature neurons. In cultured hippocampal neurons, where external polarity cues are absent, neurons maintain their intrinsic ability to develop the distinct axonal and dendritic compartments (Dotti et al., 1988). In fact, neurons re-set their developmental program after plating. They are initially round, symmetrical cells, and then grow multiple minor processes called neurites. Upon extensive growth, one of these neurites will become the axon, while the remaining, shorter, neurites will become the dendrites. Cytoskeletal rearrangements contribute to the breaking of cell symmetry and, consequently, to neuronal polarization, with both microtubules and actin filaments having fundamental roles in this process (Pacheco and Gallo, 2016; van Beuningen and Hoogenraad, 2016). In a developing neuron, actin is enriched at the tip of neurites, where the growth cone is formed. Promoting actin disruption in one of these growth cones is sufficient to promote its neurite to become the axon (Bradke and Dotti, 1999), showing that local actin instability may function as a signal for neuronal polarization. Moreover, there are different actin structures along the axon, which are thought to be important for axon outgrowth and function, including actin waves and rings (Katsuno et al., 2015; Xu et al., 2013). Even though our understanding on axonal actin structures and actin contribution for axon development has increased in recent years, the mechanisms underlying axon formation and the involvement of the actin cytoskeleton are still not fully understood.

Actin cytoskeleton complexity and function relies on a plethora of actin-binding proteins, including myosins and tropomyosins. Myosins are motor proteins that can interact with actin filaments via their motor domain, where ATP hydrolysis occurs to generate force and movement along actin filaments (Kneussel and Wagner, 2013). Myosins from class V and VI (MyoV and MyoVI) are important for transport of cargo along actin filaments, and have been recently proposed to play a role in the correct distribution of cargo between the somatodendritic and axonal compartments (Al-Bassam et al., 2012; Lewis et al., 2011). Myosins from class II (MyoII) have actin cross-linking and contractile properties, and they play important roles in neuronal migration and growth cone dynamics (Vallee et al., 2009). Tropomyosins can interact with actin filaments as well as with actin-binding proteins, and several isoforms are expressed in the brain (Brettle et al., 2016). Tropomyosins have been shown to regulate growth cone morphology and neurite extension in neuroblastoma cells (Curthoys et al., 2014), suggesting that tropomyosins may regulate the actin cytoskeleton during neurite outgrowth. The role of myosins and tropomyosins in axons is not clear. Here, we performed a targeted knockdown screen to identify myosins and tropomyosins important for axon development and outgrowth. Our data revealed that axon and dendritic outgrowth is regulated by different myosin proteins, but not by tropomysosins. We also found that MyoII proteins are involved in the establishment of the axon initial segment (AIS) upon treatment with nanomolar doses of microtubule-stabilizing drug taxol. Interestingly, depletion of MyoIIb led to the formation of bulbs at neuritic tips in taxol-treated cells, suggesting that the microtubule and actin cytoskeletons may be altered in these cells. We further observed changes in microtubule-related proteins at the proximal axon upon depletion of MyoIIb. We propose that MyoIIb may mediate the interaction between the microtubule and actin cytoskeletons during the early stages of neuronal polarization in hippocampal neurons.

RESULTS AND DISCUSSION

Different myosins are required for the development of axonal and dendritic processes

To address the role of myosins and tropomyosins in the growth of axonal and dendritic arborizations, we performed a knockdown screen of neuronal myosins and tropomyosins. Neurons were transfected at day-in-vitro (DIV) 0 and fixed 4 days later. All neurites and branches were manually traced, and the axon was identified as the longest neurite, which was negative for the somatodendritic marker Map2. We found that depletion of MyoIIc, MyoVb and MyoVI significantly decreased the total axonal arborization (Figure 1A,B). Both MyoIIc and MyoVb knockdown impaired the extension of axonal branches, while the MyoVI phenotype was due to reductions in the axon length, and in the number and length of axonal branches (Figure 1C-E). Our results are consistent with a role for MyoVb and MyoVI in the transport of proteins required for proper axonal outgrowth and branching in neurons. This would be in accordance with a previous report showing that MyoVI is necessary for the localization of axonal proteins (Lewis et al., 2011). Future studies could investigate if depletion of MyoVb and MyoVI affect the polarized distribution of axonal proteins in hippocampal neurons. We found that tropomyosins depletion had no major effects on total axonal length (Figure 1B), although TPM-α- and TPM-δ-depleted neurons showed a decrease in the mean length of axonal branches and the primary axon length, respectively (Figure 1C,E).

We also assessed if myosin depletion changed the total dendritic arborization in DIV 4 neurons. We found that MyoVa and MyoX were required for the growth of the dendritic arborization in hippocampal neurons (Figure 1F,G). The effect was mainly due to a decrease in the mean length of primary dendrites and dendritic branches (data not shown). These results suggest that MyoVa and MyoX proteins are not essential for the initial formation of dendritic processes, but rather for their extension. Interestingly, MyoVa has been shown to be involved in the proper targeting of dendritic proteins (Al-Bassam et al., 2012; Lewis et al., 2009). It was proposed that MyoVa, by walking on actin filaments at the AIS, leads to the halt and reverse of dendritic proteins, preventing their progression into the axon (Al-Bassam et al., 2012). In this way, MyoVa-depleted cells may have a deficiency in the localization of dendritic proteins to the dendrites, which may impair the dendritic arbor extension. Our finding that depletion of MyoVa and MyoVb affect dendritic and axonal development, respectively, suggests that these two related proteins have different functions in neuronal development. It will be interesting to further investigate this, by looking at the function of these proteins in young neurons. Besides roles on dendritic spine formation (Lin et al.,

Figure 1. Myosins are required for proper axon and dendritic outgrowth. ►

(A) Representative images of DIV 4 hippocampal neurons transfected at DIV 0 with pSuper (control) or MyoIIb-, MyoIIc-, MyoVI-, TPM-α-shRNA pools and GFP fill. Scale bar 100 µm.

(B) Quantification of the total axon length in DIV 4 hippocampal neurons transfected for 4 days with pSuper (control) or indicated pools of shRNAs and GFP fill. n = 15-20 cells from 2 independent experiments were analyzed per condition (for control, n = 62 cells, N = 4). Kruskal-Wallis test. * $p < 0.05$, *** $p < 0.001$.

(C-E) Quantification of primary axon length (C), number of axon branches (D) and mean length of axon branches (E) in DIV 4 hippocampal neurons transfected at DIV 0 with pSuper (control) or indicated pools of shRNAs and GFP fill. n = 15-20 cells from 2 independent experiments were analyzed per condition (for control, n = 62 cells, N = 4). Kruskal-Wallis test: * $p < 0.05$, ** $p < 0.01$, *** $p < 0.001$.

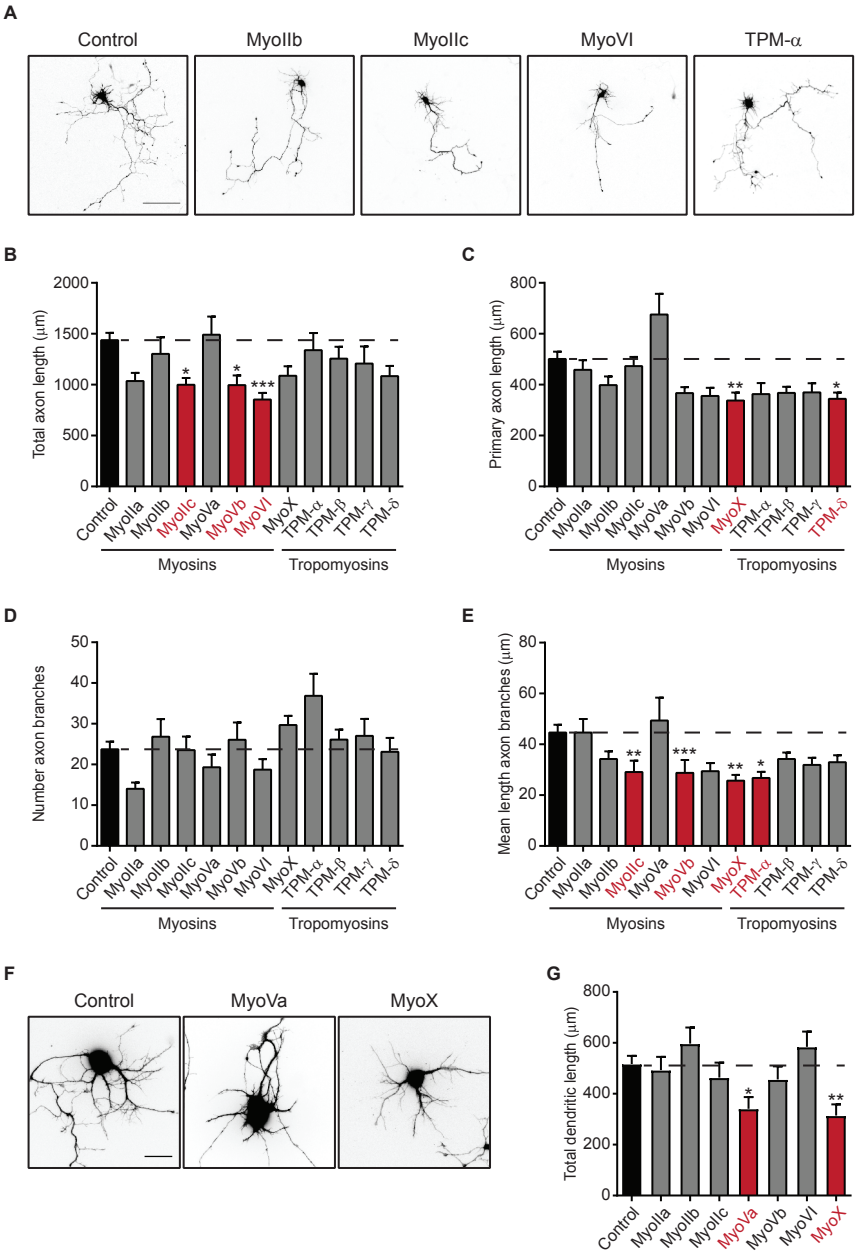

(F) Representative images of the somato-dendritic area of DIV 4 hippocampal neurons transfected at DIV 0 with pSuper (control) or MyoVa-, MyoX-shRNA pools and GFP fill. Scale bar 100 μm.

(G) Quantification of the total dendritic length in DIV 4 hippocampal neurons transfected for 4 days with pSuper (control) or indicated pools of shRNAs and GFP fill. n = 15-19 cells from 2 independent experiments were analyzed per condition (for control, n = 53 cells, N = 3). Kruskal-Wallis test: * $p < 0.05$, ** $p < 0.01$.

Data are represented as mean ± SEM. Red bars indicate $p < 0.05$.

2013), MyoX was shown to be required for proper axon extension in chick commissural and hippocampal neurons (Raines et al., 2012; Zhu et al., 2007). To our knowledge, our study is the first to show that MyoX depletion impaired dendritic development in hippocampal neurons, and future studies could examine if MyoX is localized to dendritic growth cones at the beginning of dendritogenesis.
Altogether, our results show that myosin proteins are involved in the first outgrowth stages of both axonal and dendritic processes in hippocampal neurons.

Myosins are required for axon formation in hippocampal neurons

Since depletion of myosin proteins led to impairments in neurite extension, we wondered if they are also involved in axon specification in hippocampal neurons. Neuronal polarization and axon formation occur within the first 24 hours after plating in dissociated neurons, and depletion of proteins is not effective at this stage. In this way, to determine which proteins are required for axon formation, we need to use an assay that promotes axon formation when the proteins of interest have been depleted in the cell. For this, we use nanomolar doses of the microtubule-stabilizing drug taxol, previously shown to induce the formation of multiple axons in hippocampal neurons (Witte et al., 2008). Neurons were transfected with BFP to highlight neuronal morphology and shRNAs targeting the different myosins at DIV 2, and cells were treated with taxol at DIV 4 for 48 hours. We then immunostained the neurons for the AIS marker pan-NaV channels, and quantified the number of NaV-channels-

Figure 2. MyosinIIs are required for axon initiation in hippocampal neurons. ➤

(A) Representative images of DIV 6 hippocampal neurons transfected with a BFP fill (red) and pSuper (control) or MyoIIc-shRNA pool at DIV 2 and treated at DIV 4 with 10 nM taxol for 48 h. Neurons were immunostained for pan-NaV channels (grey). Arrowheads highlight neurites positive for pan-NaV channels. Scale bar 20 µm.

(B) Average number of pan-NaV channels positive neurites in DIV 6 hippocampal neurons transfected with pSuper, indicated pools of shRNAs or dominant-negative (DN) forms, after treatment with 10 nM Taxol for 48 h. MyoIIb data from a single shRNA. n = 17-42 cells from at least 2 independent experiments (for control, n = 96 cells, N = 4). Kruskal-Wallis test: * $p < 0.05$, ** $p < 0.01$, *** $p < 0.001$.

(C) Same as B, but for the separated shRNAs of MyoIIa and MyoIIc. n = 18-29 cells from 2 independent experiments (for control, n = 55 cells, N = 2). Kruskal-Wallis test: ** $p < 0.01$, *** $p < 0.001$.

(D) Average number of AnkG positive neurites in DIV 6 control or single shRNA-depleted neurons, in the absence of taxol (-taxol). n = 20-35 cells from at least 2 independent experiments (for control, n = 58 cells, N = 5). Kruskal-Wallis test.

(E) Same as D, but neurons were treated at DIV 4 with 10 nM Taxol for 48h (+taxol). n = 13-26 cells from 2 independent experiments (for control, n = 61 cells, N = 5). Kruskal-Wallis test: * $p < 0.05$, ** $p < 0.01$, *** $p < 0.001$.

(F) Representative images of DIV 6 hippocampal neurons transfected with a BFP fill (red) and pSuper (control) or MyoIIb#1 shRNA at DIV 2 and treated at DIV 4 with control medium (-taxol) or 10 nM taxol (+taxol) for 48 h. Neurons were immunostained for AnkG (grey). Arrowheads highlight neurites positive for AnkG. Scale bar 20 µm.

(G) Quantification of different growth cone morphologies in control and single shRNA-depleted neurons. n = 14-35 cells from at least 2 independent experiments (for control, n = 77 cells, N = 6). Kruskal-Wallis test per growth cone type: * $p < 0.05$, ** $p < 0.01$, *** $p < 0.001$.

(H) Representative images of different classes of growth cones in hippocampal neurons. Scale bar 5 µm.

(I) Percentage of neurons with bulbs (growth cone diameter bigger than 7 µm). n = 14-35 cells from at least 2 independent experiments (for control, n = 77 cells, N = 6). Chi-square test: * $p < 0.05$, *** $p < 0.001$.

Data are represented as mean ± SEM. Red bars indicate $p < 0.05$.

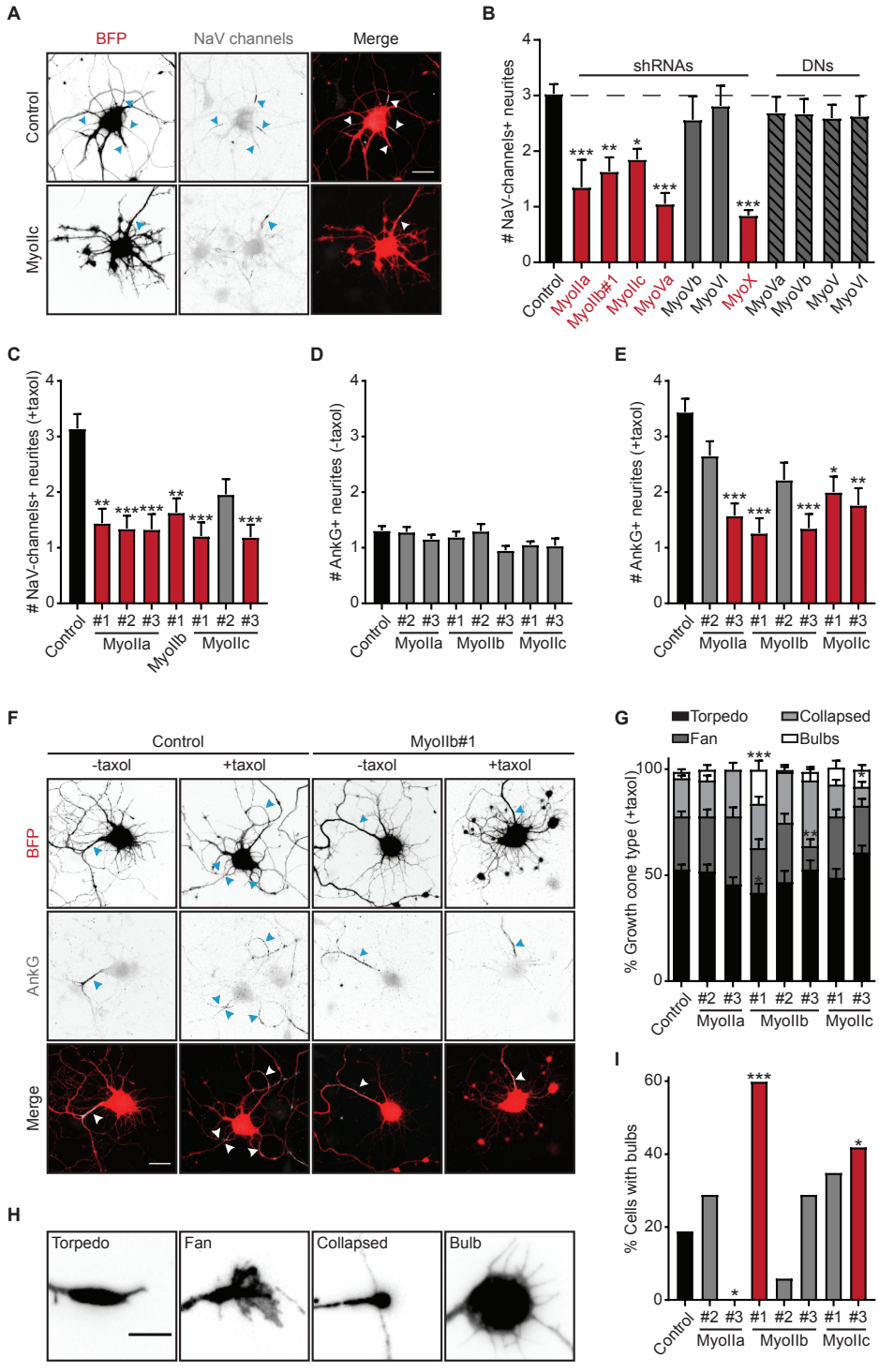
A
BFP
NaV channels
Merge
Control
MyoIIc
B
NaV-channels+ neurites
shRNAs
DNs
Control
MyoIIa
MyoIIb#1
MyoIIc
MyoVa
MyoVb
MyoVI
MyoX
MyoVa
MyoVb
MyoV
MyoVI
C
NaV-channels+ neurites (+taxol)
Control
MyoIIa
MyoIIb
MyoIIc
D
AnkG+ neurites (-taxol)
E
AnkG+ neurites (+taxol)
F
Control
MyoIIb#1
-taxol
+taxol
BFP
AnkG
Merge
G
Torpedo
Fan
Collapsed
Bulbs
% Growth cone type (+taxol)
H
Torpedo
Fan
Collapsed
Bulb
I
% Cells with bulbs

positive neurites per cell (Figure 2A). In non-treated cells, most neurons had one AIS (data not shown), but treatment with taxol increased the average number of NaV-positive neurites by 3-fold (Figure 2A,B). We found that taxol treatment did not promote an increase in the number of NaV-positive neurites in cells depleted of MyoIIa, MyoIIb, MyoIIc, MyoVa and MyoX (Figure 2A,B). More precisely, there was a reduction of at least 39 % in the average number of NaV-positive neurites in the knockdown cells in comparison to control cells (Figure 2B). It was previously shown that the recruitment of MyoX to phosphatidylinositol (3,4,5)-trisphosphate (PIP3) promotes axon formation in hippocampal neurons (Yu et al., 2012), which may explain the effects we observed upon depletion of MyoX in taxol-treated cells.

To block the function of organelle motors MyoVa, MyoVb and MyoVI, we expressed dominant negative variants that only contained the tail domain (DNs). As expected, expression of MyoVb- and MyoVI-DN had similar phenotypes to MyoVb- and MyoVI-depleted cells (Figure 2B). However, the average number of NaV-channels positive neurites in MyoVa-DN-expressing cells was similar to control cells, which was different from cells depleted of MyoVa. It will be important to assess changes on mRNA and protein levels in cells transfected with MyoVa shRNAs constructs, to further understand if our knockdown constructs are working properly and the results we observed are not due to off-target effects.

Our results show that, besides being required for axon extension, myosin proteins may also be important for the specification and formation of the axon in hippocampal neurons. In this way, myosin proteins may be important for the early stages of neuronal polarization, either by regulating actin dynamics or transporting to and confining key proteins in the future axon.

MyosinIIb is important for growth cone morphology

Non-muscle myosin II proteins regulate actin dynamics and play crucial roles in processes that promote cell reshaping and movement (Vicente-Manzanares et al., 2009). In neurons, these proteins have been shown to be important for the retrograde actin flow at growth cones and for synaptic plasticity at dendritic spines (Medeiros et al., 2006; Rex et al., 2010). Our data suggest for a new role of MyoIIa, MyoIIb and MyoIIc in axon formation induced by taxol (Figure 2B). We verified that the effects of MyoIIa and MyoIIc depletion were reproduced by transfecting individual shRNAs (Figure 2C). We then asked if AnkG, the master organizer of the AIS (Jones and Svitkina, 2016), was properly localized in MyoII-depleted cells. We found that, in the absence of taxol, there were no differences between control and depleted cells on AnkG localization to the proximal axon (Figure 2D,F). When we performed taxol treatment, AnkG was affected in a similar manner compared to NaV-channels (Figure 2E,F). Our data suggest that promoting microtubule stabilization with taxol is not sufficient to generate multiple axons in cells where actin dynamics is compromised by the absence of MyoII-induced contractility. Performing knockdown experiments earlier in neuronal development, either before neurons are plated (e.g. electroporation) or soon after plating will be needed to test if MyoIIs are indeed required for the formation of the axon and/or AIS.

We then analyzed growth cone morphology in control and MyoII-depleted cells after treatment with taxol. We found that growth cone morphology was dramatically affected in cells expressing MyoIIb knockdown constructs (Figure 2F,G). In control cells 78 % of the growth cones exhibited a torpedo- or a fan-like shape (elongating or exploratory growth cones, respectively) and hardly any collapsed or bulb-like shape. In contrast, MyoIIb#1- and

MyoIIb#3-depleted cells had almost 40 % of their growth cones in a collapsed- or bulb-like shape (retracting or stationary growth cones, respectively) (Figure 2G,H). Moreover, only 19 % of the control cells exhibited one or more bulb-like growth cones, while this was the case in 60 % of MyoIIb#1-depleted cells (Figure 2I). As the effects on growth cone morphology seem to vary between the different MyoIIb-targeting shRNAs, it will be important to verify the efficiency of knockdown of each shRNA, in order to exclude any off-target effects.

Upon taxol treatment, the increased microtubule stability may promote the appearance of bulb-shaped growth cones in MyoIIb-depleted cells. In this situation, the actin structures at the growth cone of the future axons may be more rigid and less contractile, and therefore less permissive for microtubule invasion needed for axonal outgrowth. Microtubules may become buckled or may even reverse within the growth cone, promoting the expansion of the growth cone area and the formation of the bulb-shaped growth cones. It will be interesting to perform live-imaging studies of plus-end tracking proteins on these structures may help us to understand what happens to microtubules in MyoIIb-depleted cells upon taxol treatment.

MyosinIIb interacts with several actin-binding proteins

We then assessed how MyoIIb is distributed in hippocampal neurons. Both endogenous MyoIIb (Figure 3A, top panel) and N-terminally tagged MyoIIb expression construct (data not shown) were enriched at the tips of neurites of hippocampal neurons, where the growth cones are formed. To analyze the efficiency of MyoIIb knockdown constructs, we transfected neurons with mRFP to highlight neuronal morphology and the shRNAs targeting MyoIIb (MyoIIb-Mix) or empty pSuper. After four days, cells were fixed and stained for endogenous MyoIIb, and we analyzed changes in immunofluorescent signals in the soma and the growth cones of control and MyoIIb-depleted cells (Figure 3A-C). Our preliminary results showed that MyoIIb-targeting shRNAs decreased MyoIIb intensity in the growth cones of hippocampal neurons by ~65 %, while no differences were observed in the intensity of MyoIIb at the soma (Figure 3A-C). To further validate the efficiency of MyoIIb-targeting shRNAs, we electroporated cortical neurons with empty pSuper as control or the different shRNAs before plating the cells. We prepared cortical neuron lysates four days later, and performed Western blot analysis. Our preliminary data showed ~40 % knockdown in MyoIIb intensity in neurons electroporated with either one or combined three shRNAs (MyoIIb-Mix) (Figure 3D,E). Since we found different effects on growth cone morphology with the different MyoIIb-targeting shRNAs (Figure 2G,I), we were not expecting similar depletion levels with the different shRNAs. Future studies are needed to further validate the efficiency of MyoIIb knockdown by immunocytochemistry and western blot analysis.

Axon formation relies on the crosstalk between actin and microtubules, and the specific molecules linking the two cytoskeletal compartments remain to be determined (Pacheco and Gallo, 2016). MyoIIb was previously shown to be involved in the regulation of both actin contractility and microtubule movements within the growth cone (Burnette et al., 2008; Schaefer et al., 2008), but the molecular mechanism of this process has not been determined. Therefore, we performed pull-down experiments combined with mass spectrometry analysis to identify potential interactors of MyoIIb that may provide a link with the microtubule cytoskeleton. Biotinylated and GFP-tagged (bioGFP) MyoIIb construct was co-expressed with the biotin ligase BirA in HEK293 cells, and we performed pull-down assays with rat brain lysate using the cell extracts. Mass spectrometry analysis of brain interactors

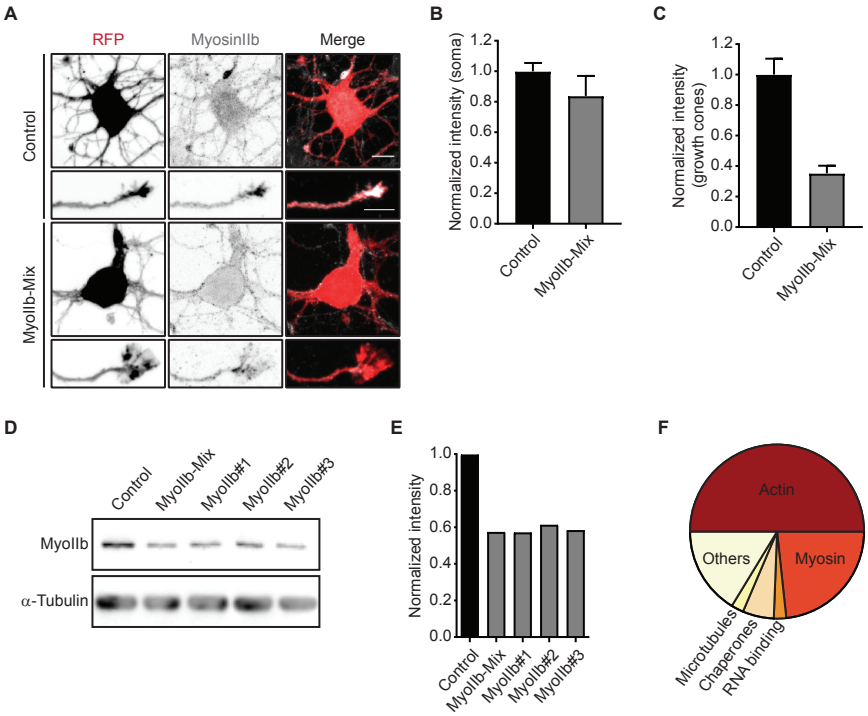

G

Acession	Protein	bio-GFP		bio-GFP-MyoIIb	
		# Peptides	# PSM	# Peptides	# PSM
G3V9Y1	**Myosin, heavy polypeptide 10, non-muscle**	**22**	**34**	**229**	**1838**
V9GZ85	Actin, cytoplasmic 2 (Fragment)	21	124	34	1102
D3ZRN3	Actin, beta-like 2	6	41	15	345
E9PTU4	Myosin-11	5	8	77	323
Q63862	Myosin-11 (fragments)	4	7	57	279
Q62707	Nonmuscle myosin heavy chain-B (Fragment)	5	7	15	261
Q68FP1	Gelsolin	4	8	30	99
F1MA36	Spectrin beta chain	29	31	69	94
Q6AZ25	Tropomyosin 1, alpha	2	2	30	90
Q91XN7	Tropomyosin alpha isoform	2	2	30	89

Figure 3. Characterization of MyosinIIb.

(A) Average intensity projection images of DIV6 hippocampal neurons, co-transfected with pSuper (control) or MyoIIb shRNA pool (MyoII-Mix) and mRFP (red) to highlight neuronal morphology for 4 days. Neurons were stained for endogenous MyoIIb (grey). Upper images show the somatic region, and bottom images show examples of growth cones of the transfected neuron. Scale bar 10 µm.

(B-C) Quantification of endogenous MyoIIb mean intensity in the soma (B) or growth cone (C) regions of neurons expressing pSuper (control) or MyoIIb shRNA pool (MyoII-Mix). Data was normalized to control. n = 7 cells (18 growth cones) from one experiment (for control, n = 10 cells, 47 growth cones, N = 1).

(D-E) Western blot analysis (D) and quantification (E) of lysates of cortical neurons electroporated with empty pSuper vector (control) or MyoIIb-shRNAs for 4 days. The extracts were loaded into 2 separate gels, and one was stained against MyoIIb (upper panel), and the other stained for α-tubulin (bottom panel). Data from one experiment, and normalized to control levels.

(F) Gene ontology analysis results. Brain specific hits were divided into 5 categories related to their molecular function.

(G) Binding partners of bioGFP-MyoIIb in HEK293 cells loaded with rat brain extracts, and identified by mass spectrometry. The table only includes the ten highest brain specific interactors. For the complete list, see Supplementary table 2. PSM, peptide spectrum matches.
Data are represented as mean ± SEM.

confirmed that MyoIIb mainly interacts with actin-related proteins (Figure 3F). In fact, the ten top hits of the brain specific interactors belong to this protein group, such as myosin11 and gelsolin (Figure 3G). Unfortunately, we did not detect novel proteins that could mediate the crosstalk between the actin and microtubule cytoskeletons.

An alternative hypothesis is that MyoIIb may act as a signaling hub for molecules that can translate extracellular cues to intracellular signaling pathways that control cytoskeleton dynamics at the growth cone of the future axon. In our mass spectrometry result lists (Supplementary table 2), we find MyoXVIIIa, a protein previously shown to co-assemble with MyoII to form mixed bipolar filaments (Billington et al., 2015). In this study, it was suggested that MyoXVIIIa may allow the recruitment of specific molecules to MyoII filaments, via its PDZ domains. Even though no roles for MyoXVIIIa have been addressed in neurons so far, it will be interesting to study if MyoXVIIIa regulates the formation of MyoII filaments in the growth cones of hippocampal neurons during neuronal polarization, or if it promotes the localization of specific molecules to the MyoII filaments.

Altered cytoskeleton organization in MyoIIb-depleted neurons

Recently, van Beuningen et al. showed that the tripartite motif containing protein 46 (TRIM46) is enriched in the proximal part of the axon, where it bundles microtubules into closely spaced arrays with their plus-end out (van Beuningen et al., 2015). Moreover, loss of TRIM46 disrupts both axon formation and AnkG clustering at the AIS, showing that TRIM46 is required for axon specification and neuronal polarization (van Beuningen et al., 2015). Therefore, we tested if TRIM46 localization was affected by depletion of MyoIIb. Even though the location and length of the TRIM46 stretch at the AIS was not different from control cells, MyoIIb-depleted cells showed a ~40 % reduction in the TRIM46 intensity signal at the proximal axon (Figure 4A-C). These results suggest that MyoIIb may be required for the maintenance of TRIM46 at the proximal axon. Even though depletion of MyoIIb did not impair axonal outgrowth (Figure 1), our results suggest that these cells may have defects in their microtubule cytoskeleton at the AIS. To further investigate this, we analyzed the intensity profiles of microtubule-associated proteins Map2 and Tau within the first 50 µm of the axon in fully polarized neurons at DIV 6 (Figure 4D). We found that Map2 intensity profile was unchanged in knockdown cells (Figure 4E). Our preliminary data showed that there is a peak in Tau intensity at ~25 µm away from the soma in control cells (~172 % from the soma intensity) (Figure 4E). In MyoIIb-depleted cells, Tau intensity profile was changed, with the highest peak being less pronounced than in control cells (~118 % from the soma intensity) (Figure 4E). We also quantified the intensity of microtubule plus-end-binding (EB) proteins EB1 and EB3 in the soma and AIS of DIV 6 neurons. MyoIIb depletion significantly increased the staining intensity of EBs at the soma of transfected cells, while it was reduced by ~20 % at the AIS (Figure 4F,G). The increase in the staining intensity of EBs at the soma was due to a ~20 % increase in the density of EB comets in the soma (Figure 4H). A similar increase in intensity of EB proteins at the soma has been reported upon AnkG depletion in hippocampal neurons (Leterrier et al., 2011), suggesting that EB intensity/staining relies on

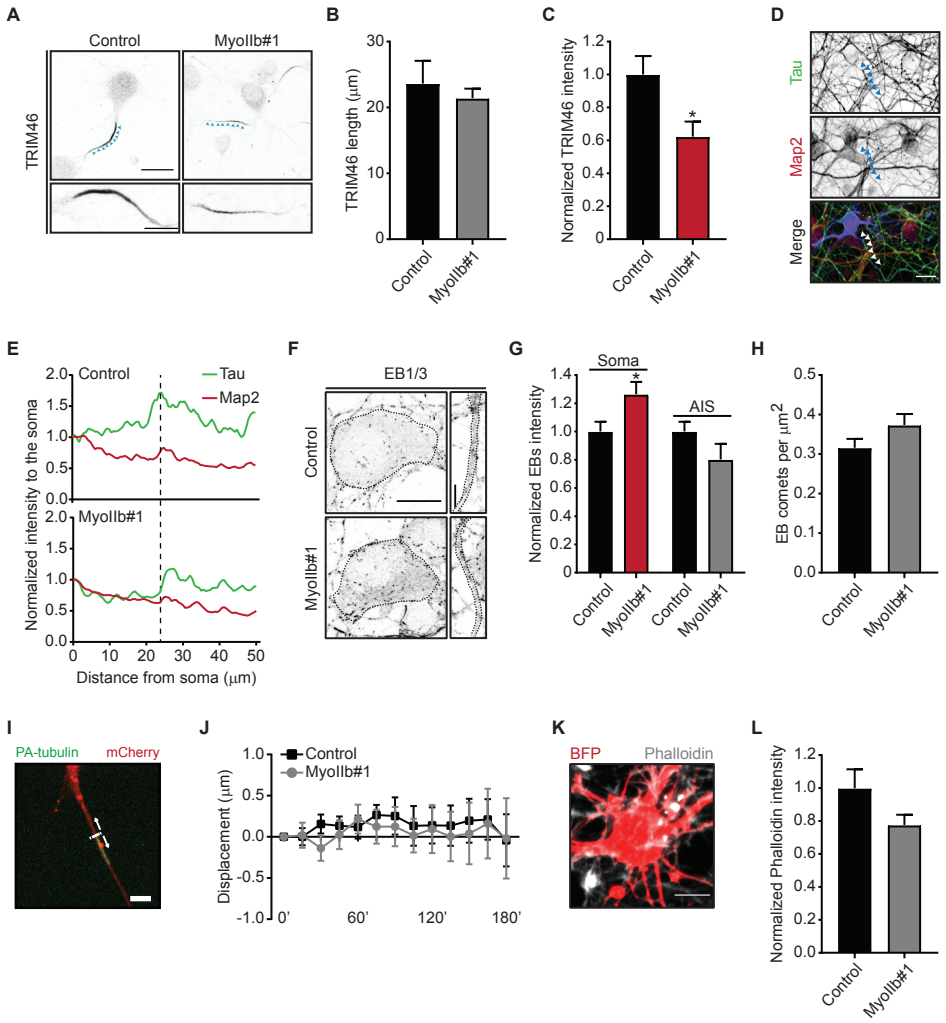

Figure 4. MyoIIb knockdown affects the microtubule and actin cytoskeletons.

(A) Representative images of hippocampal neurons at DIV 6 co-transfected at DIV 2 with control (pSuper) or MyoIIb#1 shRNA and β-galactosidase (β-gal) to highlight neuronal morphology, and stained for TRIM46 and β-gal. Blue arrowheads indicate TRIM46 positive neurites. Images are average intensity projections. Scale bar 20 μm (up) and 10 μm (bottom).

(B-C) Quantification of TRIM46 staining length (B) and average normalized fluorescent intensity (C) in control and MyoIIb#1-depleted neurons. n = 17-22 cells from 2 independent experiments. Mann-Whitney test: * $p < 0.05$.

(D) Average intensity projection images of a DIV 6 hippocampal neuron transfected with β-gal to highlight neuronal morphology and immunostained for β-gal (blue), Tau (green) and Map2 (red), in the absence of taxol. Arrowheads indicate the beginning of the axon. Scale bar 20 μm.

(E) Quantification of the average normalized fluorescent intensity profiles of Tau (green) and Map2 (red) in the first 50 μm of the axon in control (upper diagram) and MyoIIb#1-depleted (bottom diagram) neurons in the absence of taxol. Intensities were normalized to the beginning of the axon. n = 18-20 cells from 2 independent experiments.

(F) Hippocampal neurons at DIV 6 co-transfected at DIV 2 with control (pSuper) or MyoIIb#1 shRNA and

β-galactosidase (β-gal) to highlight neuronal morphology, and stained for EB1/3 and β-gal. Images are maximum intensity projections of the soma (left) and the AIS (right) regions. Scale bar 10 μm (left) and 5 μm (right).
(G-H) Quantification of endogenous EB1/3 average normalized fluorescent intensity in the soma and AIS regions (G) and the number of EB1/3 comets per μm² in the soma (H) in control and MyoIIb#1-depleted neurons. n = 22-24 cells from 2 independent experiments. Mann-Whitney test: * $p < 0.05$.
(I-J) Representative image (I) and quantification (J) of microtubule displacement in live DIV 4 control and MyoIIb#1 KD neurons, transfected with mCherry fill (red), PA-GFP-α-Tubulin (green) and empty pSuper (control) or MyoIIb#1 shRNA for 3 days. Dashed line represents the region from which the displacement was quantified. n = 13 cells from 2 independent experiments. Two-way ANOVA. Time in minutes. Scale bar 5 μm.
(K) Hippocampal neuron at DIV6 expressing BFP fill (red) and pSuper (control) for 4 days, and immunostained for actin filaments using Phalloidin A568 (grey). Image is an average intensity projection. Scale bar 10 μm.
(L) Quantification of Phalloidin intensity in control and MyoIIb-depleted neurons. Intensities were normalized to control. n = 11-12 cells from one experiment.
Data are represented as mean ± SEM. Red bars indicate $p < 0.05$.

the presence of an intact AIS scaffold. The decreased TRIM46 and Tau levels and the effects on EBs suggest that MyoIIb may be required for the integrity of the axon and the AIS scaffold, indirectly affecting the underlying microtubule cytoskeleton.

As we found that the microtubule cytoskeleton is affected at the proximal axon, we next addressed if microtubule mobility is affected upon MyoIIb depletion. We tracked the movement of photoactivated patches of microtubules at the proximal axon (Figure 4I), and found no differences between control and MyoIIb knockdown cells (Figure 4J). Our data indicate that MyoIIb does not affect the displacement of microtubules in the proximal axon, suggesting that the lack of response to taxol in MyoIIb-depleted cells is not due to defects on the transport of microtubules. Interestingly, MyoIIs were shown to be negative regulators of the bulk translocation of microtubules at the axonal growth cone (Roossien et al., 2014). It will be interesting to repeat the photoactivation experiments further in the axon or even at the axonal growth cone upon depletion of MyoIIb.

We also quantified changes in the actin cytoskeleton in polarized neurons at DIV 6, by labeling actin filaments with phalloidin (Figure 4K). Our preliminary results showed that knockdown of MyoIIb leads to a ~20 % reduction in the phalloidin soma intensity (Figure 4L). Future studies will be necessary to quantify the levels of phalloidin intensity in the axonal growth cones of MyoIIb-depleted cells. Altogether, our data suggest that MyoIIb expression levels are important for the taxol-induced axon formation, by mediating changes in the underlying actin and microtubule cytoskeleton.

FUTURE PERSPECTIVES

In this chapter, we have performed a targeted knockdown screen to identify myosin proteins involved in axon formation and outgrowth, and identified MyoIIb as a regulator of axon formation in hippocampal neurons. We found that, upon taxol treatment, MyoIIb-depleted cells did not develop multiple axons and exhibited bulb-shaped growth cones. Moreover, we found that the microtubule cytoskeleton is affected at the beginning of the axon. Two possible non-exclusive mechanisms may be the basis for our results, one happening at the growth cone and the other at the AIS. At the growth cone, actomyosin structures termed actin arcs are present, which play a role in retrograde actin flow and actin bundle recycling (Medeiros et al., 2006). Moreover, these structures exert contractile forces required for the

bundling of microtubules at the growth cone neck (Burnette et al., 2008). The formation of bulbs in MyoIIb-depleted cells may be related to a compromise on the microtubule bundling, an important feature of shaft consolidation during neuronal outgrowth (Schaefer et al., 2008). Hence, we hypothesize that microtubule dynamics and distribution may be affected in the growth cone of the future axon, promoting the formation of bulbs upon taxol-treatment. It will be important to address this by performing local uncaging of taxol (Witte et al., 2008) in a random neurite of undifferentiated neurons, and assess the distribution of dynamic microtubules within the formed growth cone at the tip of the selected neurite.

The defects we have observed at the proximal axon may be due to changes on the establishment of the AIS itself. At the AIS, EB proteins provide a functional link between the AIS microtubules and AnkG, and this is important for neuronal polarization and AIS formation (Fréal et al., 2016; Leterrier et al., 2011). Previously, it was shown that loss of AnkG leads to an upregulation of EB proteins in the soma, suggesting that AnkG may be important to capture axonal microtubules at the AIS (Leterrier et al., 2011). Here, we also found an upregulation of EBs in the soma upon MyoIIb knockdown, and a ~20 % decrease in the intensity of EBs at the AIS. The reduction of EB levels at the AIS in MyoIIb-depleted cells may suggest a loss in the link between microtubules and AnkG at the AIS, which may contribute to the observed defects in the microtubule cytoskeleton at the AIS. Future live-imaging studies on EB behavior at the AIS (Fréal et al., 2016) will be important to further understand the effect of myosin depletion on the AIS microtubule cytoskeleton. Moreover, as TRIM46 is required for the uniform distribution of microtubules along the axon (van Beuningen et al., 2015), it will be interesting to address if the reduction in TRIM46 levels upon MyoIIb depletion affects the distribution of microtubules along the axon. As we find cytoskeletal defects in both the growth cone and the proximal axon, it is also plausible that signals from the growth cone into the axon induce changes at the cytoskeleton in the proximal axon or vice-versa. In this way, the hypothesized effect on microtubule bundling at the growth cone of MyoIIb-depleted cells may promote defects on the cytoskeleton throughout the whole axon, including the AIS. On the other hand, the changes at the proximal axon may be propagated into the axon, promoting changes at the microtubule cytoskeleton at the growth cone.

One important future direction is to address if MyoIIb is normally located at the AIS. Until now, MyoIIs have been shown to be present at growth cones and at distal actin patches along the axon (Loudon et al., 2006) . Actin patches are also found along the AIS, where they are proposed to be important for filtering mechanisms to exclude non-axonal cargo from the axon (Watanabe et al., 2012). Even though not very abundant, the AIS actin patches are also observed in young neurons, at the time the AIS is established (Watanabe et al., 2012). Hence, besides the role on filtering, it is tempting to speculate that the patches may also be important to provide an initial actin scaffold for AIS formation. It is not known how these actin patches are established and regulated, and if they contain dynamic or stable actin filaments along the patch. One hypothesis could be that MyoIIs play a role in the establishment of actin patches, by providing cross-linking and contractility to the filaments. It will be interesting to address if the filtering capability of the AIS is changed upon depletion of MyoIIb. In case the actin patches are required for AIS establishment, it will also be interesting to address if this role depends on MyoIIb activity.

Overall, our study opens new doors for the study of non-muscle myosin IIb in the establishment of neuronal polarity, and may help to provide new clues on the crosstalk between actin and microtubules within the axon.

AUTHOR CONTRIBUTIONS

C.P.F. wrote the manuscript and composed all figures with advice of C.J.W. and C.C.H. C.P.F. performed and analysed all the experiments, except the experiments in Figure 4I-J, which were performed by E.T. Pull-down assay and mass spectrometry experiments were performed by R.S. under the supervision of A.F.M.A. and C.C.H. C.P.F. and C.C.H designed the study. C.J.W. and C.C.H. supervised the research.

ACKNOWLEDGMENTS

We would like to thank J. Lipka for cloning constructs used in this study. This work was supported by the Netherlands Organization for Scientific Research (NWO-ALW-VICI, C.C.H.), the European Research Council (ERC) (ERC Consolidator Grant, C.C.H.), and the Dutch Technology Foundation STW, which is part of the NOW (to C.C.H.). C.P.F. is supported by the People Programme (Marie Curie Actions; MC-ITN) of the European Union's Seventh Framework Programme FP7/2007-2013/ under REA grant agreement 473 289581. E.T. is supported by the Spanish Education Ministry and an FP7 European Union Marie Curie postdoctoral fellowship.

MATERIALS AND METHODS

Animals

All animal experiments were performed in compliance with the guidelines for the welfare of experimental animals issued by the Federal Government of The Netherlands. All animal experiments were approved by the Animal Ethical Review Committee (DEC) of Utrecht University.

Antibodies and reagents

The following antibodies were used in this study: goat anti-MyoIIb (catalog number SC-47205, Santa Cruz Biotechnology), mouse anti-AnkyrinG (clone 4G3F8, Zymed), rabbit anti-Trim46 (van Beuningen et al., 2015), mouse anti-pan-Nav (clone K58/35, Sigma-Aldrich), rabbit anti-Map2 (4542, Cell Signaling), mouse anti-Tau (MAB3420, Chemicon), mouse anti-α-tubulin (clone B-5-1-2, Sigma-Aldrich), mouse anti-EB1 (clone 5/EB1, BD Biosciences), mouse anti-EB3 (BD Biosciences), chicken anti-β-galactosidase (BGL-1040, AvesLab), Phalloidin conjugated to Alexa568 (Life Technologies), Alexa Fluor 405-, Alexa488- and Alexa568-conjugated secondary antibodies (Life Technologies), and anti-goat/mouse IgG antibody conjugated to horseradish peroxidase (DAKO). Reagents used in this study include Taxol (T7402, Sigma-Aldrich).

Expression and shRNA constructs

The following mammalian expression plasmids were described previously: pβ-actin (Kapitein et al., 2010a), pGW2 (Kapitein et al., 2010a), Bio-tag-GFP (Jaworski et al., 2009) and pSuper (Brummelkamp et al., 2002). pβactin-GFP was generated by inserting GFP in the SalI and NotI sites of pβ-actin, whereas pGW2-tagBFP was generated by inserting tagBFP in the HindIII and AscI sites of pGW2-CMV. HA-BirA and pβactin-HA-β-Galactosidase were described previously (de Boer et al., 2003; Hoogenraad et al., 2005). pEGFP-C3 MyoIIb was bought from Addgene (catalog number 11348), and it was used to amplify human full-length MyoIIb by PCR strategy and to subclone it in the Bio-GFP expression vector using the AscI and NotI restriction sites to generate a Bio-GFP MyoIIb construct. PA-GFP-α-Tubulin was created by replacing YFP of YFP-α-Tubulin (Clontech) with PA-GFP (Patterson and Lippincott-Schwartz, 2002). All shRNAs used in this study are indicated in Supplementary table 1. All shRNAs targeting rat myosin and tropomyosins mRNAs were designed using the siRNA selection program at the Whitehead Institute for Biomedical Research, and were ligated into the BglII and HindIII sites of pSuper vector. Myosin-IIb shRNA #1 was

described previously (Rex et al., 2010).

Primary hippocampal neuron culture, transfection and immunocytochemistry

Primary hippocampal cultured neurons from embryonic day 18 (E18) rat brains were prepared as described previously (Kapitein et al., 2010b). In brief, neurons were plated on coverslips coated with poly-L-lysine (37.5 µg/mL) and laminin (1.25 µg/mL) at a density of 100.000 per well, and grown in Neurobasal medium supplemented with 0.5 mM glutamine, 15.6 µM glutamate, 2 % B27 and 1 % penicillin/streptomycin. Hippocampal neurons were transfected at different days-in-vitro (DIV) using Lipofectamine 2000 (Invitrogen). Briefly, DNA (1.8 µg / well, for a 12-well plate) was mixed with 3.3 µL Lipofectamine 2000 in 200 µL NB, incubated for 30 minutes and then added to the neurons in Neurobasal supplemented with 0.5 mM glutamine at 37 °C in 5 % CO_2 for 90 minutes. Next, neurons were washed with Neurobasal and transferred to the conditioned medium at 37 °C in 5 % CO_2 for 3 or 4 days. For taxol treatments, neurons were treated at DIV 4 (two days after transfection) with 10 nM taxol dissolved in complete Neurobasal medium for 48 hours.

To perform immunostainings, dissociated hippocampal neurons were fixed with 4 % paraformaldehyde (PFA)/4 % sucrose in phosphate buffer (PBS) at room temperature for 10 minutes, or with methanol at -20 °C for 2 minutes, followed by 4 % PFA/4 % sucrose at room temperature for 8 minutes. Cells were then washed 3 times for 5 minutes in PBS at room temperature, and incubated with the primary antibody mix in GDB buffer (0.2 % Gelatin, 0.9 M NaCl, 0.6 % Triton X-100, 33.3 mM phosphate buffer, pH 7.4) overnight at 4°C. Neurons were washed 3 times for 5 minutes in PBS at room temperature, and incubated with the secondary antibody mix in GDB buffer for 1 hour at room temperature. After washing 3 times in PBS, the coverslips were mounted on slides using Vectashield mounting medium (Vector Labs) or Mowiol.

Primary cortical neuron culture and electroporation

Primary cortical cultured neurons were prepared from embryonic day 18 (E18) rat brains. Cells (1.2 x 10^6) were transfected using the AMAXA Rat Neuron Nucleofector kit (Lonza) with 3 µg of DNA, and plated on wells (for western blot analysis) coated with poly-L-lysine (37.5 µg/ml) and laminin (1.25 µg/ml). In short, cells were pelleted for 5 minutes at 200g, and ressuspended in NucleofectorTM solution supplemented with FCS. The cells were then added to the DNA, electroporated and plated in DMEM medium containing 10 % FCS. Cells were allowed to recover and adhere at 37 °C in 5 % CO_2. After an incubation of 4 hours, the medium was replaced by Neurobasal medium supplemented with 0.5 mM glutamine, 15.6 µM glutamate, 2 % B27 and 1 % penicillin/streptomycin. Cells were grown at 37 °C in 5 % CO_2 for four days prior to lysis and Western blot analysis.

Western blotting

Cortical neuron lysates were prepared at DIV 4 by aspirating the medium and scraping cells directly in sample buffer containing DTT and protease inhibitors (Roche) on ice. After scraping, samples were boiled for 10 minutes. Samples were loaded equally and ran on gradient 6% and 15% SDS-PAGE gels, and transferred to nitrocellulose membranes using a wet blotting setup. After blocking with 2 % BSA in 0.1 % Tween/PBS for 1 hour, the blots were incubated with the primary antibody mix diluted in blocking solution overnight at 4 °C. After washing 3 times in 0.1 % Tween/PBS, the membranes were incubated with the secondary antibodies conjugated to horseradish peroxidase for 1 hour at room temperature. Membranes were then washed 2 more times in 0.1 % Tween/PBS, and for a third time using 1x PBS. Blots were developed using enhanced chemiluminescent Western Blotting substrate and ImageLab software (BioRad).

Biotin-streptavidin pull-down assay and mass spectrometry analysis

For whole brain extracts, a whole brain from an adult female rat was homogenized in lysis buffer (50 mM Tris-HCl, 150 mM NaCl, 0.1 % SDS, 0.2 % NP-40, and protease inhibitors (Roche)) in a 1:10 brain (g) to lysis buffer (mL) ratio. Samples were sonicated and centrifuged at 900 rpm for 15 minutes.

For biotin-streptavidin pull-down assays, HEK-293 cells were cultured in Ø10 cm cell culture dishes at 37 °C and 5 % CO_2, and transfected with BirA and Bio-GFP constructs using polyethylenimine (PEI) transfection reagent (Polysciences). After 48 h, cells were washed and lysed in RIPA lysis buffer (50 mM Tris-HCl pH 7.4-7.8, 150

mM NaCl, 1 % Triton X-100, 0.1 % SDS, 0.5 % sodium deoxycholate) supplemented with protease inhibitors (Roche). Cells were centrifuged at 13.000 rpm for 15 minutes at 4 °C and the supernatants were incubated with Dynabeads M-280 (blocked in chicken egg albumin, Life Technologies) for 1 h at 4 °C. Beads were separated using a magnet rack (Dynal, Invitrogen) and washed five times in washing buffer (20mM Tris-HCl pH 7.4-7.8, 150 mM KCl, 0.1% Triton X-100). Samples were collected at this point for AP-MS analysis of HEK293 cells expressing each construct. For the bio-GFP pull-down with whole brain extracts, pre-incubated Dynabeads with HEK293 cell extracts expressing each construct were washed twice in low salt washing buffer (20 mM Tris-HCl pH 7.4-7.8, 100 mM KCl, 0.1 % Triton X-100), followed by two wash steps in high salt wash buffer (20 mM Tris-HCl pH 7.4-7.8, 500 mM KCl, 0.1 % Triton X-100) and two final wash steps in low salt washing buffer (20 mM Tris-HCl pH 7.4-7.8, 100 mM KCl, 0.1 % Triton X-100) to remove binding proteins from HEK293 cells. Brain lysates were centrifuged at 16.000 g for 15 min at 4°C, and the supernatant was incubated with the Dynabeads containing bio-GFP or bio-GFP-MyoIIb for 2 h at 4 °C and washed in low salt washing buffer five times. For mass spectrometry analysis, beads were resuspended in 15 µL of 4x Laemmli Sample buffer (Biorad) and supernatants were loaded on a 4-12 % gradient Criterion XT Bis-Tris precast gel (Biorad). The gel was fixed with 40 % methanol and 10 % acetic acid and then stained for 1 h using colloidal Coomassie dye G-250 (Gel Code Blue Stain Reagent, Thermo Scientific). Each lane from the gel was cut in 3 pieces, destained and digested using trypsin, as described in (Ekkebus et al., 2013). Briefly, after placed in 0.5-mL tubes, the pieces were washed with 250 µL of water, followed by 15 min dehydration in acetonitrile. Proteins were reduced (10 mM dithiothreitol, 1 h at 56 °C), dehydrated and alkylated (55 mM iodoacetamide, 1 h in the dark). After two rounds of dehydration, trypsin (Promega) was added to the samples (20 µL of 0.1 mg/mL trypsin in 50 mM Ammoniumbicarbonate) and incubated overnight at 37 °C. Peptides were extracted with acetonitrile, dried down and reconstituted in 10 % formic acid prior mass spectrometry analysis.

All samples were analyzed on aOrbitrap Q-Exactive mass spectrometer (Thermo Fisher Scientific, Germany) coupled to an Agilent 1290 Infinity LC (Agilent Technologies). Mass spectrometry was performed as described previously (Frese et al., 2017). For data analysis, raw files were processed using Proteome Discoverer 1.4 (Thermo Fisher Scientific, Germany). Database searches were performed either using the Human Uniprot database or the rat Uniprot database and Mascot (Matrix Science, UK) as the search engine. Positive protein hits were manually checked and interpreted as valid hits or discarded based on their presence in the negative control (pull-down with Bio-GFP alone).

Photoactivation experiments

For photoactivation experiments, neurons were transfected as previously described, and imaged on an inverted research microscope Nikon Eclipse Ti-E (Nikon) with perfect focus system (PFS) (Nikon), equipped with Nikon CFI Apo TIRF 100x 1.49 N.A. oil objective (Nikon), CoolSNAP HQ2 CCD camera (Roper Scientific) and controlled by MetaMorph 7.7 software (Molecular Devices). The experiments were performed using the ILas2 system (Roper Scientific). Coverslips (18 mm) were mounted in metal rings and maintained at 37 °C and 5 % CO_2 in a stage top incubator INUBG2E-ZILCS (Tokai Hit). Photoactivation of PA-GFP-α-Tubulin was done by scanning the desired region 3 times at 10 % laser power with a Vortran Stradus 405 nm (100 mW) laser. A rectangular region of PA-GFP-α-tubulin was photoactivated in the proximal axon, and tracked for a total imaging period of 225 minutes (images were taken at every 15 minutes).

Confocal microscopy

High resolution confocal laser scanning microscopy was performed on a Zeiss LSM-700 system with a Plan-Apochromat 20x, 40x and 63x objectives. Each image was a z-series comprising enough stacks to cover the whole transfected neuron, and each image was averaged 4 times. The confocal settings were kept constant during all imaging experiments, when fluorescence intensity between different conditions was analysed.

Image analysis and quantification

Image processing and analysis was performed using ImageJ (US National Institute of Health), MatLab (MathWorks) and/or MetaMorph (Molecular Devices). For the quantification of intensities, confocal images were processed using average intensity projections. For the remaining analysis, confocal images were processed using maximum intensity

projections.

Morphometric analysis. For analysis of axon morphology, GFP was used as a cell-fil, and images were acquired using Olympus BX53 upright fluorescent microscope using a 10x/0.30 NA UplanFL objective (Olympus). The axon was identified as the non-MAP2 positive neurite. Only neurons with clearly defined neuronal arborization and no overlapping neighboring cells were imaged and analyzed. All neurites and branches were quantified using ImageJ software and the NeuronJ plugin (Meijering et al., 2004). The axon length was determined by tracing the longest neurite, and total axonal length was calculated as the sum of the length of the axon and its branches. The total dendritic length was calculated as the sum of the length of all primary dendrites and their branches.

Quantification of endogenous EB comets. Confocal images were acquired using a LSM700 confocal microscope with a Plan-Apochromat 63x/1.40 NA objective. ImageJ plugin ComDet was used to quantify the number of EB1/3 comets (https://github.com/ekatrukha/ComDet).

Quantification AIS intensities. Confocal images were acquired using a LSM700 confocal microscope with a Plan-Apochromat 63x/1.40 NA objective. The quantification of fluorescence intensities profiles of different AIS proteins was performed using custom Matlab program (together with description is available at https://github.com/ekatrukha/AIS) as previously described (van Beuningen et al., 2015). AIS length was determined by quantifying intensity above a threshold, and the average intensity was quantified along the determined length.

Quantification Map2 and Tau intensities. Confocal images were acquired using a LSM700 confocal microscope with Plan-Apochromat 20x/0.8 NA objective. From the soma, the first 50 µm of axon were traced using the β-galactosidase staining as the cell-fill, and the intensity profiles were determined in this length.

Quantification of microtubule displacement. Displacement of the region nearest to the soma (dashed line) was measured relative to the cell body (negative values relate to movement towards the soma, and positive values relate to movement towards the distal axon).

Quantification of knockdown efficiency in hippocampal neurons. For the quantification of the knockdown efficiency in hippocampal neurons, growth cones and the soma were manually traced, and the average intensity was measured using ImageJ. The mean intensities were corrected for background intensities.

Statistics

Data are represented as mean values ± standard error of the mean, unless stated otherwise. Statistical analysis was performed using GraphPad Prism software. For the comparison of multiple groups, we used the Kruskal-Wallis test followed by a posthoc Dunn's comparison test. For the comparison between control and knockdown, we used a two-tailed t-test or a two-tailed Mann-Whitney test. For comparison of percentages, we used the Chi-square test. The used test is stated in each figure legend.

Differences between control and treatment were considered significant when $p < 0.05$ (*, $p < 0.05$; **, $p < 0.01$; ***, $p < 0.001$). In all figure legends and text, N indicates the number of independent experiments, and n indicates the number of cells analyzed.

REFERENCES

Al-Bassam, S., Xu, M., Wandless, T.J., and Arnold, D.B. (2012). Differential trafficking of transport vesicles contributes to the localization of dendritic proteins. Cell Rep. 2, 89-100.

Billington, N., Beach, J.R., Heissler, S.M., Remmert, K., Guzik-Lendrum, S., Nagy, A., Takagi, Y., Shao, L., Li, D., Yang, Y., et al. (2015). Myosin 18A coassembles with nonmuscle myosin 2 to form mixed bipolar filaments. Curr. Biol. 25, 942-948.

Bradke, F., and Dotti, C.G. (1999). The role of local actin instability in axon formation. Science 283, 1931-1934.

Brettle, M., Patel, S., and Fath, T. (2016). Tropomyosins in the healthy and diseased nervous system. Brain Res. Bull. 126, 311-323.

Brummelkamp, T.R., Bernards, R., and Agami, R. (2002). A system for stable expression of short interfering RNAs in mammalian cells. Science 296, 550-553.

Burnette, D.T., Ji, L., Schaefer, A.W., Medeiros, N.A., Danuser, G., and Forscher, P. (2008). Myosin II activity facilitates microtubule bundling in the neuronal growth cone neck. Dev. Cell 15, 163-169.

Curthoys, N.M., Freittag, H., Connor, A., Desouza, M., Brettle, M., Poljak, A., Hall, A., Hardeman, E., Schevzov, G., Gunning, P.W., et al. (2014). Tropomyosins induce neuritogenesis and determine neurite branching patterns in B35 neuroblastoma cells. Mol. Cell. Neurosci. 58, 11-21.

de Boer, E., Rodriguez, P., Bonte, E., Krijgsveld, J., Katsantoni, E., Heck, A., Grosveld, F., and Strouboulis, J. (2003). Efficient biotinylation and single-step purification of tagged transcription factors in mammalian cells and transgenic mice. Proc. Natl. Acad. Sci. USA 100, 7480-7485.

Dotti, C.G., Sullivan, C.A., and Banker, G.A. (1988). The establishment of polarity by hippocampal neurons in culture. J. Neurosci. 8, 1454-1468.

Ekkebus, R., van Kasteren, S.I., Kulathu, Y., Scholten, A., Berlin, I., Geurink, P.P., de Jong, A., Goerdayal, S., Neefjes, J., Heck, A.J., et al. (2013). On terminal alkynes that can react with active-site cysteine nucleophiles in proteases. J. Am. Chem. Soc. 135, 2867-2870.

Fréal, A., Fassier, C., Le Bras, B., Bullier, E., De Gois, S., Hazan, J., Hoogenraad, C.C., and Couraud, F. (2016). Cooperative Interactions between 480 kDa Ankyrin-G and EB Proteins Assemble the Axon Initial Segment. J. Neurosci. 36, 4421-4433.

Frese, C.K., Mikhaylova, M., Stucchi, R., Gautier, V., Liu, Q., Mohammed, S., Heck, A.J., Altelaar, A.F., and Hoogenraad, C.C. (2017). Quantitative Map of Proteome Dynamics during Neuronal Differentiation. Cell Rep. 18, 1527-1542.

Hoogenraad, C.C., Milstein, A.D., Ethell, I.M., Henkemeyer, M., and Sheng, M. (2005). GRIP1 controls dendrite morphogenesis by regulating EphB receptor trafficking. Nat. Neurosci. 8, 906-915.

Jaworski, J., Kapitein, L.C., Gouveia, S.M., Dortland, B.R., Wulf, P.S., Grigoriev, I., Camera, P., Spangler, S.A., Di Stefano, P., Demmers, J., et al. (2009). Dynamic microtubules regulate dendritic spine morphology and synaptic plasticity. Neuron 61, 85-100.

Jones, S.L., and Svitkina, T.M. (2016). Axon Initial Segment Cytoskeleton: Architecture, Development, and Role in Neuron Polarity. Neural Plast. 2016, 6808293.

Kapitein, L.C., Schlager, M.A., van der Zwan, W.A., Wulf, P.S., Keijzer, N., and Hoogenraad, C.C. (2010a). Probing intracellular motor protein activity using an inducible cargo trafficking assay. Biophys. J. 99, 2143-2152.

Kapitein, L.C., Yau, K.W., and Hoogenraad, C.C. (2010b). Microtubule dynamics in dendritic spines. Methods Cell Biol. 97, 111-132.

Katsuno, H., Toriyama, M., Hosokawa, Y., Mizuno, K., Ikeda, K., Sakumura, Y., and Inagaki, N. (2015). Actin Migration Driven by Directional Assembly and Disassembly of Membrane-Anchored Actin Filaments. Cell Rep. 12, 648-660.

Kneussel, M., and Wagner, W. (2013). Myosin motors at neuronal synapses: drivers of membrane transport and actin dynamics. Nat. Rev. Neurosci. 14, 233-247.

Leterrier, C., Vacher, H., Fache, M.P., d'Ortoli, S.A., Castets, F., Autillo-Touati, A., and Dargent, B. (2011). End-binding proteins EB3 and EB1 link microtubules to ankyrin G in the axon initial segment. Proc. Natl. Acad. Sci. USA 108, 8826-8831.

Lewis, T.L., Jr., Mao, T., and Arnold, D.B. (2011). A role for myosin VI in the localization of axonal proteins. PLoS Biol. 9, e1001021.

Lewis, T.L., Jr., Mao, T., Svoboda, K., and Arnold, D.B. (2009).

Myosin-dependent targeting of transmembrane proteins to neuronal dendrites. Nat. Neurosci. 12, 568-576.

Lin, W.H., Hurley, J.T., Raines, A.N., Cheney, R.E., and Webb, D.J. (2013). Myosin X and its motorless isoform differentially modulate dendritic spine development by regulating trafficking and retention of vasodilator-stimulated phosphoprotein. J. Cell Sci. 126, 4756-4768.

Loudon, R.P., Silver, L.D., Yee, H.F., Jr., and Gallo, G. (2006). RhoA-kinase and myosin II are required for the maintenance of growth cone polarity and guidance by nerve growth factor. J. Neurobiol. 66, 847-867.

Medeiros, N.A., Burnette, D.T., and Forscher, P. (2006). Myosin II functions in actin-bundle turnover in neuronal growth cones. Nat. Cell Biol. 8, 215-226.

Meijering, E., Jacob, M., Sarria, J.C., Steiner, P., Hirling, H., and Unser, M. (2004). Design and validation of a tool for neurite tracing and analysis in fluorescence microscopy images. Cytometry A 58, 167-176.

Pacheco, A., and Gallo, G. (2016). Actin filament-microtubule interactions in axon initiation and branching. Brain Res. Bull. 126, 300-310.

Patterson, G.H., and Lippincott-Schwartz, J. (2002). A photoactivatable GFP for selective photolabeling of proteins and cells. Science 297, 1873-1877.

Raines, A.N., Nagdas, S., Kerber, M.L., and Cheney, R.E. (2012). Headless Myo10 is a negative regulator of full-length Myo10 and inhibits axon outgrowth in cortical neurons. J. Biol. Chem. 287, 24873-24883.

Rex, C.S., Gavin, C.F., Rubio, M.D., Kramar, E.A., Chen, L.Y., Jia, Y., Huganir, R.L., Muzyczka, N., Gall, C.M., Miller, C.A., et al. (2010). Myosin IIb regulates actin dynamics during synaptic plasticity and memory formation. Neuron 67, 603-617.

Roossien, D.H., Lamoureux, P., and Miller, K.E. (2014). Cytoplasmic dynein pushes the cytoskeletal meshwork forward during axonal elongation. J. Cell Sci. 127, 3593-3602.

Schaefer, A.W., Schoonderwoert, V.T., Ji, L., Mederios, N., Danuser, G., and Forscher, P. (2008). Coordination of actin filament and microtubule dynamics during neurite outgrowth. Dev. Cell 15, 146-162.

Vallee, R.B., Seale, G.E., and Tsai, J.W. (2009). Emerging roles for myosin II and cytoplasmic dynein in migrating neurons and growth cones. Trends Cell Biol. 19, 347-355.

van Beuningen, S.F., and Hoogenraad, C.C. (2016). Neuronal polarity: remodeling microtubule organization. Curr. Opin. Neurobiol. 39, 1-7.

van Beuningen, S.F., Will, L., Harterink, M., Chazeau, A., van Battum, E.Y., Frias, C.P., Franker, M.A., Katrukha, E.A., Stucchi, R., Vocking, K., et al. (2015). TRIM46 Controls Neuronal Polarity and Axon Specification by Driving the Formation of Parallel Microtubule Arrays. Neuron 88, 1208-1226.

Vicente-Manzanares, M., Ma, X., Adelstein, R.S., and Horwitz, A.R. (2009). Non-muscle myosin II takes centre stage in cell adhesion and migration. Nat. Rev. Mol. Cell Biol. 10, 778-790.

Watanabe, K., Al-Bassam, S., Miyazaki, Y., Wandless, T.J., Webster, P., and Arnold, D.B. (2012). Networks of polarized actin filaments in the axon initial segment provide a mechanism for sorting axonal and dendritic proteins. Cell Rep. 2, 1546-1553.

Witte, H., Neukirchen, D., and Bradke, F. (2008). Microtubule stabilization specifies initial neuronal polarization. The Journal of cell biology 180, 619-632.

Xu, K., Zhong, G., and Zhuang, X. (2013). Actin, spectrin, and associated proteins form a periodic cytoskeletal structure in axons. Science 339, 452-456.

Yu, H., Wang, N., Ju, X., Yang, Y., Sun, D., Lai, M., Cui, L., Sheikh, M.A., Zhang, J., Wang, X., et al. (2012). PtdIns (3,4,5) P3 recruitment of Myo10 is essential for axon development. PloS one 7, e36988.

Zhu, X.J., Wang, C.Z., Dai, P.G., Xie, Y., Song, N.N., Liu, Y., Du, Q.S., Mei, L., Ding, Y.Q., and Xiong, W.C. (2007). Myosin X regulates netrin receptors and functions in axonal path-finding. Nat. Cell Biol. 9, 184-192.

SUPPLEMENTARY INFORMATION

Supplementary table 1. Overview of shRNA target sequences used in this study.

Family	Alias		shRNA sequence 5'- 3'
Myosin-II	MyoIIa	#1	GGTAAATTCATTCGTATCA
		#2	CCTCATTTATCGGGATCCT
		#3	CTGCTCGCAAGAAACTAGA
	MyoIIb	#1	GATCAAAGTTGGCCGAGAT
		#2	GGCATGCGGATCAGTATAA
		#3	GAACGCACGTTTCATATCT
	MyoIIc	#1	CCGCTCTTGAGTCTAAACT
		#2	GTGGTCATTAACCCGTACA
		#3	CTGCATCGTTCCCAATCAT
Myosin-V	MyoVa	#1	GCAAACTCGATCGGAGAAA
		#2	GATGCCTAAAGGTACCGAT
		#3	GTTTGCGTCTCGAGATTCA
	MyoVb	#1	GTGTCCTTTATACGAACAA
		#2	GGTATCGGGTGTTGATGAA
		#3	CCTGCATACATACTCTACA
Myosin-VI	MyoVI	#1	CTTCGCGATACAATCAACA
		#2	GTATGATGCACTCGTTAAA
		#3	CAGCCTAACAATTGAACCT
Myosin-X	MyoX	#1	CTCGAGGTTTGATACGGAT
		#2	GATCAACACTCTTCGACGT
		#3	GTTACCGACTCTACACGAA
Tropomyosins	TPM-α	#1	AGCACATTGCTGAAGATGCT
	TPM-β	#1	ACTGGAGCAGGCCGAGAAG
	TPM-γ	#1	AAGCTGGAGGAAGCGGAGA
	TPM-δ	#1	ATCAAGCTTCTGTCTGACAA

Supplementary table 2. Identification of binding partners of MyoIIb by mass spectrometry analysis using BioGFP pull-downs from rat brain lysates.

Accession	Protein	bio-GFP		bio-GFP-MyoIIb	
		# Peptides	# PSM	# Peptides	# PSM
G3V9Y1	**Myosin, heavy polypeptide 10, non-muscle**	**22**	**34**	**229**	**1838**
V9GZ85	Actin, cytoplasmic 2 (Fragment)	21	124	34	1102
G3V6P7	Myosin, heavy polypeptide 9, non-muscle	13	20	169	835
D3ZRN3	Actin, beta-like 2	6	41	15	345
E9PTU4	Myosin-11	5	8	77	323
F1LNF0	Myosin heavy chain 14	8	10	107	311
Q63862	Myosin-11 (fragments)	4	7	57	279
Q62707	Nonmuscle myosin heavy chain-B (Fragment)	5	7	15	261
Q9QYF3	Unconventional myosin-Va	18	20	82	193
Q07266	Drebrin	7	9	29	115
D3ZFD0	Myosin XVIIIa			58	112
Q63610	Tropomyosin alpha-3 chain	2	2	33	105
Q68FP1	Gelsolin	4	8	30	99
F1MA36	Spectrin beta chain	29	31	69	94
Q6AZ25	Tropomyosin 1, alpha	2	2	30	90
Q91XN7	Tropomyosin alpha isoform	2	2	30	89
Q32PZ3	Protein unc-45 homolog A	8	9	21	83
Q5XI32	F-actin-capping protein subunit beta	3	3	17	81
P04692	Tropomyosin alpha-1 chain	2	2	28	77
Q63583	Hepatoma alpha tropomyosin	2	2	27	76
Q923Z2	Tropomyosin 1, alpha, isoform CRA_a	2	2	26	75
D4A5I9	Myosin VI	5	5	30	70
P70566	Tropomodulin-2			22	66
P09495	Tropomyosin alpha-4 chain	2	2	30	65
F1LMV9	Coronin (fragment)	1	1	17	64
Q63357	Unconventional myosin-Id	1	1	35	59
G3V624	Coronin 1c	5	5	17	55
Q5FVG5	Similar to tropomyosin 1, embryonic fibroblast-rat	2	2	20	46
Q64119	Myosin light polypeptide 6	2	3	10	44
Q5QJC9	BAG family molecular chaperone regulator 5	2	2	15	42
D3ZCV0	Actinin alpha 2	9	12	28	41
F1M392	LIM and calponin homology domains 1	1	1	19	33
Q3T1K5	F-actin-capping protein subunit alpha-2	1	1	12	31
Q63355	Unconventional myosin-Ic	3	3	20	27
P18666	Myosin regulatory light chain 12B			9	27
B2GUZ5	F-actin-capping protein subunit alpha-1			10	26
Q6IMZ5	Tropomodulin 1			13	25
Q5RKI5	Flightless I homolog (Drosophila)	2	3	13	23
Q5XI67	F-box only protein 30			10	23
B1VKB4	Synaptopodin	2	2	16	22
F1M3R4	Unconventional myosin-Vb	4	4	12	22
Q4V7C7	Actin-related protein 3	4	5	11	21
B0BMS8	Myl9 protein			7	20
P41542	General vesicular transport factor p115	6	6	14	19
Q5RKI0	WD repeat-containing protein 1	1	1	13	19
D3ZUJ7	Ankyrin repeat domain 13 family, member D (Predicted)	2	2	13	17
Q5M7U6	Actin-related protein 2	1	1	9	17
D3ZHA7	Similar to Myosin light chain 1 slow a (Predicted)	1	1	7	17
P70620	Nonmuscle myosin heavy chain B (Fragment)			3	17
G3V940	Coronin, actin-binding protein, 1B			8	15
Q920J3	Coronin-6			6	15
Q6AY36	Coronin, actin binding protein 2A			9	14
G3V9F3	Myosin phosphatase Rho-interacting protein	1	1	12	13
Q6AXW2	Protein Tmod3			8	13
Q5RJR2	Twinfilin-1			6	13
B2GV73	Actin-related protein 2/3 complex subunit 3	2	2	5	13

Accession	Protein	bio-GFP		bio-GFP-MyoIIb	
		# Peptides	# PSM	# Peptides	# PSM
G3V9Y1	**Myosin, heavy polypeptide 10, non-muscle**	**22**	**34**	**229**	**1838**
Q99PD4	Actin-related protein 2/3 complex subunit 1A			8	12
B0BMY7	Protein Twf2			8	12
B0BN74	Bag2 protein			5	12
F1LY09	ARP3 actin-related protein 3 homolog B	1	1	8	11
P85970	Actin-related protein 2/3 complex subunit 2	1	1	7	11
Q9EPH3	Putative myosin IIC			4	11
D4ADD8	Dynactin 6 (Predicted), isoform CRA_b			3	11
B1WBY1	Cul1 protein	3	3	10	10
Q6KC51	Actin-binding LIM protein 2			7	9
D3ZWX4	NCK-interacting protein with SH3 domain	1	1	5	9
B2RZ72	Actin-related protein 2/3 complex subunit 4	3	3	5	8
P02600	Myosin light chain 1/3, skeletal muscle isoform			3	8
P60881	Synaptosomal-associated protein 25	1	1	5	7
A2RUW1	Toll-interacting protein			5	6
D4A4T0	STIP1 homology and U-Box containing protein 1			5	6
D4AA38	Holocarboxylase synthetase			4	6
B1H262	Protein phosphatase 1, regulatory subunit 9B	1	1	4	6
D3ZAN8	Protein LOC100910807	1	1	4	6
D3ZG54	WW domain-containing oxidoreductase			5	5
Q32PW9	Psmc6 protein (Fragment)			4	5
Q6XDA0	Spectrin beta chain			4	5
F1LPM3	Sorbin and SH3 domain-containing protein 2			3	5
Q5XIR5	BCL2-associated athanogene 4			4	4
O35867	Neurabin-1			4	4
D3ZDH8	Platelet glycoprotein Ib beta chain			4	4
Q4V7E8	Leucine-rich repeat flightless-interacting protein 2			4	4
Q5XI21	Target of myb1 homolog (Chicken)			3	4
P70580	Membrane-associated progesterone receptor component 1			3	3

Proteins with a number of peptide spectrum matches (#PSM) of 3 or more and an enrichment of 3 or more compared to the control (BioGFP) in the BioGFP-MyoIIb pull-down are included.

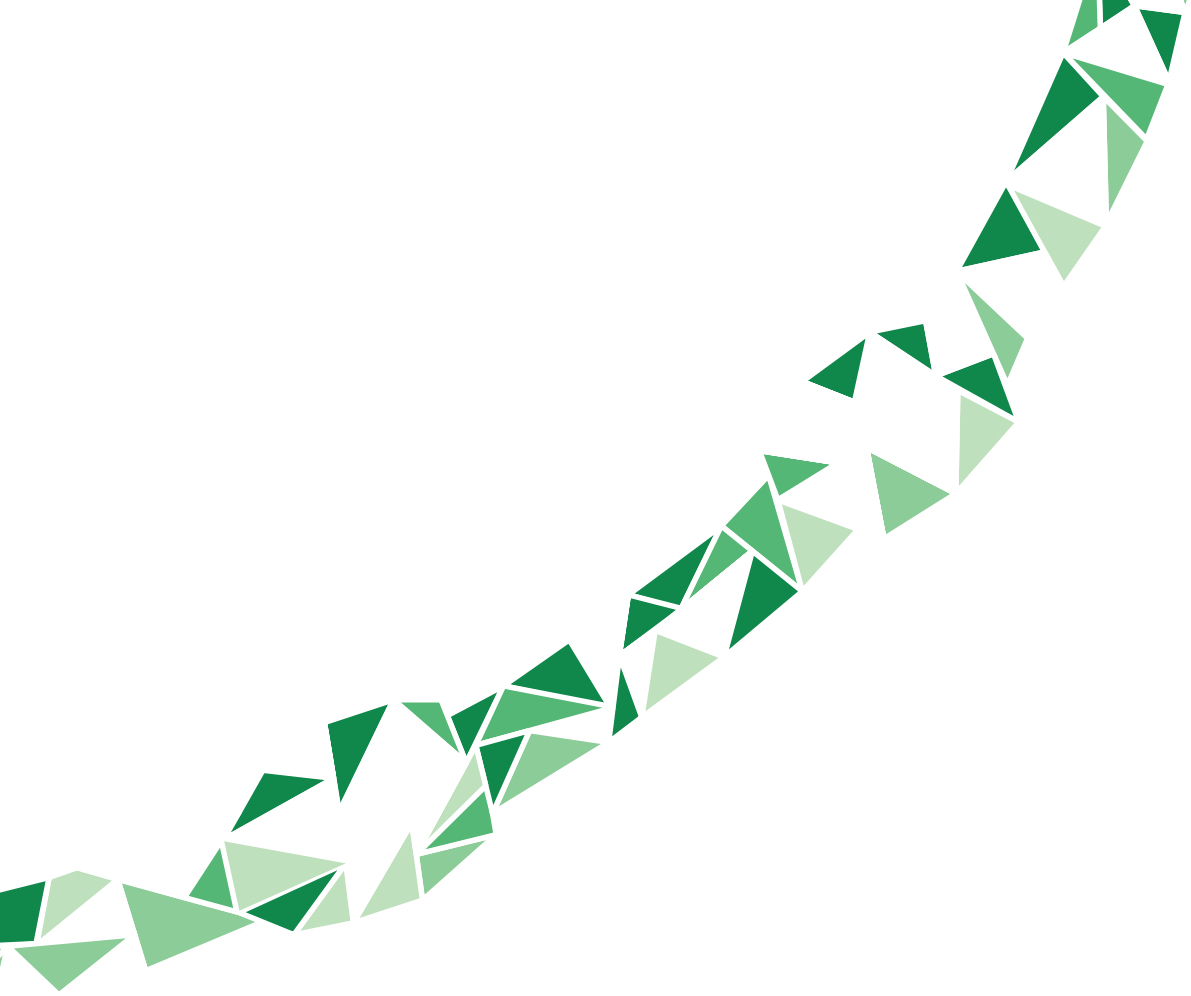

[1] Cell Biology, Department of Biology, Faculty of Science, Utrecht University, Utrecht, the Netherlands
[2] International Institute of Molecular and Cell Biology, 02-1009 Warsaw, Poland

Chapter 4

Systematic RNAi-based screening identifies KIF19 as a regulator of neuronal polarity and axon growth in hippocampal neurons

Cátia P. Frias[1], Petra van Bergeijk[1], Joanna Lipka[1,2], Loek Sanders[1], Anna Malik[2], Jacek Jaworski[2], Lukas C. Kapitein[1], Casper C. Hoogenraad[1]

ABSTRACT

The polarized architecture of neurons with functional and morphologically different compartments is central to the function of the nervous system. Even though cytoskeletal rearrangements are known to be important for neuronal polarization, the precise cascade of events underlying axonal and dendritic growth remains unknown. Kinesins are a large family of proteins that control intracellular cargo transport and the organization of the microtubule cytoskeleton. However, the contribution of kinesin proteins in neuronal development has not been systematically tested. Here, we performed a targeted knockdown screen of almost all the kinesin proteins and assessed changes in the development of cultured hippocampal neurons. We found that kinesins are important for the extension of neurites and for the establishment of the axon initial segment. More specifically, the microtubule depolymerizing proteins KIF19, KIF3C and KIF2A are required for axon initiation and neuronal polarization. We focused our study on kinesin-8 KIF19 and found that it was localized to both axonal and dendritic growth cones, and that it promoted the depolymerization of microtubules in cultured cells. We hypothesize that microtubule depolymerization at the growth cone is an essential mechanism for proper neuronal polarization and development, and that kinesins are regulators of such processes.

INTRODUCTION

The proper establishment of neuronal circuitry during development relies on the extension of axonal and dendritic processes. Neurons are polarized cells with a single axon and multiple dendrites, responsible for the transmission and reception of electrochemical signals, respectively. Axons and dendrites are functionally and morphologically distinct, and these differences may arise from modifications in the underlying cytoskeleton. In mature neurons, axons exhibit a uniform array of microtubules oriented with their plus-end towards the end of the axon (Baas et al., 1988; Heidemann et al., 1984). On the other hand, dendrites display mixed microtubule orientations (Baas et al., 1988; Yau et al., 2016), and their microtubules are less stable when compared with axonal microtubules (Baas et al., 1991).

A central question in neurobiology is how such different and compartmentalized structures arise. During neuronal development, spherical cells develop several small processes of similar length called neurites (Craig and Banker, 1994; Dotti et al., 1988). The rapid growth of one of these neurites hallmarks symmetry breaking and neuronal polarization, leading to the formation of the axon. In the remaining neurites, the microtubule orientation will change from uniformly plus-end out to mixed, and this leads to the development of the dendrites (Baas et al., 1989; Stepanova et al., 2003). Changes in the underlying cytoskeleton are responsible for the symmetry breaking and axon initiation. In fact, different microtubule-regulating proteins have been shown to regulate axon formation and outgrowth in cultured hippocampal neurons (Inagaki et al., 2001; Jiang et al., 2005; Yoshimura et al., 2005). Prior to neuronal polarization, the microtubules of one neurite retracted less upon treatment with microtubule-depolymerizer drug nocodazole in comparison to the microtubules in the remaining neurites (Witte et al., 2008), suggesting that stabilization of microtubules in one neurite may be an early event in neuronal development. Accordingly, local stabilization of microtubules using a caged form of microtubule-stabilizing drug taxol promoted axon formation in unpolarized hippocampal neurons, while treatment with nanomolar doses of taxol led to the formation of multiple axons (Witte et al., 2008). The increased microtubule stability in the future axon may be used as a cue for the polarized transport of cargo supporting the extension of the axon. Indeed, it was shown that kinesin-1, a plus-end directed motor protein, accumulated at the tip of the future axon prior to neuronal polarization (Jacobson et al., 2006; Nakata and Hirokawa, 2003), which may point towards a crucial role for microtubule-based selective transport of signaling molecules into a single neurite during axon specification.

Kinesin motors are a large family of proteins subdivided into 14 families that regulate different microtubule-related processes (Hirokawa et al., 2009). By binding to microtubules, kinesin proteins are not only able to drive the transport of membrane organelles and protein complexes, but also to control microtubule dynamics (Hirokawa et al., 2009; Walczak et al., 2013). Several mutations in different kinesin motors and their regulators have been implicated in several neurodevelopmental and neurodegenerative disorders (Franker and Hoogenraad, 2013; Hirokawa et al., 2010), suggesting that kinesin-mediated effects on microtubules are important for proper neuronal development. However, the contribution of each motor protein for the extension of axonal and dendritic processes is still unknown. In order to address the role of kinesin motor proteins in neuronal development, we performed a knockdown screen and assessed possible changes in both axonal and dendritic morphology upon kinesin protein depletion. Our data revealed that kinesins are important for proper axonal and dendritic outgrowth, suggesting they are important for the initial

extension of neuronal processes. We further showed that five kinesins are involved in the establishment and maintenance of the axon initial segment (AIS). These kinesins are microtubule-depolymerizing motors, and their depletion induced the mislocalization of both axonal and dendritic markers. We propose that microtubule depolymerization at the leading edge of the axon is crucial to promote neuronal polarization and sustain axonal outgrowth in hippocampal neurons.

RESULTS AND DISCUSSION

Kinesins from different families are important for proper neuronal development
To address the role of motor proteins in the extension of axonal and dendritic processes in hippocampal neurons in vitro, we performed a targeted knockdown screen of almost all kinesin motor proteins and the dynein heavy chain, using three shRNAs targeting the same protein. Neurons were transfected at day-in-vitro (DIV) 0 and fixed at DIV 4. All neurites and their branches were manually traced and the axon was identified as the longest neurite non-enriched for the somatodendritic marker Map2. We found that kinesins from different families induced changes in the total axonal arborization in comparison to control cells (Figure 1A-B). More specifically, members of kinesin-2 (KIF3A and KIF3C), kinesin-3 (KIF16B), kinesin-6 (KIF23), kinesin-8 (KIF18A and KIF19), kinesin-9 (KIF6), kinesin-12 (KIF12), kinesin-13 (KIF24) and kinesin-14 (KIFC2 and KIFC3) significantly reduced the total axonal arborization by decreasing the primary axon length (Figure 1C), the number of axonal branches (Figure 1D) and/or the average length of the axonal branches (Figure 1E). Members of kinesin-2, -8 and -13 families are microtubule-depolymerizing proteins (Gumy et al., 2013; Walczak et al., 2013), suggesting that axonal outgrowth depends on kinesin-mediated regulation of microtubule dynamics. The majority of these proteins did not carry out the transport of peroxisomes in an inducible cargo trafficking assay, but KIF3A, KIF16B and KIF23 were shown to selectively transport cargo in the axon (Lipka et al., 2016). Together with our results, we hypothesize that KIF3A-, KIF16B- and KIF23-based transport may be required for the proper extension of the axon. However, a recent study showed that KIF23 is almost undetectable in the axon, and that its depletion does not affect axonal navigation and branching (Lin et al., 2012). Importantly, this study is performed in rat sympathetic neurons, and we cannot exclude that there may be differences in kinesin expression, localization and function between different neuron types. In the same study, Lin and colleagues showed that KIF23 is involved in the transport of minus-end microtubules into dendrites (Lin et al., 2012). Therefore, it will be interesting to assess if KIF23 is important for microtubule orientation in axon and dendrites in early stages of development, by performing live-imaging of microtubule plus-end proteins, such as EB3 protein (Stepanova et al., 2003), in KIF23-depleted hippocampal neurons. Even though KIF5 motors are thought to play a role in the transport of cargo preceding axon formation in cultured neurons (Jacobson et al., 2006; Oksdath et al., 2016), their depletion did not induce major defects in the axonal arborization.

After extensive axonal growth, the remaining neurites develop as dendrites. We also assessed if kinesin depletion affected the extension of dendritic processes. We found that there was a partial overlap between the kinesins required for proper extension of axonal and dendritic arborizations (Figure 2A,B). Besides blocking the extension of axonal processes, depletion of KIF3C, KIF6, KIF12 and KIFC2 also decreased the total dendritic arborization

(Figure 2B-E). As KIF3C was previously shown to regulate microtubule dynamics in the axonal growth cone of dorsal root ganglion neurons (Gumy et al., 2013), our data suggest that KIF3C may play similar roles in dendritic growth cones. KIF6 and KIF12 are important for mitosis and antioxidant signaling (Lakshmikanth et al., 2004; Tikhonenko et al., 2009; Yang et al., 2014), however roles of these proteins in postmitotic neurons have never been

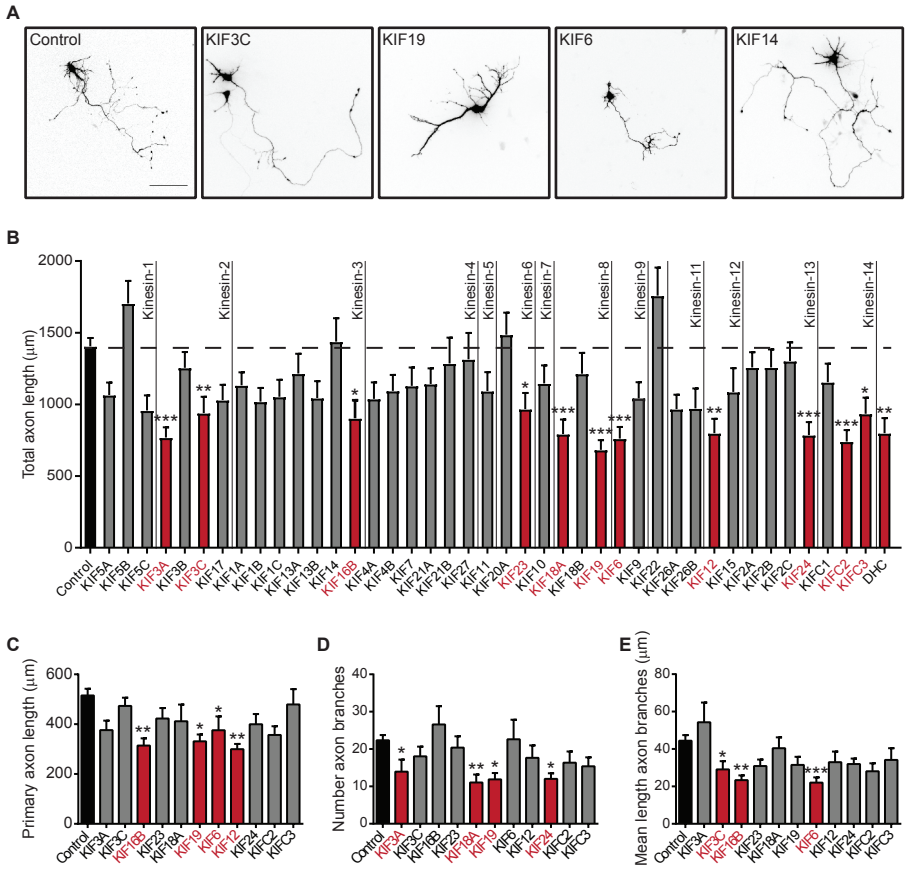

Figure 1. Kinesins from different families regulate axonal outgrowth in hippocampal neurons.

(A) Representative images of DIV 4 hippocampal neurons transfected at DIV 0 with pSuper (control) or KIF3C-, KIF19-, KIF6-, KIF14-shRNA pools and GFP fill. Scale bar 100 µm.

(B) Quantification of the total axon length in DIV 4 hippocampal neurons transfected at DIV 0 with pSuper (control) or indicated pools of shRNAs and GFP fill. n = 12-20 cells from 2 independent experiments were analyzed per condition (for control, n = 64 cells, N = 4). Kruskal-Wallis test. * $p < 0.05$, ** $p < 0.01$, *** $p < 0.001$.

(C-E) Quantification of primary axon length (C), number of axon branches (D) and mean length of axon branches (E) in DIV 4 hippocampal neurons transfected at DIV 0 with pSuper (control) or indicated pools of shRNAs and GFP fill. Only the kinesin depletions that showed a significant effect in (B) are shown. n = 14-19 cells from 2 independent experiments were analyzed per condition (for control, n = 64 cells, N = 4). Kruskal-Wallis test: * $p < 0.05$, ** $p < 0.01$, *** $p < 0.001$.

Data are represented as mean ± SEM. Red bars indicate $p < 0.05$.

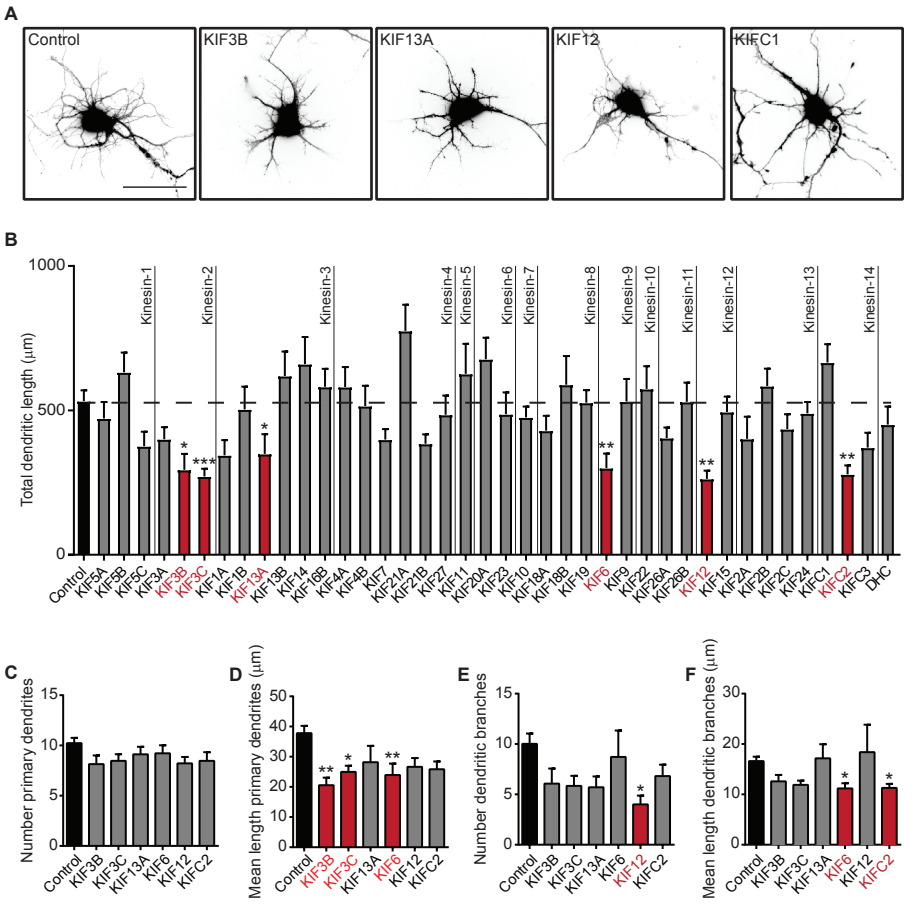

Figure 2. Kinesins important for dendritogenesis partially overlap with kinesins required for proper axon outgrowth.

(A) Representative images of the somatodendritic area of DIV 4 hippocampal neurons transfected at DIV 0 with pSuper (control) or KIF3B-, KIF13A-, KIF12-, KIFC1-shRNA pools and GFP fill. Scale bar 100 µm.

(B) Quantification of the total dendritic length in DIV 4 hippocampal neurons transfected at DIV0 with pSuper (control) or indicated pools of shRNAs and GFP fill. n = 12-20 cells from 2 independent experiments were analyzed per condition (for control, n = 43 cells, N = 2). Kruskal-Wallis test: * $p < 0.05$, ** $p < 0.01$, *** $p < 0.001$.

(C-F) Quantification of number of primary dendrites (C), mean length of the primary dendrites (D), number of dendritic branches (E) and mean length of dendritic branches (F) in DIV 4 hippocampal neurons transfected at DIV0 with pSuper (control) or indicated pools of shRNAs and GFP fill. Only the depletions that showed a significant effect in (B) are shown. n = 14-19 cells from 2 independent experiments were analyzed per condition (for control, n = 43 cells, N = 2). Kruskal-Wallis test:* $p < 0.05$, ** $p < 0.01$.

Data are represented as mean ± SEM. Red bars indicate $p < 0.05$.

described. In a study using an inducible cargo trafficking assay, both kinesins do not translocate peroxisomes in living cells (Lipka et al., 2016), suggesting that their function in cells may not be linked to transport of cargo. Therefore, it will be important to investigate the localization

of these proteins in hippocampal neurons, and if they are involved in the regulation of microtubule dynamics. We found that KIF3B- and KIF13A-depleted neurons also exhibited smaller dendritic trees, without axonal defects (Figure 2A-E, compare with Figure 1B). This suggests that these kinesins may specifically transport cargo that promotes dendritogenesis, or that they may be essential for the microtubule cytoskeleton rearrangements that take place during this process. KIF13A has been shown to be involved in the transport of dendritically-targeted serotonin receptors (Zhou et al., 2013), but no link with dendrite development has been purposed. It will be interesting to address if KIF13A is localized to dendrites in early stages of development. We also observed that depletion of KIF21A, a kinesin-4 family member, increased the total dendritic length by 46 % when compared to controls (Figure 2B). Even though this effect did not reach significance, this result suggests that KIF21A may act as a blocker of dendrite outgrowth, while massive axon extension is taking place. As KIF21A was shown to restrict microtubule growth at the cell edge (van der Vaart et al., 2013), the observed dendritic extension in KIF21A-depleted neurons may be due to increased microtubule growth at dendritic growth cones.

Overall, our data show that kinesin motor proteins are required for proper neuronal development of hippocampal neurons, by most likely regulating microtubule dynamics or promoting the transport of factors that sustain neuritic extension. As some of our candidate kinesins have never been linked to neurodevelopmental processes, it will be interesting to assess if these proteins are expressed in hippocampal neurons and if they are involved in microtubule-based processes.

Depolymerizing kinesins are involved in the establishment and maintenance of the axon initial segment

Since members of the kinesin superfamily are important for proper axonal outgrowth, we next investigated if the motor proteins are involved in the establishment of the axon identity. To address this, we performed a knockdown screen of almost all kinesin motor proteins and dynein heavy chain at DIV 0 to 1, and examined the localization of AIS marker β-IV-spectrin four days later. We found that depletion of KIF2A (kinesin-13), KIF3C (kinesin-2), KIF26B (kinesin-11), KIF6 (kinesin-9) and KIF19 (kinesin-8) showed more than 40 % decrease in the average number of β-IV-spectrin-positive neurites per neuron (Figure 3A-B). These results were confirmed by testing the individual shRNAs (data not shown). From these five kinesins, KIF2A, KIF3C and KIF19 are categorized as microtubule-depolymerizing kinesins (Gumy et al., 2013; Walczak et al., 2013), and both KIF2A and KIF3C have been shown to localize at axonal outgrowth cones (Gumy et al., 2013; Homma et al., 2003). This may suggest that dysregulation of microtubule dynamics at the growth cone may influence the establishment of the AIS. It will be also interesting to address if depletion of KIF2A and KIF3C modify the stability of the microtubule cytoskeleton at the proximal part of the axon, where the AIS is formed. Regarding KIF6 and KIF26B, not much is known on their action on microtubules, even though they have been linked to mitotic and kidney development processes, respectively (Tikhonenko et al., 2009; Uchiyama et al., 2010). As KIF6 also is required for proper axonal and dendritic growth (Figure 1B, 2B), it raises the possibility that this protein plays a central role in neuronal development. Thus, it will be important to address if this protein is expressed and where it localizes in hippocampal neurons, so we can better understand its function in neurons.

To study if the depletion of the abovementioned kinesins leads to a complete

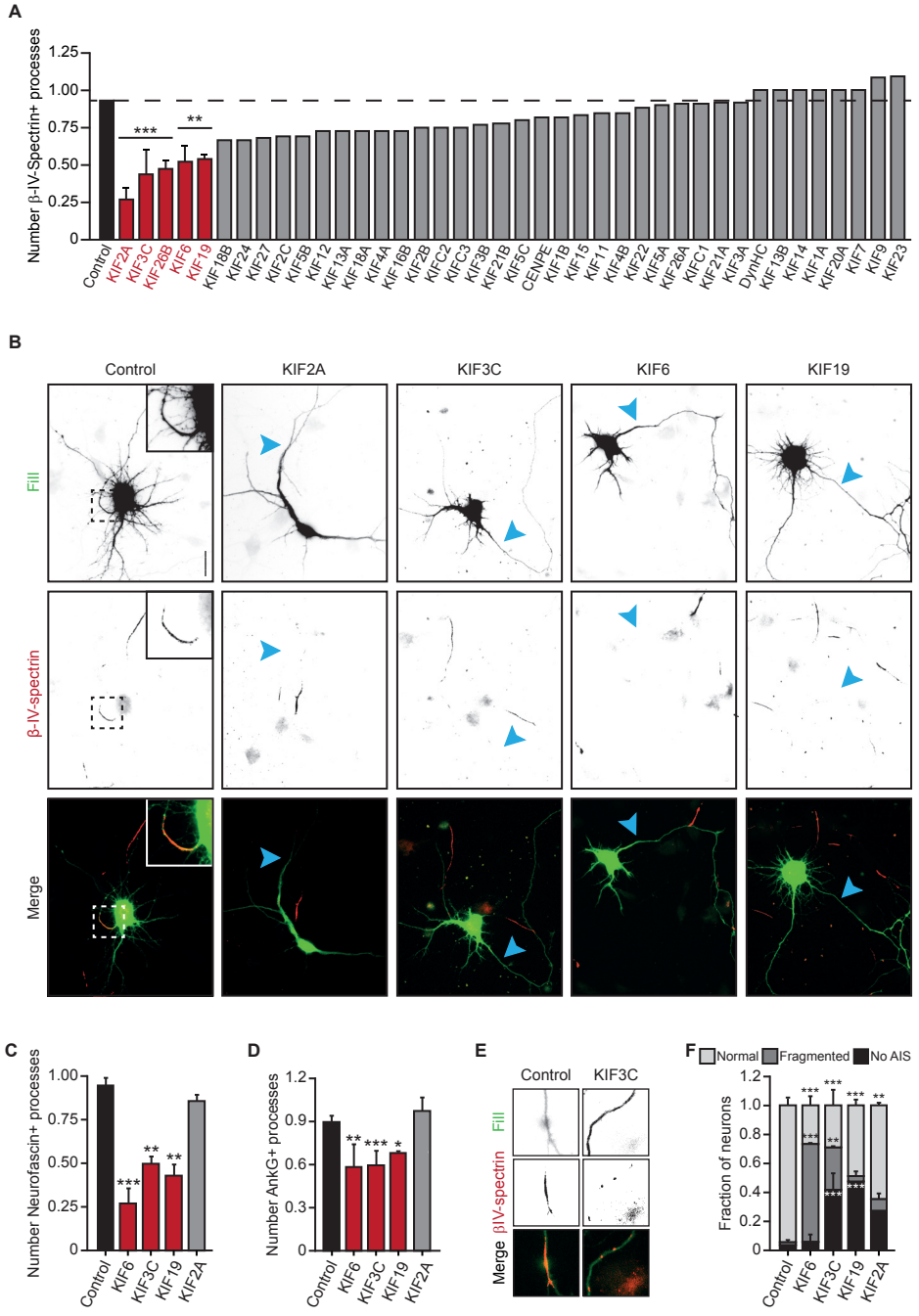

Figure 3. Depolymerizing motor proteins are involved in AIS maintenance.

(A) Average number of β-IV-Spectrin positive neurites in DIV 4-5 hippocampal neurons transfected at DIV 0-1 with pSuper (control) or indicated pools of shRNAs. n=20 cells from at least 2 independent experiments. Two-tailed

Fisher's exact test: ** $p < 0.01$, *** $p < 0.001$.
(B) Representative images of hippocampal neurons, showing a BFP fill (green) and β-IV-Spectrin staining (red) in control and KIF2A-, KIF3C-, KIF6- or KIF19-depleted neurons at DIV 4-5. Scale bar 20 µm.
(C-D) Average number of Neurofascin (C) and Ankyrin-G (D) positive neurites in DIV 4-5 hippocampal neurons transfected at DIV 0-1 with pSuper (control) or KIF6-, KIF3C-, KIF19- or KIF2A-shRNA pools. n=22 cells from at least 2 independent experiments. Two-tailed Fisher's exact test: * $p < 0.05$, ** $p < 0.01$, *** $p < 0.001$.
(E) Representative images of hippocampal neurons transfected with BFP (green) to highlight neuronal morphology and β-IV-Spectrin staining (red) in control and KIF3C-depleted neurons at DIV 4-5.
(F) Fraction of neurons showing a normal (light grey) , fragmented (dark grey) or no β-IV-Spectrin (black) staining in control or KIF6-, KIF3C-, KIF19- or KIF2A-depleted hippocampal neurons at DIV 4-5. n=22 cells from at least 2 independent experiments. Two-tailed Fisher's exact test: * $p < 0.05$, ** $p < 0.01$, *** $p < 0.001$.
Error bars indicate mean ± SEM. Red bars indicate $p < 0.05$.

disruption of the AIS, we determined if localization of other AIS markers was affected upon depletion of KIF2A, KIF6, KIF3C and KIF19. Besides the effect on β-IV-spectrin localization, depletion of KIF6, KIF3C and KIF19 also affected the localization of both Neurofascin and Ankyrin-G (Figure 3C-D), suggesting that these kinesins are important for AIS structure in hippocampal neurons. On the other hand, depletion of KIF2A did not affect the presence of Neurofascin or Ankyrin-G at the AIS (Figure 3C-D), which may suggest that KIF2A specifically affects the localization of β-IV-spectrin. In neurons that still had an AIS, we noticed that depletion of KIF6 and KIF3C induced the fragmentation of β-IV-spectrin in 67 % and 29 % of the neurons, respectively (Figure 3E,F). Altogether, these data show that motor proteins that control microtubule dynamics are required for the establishment and maintenance of the AIS structure.

Depolymerizing kinesins are required for axon formation and neuronal polarization

Three of the four studied kinesins not only induced defects on the extension of axonal processes, but also in the establishment of the AIS. The determination of the axon in hippocampal neurons in vitro is a process that occurs within the first 24 hours after plating, before the depletion of the proteins is effective. To address if axon initiation is also affected by the knockdown of KIF6, KIF3C, KIF19 and KIF2A, we performed an assay using nanomolar doses of the microtubule-stabilizing drug Taxol, previously shown to promote the formation of multiple axons (Witte et al., 2008). Neurons were transfected with the corresponding shRNAs at DIV 1, and after three days we treated the cells with 10 nM Taxol for 48 hours. We then stained the neurons against the AIS marker voltage gated sodium channels (pan-NaV), and quantified the number of positive neurites per neuron for the AIS marker. In the control situation, most neurons have one AIS, and the average number of pan-NaV-positive neurites is increased by 3-fold in Taxol-treated cells (Figure 4A-B). In kinesin-depleted cells, Taxol treatment did not induce an increase in the number of neurites positive for pan-NaV (Figure 4A-B). In fact, there was a reduction of at least 41 % in the average number of pan-NaV-positive neurites in the knockdown cells in comparison to control cells (Figure 4B). Hence, these kinesins are required for proper axon formation, suggesting that acquisition of axon identity is influenced by these proteins.

The polarized structure of neurons leads to the establishment of two distinct compartments, the axon and the dendrites. In this way, certain proteins are restricted to a

specified compartment, such as the microtubule-associated proteins Tau and Map2, found at the axonal and somatodendritic compartments, respectively. The establishment of the AIS is central for the polarized distribution of proteins (Hedstrom et al., 2008). Since we observed defects in the establishment and maintenance of the AIS, we assessed if the depletion of kinesin proteins affected the localization of Map2 and Tau. We found that depletion of kinesins induced changes in the distribution of these markers (Figure 4C-E). More precisely, knockdown of KIF6, KIF3C and KIF2A resulted in the appearance of Map2 in the axon, 4 to 5 times more often than in control cells (Figure 4C,E). Loss of Ankyrin-G, the master organizer of the AIS (Jones and Svitkina, 2016), prompts the axon to acquire dendritic-like features, such as the accumulation of Map2 (Hedstrom et al., 2008). Since we find a similar result with depletion of KIF6, KIF3C and KIF2A, our results suggest that polarity is affected in the depleted cells. Future studies will be required to assess if the uniform orientation of axonal microtubules is lost, by looking at the anterograde and retrograde growing microtubule plus-ends. Moreover, it will also be interesting to perform knockdowns later in development, to address if the assembly of excitatory postsynaptic densities and spines occurs in the axon, similar to the AnkG knockdown situation (Hedstrom et al., 2008). We also found that the axonal marker Tau was observed in the dendrites of 17 % of KIF19-silenced neurons, something that was never observed in control cells (Figure 4D-E). Overall, our data show that depletion of KIF6, KIF3C, KIF19 and KIF2A proteins induces defects on axon initiation and neuronal polarization, leading to a "leaky" and not-fully functional AIS.

KIF19 localizes to microtubules and axonal and dendritic growth cones, and depolymerizes microtubules

From the four kinesins studied, KIF19 silencing resulted in the mislocalization of axonal marker Tau, indicating that this protein may be required for axon identity maintenance and neuronal polarization. We then focused our study on KIF19, a plus-end-directed kinesin-8 family protein (Hirokawa et al., 2009). We first tested the efficiency of the KIF19-targeting shRNAs. Endogenous expression of KIF19 could not be detected with the used antibody

Figure 4. Depletion of KIF6, KIF3C, KIF19 and KIF2A impairs axon formation and mislocalizes axonal and dendritic markers. ➤

(A) Representative images of DIV 6 hippocampal neurons transfected with a BFP fill (blue) and pSuper (control) or KIF6-, KIF3C-, KIF19- or KIF2A-shRNA pools at DIV 1 and treated at DIV4 with control medium (no taxol) or 10 nM taxol for 48 h. Neurons were immunostained for pan-NaV (green) and Trim46 (red). Arrows highlight neurites positive for both markers. Scale bar 50 µm.

(B) Quantification of pan-NaV-positive neurites in DIV 6 hippocampal neurons in control or KIF6-, KIF3C-, KIF19- or KIF2A-depleted neurons after treatment with 10 nM Taxol for 48 h. n=12-31 cells from 2 independent experiments (for no-taxol group, n=59 cells, N=2; for control, n=85 cells, N=3). Chi-square test: ** $p < 0.01$, *** $p < 0.001$.

(C-D) Percentage of neurons showing Map2 (C) or Tau (D) mislocalization in DIV 4-5 hippocampal neurons transfected with pSuper (control) or KIF6-, KIF3C-, KIF19- or KIF2A-shRNA pools. n=19 cells from at least 2 independent experiments. One-tailed Fisher's exact test: * $p < 0.05$, ** $p < 0.01$, *** $p < 0.001$.

(E) Representative images of DIV 4-5 hippocampal neurons transfected with BFP fill (green) and pSuper (control) or KIF6-, KIF3C-, KIF19- or KIF2A-shRNA pools at DIV 0-1. Neurons were immunostained for the somatodendritic marker Map2 (red) and the axonal marker Tau (green). Green arrows indicate Map2 mislocalization into the axon, and red arrows indicate Tau mislocalization into the dendrites. Scale bar 40 µm.

Data are represented as mean ± SEM. Red bars indicate $p < 0.05$.

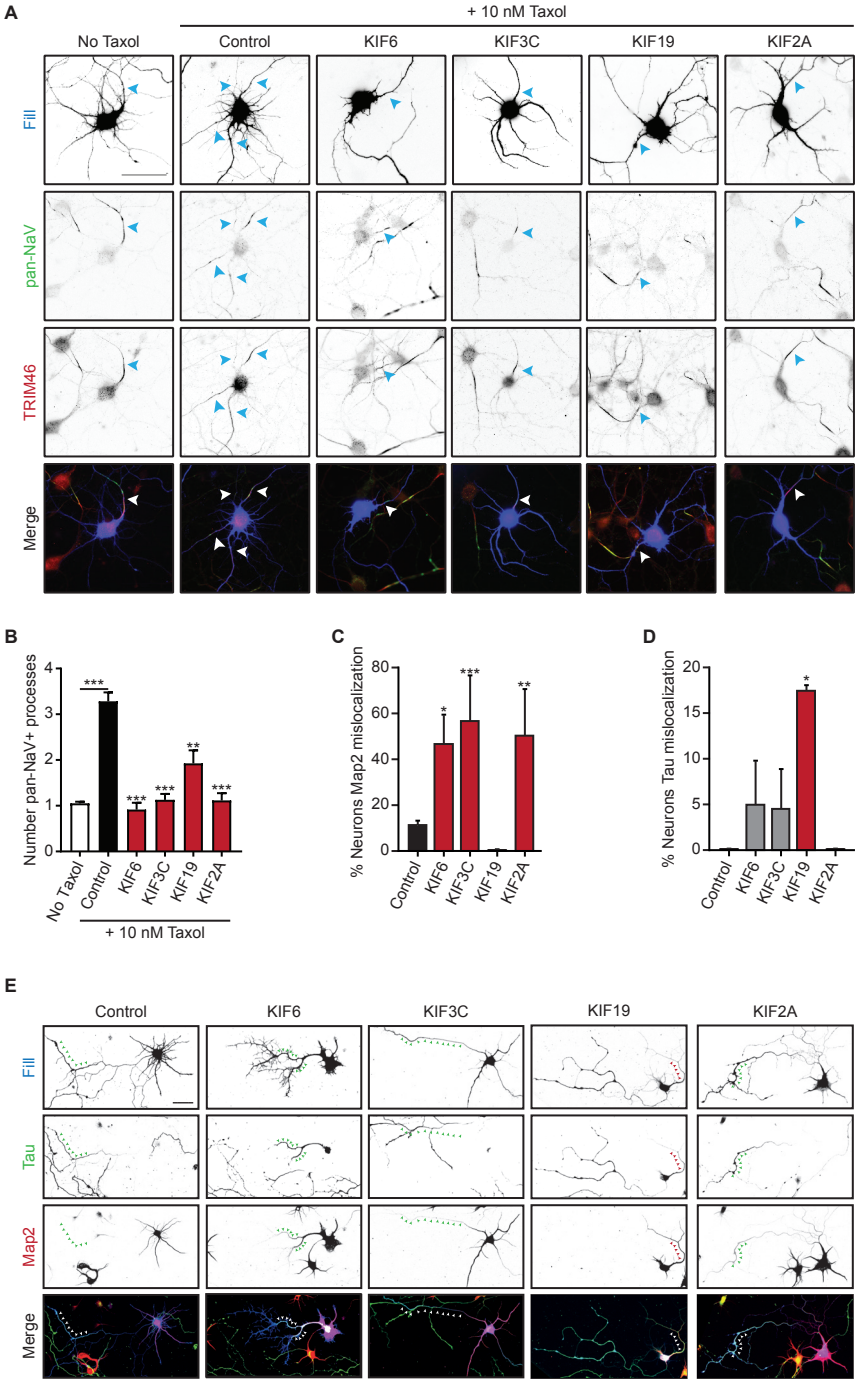
A
+ 10 nM Taxol
No Taxol
Control
KIF6
KIF3C
KIF19
KIF2A
Fill
pan-NaV
TRIM46
Merge
B
Number pan-NaV+ processes
No Taxol
Control
KIF6
KIF3C
KIF19
KIF2A
+ 10 nM Taxol
C
% Neurons Map2 mislocalization
D
% Neurons Tau mislocalization
E
Tau
Map2

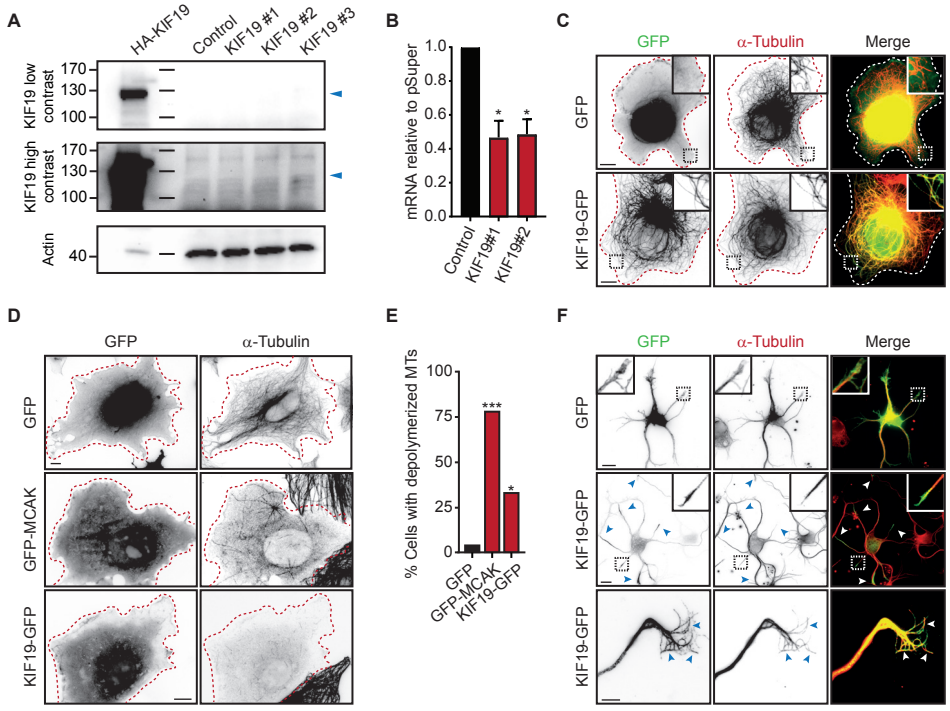

Figure 5. KIF19 localizes to microtubules of axonal growth cones, and depolymerizes microtubules.
(A) Western blot analysis of lysates of cortical neurons transfected with HA-KIF19, empty pSuper vector or KIF19-shRNAs, by using antibodies against β-actin and KIF19. Upper panel shows a low contrast image, and the middle panel shows a high contrast image of the same blot.
(B) Measurement of relative mRNA levels of KIF19 by Q-RT-PCR in cortical neurons transfected with the corresponding shRNA compared to neurons transfected with empty pSuper vector. Three experiments were performed per condition. Two-tailed t-test: * $p < 0.05$.
(C) Representative images of COS-7 cells transfected with GFP or KIF19-GFP, and immunostained for α-tubulin (red). Scale bars 10 μm.
(D) Representative images COS-7 cells transfected with GFP (upper panel), GFP-MCAK (middle panel) or KIF19-GFP (bottom panel), and immunostained for α-tubulin (red). Scale bar 10 μm.
(E) Percentage of COS-7 cells with depolymerized microtubules. n = 9 cells per condition. Two-tailed Fisher's exact test: * $p < 0.05$, *** $p < 0.001$.
(F) Representative images showing GFP (upper panel) or KIF19-GFP (middle and bottom panels) overexpression and α-tubulin (red) staining in DIV 2 cortical neurons. In the middle panel, arrows show the accumulation of KIF19-GFP on dendritic (short processes) and axonal growth cones. The bottom panel shows an axonal growth cone, where KIF19 co-localizes with microtubules. Scale bar 10 μm.
Error bars represent mean ± SEM. Red bars indicate $p < 0.05$.

(Figure 5A), making it impossible to assess changes on protein levels upon transfection with KIF19-targeting shRNAs. Therefore, we quantified the levels of KIF19 mRNA using Q-RT-PCR. KIF19 mRNA level was reduced by more than 50 % in KIF19-depleted neurons (Figure 5B), indicating that the KIF19-directed shRNAs efficiently lower the mRNA of this

kinesin. To ensure that the previously observed effects are due to depletion of KIF19, rescue experiments with the overexpression of a shRNA-resistant KIF19 should be performed in the future.

KIF19 was previously shown to control the length of cilia by inducing their depolymerization mainly from their plus-ends (Niwa et al., 2012). To gain more insight on the role of KIF19, we generated a full-length KIF19-GFP construct to determine the localization of KIF19 in both COS-7 cells and cortical neurons. In COS-7 cells, KIF19-GFP overlapped with microtubules stained for α-tubulin, showing that KIF19 is able to bind to microtubules (Figure 5C). To address if KIF19 binding to microtubules leads to their depolymerization, we transfected COS-7 cells with KIF19-GFP and GFP-MCAK, a kinesin-13 family protein with depolymerizing activity (Walczak et al., 2013), and stained the cells for α-tubulin. As expected, the majority of GFP-MCAK-transfected cells showed a disrupted microtubule cytoskeleton in comparison to control cells, characterized by a loss of polymerized α-tubulin pattern (Figure 5D-E). We also observed that 33 % of KIF19-GFP-transfected cells showed a disruption of the microtubule network, while this only happened in 4 % of control cells (Figure 5D-E). Our data show that KIF19 overexpression is able to induce depolymerization of microtubules in COS-7 cells. We then assessed the localization of KIF19-GFP in dissociated cortical neurons, and we found that KIF19-GFP localizes to the tips of both axonal and dendritic processes of DIV 2 cortical neurons (Figure 5F, middle panel). Moreover, looking at the axonal growth cone (Figure 5F, bottom panel), it is possible to observe that KIF19-GFP co-localizes with microtubules, similar to COS-7 cells. We hypothesized that the localization of KIF19 at axonal growth cones may underlie the defects observed in both axon initiation and outgrowth and neuronal polarization upon KIF19 depletion in hippocampal neurons.

KIF19 is required for proper Golgi, but not microtubule organization

We then assessed if the microtubules present at axonal growth cones were affected by KIF19 knockdown. We found that the percentage of axonal growth cones with visible microtubules or buckled microtubules did not differ between control and KIF19-depleted neurons (Figure 6A-C). Tyrosinated microtubules have been shown to be enriched at the growth cones (Tanaka et al., 1995), and this enrichment was also not affected by KIF19 depletion (Figure 6D-E). Even though we showed that overexpression of KIF19 induces microtubule depolymerization in COS-7 cells (Figure 5D-E), these results suggest that KIF19 depletion does not primarily affect microtubule organization at the growth cones. It will be important to investigate if KIF19-induced microtubule depolymerization happens at the growth cone, and if this process is essential for axonal outgrowth and guidance.

In HeLa cells, silencing of KIF19 affects the organization of the Golgi complex (Andreyeva, 2008), so we examined if KIF19 depletion changed Golgi morphology in hippocampal neurons by staining the neurons against the cis-Golgi marker GM130. In control cells, Golgi complex often showed interconnected cisternae that occupied a substantial part of the soma (Figure 6F-G). However, KIF19-depleted neurons exhibited a more condensed and packed Golgi apparatus, leading to a reduction in the overall Golgi area (Figure 6F-G). Our data indicate that KIF19 may be important for proper Golgi organization in hippocampal neurons.

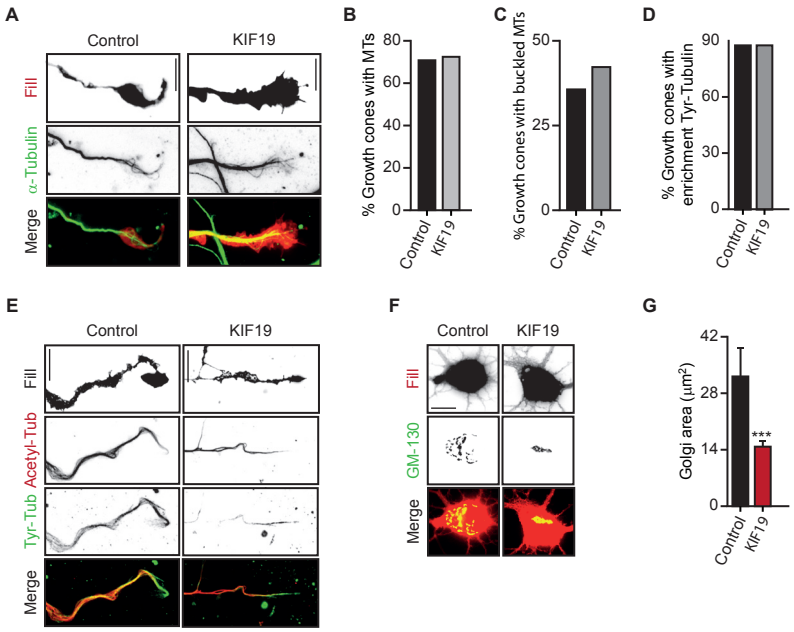

Figure 6. KIF19 is required for proper Golgi, but not microtubule organization.

(A) Representative images of DIV5 hippocampal neurons transfected at DIV 1 with BFP (fill; red) and pSuper (control) or KIF19 shRNAs, and stained for α-tubulin (green). Scale bar 10 μm.

(B-D) Percentage of growth cones in which microtubules (B), buckled microtubules (C) or enrichment of tyrosinated microtubules (D) were observed. n = 13 cells per condition. Two-tailed Mann-Whitney test.

(E) Representative images of DIV5 hippocampal neurons transfected at DIV 1 with BFP (fill) and pSuper (control) or KIF19 shRNAs, and stained for acetylated-tubulin (acetyl-tubulin, red) and tyrosinated tubulin (tyr-tubulin, green). Scale bar 10 μm.

(F) Representative images show control and KIF19-depleted DIV 5 hippocampal neurons transfected with a BFP-fill (red) at DIV 1 and stained for cis-Golgi marker GM-130 (green). Scale bar 10 μm.

(G) Quantification of the area covered by the cis-Golgi marker GM-130. n = 18 cells per condition. Two-tailed Mann-Whitney test: *** $p < 0.001$.

Data are represented as mean ± SEM. Red bars indicate $p < 0.05$.

FUTURE PERSPECTIVES

By systematically screening 39 out of the 46 mammalian kinesin proteins, we showed that three microtubule-depolymerizing kinesins (KIF3C, KIF19 and KIF2A) are required for the localization of the AIS marker β-IV-spectrin. We have also shown that these kinesins are involved in axon initiation upon treatment with nanomolar doses of the microtubule-stabilizing drug Taxol. Together, our data suggest that microtubule depolymerization is involved in axon development in hippocampal neurons. It will be interesting to assess if induction of microtubule depolymerization by kinesins at the growth cone of one neurite in non-polarized neurons could prompt this neurite to become the axon. Moreover, investigating if microtubule depolymerization could rescue the polarization and AIS defects in kinesin-depleted neurons would be important. We could then use photoswitchable inhibitors of

microtubule dynamics as Photostatin (Borowiak et al., 2015) to trigger depolymerization with high spatiotemporal precision at the growth cone of kinesin-depleted neurons.

Even though we were not able to detect KIF19 protein with the antibody used in this study, future studies should investigate the expression pattern of KIF19 in hippocampal neurons and the endogenous localization of the protein. We found that overexpressed KIF19 induces the depolymerization of microtubules in COS-7 cells and that it is localized to growth cones of cortical neurons. We hypothesize that the regulation of microtubule dynamics by KIF19 at the growth cone may be necessary for the neuronal polarization and axonal outgrowth. Microtubules can be found in a looped state as the growth cone pauses (Buck and Zheng, 2002; Dent et al., 1999; Williamson et al., 1996), and breaking of the looped microtubules coincides with the restart of directed axonal outgrowth (Dent et al., 1999). The localization of KIF19 at the growth cone and its association with growth cone microtubules suggests that it may promote the depolymerization of microtubules at the location where they are no longer required (site of repulsion) or of the looped microtubules. Reasonably, it will be important to show that KIF19 can actually promote microtubule depolymerization in hippocampal neurons. We could induce the recruitment of the kinesin to microtubules locally by using a light-induced heterodimerization assay (van Bergeijk et al., 2015), and assess changes on the microtubule cytoskeleton in the illuminated area.

Depletion of KIF19 was previously shown to induced an increase in focal adhesions size and the formation of stress fibers in HeLa cells (Andreyeva, 2008), suggesting a role for KIF19 in the regulation of the actin cytoskeleton. Actin is highly enriched in neuronal growth cones, and it will be interesting to quantify overall growth cone morphology or changes in the actin cytoskeleton upon KIF19 knockdown.

In summary, we have reported roles in axon establishment and growth of a little studied kinesin. We think that the microtubule depolymerizing activity of KIF19 may be necessary for proper neuronal polarization, axonal outgrowth and establishment of the AIS, and that the experiments discussed above may be necessary to unravel the precise mechanism by which KIF19 is required in these neurodevelopmental processes.

AUTHOR CONTRIBUTIONS

C.P.F., P.B, L.C.K and C.C.H. designed the study. C.P.F. wrote the manuscript and composed all figures with advice from C.C.H. C.P.F. performed and analysed the experiments described in Figures 1, 2 and 4A-B. Experiments in Figure 3, 4C-E, 5C-F and 6 were performed by P.B. J.L. cloned all the shRNAs constructs used in the study. Experiments in Figure 5A were performed by L.S. A.M. performed the experiments in Figure 5B under the supervision of J.J.

ACKNOWLEDGMENTS

This work was supported by the Netherlands Organization for Scientific Research (NWO-ALW-VICI, C.C.H.; NWO-ALW-VIDI, L.C.K.), the European Research Council (ERC) (ERC Consolidator Grant, C.C.H.; ERC Starting Grant, L.C.K.), and the Dutch Technology Foundation STW, which is part of the NOW (to C.C.H. and L.C.K.). C.P.F. is supported by the People Programme (Marie Curie Actions; MC-ITN) of the European Union's Seventh Framework Programme FP7/2007-2013/ under REA grant agreement 473 289581. J.L. is supported by International PhD projects Programme of Foundation of Polish Science

(Studies of nucleic acids and proteins – from basic to applied research). J.J. is supported by Polish National Science Centre Sonata Bis grant (2012/07/E/NZ3/00503) and the Foundation of Polish Science "Mistrz" Professorial Subsidy.

MATERIALS AND METHODS

Animals

All animal experiments were performed in compliance with the guidelines for the welfare of experimental animals issued by the Federal Government of The Netherlands. All animal experiments were approved by the Animal Ethical Review Committee (DEC) of Utrecht University.

Antibodies and reagents

The following antibodies were used in this study: mouse anti-AnkyrinG (clone 4G3F8, Zymed), mouse anti-pan-Neurofascin (clone L11A/41, NeuroMab), rabbit anti-β-IV-spectrin (kind gift from Dr. M. Rasband) (Ogawa et al., 2006), rabbit anti-Trim46 (van Beuningen et al., 2015), chicken anti-MAP2 (ab5392, Abcam), mouse anti-pan-Nav (clone K58/35, Sigma-Aldrich), rabbit anti-Map2 (4542, Cell Signaling), mouse anti-Tau (MAB3420, Chemicon), mouse anti-α-tubulin (clone B-5-1-2, Sigma-Aldrich), mouse anti-acetylated tubulin (clone 6-11B-1, Sigma-Aldrich), rat anti-tyrosinated tubulin (clone YL1/2, Abcam), mouse anti-GM130 (clone 610823, BD Bioscience), rabbit anti-GFP (598, MBL Sanbio), rabbit anti-KIF19 (HPA043638, Sigma-Aldrich), mouse anti-actin (clone C4, Merck Millipore), Alexa488- and Alexa568-conjugated secondary antibodies (Life Technologies) and anti-rabbit/mouse IgG antibody conjugated to horseradish peroxidase (DAKO). Reagents used in this study include: Taxol (T7402, Sigma-Aldrich) and Rapalog (AP20187, ARIAD Pharmaceuticals).

Expression and shRNA constructs

The constructs used in this study have been cloned in the following mammalian expression vectors: pβ-actin (Kapitein et al., 2010a), pGW2-CMV (Kapitein et al., 2010a), and pSuper (Brummelkamp et al., 2002). pβactin-GFP and pβactin-mGFP were generated by inserting GFP in the SalI and NotI sites of pβ-actin, whereas pGW2-CMV-tagBFP was generated by inserting tagBFP in the HindIII and AscI sites of pGW2-CMV. All shRNAs (see Supplementary Table 1) were designed using the siRNA selection program at the Whitehead Institute for Biomedical Research and were ligated into the BglII and HindIII sites of pSuper vector. p-βactin-TagRFP-TC-αTubulin was generated by inserting TagRFP-T (Evrogen) with the linker GMDELYKSGLRSSR and the N-terminus of α-Tubulin into the NheI and BamHI sites of pβ-actin. GFP-MCAK was a gift from Dr. M. Steinmetz (Honnappa et al., 2009).

To clone pβactin-KIF19-GFP, PCR amplified KIF19 (template cDNA clone MGC: 183958 IMAGE: 9087958) was cloned into AscI and SalI sites of pβactin-GFP. To make KIF19 (1-379)-FKBP*-mGFP, FKBP* was PCR amplified from pC4M-Fv2E (Ariad Pharmaceuticals), and ligated into the BamHI and SalI sites of pβactin-mGFP, followed by the upstream insertion of KIF19(1-379).

Primary hippocampal neuron culture, transfection and immunofluorescent staining

Primary hippocampal cultured neurons from embryonic day 18 (E18) rat brains were prepared as described previously (Kapitein et al., 2010b). In short, neurons were plated on coverslips coated with poly-L-lysine (37.5 µg/ml) and laminin (1.25 µg/ml) at a density of 100.000 per well (high density) or 50.000 per well (low density), and grown in Neurobasal medium supplemented with 0.5 mM glutamine, 15.6 µM glutamate, 2 % B27 and 1 % penicillin/streptomycin. Hippocampal neurons were transfected at 0 or 1 day-in-vitro (DIV) using Lipofectamine 2000 (Invitrogen). DNA (1.8 µg / well, for a 12-well plate) was mixed with 3.3 µL Lipofectamine 2000 in 200 µl NB, incubated for 30 minutes and then added to the neurons in Neurobasal supplemented with 0.5 mM glutamine at 37 °C in 5 % CO_2 for 60 minutes. Next, neurons were washed with Neurobasal and transferred to the original medium at 37 °C in 5 % CO_2 for 3 or 4 days. For taxol treatments, neurons were treated at DIV 4 with 10 nM taxol for 48 hours.

Immunocytochemistry of dissociated hippocampal neurons was performed by fixing the cells with 4 % paraformaldehyde (PFA)/4 % sucrose in phosphate buffer (PBS) at room temperature for 10 minutes. Neurons were then washed 3 times for 5 minutes in PBS at room temperature, and incubated with the primary antibody mix in GDB buffer (0.2 % Gelatin, 0.9 M NaCl, 0.6 % Triton X-100, 33.3 mM phosphate buffer, pH 7.4) overnight at 4 °C. Cells were washed 3 times for 5 minutes in PBS at room temperature, and incubated with the secondary antibody mix in GDB buffer for 1 hour at room temperature. After washing 3 times in PBS, the coverslips were mounted on slides in Vectashield mounting medium (Vector Labs) or Mowiol.

Primary cortical neuron culture and transfection

Primary cortical cultured neurons were prepared from embryonic day 18 (E18) rat brains. Cells (1.2×10^6) were transfected using the AMAXA Rat Neuron Nucleofector kit (Lonza) with 3 µg of DNA, and plated on wells (for western blot analysis) or on coverslips (for immunostainings) coated with poly-L-lysine (37.5 µg/ml) and laminin (1.25 µg/ml). In short, cells were pelleted for 5 minutes at 200g, and ressuspended in NucleofectorTM solution supplemented with FCS. The cells were then added to the DNA, electroporated and plated in DMEM medium containing 10 % FCS. Cells were allowed to recover and adhere at 37 °C in 5 % CO_2. After an incubation of 4 hours, the medium was replaced by Neurobasal medium supplemented with 0.5 mM glutamine, 15.6µM glutamate, 2 % B27 and 1 % penicillin/streptomycin. Cells were grown at 37 °C in 5 % CO_2 for 2, 4 or 7 days prior to lysis and Western blot analysis or fixation and immunocytochemistry as described for hippocampal neuron cultures.

Cultured cells, transfection and immunofluorescent staining

African Green Monkey SV40-transformed kidney fibroblast (COS-7) cells were cultured in DMEM/Ham's F10 (50 %/50 %) supplemented with 10 % FCS and 1 % penicillin/streptomycin at 37 °C and 5 % CO_2. Cells were plated on 24mm glass coverslips and transfected with Fugene6 (Promega). For live-cell imaging, coverslips were mounted in an imaging chamber.

For immunocytochemistry, cells were fixed for 10 minutes with paraformaldehyde (4 %) and washed 3 times for 5 minutes in PBS at room temperature. After permeabilization with 0.1 % Triton-X-100 in PBS for 15 minutes, cells were incubated with the primary antibody mix in GDB buffer (0.2 % Gelatin, 0.9 M NaCl, 0.6 % Triton X-100, 33.3 mM phosphate buffer, pH 7.4) overnight at 4°C. After washing 3 times in PBS, cells were incubated with the secondary antibody mix in GDB buffer for 1 hour at room temperature. Cells were then washed 3 times in PBS, and the coverslips were mounted in Mowiol.

Live-cell imaging and image processing

Time-lapse live-cell imaging of COS-7 cells was performed on a Nikon Eclipse TE2000E microscope (Nikon) with a Plan Fluor 40x objective NA 1.3 (Nikon), equipped with a CoolSnap HQ2 CCD camera (Photometrics) and an incubation chamber (INUG2-ZILCS-H2, Tokai Hit) mounted on a motorized stage (Prior). A mercury lamp (Osram) and a filter wheel containing the emission filters ET-GFP (49002), ET-dsRed (49005), ET-mCherry (49008) and ET-GFP-mCherry (59002) (all Chroma) were used for excitation. Coverslips were mounted in metal rings, immersed in Ringer's solution (10 mM HEPES, 155 mM NaCl, 5 mM KCl, 1 mM $CaCl_2$, 1 mM $MgCl_2$, 2 mM NaH_2PO_4 and 10 mM glucose, pH 7.4), and maintained at 37 °C and 5 % CO_2. Cells were imaged at every 30 s for 45 minutes. To homodimerize KIF19-FKBP*-GFP, 1 µM rapalog (previously dissolved in ethanol) was added to the culture medium during imaging.

Western blotting

4 or 7 days after transfection, the medium was aspirated, and neurons were lysed in SDS-page sample buffer containing DTT and boiled for 10 minutes. The lysates were loaded onto SDS-PAGE gels and blotted on PVDF membranes. After blocking with 3 % BSA in 0.1 % Tween/PBS for 1 hour, the blots were incubated with the primary antibody mix overnight at 4 °C. After washing 3 times in 0.1 % Tween/PBS, the blots were incubated with the secondary antibodies conjugated to horseradish peroxidase for 1 hour. Blots were washed in 0.1 % Tween/PBS and developed using enhanced chemiluminescent Western Blotting substrate (Pierce).

Quantitative RT-PCR

Freshly isolated rat cortical neurons were transfected using the AMAXA Rat Neuron Nucleofector kit (Lonza) and seeded on poly-D-lysine pre-coated plates. After 48 hours, neurons were lysed and RNA was isolated using the RNA mini kit (Qiagen). Reverse transcription was performed using the High Capacity Reverse Transcription kit (Applied Biosystems), and qPCR was performed as previously described (Malik et al., 2013). The following TaqMan rat probes were used for gene expression analysis: GAPDH Rn99999916_s1 and KIF19 Rn01470721_m1. SDS 2.4 and RQ Manager 1.2.1 programs were used for data acquisition and preliminary analysis. Data were analyzed by comparative Ct method for relative quantification.

Image analysis and quantification

Image processing and analysis was performed using ImageJ (US National Institute of Health) and MetaMorph (Molecular Devices). Unless stated otherwise, images were taken using a 40x/1.3 NA objective (Nikon) Plan Fluor objective, a 60x/1.4 NA Plan Apo VC objective or a 100x/1.4 NA Plan Apo VC objective on a Nikon Eclipse 80i microscope, equipped with a CoolSnap HQ2 CCD camera (Photometrics).

Morphometric analysis. For analysis of neuronal morphology, GFP was used as a cell-fil, and images were acquired using Olympus BX53 upright fluorescent microscope using a 10x/0.30 NA UplanFL objective (Olympus). The axon was identified as the non-MAP2 positive neurite. Only neurons with clearly defined neuronal arborization and no overlapping neighboring cells were imaged and analyzed. Total axonal length, axon length, number and mean length of axonal branches, total dendritic length, number and mean length of primary dendrites, and number and mean length of dendritic branches were quantified using ImageJ software and the NeuronJ plugin (Meijering et al., 2004). The axon length was determined by tracing the longest neurite, and total axonal length was calculated as the sum of the length of the axon and its branches. The total dendritic length was calculated as the sum of the length of all primary dendrites and their branches.

Quantification of Golgi area. To determine the area of the Golgi in the cell body of the neurons, we visualized Golgi morphology using the trans-Golgi marker GM130. Images were first binarized.

Statistics

Data are represented as mean values ± standard error of the mean, unless stated otherwise. Statistical analysis was performed using GraphPad Prism software. For the comparison of multiple groups, we used the Kruskal-Wallis test followed by a posthoc Dunn's comparison test. For the comparison of fractions, we used a one-tailed or two-tailed Fisher's exact test or a Chi-square test. For the comparison between control and knockdown, we used a two-tailed t-test or a two-tailed Mann-Whitney test. The used test is stated in each figure legend.

Differences between control and treatment were considered significant when $p < 0.05$ (*, $p < 0.05$; **, $p< 0.01$; ***, $p < 0.001$). In all figure legends and text, N indicates the number of independent experiments, and n indicates the number of cells analyzed.

REFERENCES

Andreyeva, N. (2008). Dissertation: Role of vesicular trafficking in focal adhesion turnover.

Baas, P.W., Black, M.M., and Banker, G.A. (1989). Changes in microtubule polarity orientation during the development of hippocampal neurons in culture. J. Cell Biol. 109, 3085-3094.

Baas, P.W., Deitch, J.S., Black, M.M., and Banker, G.A. (1988). Polarity orientation of microtubules in hippocampal neurons: uniformity in the axon and nonuniformity in the dendrite. Proc. Natl. Acad. Sci. USA 85, 8335-8339.

Baas, P.W., Slaughter, T., Brown, A., and Black, M.M. (1991). Microtubule dynamics in axons and dendrites. J. Neurosci. Res. 30, 134-153.

Borowiak, M., Nahaboo, W., Reynders, M., Nekolla, K., Jalinot, P., Hasserodt, J., Rehberg, M., Delattre, M., Zahler, S., Vollmar, A., et al. (2015). Photoswitchable Inhibitors of Microtubule Dynamics Optically Control Mitosis and Cell Death. Cell 162, 403-411.

Brummelkamp, T.R., Bernards, R., and Agami, R. (2002). A system for stable expression of short interfering RNAs in mammalian cells. Science 296, 550-553.

Buck, K.B., and Zheng, J.Q. (2002). Growth cone turning induced by direct local modification of microtubule dynamics. J. Neurosci. 22, 9358-9367.

Craig, A.M., and Banker, G. (1994). Neuronal polarity. Annu. Rev. Neurosci. 17, 267-310.

Dent, E.W., Callaway, J.L., Szebenyi, G., Baas, P.W., and Kalil, K. (1999). Reorganization and movement of microtubules in axonal growth cones and developing interstitial branches. J. Neurosci. 19, 8894-8908.

Dotti, C.G., Sullivan, C.A., and Banker, G.A. (1988). The establishment of polarity by hippocampal neurons in culture. J. Neurosci. 8, 1454-1468.

Franker, M.A., and Hoogenraad, C.C. (2013). Microtubule-based transport - basic mechanisms, traffic rules and role in neurological pathogenesis. J. Cell Sci. 126, 2319-2329.

Gumy, L.F., Chew, D.J., Tortosa, E., Katrukha, E.A., Kapitein, L.C., Tolkovsky, A.M., Hoogenraad, C.C., and Fawcett, J.W. (2013). The kinesin-2 family member KIF3C regulates microtubule dynamics and is required for axon growth and regeneration. J. Neurosci. 33, 11329-11345.

Hedstrom, K.L., Ogawa, Y., and Rasband, M.N. (2008). AnkyrinG is required for maintenance of the axon initial segment and neuronal polarity. J. Cell Biol. 183, 635-640.

Heidemann, S.R., Hamborg, M.A., Thomas, S.J., Song, B., Lindley, S., and Chu, D. (1984). Spatial organization of axonal microtubules. J. Cell Biol. 99, 1289-1295.

Hirokawa, N., Niwa, S., and Tanaka, Y. (2010). Molecular motors in neurons: transport mechanisms and roles in brain function, development, and disease. Neuron 68, 610-638.

Hirokawa, N., Noda, Y., Tanaka, Y., and Niwa, S. (2009). Kinesin superfamily motor proteins and intracellular transport. Nat. Rev. Mol. Cell Biol. 10, 682-696.

Homma, N., Takei, Y., Tanaka, Y., Nakata, T., Terada, S., Kikkawa, M., Noda, Y., and Hirokawa, N. (2003). Kinesin superfamily protein 2A (KIF2A) functions in suppression of collateral branch extension. Cell 114, 229-239.

Honnappa, S., Gouveia, S.M., Weisbrich, A., Damberger, F.F., Bhavesh, N.S., Jawhari, H., Grigoriev, I., van Rijssel, F.J., Buey, R.M., Lawera, A., et al. (2009). An EB1-binding motif acts as a microtubule tip localization signal. Cell 138, 366-376.

Inagaki, N., Chihara, K., Arimura, N., Menager, C., Kawano, Y., Matsuo, N., Nishimura, T., Amano, M., and Kaibuchi, K. (2001). CRMP-2 induces axons in cultured hippocampal neurons. Nat. Neurosci. 4, 781-782.

Jacobson, C., Schnapp, B., and Banker, G.A. (2006). A change in the selective translocation of the Kinesin-1 motor domain marks the initial specification of the axon. Neuron 49, 797-804.

Jiang, H., Guo, W., Liang, X., and Rao, Y. (2005). Both the establishment and the maintenance of neuronal polarity require active mechanisms: critical roles of GSK-3beta and its upstream regulators. Cell 120, 123-135.

Jones, S.L., and Svitkina, T.M. (2016). Axon Initial Segment Cytoskeleton: Architecture, Development, and Role in Neuron Polarity. Neural Plast. 2016, 6808293.

Kapitein, L.C., Schlager, M.A., van der Zwan, W.A., Wulf, P.S., Keijzer, N., and Hoogenraad, C.C. (2010a). Probing intracellular motor protein activity using an

inducible cargo trafficking assay. Biophys. J. 99, 2143-2152.

Kapitein, L.C., Yau, K.W., and Hoogenraad, C.C. (2010b). Microtubule dynamics in dendritic spines. Methods Cell Biol. 97, 111-132.

Lakshmikanth, G.S., Warrick, H.M., and Spudich, J.A. (2004). A mitotic kinesin-like protein required for normal karyokinesis, myosin localization to the furrow, and cytokinesis in Dictyostelium. Proc. Natl. Acad. Sci. USA 101, 16519-16524.

Lin, S., Liu, M., Mozgova, O.I., Yu, W., and Baas, P.W. (2012). Mitotic motors coregulate microtubule patterns in axons and dendrites. J. Neurosci. 32, 14033-14049.

Lipka, J., Kapitein, L.C., Jaworski, J., and Hoogenraad, C.C. (2016). Microtubule-binding protein doublecortin-like kinase 1 (DCLK1) guides kinesin-3-mediated cargo transport to dendrites. EMBO J. 35, 302-318.

Malik, A.R., Urbanska, M., Gozdz, A., Swiech, L.J., Nagalski A., Perycz, M., Blazejczyk, M., and Jaworski, J. (2013). Cyr61, a matricellular protein, is needed for dendritic arborization of hippocampal neurons. J. Biol. Chem. 288, 8544-8559.

Meijering, E., Jacob, M., Sarria, J.C., Steiner, P., Hirling, H., and Unser, M. (2004). Design and validation of a tool for neurite tracing and analysis in fluorescence microscopy images. Cytometry A 58, 167-176.

Nakata, T., and Hirokawa, N. (2003). Microtubules provide directional cues for polarized axonal transport through interaction with kinesin motor head. J. Cell Biol. 162, 1045-1055.

Niwa, S., Nakajima, K., Miki, H., Minato, Y., Wang, D., and Hirokawa, N. (2012). KIF19A is a microtubule-depolymerizing kinesin for ciliary length control. Dev. Cell 23, 1167-1175.

Ogawa, Y., Schafer, D.P., Horresh, I., Bar, V., Hales, K., Yang, Y., Susuki, K., Peles, E., Stankewich, M.C., and Rasband, M.N. (2006). Spectrins and ankyrinB constitute a specialized paranodal cytoskeleton. J. Neurosci. 26, 5230-5239.

Oksdath, M., Guil, A.F., Grassi, D., Sosa, L.J., and Quiroga, S. (2016). The Motor KIF5C Links the Requirements of Stable Microtubules and IGF-1 Receptor Membrane Insertion for Neuronal Polarization. Mol. Neurobiol.

Stepanova, T., Slemmer, J., Hoogenraad, C.C., Lansbergen, G., Dortland, B., De Zeeuw, C.I., Grosveld, F., van Cappellen, G., Akhmanova, A., and Galjart, N. (2003). Visualization of microtubule growth in cultured neurons via the use of EB3-GFP (end-binding protein 3-green fluorescent protein). J. Neurosci. 23, 2655-2664.

Tanaka, E., Ho, T., and Kirschner, M.W. (1995). The role of microtubule dynamics in growth cone motility and axonal growth. J. Cell Biol. 128, 139-155.

Tikhonenko, I., Nag, D.K., Robinson, D.N., and Koonce, M.P. (2009). Microtubule-nucleus interactions in Dictyostelium discoideum mediated by central motor kinesins. Eukaryot. Cell 8, 723-731.

Uchiyama, Y., Sakaguchi, M., Terabayashi, T., Inenaga, T., Inoue, S., Kobayashi, C., Oshima, N., Kiyonari, H., Nakagata, N., Sato, Y., et al. (2010). Kif26b, a kinesin family gene, regulates adhesion of the embryonic kidney mesenchyme. Proc. Natl. Acad. Sci. USA 107, 9240-9245.

van Bergeijk, P., Adrian, M., Hoogenraad, C.C., and Kapitein, L.C. (2015). Optogenetic control of organelle transport and positioning. Nature 518, 111-114.

van Beuningen, S.F., Will, L., Harterink, M., Chazeau, A., van Battum, E.Y., Frias, C.P., Franker, M.A., Katrukha, E.A., Stucchi, R., Vocking, K., et al. (2015). TRIM46 Controls Neuronal Polarity and Axon Specification by Driving the Formation of Parallel Microtubule Arrays. Neuron 88, 1208-1226.

van der Vaart, B., van Riel, W.E., Doodhi, H., Kevenaar, J.T., Katrukha, E.A., Gumy, L., Bouchet, B.P., Grigoriev, I., Spangler, S.A., Yu, K.L., et al. (2013). CFEOM1-associated kinesin KIF21A is a cortical microtubule growth inhibitor. Dev. Cell 27, 145-160.

Walczak, C.E., Gayek, S., and Ohi, R. (2013). Microtubule-depolymerizing kinesins. Annu. Rev. Cell Dev. Biol. 29, 417-441.

Williamson, T., Gordon-Weeks, P.R., Schachner, M., and Taylor, J. (1996). Microtubule reorganization is obligatory for growth cone turning. Proc. Natl. Acad. Sci. USA 93, 15221-15226.

Witte, H., Neukirchen, D., and Bradke, F. (2008). Microtubule stabilization specifies initial neuronal polarization. J. Cell Biol. 180, 619-632.

Yang, W., Tanaka, Y., Bundo, M., and Hirokawa, N. (2014). Antioxidant signaling involving the microtubule motor KIF12 is an intracellular target of nutrition excess in beta cells. Dev. Cell 31, 202-214.

Yau, K.W., Schatzle, P., Tortosa, E., Pages, S., Holtmaat, A., Kapitein, L.C., and Hoogenraad, C.C. (2016). Dendrites In Vitro and In Vivo Contain Microtubules of Opposite Polarity and Axon Formation Correlates with Uniform Plus-End-Out Microtubule Orientation. J. Neurosci. 36, 1071-1085.

Yoshimura, T., Kawano, Y., Arimura, N., Kawabata, S., Kikuchi, A., and Kaibuchi, K. (2005). GSK-3beta regulates phosphorylation of CRMP-2 and neuronal polarity. Cell 120, 137-149.

Zhou, R., Niwa, S., Guillaud, L., Tong, Y., and Hirokawa, N. (2013). A molecular motor, KIF13A, controls anxiety by transporting the serotonin type 1A receptor. Cell Rep. 3, 509-519.

SUPPLEMENTARY INFORMATION

Supplementary table 1. Overview of shRNA target sequences used in this study.

Family	Alias		shRNA sequence 5'- 3'
Kinesin-1	KIF5A	#1	GGACACCAGCGAAAACGGA
		#2	GCTGGTACGTGACAATGCA
		#3	GAGACCAATAACGAATGCA
	KIF5B	#1	GGTTATGCAAGACAGACGA
		#2	GGAATATGAATTGCTTAGT
		#3	GCCTTATGCATTTGATCGT
	KIF5C	#1	GGATCGCACACGATATTTT
		#2	CAATGCCTGTGCGAAGCAG
		#3	GCTGTCAATTACGACCAGA
Kinesin-2	KIF3A	#1	GTGCGACCAATATGAACGA
		#2	CGTATCGGAACTCTAAACT
		#3	GTTGGTGCGACCAATATGA
	KIF3B	#1	GGATACAAGAGACCACTGA
		#2	GGTCAGGGCATCTTACTTA
		#3	GGGCATCTTACTTAGAGAT
	KIF3C	#1	ATACAGGGCTGAAAATATA
		#2	GGAATTTTCTCATGACCAA
		#3	CCACGTCTAAAGTGCGAAA
Kinesin-3	KIF1A	#1	CAGGATGACCGGACCTTCT
		#2	GACCGGACCTTCTACCAGT
		#3	GTCATCAGGATACGTCCAT
	KIF1B	#1	GGGCTAAACATTTCGTTGT
		#2	GCAACGCTGTTATCAATGA
		#3	CTGGATCTAATGCGAGAGA
	KIF13A	#1	CGTACCTTATCGAGATTCA
		#2	GAACCAGTTAGACGTGTCT
		#3	GCTCATTAAACGACGGGAA
	KIF13B	#1	GAAGCCGACAAACGTTGAA
		#2	GACGAGAAATTGACTTACA
		#3	GGATGATGCTGACCGAGAG
	KIF14	#1	CATAAACAGCACTTATGTT
		#2	CATCCCGATATGAAACAAA
		#3	CGCTCTCATTCCGTTTTCA
	KIF16B	#1	CCTTCGCTATGCAAATAGA
		#2	GGCCTAGATAACATTCTCT
		#3	CTGCCAAACTTAGGGAGAA
Kinesin-4	KIF4A	#1	CTAATGTGCTCAGACGTAA
		#2	CCCAAACCTTTCCGTATTA
		#3	CCTTCGCTATGCTGACAGA
	KIF4B	#1	GAAGTCTAGAATCGGAAGT
		#2	CAAGCGGTTATCCATCTAT
		#3	GGTTATCCATCTATCAGAT
	KIF7	#1	GGTCGACACATGTGGATAA
		#2	GAGCAAGGTATTATCCCAA
		#3	GGATAAACCAGGAGCTCAA
	KIF21A	#1	CACGCACTGTGAATACAGA
		#2	CCGCGAACATAGATTACAT
		#3	GCAAACATCACGTGCGAAA
	KIF21B	#1	GACGCTCACTGCTAAGTTC
		#2	CCCTCGTTGAGATCAAAGA
		#3	CTCACTATGACGGTATCGA
	KIF27	#1	GGTGATAAATTTGCGAGAA
		#2	CGTATAGGGATGCGAAGAT
		#3	GGACCTTCACATCCGAGAA
Kinesin-5	KIF11	#1	GCTGGTATAATTCCACGTA
		#2	CCACGTACTCTTCATCAGA
		#3	GCAGAGTTATTTACGGATA

Family	Alias		shRNA sequence 5'- 3'
Kinesin-6	KIF20A	#1	CGGCAATCCTTACGTGAAA
		#2	CTTCGAATCAGACCGTTCT
		#3	GCATCTACATATGACGAAA
	KIF23	#1	GGAGAAACGACATCGCTTA
		#2	GAAGTGGTCAATAGTACAA
		#3	CCTTGTTAGAACGGCAGAA
Kinesin-7	KIF10	#1	GGAAGGATCTAGCGATGAA
		#2	GCTGTTACATAAATCGGAA
		#3	CTGAAGGTATGCGATTGAA
Kinesin-8	KIF18A	#1	GCAGCTACTAGACAATGGA
		#2	TTTGTAGAAGGCACAAATA
		#3	GACACATATAACACTCTTA
	KIF18B	#1	CCTATGAGGATACTTACAA
		#2	AGATCTTTGTGAAGCAGCA
		#3	TGACCACCATGGAACTGTA
	KIF19	#1	GCAATGACATGGAATATGA
		#2	CCAAGTGTATCTCCGTGAA
		#3	CGGGAGAAGTCATACCTCT
Kinesin-9	KIF6	#1	CAGACGGATTCGTAAACAA
		#2	CCGACATGCTAAGCTTCAT
		#3	CGTACACATATCCCTTACA
	KIF9	#1	GCAATGACATGGAATATGA
		#2	GTTAGACGAAACGCTATCT
		#3	CGGGAGAAGTCATACCTCT
Kinesin-10	KIF22	#1	GAGAGCGAATGGTACTCAT
		#2	GCTTAAGATGAAGCAAAAA
		#3	GGAATTCGGCTAAAAGAGA
Kinesin-11	KIF26A	#1	GCGGTTTCGATAACTCAGA
		#2	GGAGTGTATAGATGGCAGT
		#3	AGATCAAGGTGTATGAGAT
	KIF26B	#1	GCTCAACCGTTACAATGCT
		#2	GTGACCGACAACATTAGGA
		#3	CCTACACCATGATCGGAAG
Kinesin-12	KIF12	#1	GCCAATAGCATTAACCGCA
		#2	CTTCACCTGGCTATTAGAT
		#3	GAAGCTTTGATGGAACTAT
	KIF15	#1	GGCTATTGCTCGACTAGAA
		#2	CCTACGATAACTTACAAGA
		#3	GGAAATTGATAGGTCATCA
Kinesin-13	KIF2A	#1	GTTGTTTACTTTCCACGAA
		#2	GATCGGGATTTACGTGGAA
		#3	GAACTGACTGTGGATCCAA
	KIF2B	#1	GAAAGAAGATTGAACTGGA
		#2	CACAATGGGTGGAGCCTTT
		#3	GGCAATACAAATTCGGAAA
	KIF2C	#1	CAACGCAGCAATGGGTTAA
		#2	GTGACGTTCTTCGAGATCT
		#3	GCCAATATAAGCACGGTGA
	KIF24	#1	GGATAGAGCTGGTTATGGT
		#2	GTGCTTAGAATCAGACTCT
		#3	CAGTCGGAATCAGACATCT
Kinesin-14	KIFC1	#1	CCAGTTACGTAGAGATCTA
		#2	CTGTCACCAATGCACGATA
		#3	CACGTGCCTTACCGAAATA
	KIFC2	#1	CACACTGGGACGTACCTAA
		#2	GGCACCACTGCAGTTTTAT
		#3	CGCCCTAATTACGCTGACT
	KIFC3	#1	CGAGAACCCAGGCATTAAT
		#2	CAGCTCCGGGACAGGTTAT
		#3	CCACCTGTTAAGTATGTCA

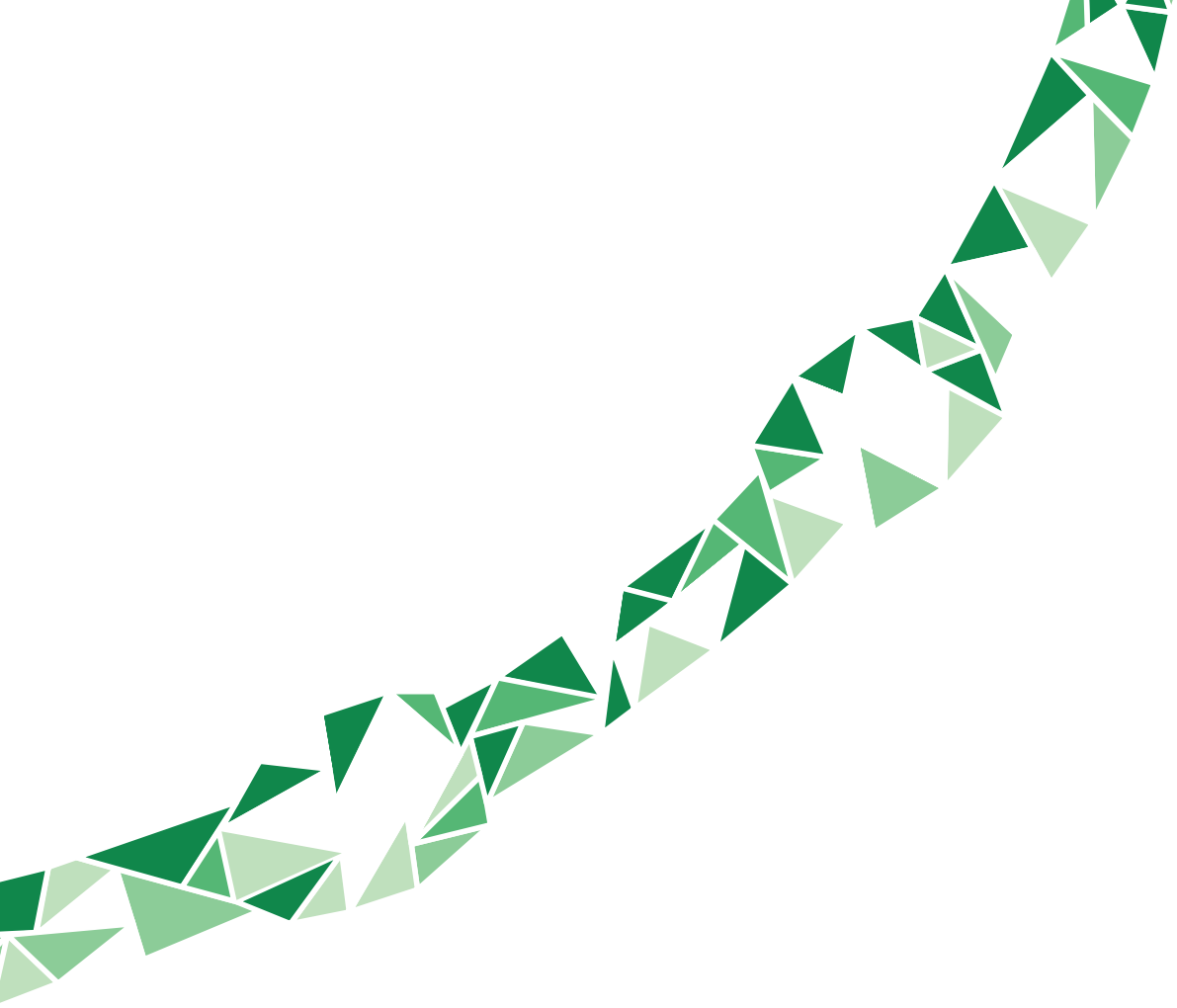

[1] Cell Biology, Department of Biology, Faculty of Science, Utrecht University, Utrecht, the Netherlands

[2] Biomolecular Mass Spectrometry and Proteomics, Bijvoet Center for Biomolecular Research, Utrecht Institute for Pharmaceutical Sciences and The Netherlands Proteomics Centre, Utrecht University, the Netherlands

Chapter 5

Screening motor proteins reveals that dynein is important for synaptic maintenance

Cátia P. Frias[1], Renske L. R. Taggenbrock[1], Feline W. Lindhout[1], Marta Esteves da Silva[1], Marijn Kuijpers[1], Riccardo Stucchi[1,2], A. F. Maarten Altelaar[2], Corette J. Wierenga[1] and Casper C. Hoogenraad[1]

ABSTRACT

During development, neurons establish precise synaptic connections that are essential for the information flow within the brain. Synaptic maintenance and function relies on the constant supply of synaptic proteins from and to the synapse. As most of the proteins are synthesized in the cell body, they need to be carried in different vesicles and protein complexes by molecular motors. Motor proteins walk along cytoskeletal filaments, and they have been shown to be important for neuronal function and plasticity. So far, the contribution of individual motor proteins for the maintenance of both excitatory and inhibitory synapses is not known. Here, we systematically addressed the role of motor proteins in the density of excitatory and inhibitory synapses within hippocampal neurons. We found that eight kinesins from different families are involved in the support of excitatory synapses, with weaker effects on inhibitory synapses. Moreover, we found that dynein-interacting proteins, some with undescribed roles in synaptic function, are required for the maintenance of both types of synapses. We uncovered roles for dynein-interacting proteins in spine maturation, in the surface level of excitatory neurotransmitter receptors and in the trafficking of recycling endosomes. Our data suggest a link between motor protein activity and synaptic structure in hippocampal neurons.

INTRODUCTION

Synapses are the basic communication units of the brain, mediating the transmission and storage of information. Synaptic function requires the release of neurotransmitter from the presynaptic terminal and the presence of neurotransmitter receptors and associated proteins at the postsynaptic site. Mainly two types of synapses are established in the brain: excitatory and inhibitory synapses. Excitatory synapses use glutamate as the neurotransmitter and induce the depolarization of the postsynaptic neuron, whereas inhibitory synapses hyperpolarize the postsynaptic neuron by releasing γ-aminobutyric acid (GABA) (Ben-Ari et al., 2007). The establishment and refinement processes of synapse assembly are critical for the proper function of the brain, and dysregulations on synaptic transmission are implicated in many neurological disorders (van Spronsen and Hoogenraad, 2010).

Most of the proteins necessary for the establishment and maintenance of pre- and postsynaptic terminals are produced at the cell body, and have to be delivered to the proper location within the axon and dendrites, respectively. Therefore, intracellular transport is crucial for synapse development and maintenance. Motor proteins are divided into 3 superfamilies (kinesin, dynein and myosin), and have been shown to promote the movement of synaptic cargoes and to regulate the underlying cytoskeletal filaments (Hirokawa et al., 2010). While in axons and dendrites microtubules and neurofilaments are the major cytoskeletal filaments, pre- and postsynaptic terminals are enriched in actin filaments (Hirokawa et al., 2010). Kinesin and dynein proteins walk along microtubule rails, which exhibit mixed polarity in dendrites (Baas et al., 1989), while in synaptic regions myosin proteins are the main delivery system by their ability to walk along actin filaments (Kneussel and Wagner, 2013). Kinesins from the kinesin-1, kinesin-2 and kinesin-3 families have been shown to be important for the transport of neurotransmitter receptors (Setou et al., 2000; Setou et al., 2002; Twelvetrees et al., 2010) and synaptic vesicles (Niwa et al., 2008; Wagner et al., 2009). Moreover, dynein-interacting proteins have been associated with the development of synapses by interacting with cell-adhesion molecules (Perlson et al., 2013) and scaffolding proteins as GKAP (Moutin et al., 2012), suggesting a role for dynein in synapse specification and stabilization. Myosin proteins are not only involved in the transport to and from the pre- and postsynaptic sites, but also in the regulation of the actin cytoskeleton dynamics (Kneussel and Wagner, 2013). Interestingly, mutations in motor protein encoding genes have been linked to neurological disorders (Franker and Hoogenraad, 2013; Hirokawa et al., 2010; Kneussel and Wagner, 2013), therefore it is important to understand the role of motor proteins in synapse formation and function. The majority of the studies so far have addressed the role of a single motor protein in the development and function of one type of synapse, and a systematic assessment of the contribution of each motor protein for the maintenance of both excitatory and inhibitory synapses is missing. In order to address the role of motor proteins in excitatory and inhibitory synaptic maintenance, we performed a targeted-knockdown screen and assessed changes in the density of excitatory and inhibitory synapses within the same hippocampal neuron. Our data revealed that eight kinesins from different families are involved in excitatory synapse maintenance, while inhibitory synapses are less affected by the depletion of kinesin proteins. On the other hand, dynein-interacting proteins are required for the maintenance of both synapse types, and are involved in dendritic spine maturation and in the delivery of excitatory neurotransmitter receptors. Therefore, we provide a mechanistic link between motor proteins and synaptic structure in hippocampal neurons.

RESULTS AND DISCUSSION

For rapid adaptation to changes in network activity, synapses need a constant supply of proteins, ranging from neurotransmitter receptors to scaffolding proteins, and this flux is established by motor proteins. In this study, we addressed the role of motor proteins in the maintenance of neuronal synapses in hippocampal neurons by using a targeted knockdown screen approach. As the timeline of synaptogenesis can differ with culturing conditions (van den Pol et al., 1998), we first assessed the time-course of excitatory and inhibitory synapse formation in our cultured hippocampal neurons. We transfected hippocampal neurons with GFP-Homer1c, in order to visualize excitatory postsynaptic densities, and empty pSuper vector at different days-in-vitro (DIV), and we fixed the cells 4 days later. We then performed immunostainings for Gephyrin, an inhibitory postsynaptic marker, and Bassoon, a presynaptic protein present in both excitatory and inhibitory terminals (Figure 1A). To analyze the density of excitatory and inhibitory synapses, we quantified the overlap between Homer and Bassoon (Figure 1B, top), and Gephyrin and Bassoon (Figure 1B, bottom), respectively (more details are given in the Methods section). The density of inhibitory synapses was low in DIV 12 neurons, but it increased as neurons mature (Figure 1C). Similar results were observed for the density of excitatory synapses, where we observed a plateau at DIV 18 (Figure

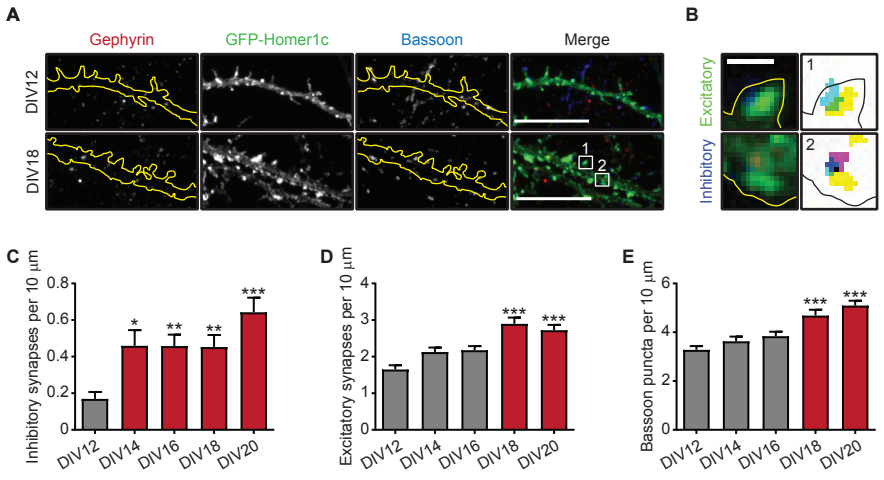

Figure 1. Synapse development in cultured hippocampal neurons.

(A) Representative images of days-in vitro (DIV) 12 and DIV 18 hippocampal neurons transfected with GFP-Homer1c and empty pSuper vector for 4 days. Neurons were immunostained for inhibitory postsynaptic protein Gephyrin (red) and presynaptic protein Bassoon (blue). Scale bar 10 µm.

(B) Example of an excitatory (up; box 1 in A) and an inhibitory (down; box 2 in A) synapse upon analysis using PunctaAnalyzer. An excitatory synapse (green) was defined by the co-localization of GFP-Homer1c (yellow) and Bassoon (blue), while an inhibitory synapse (dark blue) was defined by the co-localization of Gephyrin (magenta) and Bassoon (blue). Scale bar 1 µm.

(C-E) Quantification of inhibitory (C) and excitatory (D) synapses, and bassoon puncta (E) per 10 µm in hippocampal neurons at the indicated DIV. 3 stretches of dendrite were analyzed per cell (n = 10 cells per condition). Kruskal-Wallis test followed by post-hoc Dunn's multiple comparison test (comparison between DIV 12 and remaining DIVs). * $p < 0.05$, ** $p < 0.01$, *** $p < 0.001$.

Error bars represent mean ± SEM. Red bars indicate $p < 0.05$.

1D). The observed increases in synaptic density as the neuron matures are illustrated by increases on the density of individual synaptic puncta, such as Bassoon along the dendrites of transfected cells (Figure 1A,E). We also found that, from DIV 14 onwards, the rate of synapse formation seems to decrease, and the global neuronal network seems to be stabilized by DIV 18 (Figure 1C,D). Together, these data show that performing transfections of hippocampal neurons at DIV 14 and fixing the cells at DIV 18 is an appropriate window to identify motor proteins that play a role in synaptic maintenance.

Eight kinesin proteins are involved in the maintenance of excitatory synapses in hippocampal neurons

We performed a targeted knockdown screen of almost all kinesin motor proteins, using a pool of three shRNAs targeting the same protein. We found that the knockdown of seven kinesin proteins from different families decreased the density of excitatory synapses in comparison to control cells (Figure 2A,B). Specifically, knocking down KIF1A (kinesin-3), KIF13A (kinesin-3), KIF21B (kinesin-4), KIF10 (kinesin-7), KIF15 (kinesin-12), KIF24 (kinesin-13) and KIFC1 (kinesin-14) significantly reduced the density of excitatory synapses by at least 42 % (Figure 2B). The depletion of these proteins did not induce significant changes on the density of inhibitory synapses (Figure 2E). Except for KIFC1 depletion, the reduction on excitatory synapse density seems to be due to a decrease in the density of excitatory postsynaptic specializations, rather to a decrease in presynaptic structures formed onto the dendrites of the transfected neuron (Figure 2C,D). Oppositely to these seven kinesins, we found that depletion of KIF6 (kinesin-9) increased the density of excitatory synapses (Figure 2B), suggesting that KIF6 may act as a brake for synaptic development. Regarding inhibitory synapses, we observed that only KIF22-depleted neurons exhibited significant changes in the density of inhibitory synapses, with a ~75 % reduction in the density of inhibitory synapses (Figure 2A,E). These results indicate that KIF22, a plus-end directed kinesin with described roles in mitosis (Ohsugi et al., 2008), may be important for the maintenance of inhibitory synapses.

To further validate our results, we performed transfections using a single shRNA per kinesin. We could reproduced the results for single shRNAs targeting KIF1A, KIF13A and KIF21B, but not KIF24 and KIF22 (Figure 2F,G), suggesting a possible off-target effect. Our results point towards a dendritic function of KIF1A and KIF13A in excitatory synaptic maintenance, even though KIF1A is normally regarded as an important axon motor protein (Niwa et al., 2008; Wagner et al., 2009; Zhang et al., 2017). However, depletion of KIF1A was recently shown to affect the transport of dense-core vesicles in dendrites of hippocampal neurons (Lipka et al., 2016), consistent with our results. It would therefore be interesting to address which cargo is transported by KIF1A and KIF13A to support excitatory synapses. The phenotype observed after KIF21B depletion is in line with a study characterizing the KIF21B knockout mouse, in which KIF21B-/- neurons exhibited a reduction in spine density and surface expression of synaptic receptors (Muhia et al., 2016). As KIF21B is a motor protein with roles in both trafficking and microtubule dynamics in neuronal cells (Ghiretti et al., 2016; Muhia et al., 2016), it would be interesting to understand which KIF21B function is related to the maintenance of excitatory synapses. Altogether, our data show that kinesin motor proteins are essential for the maintenance of excitatory synapses in hippocampal neurons, and suggest that kinesin function may be required for the proper functionality or localization of postsynaptic density proteins.

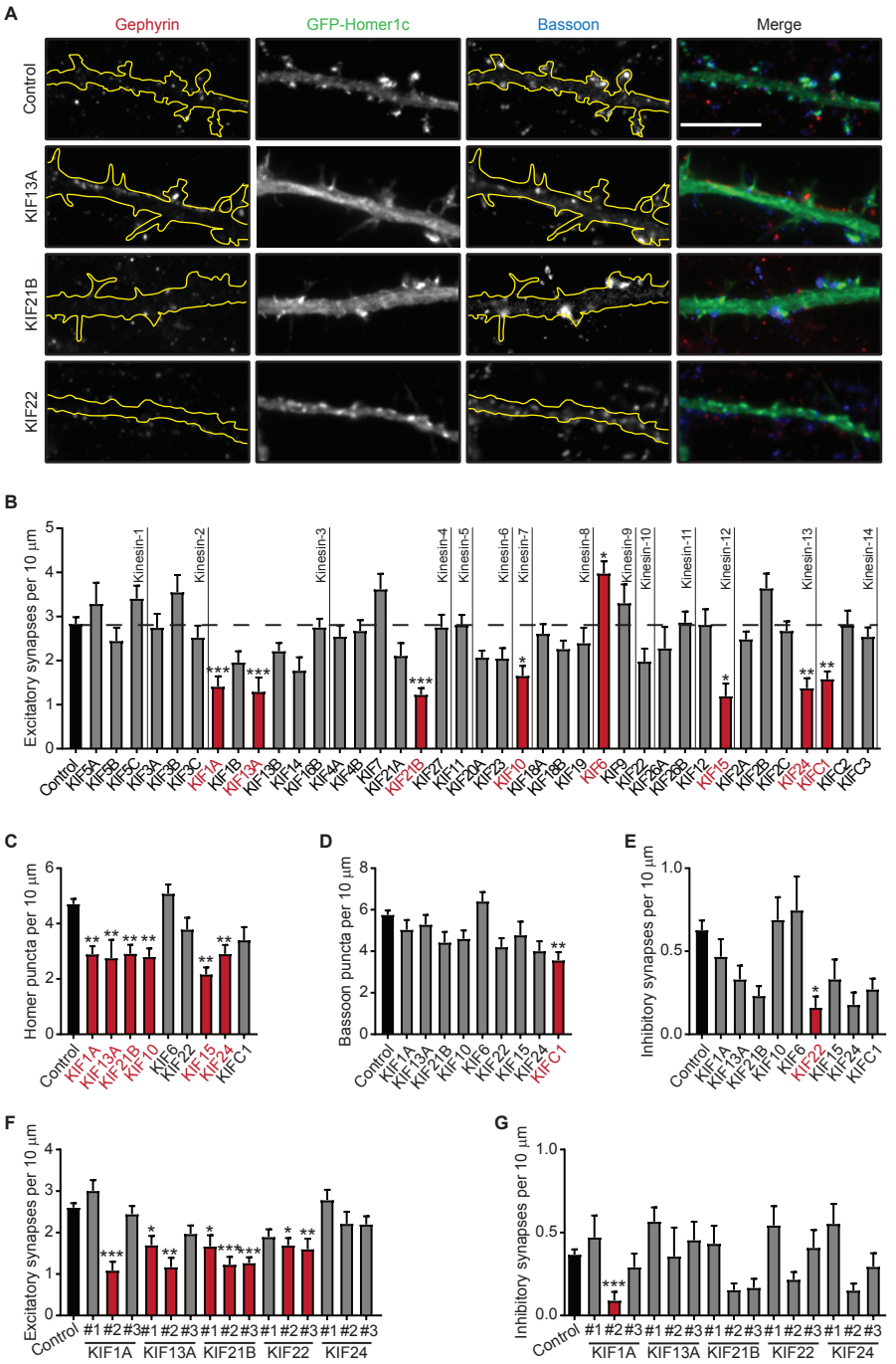

Figure 2. KIF1A, KIF13A, KIF21B and KIF24 are involved in the development of excitatory synapses in hippocampal neurons.

(A) Representative images of DIV 18 hippocampal neurons transfected at DIV 14 with pSuper (control) or KIF13A-, KIF21B-, and KIF22-shRNA pools and GFP-Homer1c. Neurons were immunostained for Gephyrin (red) and Bassoon (blue). Scale bar 10 µm.
(B) Average excitatory synapse number per 10 µm of dendrite in DIV 18 hippocampal neurons transfected at DIV 14 with pSuper (control) or indicated kinesin-shRNA pools and GFP-Homer1c. n = 16-20 cells from 2 independent experiments were analyzed per condition (for control, n = 125 cells, N = 3), except for KIF26 and KIF15 (n = 9 cells). Kruskal-Wallis test followed by post-hoc Dunn's multiple comparison test. * $p < 0.05$, *** $p < 0.001$.
(C-E) Average number of Homer (C) and Bassoon (D) puncta, and inhibitory synapses (E) per 10 µm of dendrite in DIV 18 hippocampal neurons transfected at DIV 14 with pSuper (control) or indicated kinesin-shRNA pools and GFP-Homer1c. n = 18-20 cells from 2 independent experiments were analyzed per condition (for control, n = 125 cells, N = 3), except for KIF15 (n = 9 cells). Kruskal-Wallis test followed by post-hoc Dunn's multiple comparison test. * $p < 0.05$, ** $p < 0.01$.
(F-G) Average excitatory (F) and inhibitory (G) synapse number per 10 µm of dendrite in DIV 18 hippocampal neurons transfected for 4 days with pSuper (control) or indicated single shRNAs and GFP-Homer1c. n = 16-20 cells from 2 independent experiments were analyzed per condition (for control, n = 126 cells, N = 5), except for KIF13A-#2 (n = 10 cells, N = 1). Kruskal-Wallis test followed by post-hoc Dunn's multiple comparison test. * $p < 0.05$, ** $p < 0.01$, *** $p < 0.001$.
Error bars represent mean ± SEM. Red bars indicate $p < 0.05$.

Depletion of MyosinX decreases the density of excitatory synapses

Actin is highly enriched in synaptic regions, and here myosin proteins are important for short-range transport and regulation of actin dynamics. Therefore, we assessed the contribution of neuronal myosin proteins for sustaining excitatory and inhibitory synapses. Similar to the kinesin screen, we used a pool of three shRNAs targeting the same protein. Knocking down non-muscle MyoIIb and MyoX changed the density of synapses along the dendrites of hippocampal neurons (Figure 3A). MyoX-depleted neurons showed a significant decrease in the density of excitatory synapses (Figure 3B) by reducing the number of Homer-positive protrusions (data not shown). This effect was confirmed when we tested the individual shRNAs (Figure 3D). In the brain, MyoX has been shown to be involved in early stages of synaptogenesis and spinogenesis (Lin et al., 2013). Moreover, knocking down MyoX showed a previously undescribed role in inhibitory synapses, as MyoX-depleted neurons showed a decrease of ~60 % in the density of inhibitory synapses (Figure 3C). MyoIIb also reduced the density of both excitatory and inhibitory synapses by 33 % and 37 %, respectively, but these effects did not reach significance. Even though MyoIIb has been linked to excitatory synapse formation and plasticity (Hodges et al., 2011; Rex et al., 2010), MyoIIb role on inhibitory synapse function has not been addressed. As the effects of MyoX and MyoIIb depletion seem to be similar in both types of synapses, our results suggest that these proteins are required for general processes underlying synapse formation. Therefore, it would be interesting to further investigate the role of both MyoX and MyoIIb in regulating actin-based processes at inhibitory synapses, similar to the ones observed at excitatory synapses. Given their prominent role in the delivery of synaptic cargo (Kneussel and Wagner, 2013), it was surprising that the MyoV and MyoVI did not induce major changes in either type of synapse.

Dynein-interacting proteins are necessary for supporting of excitatory and inhibitory synapses

Cytoplasmic dynein promotes minus-end directed transport of cargoes along the microtubule cytoskeleton, and consists of a massive complex of proteins of 1-2 MDa. This complex is

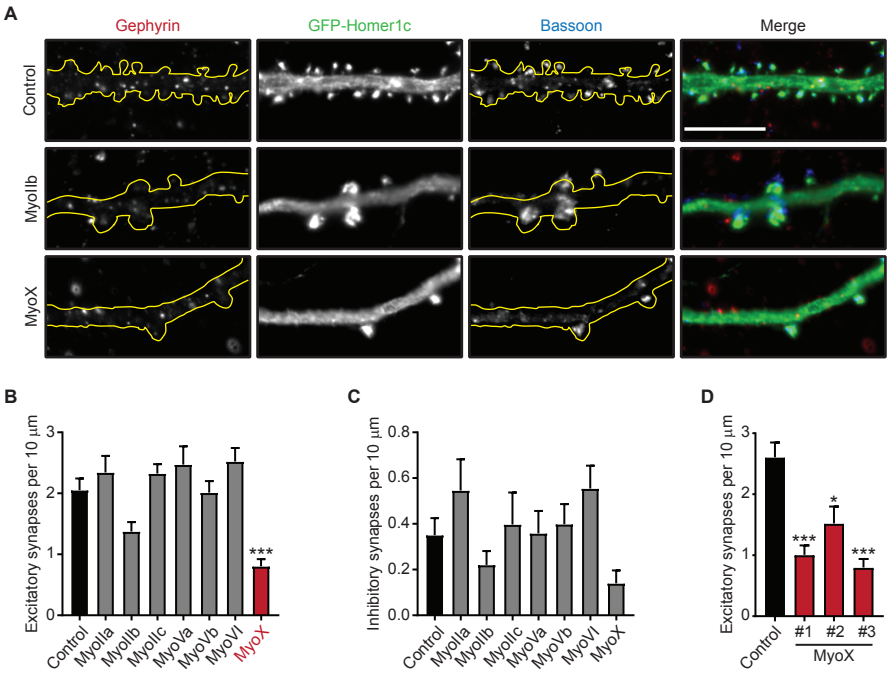

Figure 3. MyoX depletion reduces the density of excitatory synapses.

(A) Representative images of DIV 18 hippocampal neurons transfected for 4 days with pSuper (control) or MyoIIb- and MyoX-shRNA pools and GFP-Homer1c. Neurons were immunostained for Gephyrin (red) and Bassoon (blue). Scale bar 10 µm.

(B-C) Average excitatory (B) and inhibitory (C) synapse number per 10 µm of dendrite in DIV 18 hippocampal neurons transfected at DIV 14 with pSuper (control) or indicated myosin-shRNA pools and GFP-Homer1c. n = 18-20 cells from 2 independent experiments were analyzed per condition (for control, n = 39 cells, N = 3). Kruskal-Wallis test followed by post-hoc Dunn's multiple comparison test. *** $p < 0.001$.

(D) Average excitatory synapse number per 10 µm of dendrite in DIV 18 hippocampal neurons transfected for 4 days with pSuper (control) or single shRNAs targeting MyoX. n = 20 cells from 2 independent experiments were analyzed per condition (for control, n = 38 cells, N = 2).

Error bars represent mean ± SEM. Red bars indicate $p < 0.05$.

composed of different subunits that include heavy chains, intermediate chains, intermediate light chains and light chains, and can further associate with the dynactin complex and accessory factors that can influence dynein activity (van den Berg and Hoogenraad, 2012). Dynein has been shown to be involved in the transport of several synaptic cargoes, including α-amino-3-hydroxy-5-methyl-4-isoxazolepropionic acid receptor (AMPAR) and glycine receptor vesicles (Kapitein et al., 2010a; Maas et al., 2006). However, the contribution of the dynein complex for synaptic maintenance remains obscure. Therefore, we extended our screen to investigate the contribution of each dynein-interacting protein for the support of synapses in hippocampal neurons. We adapted a previously published library of siRNAs targeting the human sequences of each individual subunit of the dynein-dynactin complex and dynein adaptor proteins (Raaijmakers et al., 2013). We transfected DIV 14 hippocampal

neurons with GFP-Homer1c and single shRNA targeting the different dynein-interacting proteins for 4 days, and performed immunostainings for Gephyrin and Bassoon. Depleting dynein regulators generally affected the morphology of hippocampal neurons, and revealed that they are important for the proper maintenance of synapses (Figure 4A-C). As expected, impairing dynein movement by depleting the two dynein heavy chains (DHC1/2) prominently reduced the density of both types of synapses (Figure 4B,C). Besides dynein heavy chains, neurons depleted of dynactin subunit 6 (DCTN6) and dynein light chain LC8-type 1/2 (DLL1/2) also showed impairments in the maintenance of both types of synapses (Figure 4B,C). Interestingly, DLLs can associate with excitatory postsynaptic marker GKAP (Naisbitt et al., 2000) and gephyrin (Fuhrmann et al., 2002), which may explain our findings.

Opposite to kinesin proteins, several dynein interactors seem to be specifically important for sustaining inhibitory synapses, including dynactin subunit 3 (DCTN3) and Centromere/kinetochore protein zw10 homolog (ZW10) (Figure 4C). We could reproduce the effect of DCTN3, DCTN6 and ZW10 on synapses by transfecting neurons with other shRNAs targeting these proteins (Figure 4D,E). In control neurons, approximately 30 % of the gephryin puncta is associated with presynaptic Bassoon, but this percentage is decreased by the depletion of DCTN3, DCTN6 and ZW10 (Figure 4F), further confirming that these proteins are important for inhibitory synapses. These results show that dynein interactors are generally central for synaptic maintenance, and that three proteins with no previously reported role in synapses are important for this process.

Characterization of DCTN3, DCTN6 and ZW10

DCTN3 (p22/24) has been reported to interact with DCTN1 (p150) and two DCTN2 (p50) subunits, stabilizing the shoulder complex of dynactin (Terasawa et al., 2010). DCTN6 (p27) seems to have a distinct function from DCTN3, as it forms heterodimers with DCTN5 (p25) to mediate the binding of dynactin/dynein complex to early and recycling endosomes (Yeh et al., 2012). It is therefore interesting that deletion of DCTN3 and DCTN6, but not of other dynactin subunits, decreased the density of inhibitory synapses, suggesting that these proteins may have dynactin-independent roles in hippocampal neurons. ZW10 (Zeste-white in Drosophila and C. elegans) is mainly known for its role in mitosis (Chan et al., 2000; Starr et al., 1998), but it is also involved in ER-Golgi trafficking during interphase (Arasaki et al., 2007; Hirose et al., 2004). In order to study the molecular function of DCTN3, DCTN6 and ZW10, we generated N-terminally tagged expression constructs and purchased antibodies previously used in published studies. We validated the antibodies reactivity and specificity using immunocytochemistry in HeLa cells and hippocampal neurons (Figure 5A,D,G), where the antibodies could recognize the overexpressed protein. We then assessed the efficiency of the two shRNAs targeting the different proteins in hippocampal neurons and in A7r5 rat fibroblast cells. Our preliminary results showed that DCTN3-targeting shRNAs do not decrease DCTN3 intensity in the soma of hippocampal neurons (Figure 5B), but that the shRNA #1 is able to decrease the fluorescence signal by ~34 % in A7r5 cells (Figure 5C). Moreover, we also found that DCTN6-targeting shRNA #1 reduced the DCTN6 intensity signal by ~42 % in hippocampal neurons (Figure 5E). However, we could not confirm this effect in A7r5 cells (Figure 5F). Even though we could not observe a reduction in the fluorescence signal of ZW10 in ZW10-depleted neurons (Figure 5H), we found that more than 90 % of the cells transfected with shRNA #1 exhibited an abnormal Golgi morphology (Figure 5I). Depletion of ZW10 promotes Golgi morphology disruption in human cells (Sun

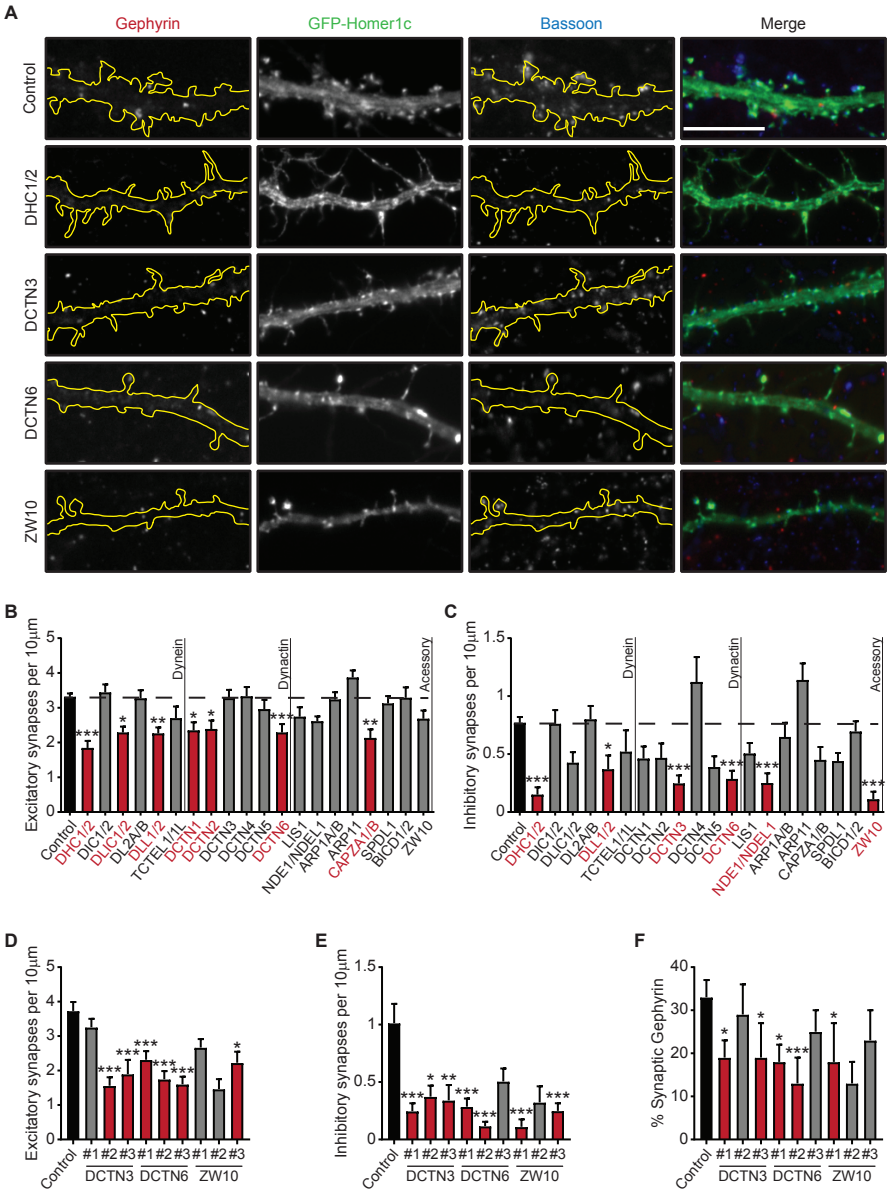

Figure 4. Dynein-interacting proteins are necessary for proper maintenance of excitatory and inhibitory synapses.

(A) Representative images of DIV 18 hippocampal neurons transfected for 4 days with pSuper (control) or DHC1/2-, DCTN3-, DCTN6- or ZW10-shRNA and GFP-Homer1c. Neurons were immunostained for Gephyrin (red) and Bassoon (blue). Scale bar 10 µm.

(B-C) Average excitatory (B) and inhibitory (C) synapse number per 10 µm of dendrite in DIV 18 hippocampal neurons transfected at for 4 days with pSuper (control) or indicated shRNAs and GFP-Homer1c. n = 16-30 cells

from at least 2 independent experiments were analyzed per condition, except for TCTEL1/1L (n=10 cells) (for control, n = 137 cells, N = 5). Kruskal-Wallis test followed by post-hoc Dunn's multiple comparison test. * $p < 0.05$, ** $p < 0.01$, *** $p < 0.001$.

(D-E) Average excitatory (D) and inhibitory (E) synapse number per 10 µm of dendrite in DIV 18 hippocampal neurons transfected for 4 days with pSuper (control) or indicated single shRNAs and GFP-Homer1c. n = 15-20 cells from 2 independent experiments were analyzed per condition (for control, n = 19 cells, N = 2), except for ZW10-#2 (n = 9 cells, N = 1). The shRNA #1 represents the data obtained in B and C. Kruskal-Wallis test followed by post-hoc Dunn's multiple comparison test. * $p < 0.05$, ** $p < 0.01$, *** $p < 0.001$.

(F) Percentage of synaptic Gephyrin puncta, determined by dividing the density of inhibitory synapses by the density of Gephyrin puncta, in DIV 18 hippocampal neurons transfected for 4 days with pSuper (control) or indicated single shRNAs and GFP-Homer1c. n = 15-20 cells from 2 independent experiments were analyzed per condition (for control, n = 19 cells, N = 2), except for ZW10-#2 (n = 9 cells, N = 1). The shRNA #1 represents the data obtained in B and C. Chi-square test. * $p < 0.05$, *** $p < 0.001$.

Error bars represent mean ± SEM. Red bars indicate $p < 0.05$.

et al., 2007), so the phenotype we observed may indicate that we are indeed changing ZW10 expression levels. Overall, our preliminary immunocytochemistry results do not show a consistent reduction in the expression of the studied proteins in hippocampal neurons and A7r5 cells. Future experiments involving electroporation of cortical neurons and western blot analysis or quantification of mRNA levels using Q-RT-PCR will be necessary to validate our shRNA constructs.

To gain more insights into the possible role of DCTN3, DCTN6 and ZW10 in maintaining inhibitory synapses, we performed pull-down experiments combined with mass spectrometry analysis to identify potential interactors of these proteins. Biotinylated and GFP-tagged (bioGFP) DCTN3, DCTN6 and ZW10 constructs were co-expressed with the biotin ligase BirA in HEK293 cells, and the cell extracts were used for pull-down assays with rat brain lysate. Interestingly, the mass spectrometry analysis of DCTN6 and ZW10 pull-downs identified a possible interaction with neurobeachin and neuroplastin, respectively (Figure 5J). Neurobeachin is a brain-specific A-kinase anchor protein (AKAP) recently shown to regulate the targeting of γ-aminobutyric acid type A receptors ($GABA_AR$) to synapses (Farzana et al., 2016). Neuroplastins are cell-adhesion proteins from the immunoglobulin superfamily that comprise two isoforms, Neuroplastin-55 (Np55) and Neuroplastin-65 (Np65). Np65 is present in both pre- and postsynaptic sites and is able to interact with GABAAR (Herrera-Molina et al., 2014; Sarto-Jackson et al., 2012). These results may provide a possible link to the effect of DCTN6 and ZW10 on inhibitory synapses, and it will therefore be interesting to address if Neurobeachin interacts biochemically with DCTN6, as well if Np65 does so with ZW10.

Dynein-interacting proteins are necessary for spine maturation and receptor delivery to excitatory synapses

We have also found that dynein-interacting proteins are required for the proper maintenance of excitatory synapses, such as dynein heavy chain1/2 (DHC1/2), dynein light intermediate chains 1/2 (DLIC1/2) and dynactin subunit 1 (DCTN1) (Figure 4B). To determine the role of these proteins in spine morphology, we co-transfected DIV 15 hippocampal neurons with the indicated shRNAs or empty pSuper vector, and MARCKS-GFP to highlight neuronal morphology for 3 days. We also used a dominant-negative construct of DCTN1 (DCTN1-cc1), which only includes the first coiled-coil domain (amino acid 217-546), to

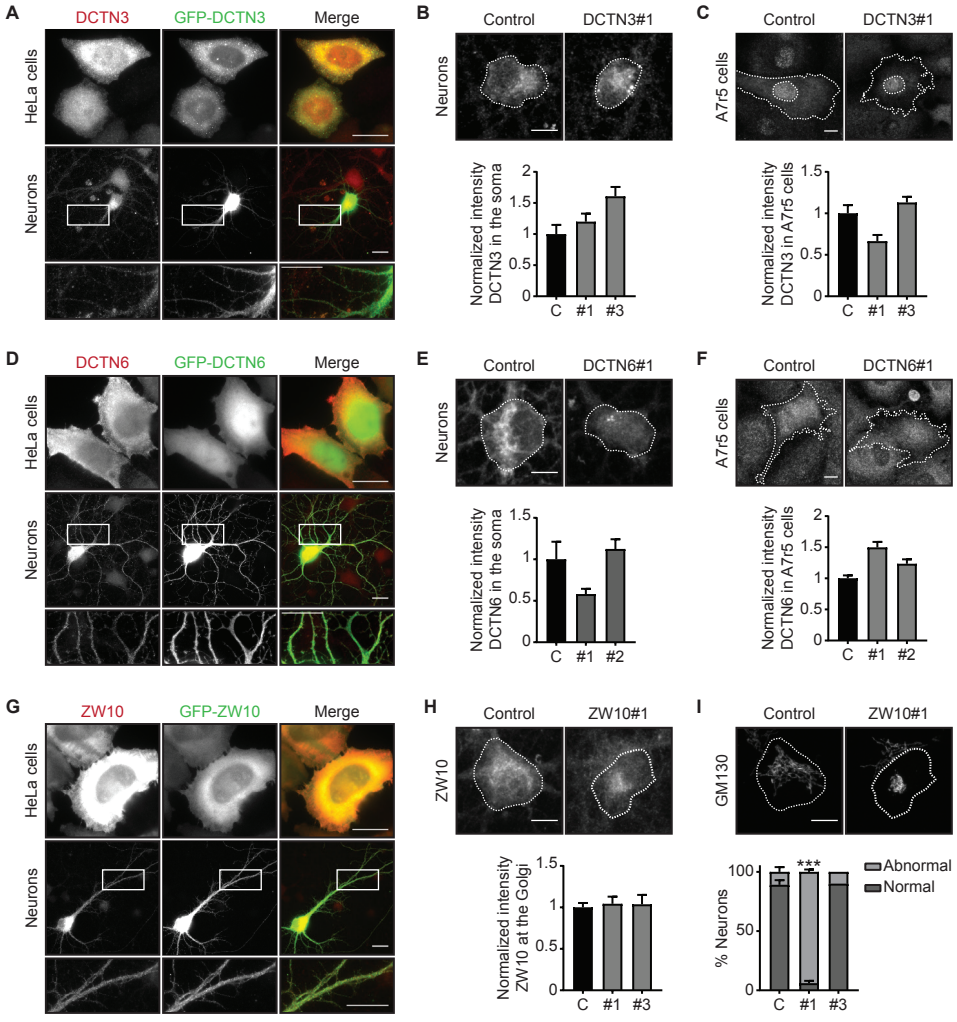

J

Accession	Protein	bio-GFP		bio-GFP-DCTN6		bio-GFP-DCTN3		bio-GFP-ZW10	
		# Pept	# PSM	# Pept	# PSM	# Pept	# PSM	# Pept	# PSM
D4ADD8	**Dynactin subunit 6**			**8**	**332**				
D4A1B8	**Dynactin subunit 3**					**10**	**163**		
Q4V8C2	**Centromere/kinetochore protein zw10 homolog**	**3**	**3**					**30**	**351**
P97546	Neuroplastin	1	1					6	8
P60881	Synaptosomal-associated protein 25	1	1			6	6	4	4
Q63564	Synaptic vesicle glycoprotein 2B	1	1	5	6				
G3V852	Talin 1			5	5	5	5		
D3ZWS0	Scribbled planar cell polarity protein	1	1	5	5				
F1LX73	Neurobeachin			4	4				
P85845	Fascin1	1	1					4	4
P09606	Glutamine synthetase					3	4	2	3
D3ZPP8	Neuronal-specific septin-3							3	3
Q812E9	Neuronal membrane glycoprotein M6-a					3	3	2	3

Figure 5. Characterization of candidates DCTN6, DCTN3 and ZW10.

(A) Representative images of HeLa cells (up) and DIV 13 hippocampal neurons (bottom) transfected for 1 (HeLa) or 2 days (neurons) with GFP-DCTN3. Cells were immunostained for DCTN3 (red). The lower panel represents

the zoomed region indicated by the white box. Scale bars 20 µm.
(B) Quantification of knockdown efficiency of DCTN3 shRNAs in hippocampal neurons, normalized to control. Neurons were transfected at DIV 14 with MARCKS-GFP to highlight neuronal morphology and empty pSUPER vector (control) or indicated DCTN3 shRNAs, fixed 4 days later and immunostained for DCTN3. Dotted lines highlight the somatic area of the transfected neuron. n = 12 cells from 2 independent experiments were analyzed for DCTN3#1 and n = 6 cells from one experiment were analyzed for DCTN3#3 (for control, n = 16 cells, N = 2). Kruskal-Wallis test followed by post-hoc Dunn's multiple comparison test.
(C) Quantification of knockdown efficiency of DCTN3 shRNAs in A7r5 cells, normalized to control. Cells were transfected for 2 days with empty pSUPER vector (control) or DCTN3 shRNAs and GFP, and immunostained for DCTN3. Dotted lines highlight the area of the nucleus (inner line) and the outline of the transfected cell. n = 9/10 cells from one experiment were analysed per condition (for control, n = 8 cells, N = 1).
(D) Same as A, but HeLa cells and hippocampal neurons were transfected with GFP-DCTN6, and immunostained for DCTN6 (red).
(E) Same as B, but neurons were transfected with empty pSUPER vector (control) or indicated DCTN6 shRNAs. n = 13-16 cells from 2 independent experiments were analysed per condition (for control, n = 19 cells, N = 2). Kruskal-Wallis test followed by post-hoc Dunn's multiple comparison test.
(F) Same as C, but cells were transfected with empty pSUPER vector (control) or DCTN6 shRNAs. n = 7 cells from one experiment were analysed per condition (for control, n = 9 cells, N = 1).
(G) Same as A, but HeLa cells and hippocampal neurons were transfected with GFP-ZW10, and immunostained for ZW10 (red).
(H-I) Quantification of knockdown efficiency of ZW10 shRNAs (H), and percentage of hippocampal neurons with normal (control) and abnormal (ZW10#1) Golgi morphology (I). Neurons were transfected with empty pSUPER vector (control) or indicated ZW10 shRNAs and MARCKS-GFP at DIV 14, fixed 4 days later and immunnostained for ZW10 (H) and GM-130 (cis- Golgi marker; I). n = 17 cells from 2 independent experiments were analyzed for ZW10#1 and n = 10 cells from one experiment were analyzed for ZW10#3 (for control, n = 19 cells, N = 2). Kruskal-Wallis test followed by post-hoc Dunn's multiple comparison test in H, and Chi-square test in I. *** $p < 0.001$.
(J) Binding partners of bioGFP-DCTN3, bioGFP-DCTN6 and bioGFP-ZW10 in HEK293 cells loaded with rat brain extracts, and identified by mass spectrometry. The table only includes hits that have been associated with synapses. For the complete lists, see Supplementary tables 4-6. PSM, peptide spectrum matches; Pept, number of peptides.
Error bars represent mean ± SEM.

compare with the effects of the DCTN1-targeting shRNA. Then, we fixed the cells and performed immunostainings for excitatory postsynaptic marker Homer1 and presynaptic protein Bassoon. We first quantified the density of dendritic protrusions outgrowing from the dendrite of the transfected neurons. We found that knockdown of dynein-interacting proteins affects the maturation level of dendritic protrusions (Figure 6A,B). More precisely, we observed that depletion of DHC1/2 and DLIC1/2 decreased the density of dendritic spines, similar to the overexpression of the DCTN1 dominant negative (Figure 6B). DLIC1/2-depleted neurons also showed a significant increase in the density of filopodia (Figure 6B). To determine if the morphological changes were translated to deficiencies in synapse number, we quantified the density of excitatory synapses formed at the protrusion level by analyzing co-localization of endogenous Homer and Bassoon puncta. The number of excitatory synapses was significantly decreased upon depletion of DHC1/2 and DCTN1 similar to the effect observed before (Figure 4B), while depletion of DLIC1/2 led to a decrease of ~36 % in the density of spine synapses (Figure 6C). Interestingly, DLIC1/2-depleted neurons also showed an almost 2-fold increase in the density of excitatory shaft synapses, an effect also observed for the depletion of Rab11-FIP3, an adaptor of Rab11 recycling endosomes shown to interact with DLIC1 and 2 (Horgan et al., 2010a, b) (Figure 6D). The similar phenotype of

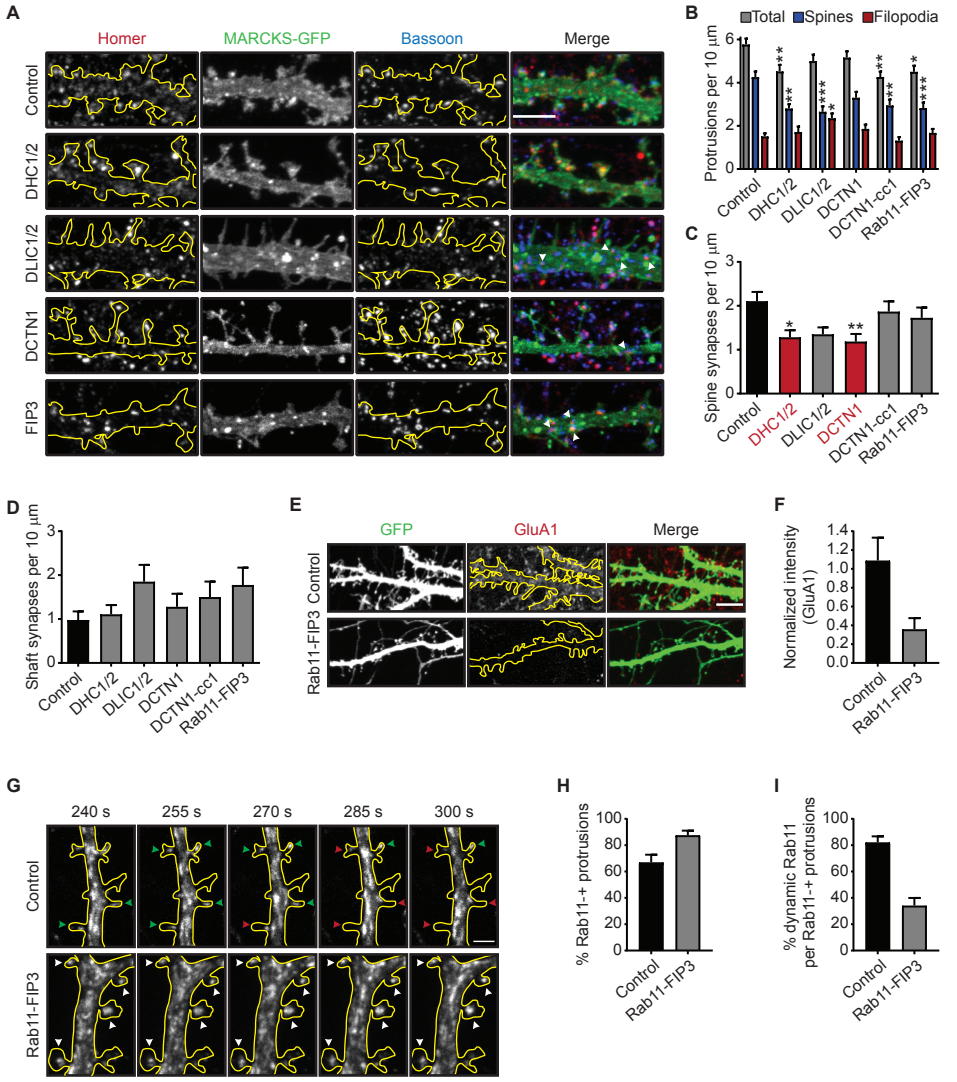

Figure 6. Dynein-interacting proteins are important for spine maturation in hippocampal neurons.
(A) Representative images of DIV 18 hippocampal neurons transfected with MARCKS-GFP and indicated shRNAs, empty pSuper vector (control) or a dominant negative form of p150 (p150-DN) at DIV 15, and immunostained for postsynaptic excitatory marker Homer (red) and presynaptic marker Bassoon (blue). White arrowheads represent excitatory synapses formed at the dendritic shaft. Scale bar 10 µm.
(B) Quantification of the number of protrusions per 10 µm of dendrite. Classification was based on the morphology of the spine observed through the acquired z-stacks. n = 22-27 cells from 3 independent experiments, except for Lis1 (n = 14 cells, N = 2) (for control, n = 27 cells, N = 3). Kruskal-Wallis test followed by post-hoc Dunn's multiple comparison test. * $p < 0.05$, ** $p < 0.01$, *** $p < 0.001$.
(C-D) Quantification of number of excitatory synapses formed at the protrusion (C) or at the dendritic shaft (D) per 10 µm of dendrite. An excitatory synapse was quantified when presynaptic Bassoon and postsynaptic Homer

co-localized in at least one of the z-stacks. n = 22-27 cells from 3 independent experiments, except for Lis1 (n = 14 cells, N = 2) (for control, n = 27 cells, N = 3). Kruskal-Wallis test followed by post-hoc Dunn's multiple comparison test. * $p < 0.05$, ** $p < 0.01$.

(E) Representative images of hippocampal neurons transfected with GFP (green), to highlight neuronal morphology, and empty pSuper vector (control) or Rab11-FIP3 shRNA. Neurons were stained for surface AMPAR subunit GluA1 (red). Scale bar 10 µm.

(F) Quantification of the surface intensity of GluA1 along the dendrites of Rab11-FIP3-depleted cells, normalized to control. n = 5 cells from one experiment (for control, n = 6 cells, N = 1).

(G) Stills from a 5 minute time-lapse recording of rat hippocampal neurons at DIV14-17 expressing GFP-Rab11 and empty pSuper vector (control) or Rab11-FIP3 shRNA. Green and red arrows indicate the entrance and exit of Rab11 endosomes to and from dendritic protrusions, respectively, and white arrows indicate static Rab11 endosomes (no movement in or out of the dendritic protrusion). Time in seconds. Scale bar is 2 µm.

(H-I) Quantification of the percentage of dendritic protrusions targeted by Rab11-positive recycling endosomes along 20 µm of dendrite during the time-lapse recordings (H) and percentage of dynamic Rab11-positive recycling endosomes per number of targeted protrusions (I), in control and Rab11-FIP3-depleted cells. n = 15 cells from one experiment (for control, n = 12 cells, N = 1).

Error bars represent mean ± SEM. Red bars indicate $p < 0.05$.

DLIC1/2 and Rab11-FIP3 depletion may suggest that the interaction between these proteins is necessary for proper excitatory synapse formation.

Excitatory shaft synapses have been linked to impairments on spine morphogenesis (Sugiura et al., 2015), and may act as a compensatory mechanism for decreased excitatory transmission prompted by a decrease on spine synapses. Synapse shaft formation observed upon depletion of Rab11-FIP3 and DLIC1/2 may be due to defects in spinogenesis or in the delivery of excitatory synaptic proteins to the postsynaptic specialization. We next assessed if the surface expression levels of AMPAR subunit GluA1 was affected by depletion of Rab11-FIP3 (Figure 6E). Our preliminary data showed that the surface intensity of GluA1 is reduced by ~60 % in neurons transfected with Rab11-FIP3 shRNA or a Rab11-FIP3 dominant negative construct (Figure 6F). Depletion of Rab11-FIP3 also decreased the surface intensity of GluA2 (data not shown). These results suggest that the movement of AMPARs along the dendrites of hippocampal neurons is modulated by Rab11-FIP3. We have previously shown that Rab11 endosomes transport intracellular AMPARs, and removal of Rab11-positive endosomes from dendritic spines affects synaptic architecture (Esteves da Silva et al., 2015). We then addressed if Rab11 movement was affected by depletion of Rab11-FIP3, and found that it increased the fraction of protrusions positive for Rab11 (Figure 6G,H). However, the dynamics of Rab11 vesicles were decreased in Rab11-FIP3-depleted cells (Figure 6G,I), suggesting that recycling endosomes are trapped in dendritic spines under this condition. It would be interesting to address if DLIC1/2 depletion leads to similar phenotypes. Moreover, as we observed an increase in shaft synapses, future studies could address if the depletion of Rab11-FIP3 or DLIC1/2 induce the formation of immobile clusters of Rab11 endosomes along the dendritic shaft. Overall, our data points towards a role of Rab11-FIP3 and DLIC1/2 in the proper flow of glutamate receptors from the synapse, which may contribute to the proper development of spine synapses.

FUTURE PERSPECTIVES

Although our results provide valuable new insights into the molecular processes of synaptic maintenance, it also raises new interesting questions. Regarding the effects of DCTN3, DCTN6 and ZW10 depletion in inhibitory synapses, we do not know if these proteins are important for synaptic structure and if the overall synaptic morphology is affected. For example, it will be interesting to estimate if the levels of surface GABAARs or specific inhibitory synapse proteins, such as gephyrin, and neuroligin-2, are affected in depleted cells. Moreover, we cannot distinguish if the observed effects are related to the role of these proteins in regulating dynein-based transport, or if these proteins act as signaling factors from and to the synapse. Future studies will be important to assess the transport of synaptic cargo along dendrites of DCTN3, DCTN6 and ZW10-depleted neurons. In general, changes in synaptic density are related to changes in synaptic function. It will therefore be valuable to understand how the depletion of DCTN3, DCTN6 and ZW10 affects inhibitory synaptic transmission in postsynaptic neurons. Our mass spectrometry results may guide us to further unveil and characterize the molecular pathway underlying the role of these proteins in inhibitory synapses. In case we verify the interactions biochemically, it will then be interesting to address if Neuroplastin and Neurobeachin co-localize with ZW10 and DCTN6 in hippocampal neurons, respectively, and if such interactions are activity-dependent. Blocking network activity with tetrodotoxin (TTX) may help us to understand if activity is required for such interactions.

We also show that dynein light intermediate chains and Rab-11 adaptor Rab11-FIP3 promote the formation of shaft excitatory synapses. Furthermore, we show that depletion of Rab11-FIP3 diminishes the surface level of AMPARs and the dynamics of recycling endosomes. Modifying the dynamics of recycling endosomes has previously been shown to change the structural organization of excitatory postsynaptic densities. (Esteves da Silva et al., 2015) It will be important to address if depletion of Rab11-FIP3 or DLIC1/2 promote similar changes in the synaptic architecture, and if synaptic plasticity is also affected in such conditions.

AUTHOR CONTRIBUTIONS

C.P.F. wrote the manuscript and composed all figures with advice of C.J.W. and C.C.H. C.P.F. performed and analysed the experiments described in Figure 4D-F, 5 and 6A-D. Experiments in Figure 2 and 3 were performed and analysed by R.L.R.T under the supervision of C.P.F. F.W.L. performed and analysed the experiments in Figure 1 and 4A-C under the supervision of C.P.F. Experiments in Figure 6G-H were performed by M.E.S. M.K. performed the experiments in Figure 6E-F. C.P.F., M.E.S. and M.K. cloned constructs used in the study. Pull-down assay and mass spectrometry experiments were performed by R.S. under the supervision of A.F.M.A. and C.C.H. C.P.F., C.J.W. and C.C.H designed the study. C.J.W. and C.C.H. supervised the research.

ACKNOWLEDGMENTS

We would like to thank J. Lipka, M.A. Schlager, P. Schätzle and M. Adrian for cloning constructs used in this study. This work was supported by the Netherlands Organization for Scientific Research (NWO-ALW-VICI, C.C.H.; NWO-ALW-VIDI, C.J.W.), the European Research

Council (ERC) (ERC Consolidator Grant, C.C.H.), and the European Commission (Marie Curie Reintegration Grant 256284, C.J.W.). C.P.F. is supported by the People Programme (Marie Curie Actions; MC-ITN) of the European Union's Seventh Framework Programme FP7/2007-2013/ under REA grant agreement 473 289581. M.E.d.S. is supported by Fundação para a Ciência e Tecnologia (FCT-Portugal).

MATERIALS AND METHODS

Animals

All animal experiments were performed in compliance with the guidelines for the welfare of experimental animals issued by the Federal Government of The Netherlands. All animal experiments were approved by the Animal Ethical Review Committee (DEC) of Utrecht University.

Antibodies

The following antibodies were used in this study: mouse anti-Gephyrin (clone mAb7a, Synaptic Systems), rabbit anti-Bassoon (141 002, Synaptic Systems), mouse anti-Bassoon (clone SAP7F407, ENZO Life Sciences), rabbit anti-Homer1 (160 002, Synaptic Systems), rabbit anti-DCTN6 (16947-1-AP, Proteintech), rabbit anti-ZW10 (ab21582, Abcam), rabbit anti-DCTN3 (clone EPR5097, GeneTex), mouse anti-GM130 (610823, BD Bioscience), rabbit anti-GluA1 (PC246, Calbiochem), mouse anti-GluA2 (clone 6C4, Millipore) and Alexa-405, Alexa488-, Alexa568-, and Alexa-647-conjugated secondary antibodies (Life Technologies).

Expression and shRNA constructs

The following mammalian expression plasmids were described previously: pGW1 (Hoogenraad et al., 2005), pGW2 (Kapitein et al., 2010b), Bio-tag-GFP (Jaworski et al., 2009) and pSuper (Brummelkamp et al., 2002). GW1-GFP-ZW10 was a kind gift of Thijs van Vlijmen. HA-BirA and GFP-Rab11a were described previously (de Boer et al., 2003; Hoogenraad et al., 2010). GW2-GFP-Homer1c was generated by inserting PCR-amplified Homer1c in the EcoRI and BamHI sites of Gw2-GFP, and pGW2-tagBFP was generated by inserting tagBFP in the HindIII and AscI sites of pGW2-CMV. MARCKS-eGFP (De Paola et al., 2003) was subcloned into GW2 expression vector, using the restriction sites HindIII and XbaI, and MARCKS-tagRFP-T was subcloned using the restriction sites BamHI and XbaI of GW2. HA-DCTN1-cc1 was obtained by cloning DCTN1 into the AscI and EcoRI sites of GW1 from a previously described construct (van Spronsen et al., 2013). DCTN6 and DCTN3 cDNAs were obtained from a human cDNA library, kindly provided by Mike Boxem. Full-length ZW10, DCTN6 and DCTN3 were amplified by PCR and subcloned in the Bio-GFP expression vector to generate Bio-GFP tagged ZW10, DCTN6 and DCTN3 using the AscI and SalI restriction sites. N-terminally GFP tagged ZW10, DCTN6 and DCTN3 constructs were generated by recloning the Bio-GFP constructs into pGW2-GFP expression vectors, using the restriction sites AscI and SalI.

All shRNAs used in this study are indicated in Supplementary Tables 1, 2 and 3. All shRNAs targeting kinesin and myosin mRNAs were designed using the siRNA selection program at the Whitehead Institute for Biomedical Research. Myosin-IIb shRNA#1 was described previously (Rex et al., 2010). shRNAs targeting dynein-interacting proteins were designed based on previously published sequences (Raaijmakers et al., 2013), while Rab11-FIP3 shRNA was based on previously published sequence (Inoue et al., 2008). All shRNAs were ligated into the BglII and HindIII sites of pSuper vector.

Primary hippocampal neuron culture, transfection and immunofluorescent staining

Primary hippocampal cultured neurons from embryonic day 18 (E18) rat brains were prepared as described previously (Kapitein et al., 2010c). In brief, neurons were plated on coverslips coated with poly-L-lysine (37.5 µg/mL) and laminin (1.25 µg/mL) at a density of 100.000 per well, and grown in Neurobasal medium supplemented with 0.5 mM glutamine, 15.6 µM glutamate, 2 % B27 and 1 % penicillin/streptomycin. Hippocampal neurons were

transfected at 14 or 15 days-in-vitro (DIV) using Lipofectamine 2000 (Invitrogen). Briefly, DNA (1.8 µg / well, for a 12-well plate) was mixed with 3.3 µL Lipofectamine 2000 in 200 µL NB, incubated for 30 minutes and then added to the neurons in Neurobasal supplemented with 0.5 mM glutamine at 37 °C in 5 % CO_2 for 90 minutes. Next, neurons were washed with Neurobasal and transferred to a mix of the original and fresh medium at 37 °C in 5 % CO_2 for 3 or 4 days.

To perform immunostainings, dissociated hippocampal neurons were fixed with 4 % paraformaldehyde (PFA)/4 % sucrose in phosphate buffer (PBS) at room temperature for 10 minutes. Cells were then washed 3 times for 5 minutes in PBS at room temperature, and incubated with the primary antibody mix in GDB buffer (0.2 % Gelatin, 0.9 M NaCl, 0.6 % Triton X-100, 33.3 mM phosphate buffer, pH 7.4) overnight at 4°C. Neurons were washed 3 times for 5 minutes in PBS at room temperature, and incubated with the secondary antibody mix in GDB buffer for 1 hour at room temperature. After washing 3 times in PBS, the coverslips were mounted on slides in Vectashield mounting medium (Vector Labs).

Cultured cells, transfection and immunofluorescent staining

HeLa and rat smooth muscle-derived A7r5 cells were cultured in DMEM/Ham's F10 (50 %/50 %), supplemented with 10 % FCS and 1 % penicillin/streptomycin at 37 °C and 5 % CO_2. Cells were plated on 12 mm or 24 mm glass coverslips and transfected with Fugene6, accordingly to manufacturer's protocol (Promega). For immunocytochemistry, cells were fixed for 10 minutes with paraformaldehyde (4 %) and washed 3 times for 5 minutes in phosphate buffer (PBS) at room temperature. After permeabilization with 0.1 % Triton-X-100 in PBS for 15 minutes, cells were incubated with the primary antibody mix in GDB buffer (0.2 % Gelatin, 0.9 M NaCl, 0.6 % Triton X-100, 33.3 mM phosphate buffer, pH 7.4) overnight at 4 °C. After washing 3 times in PBS, cells were incubated with the secondary antibody mix in GDB buffer for 1 hour at room temperature. Cells were then washed 3 times in PBS, and the coverslips were mounted in Mowiol.

Biotin-streptavidin pull-down assay and mass spectrometry analysis

For whole brain extracts, a whole brain from an adult female rat was homogenized in lysis buffer (50 mM Tris-HCl, 150 mM NaCl, 0.1 % SDS, 0.2 % NP-40, and protease inhibitors (Roche)) in a 1:10 brain (g) to lysis buffer (mL) ratio. Samples were sonicated and centrifuged at 900 rpm for 15 minutes.

For biotin-streptavidin pull-down assays, HEK-293 cells were cultured in Ø10 cm cell culture dishes at 37 °C and 5 % CO_2, and transfected with BirA and Bio-GFP constructs using polyethylenimine (PEI) transfection reagent (Polysciences). After 48 h, cells were washed and lysed in RIPA lysis buffer (50 mM Tris-HCl pH 7.4-7.8, 150 mM NaCl, 1 % Triton X-100, 0.1 % SDS, 0.5 % sodium deoxycholate) supplemented with protease inhibitors (Roche). Cells were centrifuged at 13.000 rpm for 15 minutes at 4 °C and the supernatants were incubated with Dynabeads M-280 (blocked in chicken egg albumin, Life Technologies) for 1 h at 4 °C. Beads were separated using a magnet rack (Dynal, Invitrogen) and washed five times in washing buffer (20mM Tris-HCl pH 7.4-7.8, 150 mM KCl, 0.1% Triton X-100). Samples were collected at this point for AP-MS analysis of HEK293 cells expressing each construct. For the bio-GFP pull-down with whole brain extracts, pre-incubated Dynabeads with HEK293 cell extracts expressing each construct were washed twice in low salt washing buffer (20 mM Tris-HCl pH 7.4-7.8, 100 mM KCl, 0.1 % Triton X-100), followed by two wash steps in high salt wash buffer (20 mM Tris-HCl pH 7.4-7.8, 500 mM KCl, 0.1 % Triton X-100) and two final wash steps in low salt washing buffer (20 mM Tris-HCl pH 7.4-7.8, 100 mM KCl, 0.1 % Triton X-100) to remove binding proteins from HEK293 cells. Brain lysates were centrifuged at 16.000 g for 15 min at 4°C, and the supernatant was incubated with the Dynabeads containing bio-GFP or bio-GFP-MyoIIb for 2 h at 4 °C and washed in low salt washing buffer five times. For mass spectrometry analysis, beads were resuspended in 15 µL of 4x Laemmli Sample buffer (Biorad) and supernatants were loaded on a 4-12 % gradient Criterion XT Bis-Tris precast gel (Biorad). The gel was fixed with 40 % methanol and 10 % acetic acid and then stained for 1 h using colloidal Coomassie dye G-250 (Gel Code Blue Stain Reagent, Thermo Scientific). Each lane from the gel was cut in 3 pieces, destained and digested using trypsin, as described in (Ekkebus et al., 2013). Briefly, after placed in 0.5-mL tubes, the pieces were washed with 250 µL of water, followed by 15 min dehydration in acetonitrile. Proteins were reduced (10 mM dithiothreitol, 1 h at 56 °C), dehydrated and alkylated (55 mM iodoacetamide, 1 h in the dark). After two rounds of dehydration, trypsin (Promega) was added to the samples (20 µL of 0.1 mg/mL trypsin in 50

mM Ammoniumbicarbonate) and incubated overnight at 37 °C. Peptides were extracted with acetonitrile, dried down and reconstituted in 10 % formic acid prior mass spectrometry analysis.

All samples were analyzed on aOrbitrap Q-Exactive mass spectrometer (Thermo Fisher Scientific, Germany) coupled to an Agilent 1290 Infinity LC (Agilent Technologies). Mass spectrometry was performed as described previously (Frese et al., 2017). For data analysis, raw files were processed using Proteome Discoverer 1.4 (Thermo Fisher Scientific, Germany). Database searches were performed either using the Human Uniprot database or the rat Uniprot database and Mascot (Matrix Science, UK) as the search engine. Positive protein hits were manually checked and interpreted as valid hits or discarded based on their presence in the negative control (pull-down with Bio-GFP alone). All the hits are listed in Supplementary Tables 4-6.

Confocal microscopy

High resolution confocal laser scanning microscopy was performed on a Zeiss LSM-700 system with a Plan-Apochromat 63x 1.4 NA oil immersion objective. Each image was a z-series of 8-19 images, each averaged 4 times. For the imaging of dendritic spines and A7r5 cells, the imaged area was 78 x 78 µm (1024 x 1024 pixels). The confocal settings were kept constant during all parallel imaging experiments.

Live cell-imaging microscopy

Live-cell imaging was performed using laser confocal spinning-disk microscopy as previously described (Esteves da Silva et al., 2015). All imaging was performed in full conditioned medium at 37 °C and 5 % CO_2. To image Rab11-positive recycling endosomes dynamics in dendritic spines, time-lapses of 5 minutes were acquired, with 5 seconds interval between acquisition and a z-stack stream at every time point, to guarantee the entire dendritic complexity is imaged. MARCKS-tagRFP-t was also imaged to assess neuronal morphology.

Image analysis and quantification

Image processing and analysis was performed using ImageJ (US National Institute of Health) and MetaMorph (Molecular Devices).

Quantification of synaptic density in hippocampal neurons. Neuronal morphology was highlighted using Homer-1c-GFP, and images were acquired using an Olympus BX53 upright fluorescent microscope equipped with a 60x/1.35 NA UplanFL objective (Olympus) and the MicroManager software. A representative stretch of dendrite per neuron was selected and analyzed using the PunctaAnalyzer plugin. After determining the individual puncta, we used a Macro to determine the overlap between the different synaptic puncta. An excitatory/inhibitory synapse was counted when there was overlap between Homer/Gephyrin and Bassoon puncta. Data were then normalized per 10 µm of dendrite.

Quantification of spine morphology. For the analysis of spine morphology, one or two stretches of 10 µm were traced along proximal dendrites. We manually inspected and quantified individual protrusions through all z-sections in each dendritic stretch, and divided them into 2 categories: filopodia (immature long protrusions, without obvious spine head) and spine (mature spines with short necks). We then checked if these protrusions were excitatory synapses, by counting the co-localizations between excitatory postsynaptic marker Homer and presynaptic marker Bassoon. We also measured the density of excitatory synapses formed onto the dendritic shaft.

Quantification of fluorescent intensity. To quantify fluorescent intensity in neurons and dissociated cells, the obtained z-stack was projected into a single imaging, using the average intensity projection. Then, a region of interest was manually drawn around the cell body or cytoplasm, and the average intensity was measured using Image J. For the quantification of the knockdown efficiency in hippocampal neurons, the mean intensities were corrected for background intensities.

Classification Golgi morphology. The Golgi morphology was visualized by using the trans-Golgi marker GM130, and we used a maximum intensity projection to classify if the morphology was normal (triangular-like shape) or abnormal (rounded and/or fragmented).

Quantification of GluA1 and GluA2 surface levels. Per neuron, 2 dendrites were traced to quantify the surface levels of GluA1 and GluA2. Intensity per cell was normalized to a non-transfected cell in the same imaged area.
Quantification of Rab11 endosome dynamics in dendritic protrusions

Rab11 recycling endosome dynamics was quantified as previously described (Esteves da Silva et al., 2015).

Statistics

Data are represented as mean values ± standard error of the mean, unless stated otherwise. Statistical analysis was performed using GraphPad Prism software. For the comparison of multiple groups, we used the Kruskal-Wallis test followed by a posthoc Dunn's comparison test. For the comparison between control and knockdown, we used a two-tailed t-test or a two-tailed Mann-Whitney test. For comparison of percentages, we used the Chi-square test. The used test is stated in each figure legend.

Differences between control and treatment were considered significant when $p < 0.05$ (*, $p < 0.05$; **, $p< 0.01$; ***, $p < 0.001$). In all figure legends and text, N indicates the number of independent experiments, and n indicates the number of cells analyzed.

REFERENCES

Arasaki, K., Uemura, T., Tani, K., and Tagaya, M. (2007). Correlation of Golgi localization of ZW10 and centrosomal accumulation of dynactin. Biochem. Biophys. Res. Commun. 359, 811-816.

Baas, P.W., Black, M.M., and Banker, G.A. (1989). Changes in microtubule polarity orientation during the development of hippocampal neurons in culture. J. Cell Biol. 109, 3085-3094.

Ben-Ari, Y., Gaiarsa, J.L., Tyzio, R., and Khazipov, R. (2007). GABA: a pioneer transmitter that excites immature neurons and generates primitive oscillations. Physiol. Rev. 87, 1215-1284.

Brummelkamp, T.R., Bernards, R., and Agami, R. (2002). A system for stable expression of short interfering RNAs in mammalian cells. Science 296, 550-553.

Chan, G.K., Jablonski, S.A., Starr, D.A., Goldberg, M.L., and Yen, T.J. (2000). Human Zw10 and ROD are mitotic checkpoint proteins that bind to kinetochores. Nat. Cell Biol. 2, 944-947.

de Boer, E., Rodriguez, P., Bonte, E., Krijgsveld, J., Katsantoni, E., Heck, A., Grosveld, F., and Strouboulis, J. (2003). Efficient biotinylation and single-step purification of tagged transcription factors in mammalian cells and transgenic mice. Proc. Natl. Acad. Sci. 100, 7480-7485.

De Paola, V., Arber, S., and Caroni, P. (2003). AMPA receptors regulate dynamic equilibrium of presynaptic terminals in mature hippocampal networks. Nat. Neurosci. 6, 491-500.

Ekkebus, R., van Kasteren, S.I., Kulathu, Y., Scholten, A., Berlin, I., Geurink, P.P., de Jong, A., Goerdayal, S., Neefjes, J., Heck, A.J., et al. (2013). On terminal alkynes that can react with active-site cysteine nucleophiles in proteases. J. Am. Chem. Soc. 135, 2867-2870.

Esteves da Silva, M., Adrian, M., Schatzle, P., Lipka, J., Watanabe, T., Cho, S., Futai, K., Wierenga, C.J., Kapitein, L.C., and Hoogenraad, C.C. (2015). Positioning of AMPA Receptor-Containing Endosomes Regulates Synapse Architecture. Cell Rep. 13, 933-943.

Farzana, F., Zalm, R., Chen, N., Li, K.W., Grant, S.G., Smit, A.B., Toonen, R.F., and Verhage, M. (2016). Neurobeachin Regulates Glutamate- and GABA-Receptor Targeting to Synapses via Distinct Pathways. Mol. Neurobiol. 53, 2112-2123.

Franker, M.A., and Hoogenraad, C.C. (2013). Microtubule-based transport - basic mechanisms, traffic rules and role in neurological pathogenesis. J. Cell Sci. 126, 2319-2329.

Frese, C.K., Mikhaylova, M., Stucchi, R., Gautier, V., Liu, Q., Mohammed, S., Heck, A.J., Altelaar, A.F., and Hoogenraad, C.C. (2017). Quantitative Map of Proteome Dynamics during Neuronal Differentiation. Cell Rep. 18, 1527-1542.

Fuhrmann, J.C., Kins, S., Rostaing, P., El Far, O., Kirsch, J., Sheng, M., Triller, A., Betz, H., and Kneussel, M. (2002). Gephyrin interacts with Dynein light chains 1 and 2, components of motor protein complexes. J. Neurosci. 22, 5393-5402.

Ghiretti, A.E., Thies, E., Tokito, M.K., Lin, T., Ostap, E.M., Kneussel, M., and Holzbaur, E.L. (2016). Activity-Dependent Regulation of Distinct Transport and Cytoskeletal Remodeling Functions of the Dendritic Kinesin KIF21B. Neuron 92, 857-872.

Herrera-Molina, R., Sarto-Jackson, I., Montenegro-Venegas, C., Heine, M., Smalla, K.H., Seidenbecher, C.I., Beesley, P.W., Gundelfinger, E.D., and Montag, D. (2014). Structure of excitatory synapses and GABAA receptor localization at inhibitory synapses are regulated by neuroplastin-65. J. Biol. Chem. 289, 8973-8988.

Hirokawa, N., Niwa, S., and Tanaka, Y. (2010). Molecular motors in neurons: transport mechanisms and roles in brain function, development, and disease. Neuron 68, 610-638.

Hirose, H., Arasaki, K., Dohmae, N., Takio, K., Hatsuzawa, K., Nagahama, M., Tani, K., Yamamoto, A., Tohyama, M., and Tagaya, M. (2004). Implication of ZW10 in membrane trafficking between the endoplasmic reticulum and Golgi. EMBO J. 23, 1267-1278.

Hodges, J.L., Newell-Litwa, K., Asmussen, H., Vicente-Manzanares, M., and Horwitz, A.R. (2011). Myosin IIb activity and phosphorylation status determines dendritic spine and post-synaptic density morphology. PloS one 6, e24149.

Hoogenraad, C.C., Milstein, A.D., Ethell, I.M., Henkemeyer, M., and Sheng, M. (2005). GRIP1 controls dendrite morphogenesis by regulating EphB receptor trafficking. Nat. Neurosci. 8, 906-915.

Hoogenraad, C.C., Popa, I., Futai, K., Martinez-Sanchez, E., Wulf, P.S., van Vlijmen, T., Dortland, B.R., Oorschot, V., Govers, R., Monti, M., et al. (2010). Neuron specific Rab4 effector GRASP-1 coordinates membrane specialization and maturation of recycling endosomes. PLoS Biol. 8, e1000283.

Horgan, C.P., Hanscom, S.R., Jolly, R.S., Futter, C.E., and McCaffrey, M.W. (2010a). Rab11-FIP3 binds dynein light intermediate chain 2 and its overexpression fragments the Golgi complex. Biochem. Biophys. Res. Commun. 394, 387-392.

Horgan, C.P., Hanscom, S.R., Jolly, R.S., Futter, C.E., and McCaffrey, M.W. (2010b). Rab11-FIP3 links the Rab11 GTPase and cytoplasmic dynein to mediate transport to the endosomal-recycling compartment. J. Cell Sci. 123, 181-191.

Inoue, H., Ha, V.L., Prekeris, R., and Randazzo, P.A. (2008). Arf GTPase-activating protein ASAP1 interacts with Rab11 effector FIP3 and regulates pericentrosomal localization of transferrin receptor-positive recycling endosome. Mol. Biol. Cell 19, 4224-4237.

Jaworski, J., Kapitein, L.C., Gouveia, S.M., Dortland, B.R., Wulf, P.S., Grigoriev, I., Camera, P., Spangler, S.A., Di Stefano, P., Demmers, J., et al. (2009). Dynamic microtubules regulate dendritic spine morphology and synaptic plasticity. Neuron 61, 85-100.

Kapitein, L.C., Schlager, M.A., Kuijpers, M., Wulf, P.S., van Spronsen, M., MacKintosh, F.C., and Hoogenraad, C.C. (2010a). Mixed microtubules steer dynein-driven cargo transport into dendrites. Curr. Biol. 20, 290-299.

Kapitein, L.C., Schlager, M.A., van der Zwan, W.A., Wulf, P.S., Keijzer, N., and Hoogenraad, C.C. (2010b). Probing intracellular motor protein activity using an inducible cargo trafficking assay. Biophys. J. 99, 2143-2152.

Kapitein, L.C., Yau, K.W., and Hoogenraad, C.C. (2010c). Microtubule dynamics in dendritic spines. Methods Cell Biol. 97, 111-132.

Kneussel, M., and Wagner, W. (2013). Myosin motors at neuronal synapses: drivers of membrane transport and actin dynamics. Nat. Rev. Neurosci. 14, 233-247.

Lin, W.H., Hurley, J.T., Raines, A.N., Cheney, R.E., and Webb, D.J. (2013). Myosin X and its motorless isoform differentially modulate dendritic spine development by regulating trafficking and retention of vasodilator-stimulated phosphoprotein. J. Cell Sci. 126, 4756-4768.

Lipka, J., Kapitein, L.C., Jaworski, J., and Hoogenraad, C.C. (2016). Microtubule-binding protein doublecortin-like kinase 1 (DCLK1) guides kinesin-3-mediated cargo transport to dendrites. EMBO J. 35, 302-318.

Maas, C., Tagnaouti, N., Loebrich, S., Behrend, B., Lappe-Siefke, C., and Kneussel, M. (2006). Neuronal cotransport of glycine receptor and the scaffold protein gephyrin. J. Cell Biol. 172, 441-451.

Moutin, E., Raynaud, F., Fagni, L., and Perroy, J. (2012). GKAP-DLC2 interaction organizes the postsynaptic scaffold complex to enhance synaptic NMDA receptor activity. J. Cell Sci. 125, 2030-2040.

Muhia, M., Thies, E., Labonte, D., Ghiretti, A.E., Gromova, K.V., Xompero, F., Lappe-Siefke, C., Hermans-Borgmeyer, I., Kuhl, D., Schweizer, M., et al. (2016). The Kinesin KIF21B Regulates Microtubule Dynamics and Is Essential for Neuronal Morphology, Synapse Function, and Learning and Memory. Cell Rep. 15, 968-977.

Naisbitt, S., Valtschanoff, J., Allison, D.W., Sala, C., Kim, E., Craig, A.M., Weinberg, R.J., and Sheng, M. (2000). Interaction of the postsynaptic density-95/guanylate kinase domain-associated protein complex with a light chain of myosin-V and dynein. J. Neurosci. 20, 4524-4534.

Niwa, S., Tanaka, Y., and Hirokawa, N. (2008). KIF1Bbeta- and KIF1A-mediated axonal transport of presynaptic regulator Rab3 occurs in a GTP-dependent manner through DENN/MADD. Nat. Cell Biol. 10, 1269-1279.

Ohsugi, M., Adachi, K., Horai, R., Kakuta, S., Sudo, K., Kotaki, H., Tokai-Nishizumi, N., Sagara, H., Iwakura, Y., and Yamamoto, T. (2008). Kid-mediated chromosome compaction ensures proper nuclear envelope formation. Cell 132, 771-782.

Perlson, E., Hendricks, A.G., Lazarus, J.E., Ben-Yaakov, K., Gradus, T., Tokito, M., and Holzbaur, E.L. (2013). Dynein interacts with the neural cell adhesion molecule (NCAM180) to tether dynamic microtubules and maintain synaptic density in cortical neurons. J. Biol. Chem. 288, 27812-27824.

Raaijmakers, J.A., Tanenbaum, M.E., and Medema, R.H. (2013). Systematic dissection of dynein regulators in mitosis. J. Cell Biol. 201, 201-215.

Rex, C.S., Gavin, C.F., Rubio, M.D., Kramar, E.A., Chen,

L.Y., Jia, Y., Huganir, R.L., Muzyczka, N., Gall, C.M., Miller, C.A., et al. (2010). Myosin IIb regulates actin dynamics during synaptic plasticity and memory formation. Neuron 67, 603-617.

Sarto-Jackson, I., Milenkovic, I., Smalla, K.H., Gundelfinger, E.D., Kaehne, T., Herrera-Molina, R., Thomas, S., Kiebler, M.A., and Sieghart, W. (2012). The cell adhesion molecule neuroplastin-65 is a novel interaction partner of gamma-aminobutyric acid type A receptors. J. Biol. Chem. 287, 14201-14214.

Setou, M., Nakagawa, T., Seog, D.H., and Hirokawa, N. (2000). Kinesin superfamily motor protein KIF17 and mLin-10 in NMDA receptor-containing vesicle transport. Science 288, 1796-1802.

Setou, M., Seog, D.H., Tanaka, Y., Kanai, Y., Takei, Y., Kawagishi, M., and Hirokawa, N. (2002). Glutamate-receptor-interacting protein GRIP1 directly steers kinesin to dendrites. Nature 417, 83-87.

Starr, D.A., Williams, B.C., Hays, T.S., and Goldberg, M.L. (1998). ZW10 helps recruit dynactin and dynein to the kinetochore. J. Cell Biol. 142, 763-774.

Sugiura, H., Yasuda, S., Katsurabayashi, S., Kawano, H., Endo, K., Takasaki, K., Iwasaki, K., Ichikawa, M., Kobayashi, T., Hino, O., et al. (2015). Rheb activation disrupts spine synapse formation through accumulation of syntenin in tuberous sclerosis complex. Nat. Commun. 6, 6842.

Sun, Y., Shestakova, A., Hunt, L., Sehgal, S., Lupashin, V., and Storrie, B. (2007). Rab6 regulates both ZW10/RINT-1 and conserved oligomeric Golgi complex-dependent Golgi trafficking and homeostasis. Mole. Biol. Cell 18, 4129-4142.

Terasawa, M., Toya, M., Motegi, F., Mana, M., Nakamura, K., and Sugimoto, A. (2010). Caenorhabditis elegans ortholog of the p24/p22 subunit, DNC-3, is essential for the formation of the dynactin complex by bridging DNC-1/p150(Glued) and DNC-2/dynamitin. Genes Cells 15, 1145-1157.

Twelvetrees, A.E., Yuen, E.Y., Arancibia-Carcamo, I.L., MacAskill, A.F., Rostaing, P., Lumb, M.J., Humbert, S., Triller, A., Saudou, F., Yan, Z., et al. (2010). Delivery of GABAARs to synapses is mediated by HAP1-KIF5 and disrupted by mutant huntingtin. Neuron 65, 53-65.

van den Berg, R., and Hoogenraad, C.C. (2012). Molecular motors in cargo trafficking and synapse assembly. Adv. Exp. Med. Biol. 970, 173-196.

van den Pol, A.N., Obrietan, K., Belousov, A.B., Yang, Y., and Heller, H.C. (1998). Early synaptogenesis in vitro: role of axon target distance. J. Comp. Neurol. 399, 541-560.

van Spronsen, M., and Hoogenraad, C.C. (2010). Synapse pathology in psychiatric and neurologic disease. Curr. Neurol. Neurosci. Rep. 10, 207-214.

van Spronsen, M., Mikhaylova, M., Lipka, J., Schlager, M.A., van den Heuvel, D.J., Kuijpers, M., Wulf, P.S., Keijzer, N., Demmers, J., Kapitein, L.C., et al. (2013). TRAK/Milton motor-adaptor proteins steer mitochondrial trafficking to axons and dendrites. Neuron 77, 485-502.

Wagner, O.I., Esposito, A., Kohler, B., Chen, C.W., Shen, C.P., Wu, G.H., Butkevich, E., Mandalapu, S., Wenzel, D., Wouters, F.S., et al. (2009). Synaptic scaffolding protein SYD-2 clusters and activates kinesin-3 UNC-104 in C. elegans. Proc. Natl. Acad. Sci. 106, 19605-19610.

Yeh, T.Y., Quintyne, N.J., Scipioni, B.R., Eckley, D.M., and Schroer, T.A. (2012). Dynactin's pointed-end complex is a cargo-targeting module. Mol. Biol. Cell 23, 3827-3837.

Zhang, Y.V., Hannan, S.B., Kern, J.V., Stanchev, D.T., Koc, B., Jahn, T.R., and Rasse, T.M. (2017). The KIF1A homolog Unc-104 is important for spontaneous release, postsynaptic density maturation and perisynaptic scaffold organization. Sci. Rep. 7, 38172.

SUPPLEMENTARY INFORMATION

Supplementary table 1. Overview of shRNA sequences targeting kinesin proteins used in this study.

Family	Alias		shRNA sequence 5'- 3'
Kinesin-1	KIF5A	#1	GGACACCAGCGAAAACGGA
		#2	GCTGGTACGTGACAATGCA
		#3	GAGACCAATAACGAATGCA
	KIF5B	#1	GGTTATGCAAGACAGACGA
		#2	GGAATATGAATTGCTTAGT
		#3	GCCTTATGCATTTGATCGT
	KIF5C	#1	GGATCGCACACGATATTTT
		#2	CAATGCCTGTGCGAAGCAG
		#3	GCTGTCAATTACGACCAGA
Kinesin-2	KIF3A	#1	GTGCGACCAATATGAACGA
		#2	CGTATCGGAACTCTAAACT
		#3	GTTGGTGCGACCAATATGA
	KIF3B	#1	GGATACAAGAGACCACTGA
		#2	GGTCAGGGCATCTTACTTA
		#3	GGGCATCTTACTTAGAGAT
	KIF3C	#1	ATACAGGGCTGAAAATATA
		#2	GGAATTTTCTCATGACCAA
		#3	CCACGTCTAAAGTGCGAAA
Kinesin-3	KIF1A	#1	CAGGATGACCGGACCTTCT
		#2	GACCGGACCTTCTACCAGT
		#3	GTCATCAGGATACGTCCAT
	KIF1B	#1	GGGCTAAACATTTCGTTGT
		#2	GCAACGCTGTTATCAATGA
		#3	CTGGATCTAATGCGAGAGA
	KIF13A	#1	CGTACCTTATCGAGATTCA
		#2	GAACCAGTTAGACGTGTCT
		#3	GCTCATTAAACGACGGGAA
	KIF13B	#1	GAAGCCGACAAACGTTGAA
		#2	GACGAGAAATTGACTTACA
		#3	GGATGATGCTGACCGAGAG
	KIF14	#1	CATAAACAGCACTTATGTT
		#2	CATCCCGATATGAAACAAA
		#3	CGCTCTCATTCCGTTTTCA
	KIF16B	#1	CCTTCGCTATGCAAATAGA
		#2	GGCCTAGATAACATTCTCT
		#3	CTGCCAAACTTAGGGAGAA
Kinesin-4	KIF4A	#1	CTAATGTGCTCAGACGTAA
		#2	CCCAAACCTTTCCGTATTA
		#3	CCTTCGCTATGCTGACAGA
	KIF4B	#1	GAAGTCTAGAATCGGAAGT
		#2	CAAGCGGTTATCCATCTAT
		#3	GGTTATCCATCTATCAGAT
	KIF7	#1	GGTCGACACATGTGGATAA
		#2	GAGCAAGGTATTATCCCAA
		#3	GGATAAACCAGGAGCTCAA
	KIF21A	#1	CACGCACTGTGAATACAGA
		#2	CCGCGAACATAGATTACAT
		#3	GCAAACATCACGTGCGAAA
	KIF21B	#1	GACGCTCACTGCTAAGTTC
		#2	CCCTCGTTGAGATCAAAGA
		#3	CTCACTATGACGGTATCGA
	KIF27	#1	GGTGATAAATTTGCGAGAA
		#2	CGTATAGGGATGCGAAGAT
		#3	GGACCTTCACATCCGAGAA
Kinesin-5	KIF11	#1	GCTGGTATAATTCCACGTA
		#2	CCACGTACTCTTCATCAGA
		#3	GCAGAGTTATTTACGGATA

Family	Alias		shRNA sequence 5'- 3'
Kinesin-6	KIF20A	#1	CGGCAATCCTTACGTGAAA
		#2	CTTCGAATCAGACCGTTCT
		#3	GCATCTACATATGACGAAA
	KIF23	#1	GGAGAAACGACATCGCTTA
		#2	GAAGTGGTCAATAGTACAA
		#3	CCTTGTTAGAACGGCAGAA
Kinesin-7	KIF10	#1	GGAAGGATCTAGCGATGAA
		#2	GCTGTTACATAAATCGGAA
		#3	CTGAAGGTATGCGATTGAA
Kinesin-8	KIF18A	#1	GCAGCTACTAGACAATGGA
		#2	TTTGTAGAAGGCACAAATA
		#3	GACACATATAACACTCTTA
	KIF18B	#1	CCTATGAGGATACTTACAA
		#2	AGATCTTTGTGAAGCAGCA
		#3	TGACCACCATGGAACTGTA
	KIF19	#1	GCAATGACATGGAATATGA
		#2	CCAAGTGTATCTCCGTGAA
		#3	CGGGAGAAGTCATACCTCT
Kinesin-9	KIF6	#1	CAGACGGATTCGTAAACAA
		#2	CCGACATGCTAAGCTTCAT
		#3	CGTACACATATCCCTTACA
	KIF9	#1	GCAATGACATGGAATATGA
		#2	GTTAGACGAAACGCTATCT
		#3	CGGGAGAAGTCATACCTCT
Kinesin-10	KIF22	#1	GAGAGCGAATGGTACTCAT
		#2	GCTTAAGATGAAGCAAAAA
		#3	GGAATTCGGCTAAAAGAGA
Kinesin-11	KIF26A	#1	GCGGTTTCGATAACTCAGA
		#2	GGAGTGTATAGATGGCAGT
		#3	AGATCAAGGTGTATGAGAT
	KIF26B	#1	GCTCAACCGTTACAATGCT
		#2	GTGACCGACAACATTAGGA
		#3	CCTACACCATGATCGGAAG
Kinesin-12	KIF12	#1	GCCAATAGCATTAACCGCA
		#2	CTTCACCTGGCTATTAGAT
		#3	GAAGCTTTGATGGAACTAT
	KIF15	#1	GGCTATTGCTCGACTAGAA
		#2	CCTACGATAACTTACAAGA
		#3	GGAAATTGATAGGTCATCA
Kinesin-13	KIF2A	#1	GTTGTTTACTTTCCACGAA
		#2	GATCGGGATTTACGTGGAA
		#3	GAACTGACTGTGGATCCAA
	KIF2B	#1	GAAAGAAGATTGAACTGGA
		#2	CACAATGGGTGGAGCCTTT
		#3	GGCAATACAAATTCGGAAA
	KIF2C	#1	CAACGCAGCAATGGGTTAA
		#2	GTGACGTTCTTCGAGATCT
		#3	GCCAATATAAGCACGGTGA
	KIF24	#1	GGATAGAGCTGGTTATGGT
		#2	GTGCTTAGAATCAGACTCT
		#3	CAGTCGGAATCAGACATCT
Kinesin-14	KIFC1	#1	CCAGTTACGTAGAGATCTA
		#2	CTGTCACCAATGCACGATA
		#3	CACGTGCCTTACCGAAATA
	KIFC2	#1	CACACTGGGACGTACCTAA
		#2	GGCACCACTGCAGTTTTAT
		#3	CGCCCTAATTACGCTGACT
	KIFC3	#1	CGAGAACCCAGGCATTAAT
		#2	CAGCTCCGGGACAGGTTAT
		#3	CCACCTGTTAAGTATGTCA

Supplementary table 2. Overview of shRNA sequences targeting myosin proteins used in this study.

Family	Alias		shRNA sequence 5'- 3'
Myosin-II	MyoIIa	#1	GGTAAATTCATTCGTATCA
		#2	CCTCATTTATCGGGATCCT
		#3	CTGCTCGCAAGAAACTAGA
	MyoIIb	#1	GATCAAAGTTGGCCGAGAT
		#2	GGCATGCGGATCAGTATAA
		#3	GAACGCACGTTTCATATCT
	MyoIIc	#1	CCGCTCTTGAGTCTAAACT
		#2	GTGGTCATTAACCCGTACA
		#3	CTGCATCGTTCCCAATCAT
Myosin-V	MyoVa	#1	GCAAACTCGATCGGAGAAA
		#2	GATGCCTAAAGGTACCGAT
		#3	GTTTGCGTCTCGAGATTCA
	MyoVb	#1	GTGTCCTTTATACGAACAA
		#2	GGTATCGGGTGTTGATGAA
		#3	CCTGCATACATACTCTACA
Myosin-VI	MyoVI	#1	CTTCGCGATACAATCAACA
		#2	GTATGATGCACTCGTTAAA
		#3	CAGCCTAACAATTGAACCT
Myosin-X	MyoX	#1	CTCGAGGTTTGATACGGAT
		#2	GATCAACACTCTTCGACGT
		#3	GTTACCGACTCTACACGAA
Tropomyosins	TPM-α	#1	AGCACATTGCTGAAGATGCT
	TPM-β	#1	ACTGGAGCAGGCCGAGAAG
	TPM-γ	#1	AAGCTGGAGGAAGCGGAGA
	TPM-δ	#1	ATCAAGCTTCTGTCTGACAA

Supplementary table 3. Overview of shRNA sequences targeting dynein-interacting proteins used in this study.

Targeted mRNA	Alias		shRNA sequence 5'- 3'
Dynein subunits	DHC1		GCTCAAACATGACAGAATT
	DHC2		TTGGGTGTAGTCCTACGAA
	DIC1		GGAAGGTGCGGTTGAGTTA
	DIC2		CTTTGGTCAACTAAGAATA
	DLIC1		AGATGACAGTGTCGTCCTA
	DLIC2		GCCAGAAGATGCATATGAA
	DL2A		TGAATAAGGCACTGTCTTG
	DL2B		GTACAGTCAGGGACATTGA
	DLL1		ATGCAGACATGTCGGAAGA
	DLL2		GTTGCAATCCTCCTCTTCA
	TCTEL1		GAAGTGAGCAACATTGTAA
	TCTE1L		GATGGCACCTGTACCGTTA
Dynactin subunits	DCTN1		GATCGAGAGACAGTCATCA
	DCTN2		TTATGAAACCAGCGACCTA
	DCTN3	#1	GGTGAAGATTCTCTACAAA
		#2	TGGCAGAGGAACAGTTCAT
		#3	GAGGAGTATAACAAGACTA
	DCTN4		GAAACTGGCACGGCGAAGA
	DCTN5		TGTAAGAGTTGGACGTCAC
	DCTN6	#1	AGATGTAACCATAGGTCCT
		#2	AAGCGTACGTAGGCAGGAA
		#3	ATAAACGCCCATCCAGATA
Acessory factors	LIS1		CAATTAAGGTGTGGGATTA
	NDE1		GGATCCAGCTCTGGTTTGA
	NDEL1		GCAGGTCTCAGTGTTAGAA
	ARP1A		GAAAGGAGGGCTACGATTT
	ARP1B		CGCAACAGGACGCACTACT
	ARP11		CCAGAGGAAGTTCATTATA
	CAPZA1		CAGTAACTGTTTCTAATGA
	CAPZB		GGAGTGATCCTCATAAAGA
	SPDL1		GGGAAGACGTTTCTAGACT
	BICD1		ACAGCTGTCTCGTCAAAGA
	BICD2		AGACAGAGCGAGAGCAGAA
	ZW10	#1	GCAATATGATCAGCAAGAA
		#2	GATCCAGTTGGTATTGGAA
		#3	CATATCAACTGTTGAGTTT
Other	Rab11-FIP3		GCAGCTGGATGAGGAGAACAGTGAG

Supplementary table 4. Identification of binding partners of Dynactin 6 (DCTN6) by mass spectrometry analysis using BioGFP pull-downs from rat brain lysates.

Accession	Protein	bio-GFP		bio-GFP-MyoIIb	
		# Peptides	# PSM	# Peptides	# PSM
D4ADD8	**Dynactin 6**			**8**	**332**
P85515	Alpha-centractin	1	1	16	49
B2RYJ7	ARP1 actin-related protein 1 homolog B			11	30
Q6AYH5	Dynactin subunit 2			15	28
Q498N3	Dynactin 4			11	26
F1M265	Palladin			9	19
D4A1B8	Dynactin 3			8	18
E9PTE5	Zinc finger MYM-type-containing 3			10	17
D3ZER1	Homeobox-containing 1			9	12
Q4KM59	Dynactin 5			6	11
Q5M9F7	ARP10 actin-related protein 10 homolog			6	10
D4A069	Zinc finger MYM-type-containing 4			8	9
Q5XIR5	BCL2-associated athanogene 4			6	9
F1MA31	Lysine demethylase 1A	1	1	6	9
Q3T1K5	F-actin-capping protein subunit alpha-2	1	1	6	7
F1M0Y0	Clustered mitochondria protein homolog			6	6
E9PTK9	Ankyrin repeat and KH domain-containing 1	1	1	6	6
Q63564	Synaptic vesicle glycoprotein 2B	1	1	5	6
B2GUZ5	F-actin-capping protein subunit alpha-1			4	6
G3V852	Talin 1			5	5
D3ZWS0	Scribbled planar cell polarity protein	1	1	5	5
Q9EQX9	Ubiquitin-conjugating enzyme E2 N			4	5
Q5XFX0	Transgelin-2			4	4
F1LX73	Neurobeachin			4	4
G3V678	DNA-directed RNA Poly. I, II, and III subunit RPABC3-like	1	1	4	4
D4AAT4	Small nuclear ribonucleoprotein polypeptide F			3	4
B0BN74	Bag2 protein			3	4
A0A096MJ33	Platelet-derived growth factor D			3	4
D4AA38	Holocarboxylase synthetase			3	3
Q156J1	Bcl-2-interacting death suppressor			3	3
D4A554	Eukaryotic translation initiation factor 4 gamma, 3			3	3
B2RZD1	Sec61 beta subunit			3	3
D3ZAF6	ATP synthase subunit f			3	3
Q9WV97	Mitochondrial import translocase subunit Tim9			3	3
M0RDN9	Ubiquitin carboxyl-terminal hydrolase 19			3	3
V9GZ88	Phosphatidylinositol 3,4,5-trisphosphate 5-phosphatase2			3	3
D3ZHS5	Carboxypeptidase A4			2	3
P29419	ATP synthase subunit e			2	3
Q5U2U2	Crk-like protein			2	3

Proteins with a number of peptide spectrum matches (#PSM) of 3 or more and an enrichment of 3 or more compared to the control (BioGFP) in the BioGFP-DCTN6 pull-down are included.

Supplementary table 5. Identification of binding partners of Dynactin 3 (DCTN3) by mass spectrometry analysis using BioGFP pull-downs from rat brain lysates.

Accession	Protein	bio-GFP		bio-GFP-MyoIIb	
		# Peptides	# PSM	# Peptides	# PSM
D4A1B8	**Dynactin subunit 3**			**10**	**163**
Q5QJC9	BAG family molecular chaperone regulator 5	2	2	26	106
Q66HA8	Heat shock protein 105 kDa	5	6	28	79
D3ZUJ7	Ankyrin repeat domain 13 family, member D	2	2	18	31
B0BN74	Bag2 protein			8	20
Q6MG49	Large proline-rich protein BAG6	2	2	10	13
D4A4T0	Protein Stub1			7	13
B0BNK1	Protein Rab5c	1	1	7	12
D3Z8Q5	Protein Tusc2			4	12
D4ADD8	Dynactin subunit 6			3	7
P60881	Synaptosomal-associated protein 25	1	1	6	6
D4AA38	Protein Hlcs			5	6
Q5XIR5	BCL2-associated athanogene 4			5	5
G3V852	Protein Tln1			5	5
P70580	Membrane-associated progesterone receptor 1			4	5
D3ZDH8	Platelet glycoprotein Ib beta chain			4	4
P09606	Glutamine synthetase			3	4
P97849	Long-chain fatty acid transport protein 1			3	4
A0JN29	Limb and neural patterns			3	3
Q812E9	Neuronal membrane glycoprotein M6-a			3	3
F1M0Y0	Clustered mitochondria protein homolog			3	3
Q4FZS2	Budding uninhibited by benzimidazoles 3 homolog			3	3
D3ZPN3	Myeloid leukemia factor 2			2	3
D3ZHS5	Protein Cpa4			2	3

Proteins with a number of peptide spectrum matches (#PSM) of 3 or more and an enrichment of 3 or more compared to the control (BioGFP) in the BioGFP-DCTN3 pull-down are included.

Supplementary table 6. Identification of binding partners of Centromere/kinetochore protein zw10 homolog (ZW10) by mass spectrometry analysis using BioGFP pull-downs from rat brain lysates.

Accession	Protein	bio-GFP		bio-GFP-MyoIIb	
		# Peptides	# PSM	# Peptides	# PSM
Q4V8C2	**Centromere/kinetochore protein zw10 homolog**	**3**	**3**	**30**	**351**
P21213	Histidine ammonia-lyase	1	2	6	9
P00507	Aspartate aminotransferase			7	8
P97546	Neuroplastin	1	1	6	8
D3ZWT8	ATP synthase subunit d	1	1	5	6
Q45QM4	Guanine nucleotide binding protein alpha q subunit			5	5
Q5U2Z3	Nucleosome assembly protein 1-like 4	1	1	5	5
D3ZY51	Plakophilin 1	1	1	4	5
Q5XIV1	Phosphoglycerate kinase	1	1	4	5
Q5FVI4	Cell cycle exit and neuronal differentiation protein 1			4	4
P60881	Synaptosomal-associated protein 25	1	1	4	4
Q6LDP3	Glutathione S-transferase			4	4
P97849	Long-chain fatty acid transport protein 1			4	4
P19627	Guanine nucleotide-binding protein G(z) subunit alpha			4	4
Q63768	Adapter molecule crk			4	4
G3V6H9	Nucleosome assembly protein 1-like 1	1	1	4	4
P62997	Transformer-2 protein homolog beta	1	1	4	4
P85845	Fascin1	1	1	4	4
Q920L2	Succinate dehydrogenase [ubiquinone] flavoprotein	1	1	4	4
D3ZTW9	Endonuclease G-like 1			3	4
P29419	ATP synthase subunit e			3	4
D3ZDH8	Platelet glycoprotein Ib beta chain			3	4
D3ZAA0	PRA1 family protein			2	4
M0R9D5	Protein Ahnak			2	4
D4AAT4	Protein Snrpf			3	3
Q6LDS4	Superoxide dismutase			3	3
Q04970	GTPase NRas			3	3
Q5XFX0	Transgelin-2			3	3
P37805	Transgelin-3			3	3
D4AA38	Protein Hlcs			3	3
D3ZPP8	Neuronal-specific septin-3			3	3
Q5XIU9	Membrane-associated progesterone receptor component 2			3	3
P97612	Fatty-acid amide hydrolase 1			3	3
P10888	Cytochrome c oxidase subunit 4 isoform 1			3	3
P09606	Glutamine synthetase			2	3
Q75Q41	Mitochondrial import receptor subunit TOM22			2	3
B2RYW7	Protein Srp14			2	3
D3ZLH9	Protein LOC680385			2	3
F1M0U5	Protein Nbas			2	3
B2RZD1	Protein Sec61b			2	3
P20171	GTPase HRas			2	3
F1M882	Secretory carrier-associated membrane protein 5			2	3
Q9EQX9	Ubiquitin-conjugating enzyme E2 N			2	3
P70580	Membrane-associated progesterone receptor component 1			2	3
Q812E9	Neuronal membrane glycoprotein M6-a			2	3
D3ZBE6	ATP synthase, H+ transporting, mitochondrial Fo, d-like 1			2	3

Proteins with a number of peptide spectrum matches (#PSM) of 3 or more and an enrichment of 3 or more compared to the control (BioGFP) in the BioGFP-ZW10 pull-down are included.

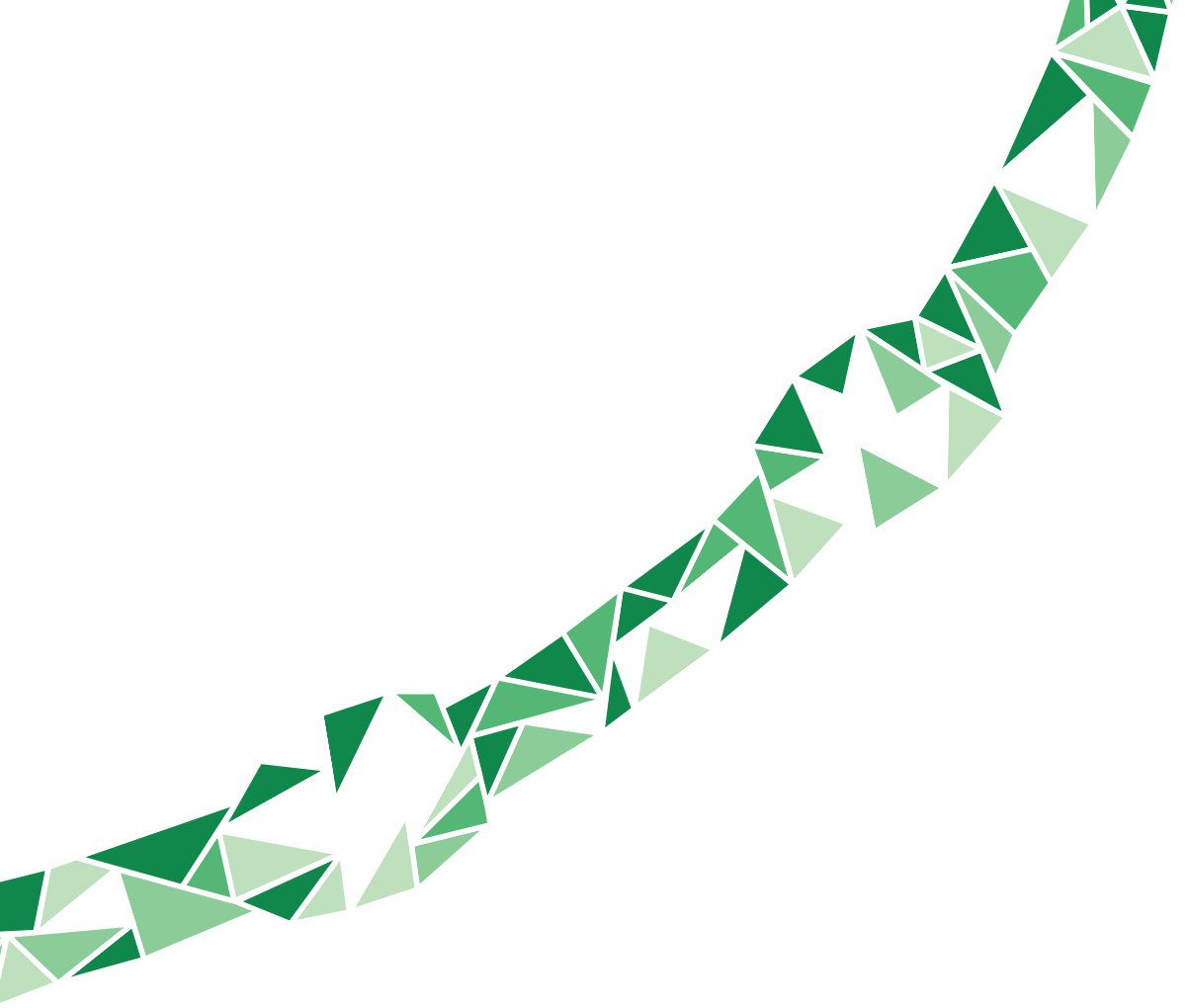

Cell Biology, Department Biology, Faculty of Science, Utrecht University, Utrecht, the Netherlands

Chapter 6

Molecular pathway underlying bouton stabilization by Semaphorin4D during inhibitory synapse formation

Cátia P. Frias, Tom Bresser, Lisa Scheefhals, Hai Yin Hu, Paul M. P. van Bergen en Henegouwen, Casper C. Hoogenraad and Corette J. Wierenga

In revision

SUMMARY

Changes in inhibitory connections are essential for experience-dependent circuit adaptations, but the underlying molecular processes are not well known. By monitoring inhibitory axons over time in organotypic hippocampal slices, we found that inhibitory axons and their presynaptic boutons are remarkably dynamic and can rapidly respond to environmental signals. We show that Semaphorin4D (Sema4D) signaling increases inhibitory synapses by inducing stabilization of presynaptic boutons within tens of minutes, which is followed by recruitment of pre- and postsynaptic proteins over the next 24 hours. Sema4D-induced inhibitory bouton stabilization involves actin remodeling and requires activation of the receptor tyrosine kinase MET, a known autism risk factor. We further show that this Sema4D signaling pathway requires ongoing neuronal activity and can induce local changes in bouton density. Our data indicate a role for Sema4D signaling in activity-dependent circuit adaptation and suggest that defects in inhibitory adaptation are important in autism spectrum disorders (ASD).

INTRODUCTION

For proper information processing during the ongoing stream of events in life, synaptic connections in the brain are continuously updated. Recent imaging studies have demonstrated that axons and their presynaptic terminals (e.g. boutons) are highly dynamic structures that can rapidly adapt to changes. Intra-axonal exchange of synaptic vesicles occurs between neighboring boutons at a time scale of minutes (Staras, 2007) and entire boutons can appear, disappear and reappear over the course of minutes to hours (Sabo et al., 2006; Wierenga et al., 2008). These ongoing axonal dynamics are thought to allow quick implementation of changes in synaptic connectivity in response to activity or other environmental signals (Frias and Wierenga, 2013; Staras, 2007). Inhibitory axons appear particularly dynamic (Chen et al., 2015; Fu et al., 2012; Keck et al., 2011; Schuemann et al., 2013). Recent in vivo data demonstrated that inhibitory adaptation occurs within 24 hours and can serve as a gating mechanism for plasticity at nearby excitatory synapses, which occurs at a slower time scale (Chen et al., 2015; Froemke et al., 2007; Keck et al., 2011; Villa et al., 2016), and this may be a general aspect of circuit development and adaptation (Froemke, 2015; Hensch, 2005). We currently do not understand the molecular processes taking place during rapid adaptation of inhibitory axons and how these are regulated.

We previously showed that new inhibitory synapses form by the occurrence of new presynaptic boutons at pre-existing axon-dendrite crossings (Schuemann et al., 2013; Wierenga et al., 2008). The apparently stochastic dynamics of inhibitory boutons during this process seem to contrast with studies in which a local signaling event, such as specific adhesion between the pre- and postsynaptic membranes, is followed by the recruitment of presynaptic proteins and synaptic vesicles within minutes (Siddiqui and Craig, 2011; Wierenga, 2016). In studies using heterologous culture systems, presynaptic assembly may occur as a sequential process, but it is important to understand the sequence of events that takes place during synapse formation in intact tissue.

The class 4 semaphorin Sema4D has recently been shown to signal rapid changes in inhibitory synapses in primary cultures, which makes it an interesting candidate for mediating activity-dependent changes in inhibitory axons. It is currently not known how Sema4D affects presynaptic bouton dynamics. Knockdown of postsynaptic Sema4D leads to a reduction in the density of GABAergic synapses (Paradis et al., 2007), while addition of soluble Sema4D to primary hippocampal cultures induces an increase of functional inhibitory synapses (Kuzirian et al., 2013). However, from these studies it is not clear if Sema4D directly promotes synapse formation or rather prevents ongoing synapse elimination. Sema4D acts as a postsynaptic protein and requires only its extracellular domain to induce inhibitory synapses through its receptor PlexinB1 (Kuzirian et al., 2013; Raissi et al., 2013). Depending on the association of PlexinB1 with receptor tyrosine kinases, different downstream signal cascades involving small GTPases (Oinuma et al., 2004; Vodrazka et al., 2009) can be activated, which can have opposing effects on the actin cytoskeleton (Swiercz et al., 2002; Tasaka et al., 2012). It is currently not clear how actin remodeling is linked with signaling molecules at the membrane and inhibitory synapse formation.

In the current study, we examine the link between Sema4D signaling and actin in regulating the dynamics of inhibitory presynapses in intact tissue. We find that Sema4D signaling specifically regulates the stabilization of inhibitory boutons along the axon and can induce local changes in bouton density within tens of minutes. This early step in inhibitory synapse formation is followed by subsequent recruitment of pre- and postsynaptic proteins

over the course of the next 24 hours. We further characterized the molecular pathway of Sema4D-induced bouton stabilization and found that it is activity-dependent, involves actin remodeling, and requires the activation of the receptor tyrosine kinase MET. Our study demonstrates that inhibitory axons can rapidly respond to environmental signals. We elucidate an important regulatory pathway of activity-dependent inhibitory synapse formation and reveal a novel role for the receptor tyrosine kinase MET in Sema4D-induced formation of inhibitory synapses.

RESULTS

We performed time-lapse two-photon microscopy in organotypic hippocampal cultures from GAD65-GFP mice to monitor the dynamics of inhibitory boutons in the CA1 region of the hippocampus (Schuemann et al., 2013; Wierenga et al., 2008). High-resolution image stacks of GFP-labeled inhibitory axons were acquired every 10 minutes, for a total period of 150 minutes. We found that inhibitory boutons were remarkably dynamic and many boutons appear, disappeared and reappeared during the course of the imaging period. To bias our analysis towards synaptic events, we only included boutons that appeared for at least 2 time points at the same location during the imaging period. We distinguished two main classes of boutons: persistent boutons, which were present during all time points, and non-persistent boutons, which were absent during one or more time points during the imaging session (Figure 1A and 1B). Approximately 77 % (with standard deviation of 12 %) of inhibitory boutons at any given time point were persistent (Figure 1C), and they reflect inhibitory synapses (Figure 1E) (Müllner et al., 2015; Wierenga et al., 2008). Non-persistent boutons reflect locations where inhibitory synapses are 'in transition', e.g. where synapses are being formed or disassembled (Dobie and Craig, 2011; Schuemann et al., 2013; Wierenga et al., 2008). Based on the presence or absence of non-persistent boutons during a baseline and

Figure 1. Classification of presynaptic inhibitory boutons by their dynamics. ➤

(A) Time-lapse two-photon images of two inhibitory boutons (blue arrowheads) along a GAD65-GFP-labeled axon in the CA1 region of the hippocampus. These boutons were present at all time points, and therefore categorized as persistent boutons. Only every second image is shown for clarity. On the right, the same region is shown after fixation and staining against vesicular GABA transporter (VGAT, magenta). The zoom shows a single optical plane through the bouton to demonstrate overlap (white) of VGAT and GFP boutons. Time in minutes. Scale bars 2 µm and 1 µm (zoom).

(B1-5) Same as in A, showing examples of new (B1; absent during baseline), lost (B2; absent during wash-in), stabilizing (B3; non-persistent during baseline, and persistent during wash-in), destabilizing (B4; persistent during the baseline, and non-persistent during the wash-in) and transient (B5; non-persistent during both baseline and wash-in) boutons. Filled yellow arrowheads indicate that the bouton is present, and empty yellow arrowheads indicate that the bouton is absent at the time point shown.

(C) Average fraction of persistent (P) and non-persistent (NP) boutons at any given time point, and average fraction of the 5 subgroups of non-persistent boutons normalized to the total number of non-persistent boutons (N – new; L – lost; S – stabilizing; D – destabilizing; T – transient).

(D) Percentage of time points in which boutons were present during baseline (white) and wash-in (gray) periods. #: values for D were significantly different from N and T for wash-in ($p < 0.01$; χ^2).

(E) Fraction of boutons positive for VGAT per axon. Numbers indicate the number of boutons analyzed per group. Confocal images are maximum intensity projections of 5-8 z stacks, while two-photon images are maximum intensity projections of 13-15 z stacks. Data are represented as mean ± SEM. In C and D, data from 90 axons from 24 independent experiments, and in E from 21 axons from 5 independent experiments.

wash-in period (details are given in the methods section), we distinguished 5 subgroups of non-persistent boutons: new (N; absent during baseline), lost (L; absent during wash-in), stabilizing (S; non-persistent during baseline, persistent during wash-in), destabilizing (D; persistent during baseline, non-persistent during wash-in) and transient (non-persistent in both periods). These different subgroups of non-persistent boutons not only differed in their incidence and duration (Figure 1C and 1D), but also in their presynaptic vesicular GABA transporter (VGAT) content (Figure 1E). Stabilizing boutons, which were present for at least 90 minutes before fixation, showed similar association with VGAT as persistent boutons, indicating that nascent inhibitory synapses recruit synaptic vesicles within this period. New boutons, which were present for a shorter period before fixation, showed a lower percentage of VGAT association. These data demonstrate that inhibitory presynaptic

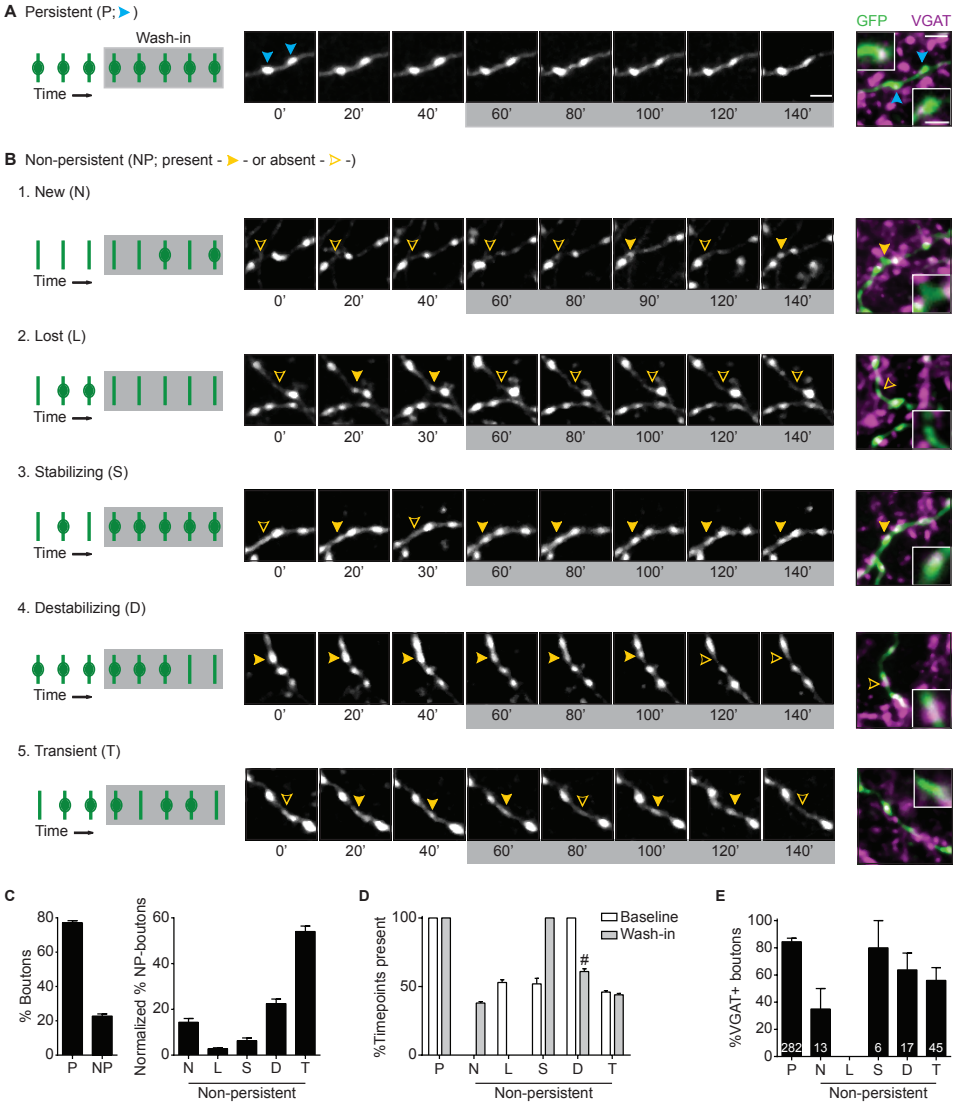

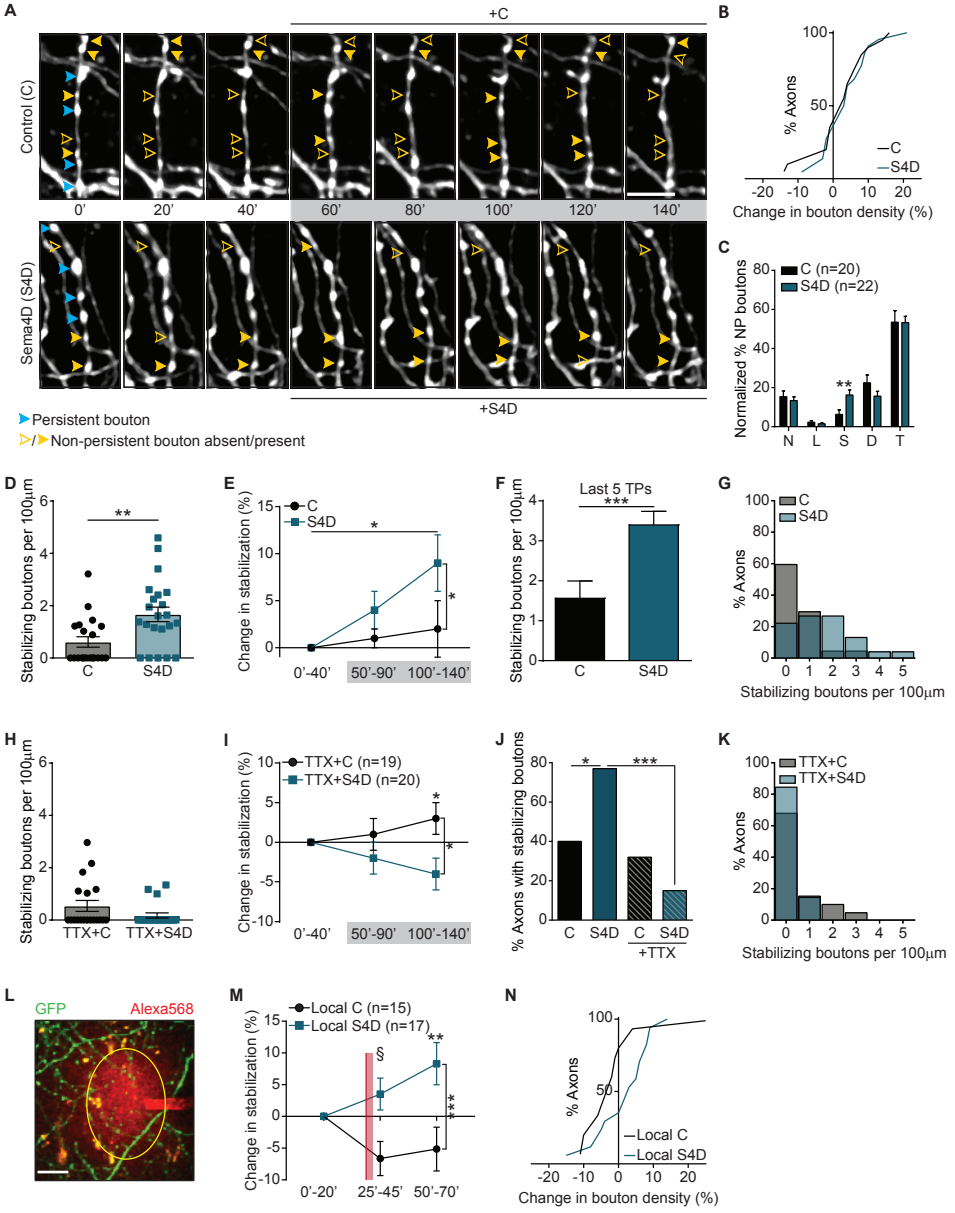

Figure 2. Sema4D treatment promotes inhibitory bouton stabilization.

(A) Time-lapse two-photon images of GFP-labeled inhibitory axons in the CA1 region of the hippocampus during baseline (5 time points) and wash-in (10 time points; grey box) of 1 nM Fc - control (C; upper panel) or 1 nM Sema4D-Fc (S4D; bottom panel). Only every second image is shown for clarity. Persistent (blue) and non-persistent (yellow) boutons are indicated by arrowheads. Filled arrowheads indicate that the bouton is present, and empty arrowheads indicate that the bouton is absent at that time point. Images are maximum intensity projections of 11-18 z stacks. Time in minutes. Scale bar 5 µm.

(B) Cumulative distribution of the change in mean bouton density during the wash-in period compared to baseline

after wash-in of C or S4D. $p = 0.83$ (MW).

(C) Average fraction of subgroups of non-persistent boutons in C- and S4D-treated axons: N – new; L – lost; S – stabilizing; D – destabilizing; T - transient. ** $p < 0.01$ (MW per subgroup).

(D) Density of stabilizing boutons in C- and S4D-treated axons. Each dot represents an individual axon. ** $p < 0.01$ (MW).

(E) Stabilization of inhibitory boutons, as determined by the change (compared to baseline) in density of boutons that were present at 5 consecutive time points during the imaging period: 0'-40' (baseline), 50'-90' (wash-in) and 100'-140' (wash-in). Two-way ANOVA analysis showed a significant effect of both treatment and time. * $p < 0.05$ (Two-Way ANOVA).

(F) Density of boutons that stabilized in the last 5 time points (TPs). *** $p < 0.001$ (MW).

(G) Frequency distribution of the stabilizing bouton density in C- and S4D-treated axons.

(H-I) Same as in D-E, but in the presence of 0.5 µM TTX. In H, p = 0.17 (MW). In I, Two-way ANOVA analysis showed a significant effect of treatment. * $p < 0.05$ (Two-Way ANOVA).

(J) Fraction of axons with stabilizing boutons in axons treated with C or S4D, in normal or activity-depleted slices (0.5 µM TTX). * $p < 0.05$, ** $p < 0.01$ (χ^2).

(K) Same as in G, but in the presence of 0.5 µM TTX.

(L) Representative image of the local treatment of GFP-labeled inhibitory axons in the CA1 region of the hippocampus. The pipette was filled with Alexa568 (red) to visualize the area of the puff (yellow circle). Scale bar 10 µm.

(M) Same as E, but for local treatment with 10 nM Fc (control, C) or 10 nM S4D. Red line marks the puffing. Two-way ANOVA analysis showed a significant effect of treatment and an interaction between treatment and time (§). §,* $p < 0.05$, *** $p < 0.001$ (Two-Way ANOVA).

(N) Same as B, but after local treatment with C or S4D. * $p < 0.05$ (MW).

Data are represented as mean ± SEM. Data in B-G from 20 control axons (N=6) and 22 S4D-treated axons. (N=5), in H,I,K from 19 control axons (N=5) and 20 S4D-treated axons (N=5), and in M-N from 15 control axons (N=6) and 17 S4D-treated axons (N=6).

boutons are dynamic structures that are continuously being formed and disassembled along the axons, and suggest that non-persistent boutons reflect boutons at different stages of inhibitory synapse assembly and disassembly.

Inhibitory bouton stabilization during treatment with Sema4D

It was recently shown that class 4 semaphorin Sema4D can rapidly induce the assembly of functional inhibitory synapses in hippocampal dissociated cultures (Kuzirian et al., 2013), but the underlying mechanisms remain unknown. To examine the effect of Sema4D on inhibitory bouton dynamics, we bath applied the extracellular domain of mouse Sema4D conjugated to the Fc region of mouse IgG2A (Sema4D; 1 nM) and compared inhibitory bouton dynamics during a baseline period of 5 time points and during Sema4D treatment in the subsequent 10 time points (Figure 2A). We used Fc alone (1 nM) as a control (Kuzirian et al., 2013). Bath application of Sema4D did not affect overall axonal morphology (Figure 2A), and did not change the density of inhibitory boutons (Figure 2B). However, when we analyzed the different subgroups of non-persistent boutons, we found that Sema4D treatment specifically enhanced the fraction of stabilizing boutons from 6 % ± 2% to 16 % ± 3 %, while leaving the other subgroups unaffected (Figure 2C and S1A-S1E). Indeed, treatment with Sema4D induced a >2-fold increase in the absolute density of stabilizing boutons (Figure 2D). To examine how Sema4D-induced stabilization developed over time, we quantified the number of boutons that were present for 5 consecutive time points during the baseline and the wash-in period. We found that Sema4D induced a marked increase in these boutons over the course of the wash-in period (% stabilization, Figure 2E), and strongly enhanced the number of

boutons that had stabilized at the end of this period (last 5 time points; Figure 2F). Stabilizing boutons are relatively rare in our slices, as under control conditions only 40% of the axons display one or more stabilizing boutons. Treatment with Sema4D significantly increased this fraction to 77% (Figure 2G). Altogether, these data show that Sema4D treatment specifically promotes the stabilization of inhibitory boutons within tens of minutes in intact tissue.

Sema4D-induced bouton stabilization relies on network activity

We previously showed that inhibitory bouton dynamics are regulated by neuronal activity (Schuemann et al., 2013). We therefore asked whether Sema4D-induced stabilization of inhibitory boutons depended on network activity. Blocking activity by bath application of tetrodotoxin (TTX) only slightly decreased overall bouton dynamics in our slices (Figure S1F), which is in accordance with our previous findings (Schuemann et al., 2013). However, we found that in the presence of TTX Sema4D no longer induced stabilization of inhibitory boutons, and that Sema4D treatment even led to a reduction in bouton stabilization compared to control (Figure 2H and 2I) and decreased the fraction of lost boutons (Figure S1G). Indeed, whereas under control conditions Sema4D treatment increased the number of axons that displayed stabilizing boutons, it led to a decrease in the presence of TTX (Figure 2J and 2K). These findings show that Sema4D treatment affected bouton dynamics in an activity-dependent manner, and indicate that Sema4D promotes the stabilization of inhibitory presynaptic boutons only in active neuronal networks.

Local Sema4D-induced bouton stabilization

Under physiological circumstances, Sema4D is a membrane-attached protein and local Sema4D signaling may be different from our bath application. We therefore locally applied Sema4D to short stretches (~40 µm) of inhibitory axons (Figure 2L). We found that Sema4D induced robust stabilization of inhibitory boutons in these axons, and prevented bouton destabilization, which was induced in control axons by the local application (Figure 2M). In these short axon stretches, these two effects together led to a significant increase in bouton density in Sema4D-treated axons compared to control axons (Figure 2N), indicating that local application of Sema4D was more potent to induce axonal changes than bath application (compare Figure 2B). This demonstrates that local Sema4D signaling can induce local changes in inhibitory bouton density within tens of minutes. Together with the results described above, our data indicate that Sema4D-signaling can mediate rapid changes in local bouton density of inhibitory axons in an activity-dependent manner.

Sema4D-induced stabilization of inhibitory boutons precedes inhibitory synapse formation

We next assessed whether Sema4D-induced bouton stabilization results in formation of new inhibitory synapses. We first examined if longer Sema4D treatment enhanced the bouton stabilization effect. We compared dynamics of individual boutons during baseline and after 6 h treatment (400 minutes total treatment) and found that longer Sema4D treatment also induced prominent bouton stabilization (Figure 3A and S1H). However, the 6 h treatment did not increase bouton stabilization beyond the 2 h level (Figure 3B), suggesting that the number of inhibitory boutons that can be stabilized by Sema4D is limited. In addition to promoting bouton stabilization, longer treatments also induced a reduction in the density of transient boutons (Figure 3C). This secondary effect was only revealed by analyzing the

effect over time, suggesting a more general reduction of dynamics as an indirect effect of prolonged bouton stabilization. These results indicate that the Sema4D-induced stabilization of inhibitory boutons persists, but does not further increase, with longer treatments.

We next asked if Sema4D-induced inhibitory bouton stabilization leads to the formation of new synapses. We treated organotypic hippocampal slices with 1 nM Fc or 1nM Sema4D for 2, 6 and 24 h, and determined overall inhibitory synapse density by immunohistochemistry. We used antibodies against presynaptic VGAT and postsynaptic gephyrin to visualize inhibitory synapses (Figure 3D and 3E). Sema4D induced a clear increase in the density of inhibitory synapses after 24 h (Figure 3F), suggesting that Sema4D-induced bouton stabilization resulted in the formation of new synapses. Treatment with Sema4D induced an increase in the area of VGAT puncta, without affecting their density (Figure 3G-3I). For gephyrin, Sema4D treatment caused an increase in puncta density, but not in their size (Figure 3J-3L). The average puncta intensity was not affected (at 24h, VGAT: 107 % ± 4 % of control, $p = 0.35$ (MW); gephyrin: 106 % ± 5 % of control, $p = 0.51$ (MW)). Interestingly, the time course for presynaptic and postsynaptic changes was different. Whereas the increase in presynaptic VGAT area could be detected after 6 h, the increase in postsynaptic gephyrin density was only evident after 24 h. Note that the increase in presynaptic VGAT could already be detected in individual boutons after 2 h (Figure 1E). The slower postsynaptic response compared to a previous report in primary cultures (Kuzirian et al., 2013) may reflect a difference in overall neuronal maturation (Oh et al., 2016). The observed time course in our slices fits well with previous in vivo reports (Chen et al., 2015; Keck et al., 2011; Villa et al., 2016). Together, these data indicate that the initial Sema4D-induced stabilization of inhibitory boutons is followed by a slower maturation process, through an increase in presynaptic vesicle content and subsequent acquisition of postsynaptic scaffolds (Dobie and Craig, 2011; Wierenga et al., 2008), resulting in an overall increase in inhibitory synapses after Sema4D treatment.

Actin remodeling by low doses of LatrunculinB promotes stabilization of inhibitory boutons

The assembly of inhibitory synapses induced by Sema4D in dissociated hippocampal neurons was shown to be dependent on its receptor PlexinB1 (Kuzirian et al., 2013), and PlexinB1 activation can induce changes in the actin cytoskeleton (Swiercz et al., 2002; Tasaka et al., 2012). To examine how the actin cytoskeleton is involved in inhibitory bouton dynamics, we studied the effect of the actin monomer sequestering drug LatrunculinB (LatB) and the actin filament stabilizer drug Jasplakinolide (Jasp) in our system. In the low concentrations that we use here (100 nM LatB and 200 nM Jasp) these drugs perturb the actin cytoskeleton without affecting synaptic function (Honkura et al., 2008; Rex et al., 2009). None of the treatments changed overall axon morphology (Figure 4A). We found that the fraction of stabilizing boutons was increased in the presence of LatB, but not of Jasp (Figure 4B and 4C). Other bouton subgroups were not affected (Figure S2). In fact, we found that LatB specifically increased the absolute density of stabilizing boutons by almost 2-fold (Figure 4D and 4E), similar to Sema4D (Figure 2D and 2G). These findings show that inhibitory bouton dynamics are regulated by changes in the actin cytoskeleton.

The similar stabilization of inhibitory boutons induced by treatment with LatB or Sema4D suggests that they act in a common underlying pathway at the same subset of boutons. We therefore treated slices with a combination of LatB and Fc or LatB and Sema4D,

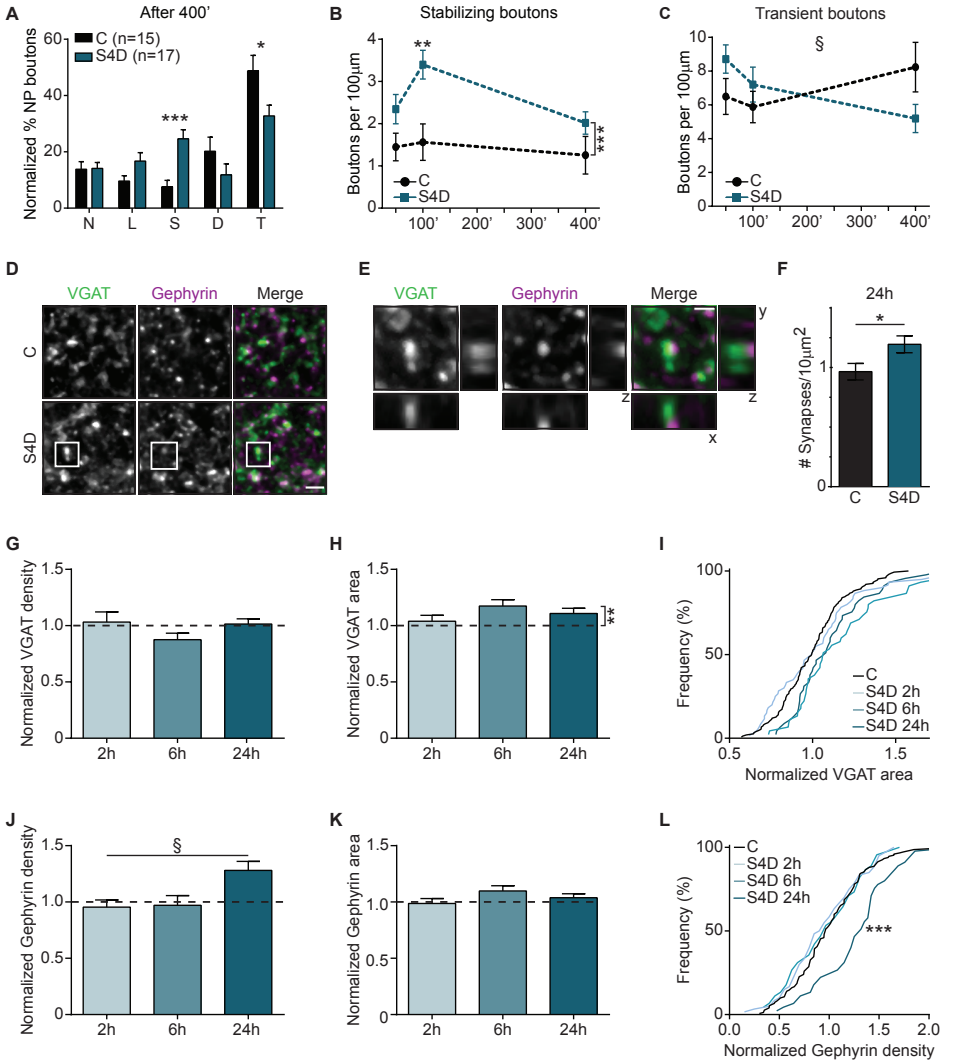

Figure 3. Sema4D increases overall inhibitory synaptic density.

(A) Average fraction of subgroups of non-persistent boutons after treatment with 1 nM Fc (control; C) or 1 nM Sema4D-Fc (S4D) for 6 hours (400 minutes of total treatment): N – new; L – lost; S – stabilizing; D – destabilizing; T - transient. * $p < 0.05$, *** $p < 0.001$ (MW per subgroup).

(B) Density of stabilizing boutons after treatment with Fc or S4D for 50, 100 and 400 minutes. Two-way ANOVA analysis showed that S4D increased density independent of time. ** $p < 0.01$, *** $p < 0.001$ (Two-Way ANOVA).

(C) Same as B, but for transient boutons. Two-Way ANOVA analysis indicated a significant interaction between treatment and time (§). § $p < 0.05$ (Two-Way ANOVA).

(D) Representative images of CA1 dendritic area of GAD65-GFP hippocampal slices treated with 1 nM Fc (C) or 1 nM Sema4D-Fc (S4D) for 24 h, and immunostained for VGAT (green) and gephyrin (magenta). Images are average intensity projections of 5 z stacks. Scale bar 2 µm.

(E) Example of an inhibitory synapse (white box in D), identified as the apposition of VGAT (green) and gephyrin (magenta) puncta. The respective xz and yz projections show the close apposition of the two markers. Images are

maximum intensity projections of 6 z stacks. Scale bar 1 µm.
(F) Density of inhibitory synapses in slices treated with Fc or Sema4D for 24 h. * $p < 0.05$ (MW).
(G) Normalized density of presynaptic vesicular GABA transporter (VGAT) puncta (after treatment with 1 nM S4D for 2 h, 6 h and 24 h. Dotted line represents control (treatment with 1nM Fc for 2 h, 6 h and 24 h).
(H) Same as in G, but for VGAT puncta area. Two-way ANOVA analysis showed that S4D treatment increased VGAT area independent of time. ** $p < 0.01$ (Two-Way ANOVA).
(I) Cumulative distributions of the normalized area of VGAT after treatment with 1 nM S4D for 2, 6 and 24 h. Black line represents the normalized control values. p = 0.81, 0.08 and 0.14 (KS) for 2, 6 and 24 h, respectively.
(J-K) Same as in G-H, but for density (J) and area (K) of postsynaptic gephyrin puncta. In J, Two-way ANOVA analysis showed a significant effect of time and an interaction between treatment and time in I (§). § $p < 0.05$ (Two-Way ANOVA).
(L) Same as in I, but for normalized gephyrin density. $p = 0.99$ and 0.99 (KS) for 2 and 6 h, respectively. *** $p < 0.001$ (KS).
Data are represented as mean ± SEM. In A, data from 15 control axons (N=4) and 17 S4D-treated axons (N=4), and in F-L from 15/20 control images (N=3/4) and 15/20 S4D images (N=3/4).

and found that bouton stabilization by LatB occluded a further increase by co-application with Sema4D (Figure 4F and 4G). Co-treatment with LatB and Sema4D only increased the fraction of new boutons. These data suggest that LatB and Sema4D induced stabilization of the same subgroup of inhibitory boutons and act in a common signaling pathway.

MET is enriched at a subset of inhibitory presynaptic boutons

The outcome of Sema4D/PlexinB1 signaling on the underlying actin cytoskeleton relies on the co-activation of receptor tyrosine kinase receptors. Co-activation of MET upon Sema4D treatment has been shown to promote anti-migratory effects in some breast cancer lines through actin remodeling by the inactivation of small RhoGTPase RhoA (Sun et al., 2012; Swiercz et al., 2008). Based on our observation that Sema4D and LatB act in a common pathway regulating inhibitory bouton dynamics, we wondered if MET plays a role in Sema4D-induced bouton stabilization. MET has previously been shown to be enriched in axonal tracts and to co-localize with presynaptic markers of excitatory synapses (Eagleson et al., 2013; Judson et al., 2009; Xie et al., 2016), but its presence in inhibitory neurons is debated (Eagleson et al., 2011). To address a possible localization of MET at inhibitory synapses, we made use of a nanobody against MET (Heukers et al., 2014). We confirmed that this nanobody labels synapses in primary hippocampal cultures (Figure S3A). The majority of MET puncta overlapped with excitatory synapses as previously reported (Eagleson et al., 2013; Tyndall and Walikonis, 2006), but clear association of MET with inhibitory presynapses was also observed (Figure S3B). When we labeled MET in our hippocampal slices of GAD65-GFP mice, we observed that 21 % ± 3 % of the GFP-labeled inhibitory boutons were enriched for MET (Figure 5A-5C). Comparing the MET staining pattern with staining for postsynaptic gephyrin (compare Figure 5B with Figure 3E) suggests a presynaptic localization of MET at these inhibitory synapses. These data show that with our method we are able to detect enrichment of MET in inhibitory presynaptic boutons.

Inhibitory bouton stabilization by Sema4D requires MET

We next assessed if MET activation is necessary for the observed Sema4D-induced stabilization of boutons. After the baseline period, we treated our slices with Sema4D as before or in combination with PHA-665752 (PHA), a highly specific MET inhibitor (Lim and Walikonis, 2008). We observed that adding the PHA blocker alone did not affect bouton dynamics (Figure S3C and S3D), suggesting that MET is not activated under baseline conditions

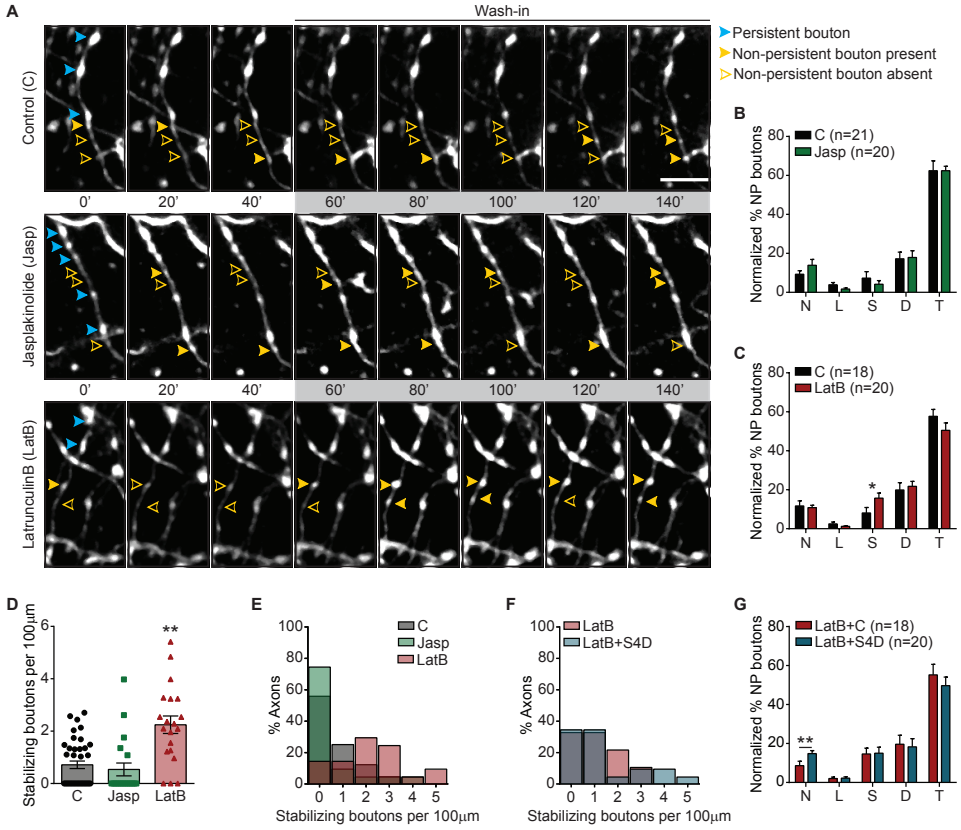

Figure 4. Inhibitory bouton dynamics are regulated by actin.

(A) Time-lapse two-photon images of GAD65-GFP-labeled axons in the CA1 region of the hippocampus during baseline (5 time points) and wash-in (10 time points; grey box) of DMSO - control (C; upper panel), 200 nM Jasplakinolide (Jasp; middle panel) or 100 nM LatrunculinB (LatB; bottom panel). Only every second image is shown for clarity. Persistent and non-persistent boutons are indicated as in Figure 2. Images are maximum intensity projections of 12-14 z stacks. Time in minutes. Scale bar 5 µm.

(B) Average fraction of the five subgroups of non-persistent (NP) boutons (N – new; L – lost; S – stabilizing; D – destabilizing; T – transient) in C and Jasp-treated axons.

(C) Same as in B, but for C and LatB-treated axons. * $p < 0.05$ (MW per subgroup).

(D) Density of stabilizing boutons in control, Jasp- and LatB-treated axons. ** $p < 0.01$ (MW).

(E) Frequency distribution of the stabilizing bouton density in C, Jasp- and LatB-treated slices.

(F) Same as E, but for combined treatment with 100 nM LatB/1 nM Fc (LatB+C) or 100 nM LatB/1 nM Sema4D (LatB+S4D).

(G) Same as B, but for combined treatment with LatB/C or LatB/S4D. ** $p < 0.01$ (MW per subgroup).

Data are represented as mean ± SEM. Data from 21 control axons (N=6) and 20 Jasp-treated axons (N=5) in B, from 18 control axons (N=5) and 20 LatB-treated axons (N=5) in C, and from 18 LatB/Fc- (N=4) and 20 LatB/S4D-treated axons (N=5).

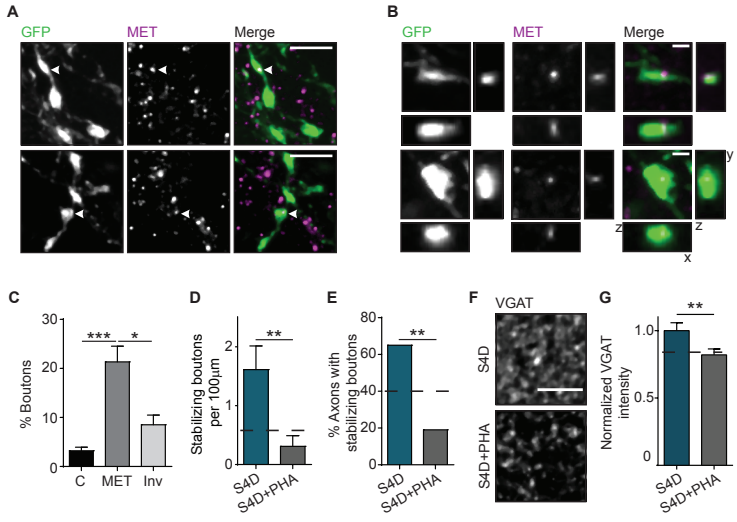

Figure 5. Inhibitory bouton stabilization by Sema4D requires MET.

(A) Representative images of GFP-labeled inhibitory boutons (green) in hippocampal slices, stained for MET (magenta). Images are maximum intensity projections of 6 z stacks. White arrows indicate boutons MET enrichments in GFP-labeled boutons. Scale bar 5 µm.

(B) Example of two inhibitory boutons (green) in hippocampal slices showing enrichment in MET (magenta), and the respective xz and yz projections. Images are maximum intensity projections of 6 z stacks. Scale bar 1 µm.

(C) Fraction of GFP boutons positive for MET. Aspecific staining was determined by anti-myc staining without nanobody ('C'; black) and random co-localization was determined by inverting the MET channel ('Inv'; light gray). * $p < 0.05$, *** $p < 0.001$ (KW).

(D) Density of stabilizing boutons in slices treated with a combination of 1 nM Sema4D/DMSO (S4D) or 1 nM Sema4D/1 µM PHA-665752 (S4D+PHA). Dotted line represents control values. ** $p < 0.01$ (MW).

(E) Fraction of axons with stabilizing boutons. Dotted line represents control values. ** $p < 0.01$ (χ^2).

(F) Representative images of hippocampal slices treated with S4D (upper panel) or S4D+PHA (bottom panel) for 100', and stained for presynaptic VGAT. Images are average intensity projections of 5 z stacks. Scale bar 5 µm.

(G) Normalized mean staining intensity for VGAT. Control value is indicated with dotted line. ** $p < 0.01$ (MW).

Data are represented as mean ± SEM. In C, data from 10 control images (N=2) and 12 images in MET and inverted group (N=3), in D-E from 17 S4D/DMSO-treated axons (N=4) and 16 S4D/PHA-treated axons (N=4), and in G from 16 images of S4D-treated slices (N=3) and 23 images of S4D+PHA-treated slices (N=4).

in our slices. However, blocking MET completely abolished the Sema4D-induced increase in the density of stabilizing boutons (Figure 5D). In fact, blocking MET in combination with Sema4D treatment almost entirely abolished the occurrence of stabilizing boutons (Figure 5E). Sema4D treatment in the presence of PHA had only a mild effect on the other bouton subgroups (Figure S4). Consistent with the live imaging data, inhibiting MET with PHA also blocked the increase in VGAT staining intensity after Sema4D treatment (Figure 5F and 5G). Taken together, these data indicate that activation of MET is required for the Sema4D-induced stabilization of inhibitory boutons.

DISCUSSION

Ongoing formation and disassembly of inhibitory synapses in the brain play an important role in experience-dependent circuit adaptation. We found that Sema4D signaling affects these dynamics in a highly specific manner. Sema4D signaling induces actin remodeling, which leads to inhibitory bouton stabilization within tens of minutes, followed by subsequent maturation of inhibitory synapses over the next 24 hours. Our data indicate that Sema4D can mediate local changes in inhibitory bouton density in an activity-dependent manner, suggesting an important role for this signaling pathway in circuit adaptation processes. We further found that Sema4D-induced inhibitory synapse formation requires activation of the receptor tyrosine kinase MET. Our results elucidate an important regulatory pathway of activity-dependent inhibitory synapse formation and reveal a novel role for MET in inhibitory synapses.

Inhibitory axons can rapidly respond to environmental signals

Our live imaging experiments give unique insight in the dynamics of the process of inhibitory synapse formation in brain slices, which would have remained undetected with methods using stationary comparisons before and after treatment. In postnatal brain tissue, in which the majority of inhibitory connections have been established, synapse formation and disassembly is still ongoing. In our slices, many GFP-labeled boutons are persistent and display pre- and postsynaptic markers of mature inhibitory synapses, but a significant portion (~20%) of inhibitory boutons are non-persistent. Non-persistent boutons represent locations where inhibitory synapses are 'in transition'. At these axonal locations, inhibitory synapses seem to be formed and disassembled in an trial-and-error fashion (Dobie and Craig, 2011; Fu et al., 2012; Schuemann et al., 2013; Wierenga, 2016; Wierenga et al., 2008). Here we show that inhibitory axons can respond very rapidly to signals from their environment. Local signaling through Sema4D can promote rapid stabilization of non-persistent inhibitory boutons, resulting in a local increase of inhibitory synapses. This suggests that ongoing bouton dynamics in inhibitory axons play a major role in rapid adaptation of inhibitory connections, such that inhibitory connections can be quickly updated when needed. As rapid changes in inhibitory connections are an essential aspect of circuit rewiring during development and learning, it is important to characterize the molecular processes underlying presynaptic dynamics in inhibitory axons.

Sema4D regulates stabilization of non-persistent inhibitory boutons

We found that Sema4D treatment specifically increased the number of non-persistent boutons that stabilized during the imaging period. Sema4D-induced bouton stabilization was not enhanced by longer treatment (>2 h) or co-application with LatB, suggesting that the number of boutons susceptible to Sema4D at any given time is limited. This suggests that Sema4D signaling is involved only at a specific stage during synapse formation and that boutons which are more mature or too immature do not respond to Sema4D. Indeed, we observed that Sema4D signaling did not induce formation of inhibitory synapses de novo, but stabilized boutons at locations where a bouton had occurred before. At first sight, this seems to contrast with a previous report in primary cultures, where Sema4D application induced the formation of new inhibitory synapses (Kuzirian et al., 2013). However, in the latter study, presynaptic dynamics were not monitored and it is not known if Sema4D-induced synapses occurred de novo, or at locations where inhibitory boutons had occurred before.

In primary cultures, a much larger fraction of synapses may be immature compared to intact tissue (Dobie and Craig, 2011; Kuriu et al., 2012), which may underlie the stronger effect of Sema4D on inhibitory synapse formation in this preparation. In our slices, Sema4D treatment increased inhibitory synapse density by ~20% after 24 hours (Fig. 3F), which is in line with in vivo studies (Chen et al., 2015; Keck et al., 2011; Villa et al., 2016). In addition to stabilizing inhibitory boutons, we found that Sema4D signaling also reduced bouton destabilization (Figure 2M and 3A), possibly reflecting an enhanced sensitivity of destabilizing boutons to the Sema4D stabilization signal. Our results suggest that Sema4D signaling regulates a specific step of inhibitory synapse formation.

A novel role for MET in inhibitory synapse formation

It was previously shown that Sema4D acts as a postsynaptic protein and requires PlexinB1 for promoting inhibitory synapse formation (Kuzirian et al., 2013; Raissi et al., 2013). Future studies will need to determine if presynaptic PlexinB1 receptors are sufficient or if additional PlexinB isoforms or postsynaptic receptors are also involved. Here we found that activation of the receptor tyrosine kinase MET is required for Sema4D-induced inhibitory bouton stabilization, suggesting that MET acts as a co-receptor for the Sema4D receptor PlexinB1 (Swiercz et al., 2008) to promote an intracellular pathway that ultimately leads to actin remodeling within the axon. Consistent with this scenario, we found that MET is enriched in inhibitory synapses, both in primary hippocampal cultures and organotypic slices. Our data suggest a presynaptic localization of MET at inhibitory synapses, which would be consistent with the observation of MET in symmetric presynaptic terminals in a previous immunoelectron microscopy study (Eagleson et al., 2013). However, expression of MET in inhibitory neurons is debated, since expression could not be detected in vivo, but only when cells were challenged in vitro (Eagleson et al., 2011). Future studies are needed to clarify this point further, and if expression of MET happens at specific stages of inhibitory synapse formation or if it is related with neuronal activity. Our data suggest that activation of MET is part of the Sema4D-signaling pathway promoting inhibitory bouton stabilization. Previous studies have implicated MET in regulating postsynaptic strength in excitatory neurons (Lo et al., 2016; Qiu et al., 2014), and in interneuron migration during early stages of neuronal development (Martins et al., 2011). Our data indicate a novel role for MET in the assembly of inhibitory presynapses.

Actin remodeling is one of the first events in inhibitory synapse formation

Activation of the Sema4D/PlexinB1 signaling pathway via MET ultimately leads to changes in the actin cytoskeleton (Sun et al., 2012; Swiercz et al., 2008). Indeed, we could mimic the Sema4D effect by applying low levels of the actin-depolymerizing drug LatB. Our observations indicate that presynaptic actin remodeling is one of the first events occurring during inhibitory synapse formation. This finding complements two recent studies that show a similar role for presynaptic actin in synaptogenesis in C. elegans (Chia et al., 2014) and Drosophila (Piccioli and Littleton, 2014). Our study shows that the dynamics of inhibitory boutons are regulated by intracellular modification of actin structures. It has been previously shown that bouton dynamics reflect intra-axonal transport of presynaptic components, including clusters of synaptic vesicles and active zone proteins (Fu et al., 2012; Sabo et al., 2006; Staras, 2007). We show that Sema4D and LatB treatments induce similar actin changes in immature boutons to promote stabilization, suggesting that the affinity for vesicle capture

may be defined by local actin structures (Sun and Bamji, 2011; Wu et al., 2013). Low doses of monomer sequestering drugs, such as LatB used in our study, presumably do not lead to the complete disassembly of actin structures (Bleckert et al., 2012; Ganguly et al., 2015; Honkura et al., 2008). Instead, limited availability of actin monomers may indirectly affect actin-regulating factors resulting in structural changes of the actin cytoskeleton (Ganguly et al., 2015; Suarez et al., 2015). Future studies will be necessary to unravel precise actin structures and the role of actin-regulating factors in axonal boutons, and the specific changes that occur during synapse formation.

Activity-dependent inhibitory adaptation

Our observation that Sema4D-induced bouton stabilization requires ongoing neuronal activity suggests that this process plays a role during activity-dependent inhibitory plasticity. A local Sema4D signal can induce a rapid increase in inhibitory synapses, shaping local inhibitory connections and thereby affecting information processing. It is becoming clear that adaptation of inhibitory synapses play an important role in the rewiring of circuits during development, and in response to behavioral demands during adulthood. A transient change in inhibitory connectivity may serve as a gating mechanism for plasticity at nearby excitatory synapses, which takes place at a slower time scale (Froemke, 2015; Froemke et al., 2007; Hensch, 2005; Keck et al., 2011; Villa et al., 2016). However, our understanding of the molecular processes underlying activity-dependent inhibitory adaptation is very limited. Our data suggest that Sema4D signaling may be one of the pathways regulating this process. Another pathway may involve GABAB signaling (Fu et al., 2012), and there may be many more. Defects in inhibitory adaptation may contribute to neurodevelopmental disorders, including autism spectrum disorder (ASD). It is therefore interesting that mutations in the MET gene are an established risk factor for ASD, as determined by various human imaging and genetic studies (Peng et al., 2013). Our discovery of a role for MET in Sema4D-mediated inhibitory synapse formation suggests that defects in inhibitory adaptation may contribute to problems in information processing as seen in ASD. It will be important to study inhibitory adaptation processes in ASD mouse models in future studies.

Together, our study demonstrates that inhibitory axons can respond to environmental signals within tens of minutes. We elucidate here the molecular pathway underlying rapid inhibitory bouton stabilization by activity-dependent Sema4D signaling and reveal a novel role for the receptor tyrosine kinase MET in inhibitory synapses. Our findings contribute to unraveling the molecular processes underlying local activity-dependent changes in inhibitory connections during circuit adaptation.

ACKNOWLEDGMENTS

We would like to thank G. Szábo for kindly providing the GAD65-GFP mice, R. van Dorland for technical support, S. Paradis for helpful comments and scientific discussions and A. Akhmanova, G.G. Turrigiano and R.J. Pasterkamp for critically reading the manuscript. This work was supported by the People Programme (Marie Curie Actions) of the European Union's Seventh Framework Programme FP7/2007-2013/ under REA grant agreement 289581 (C.P.F.), a Marie Curie Reintegration Grant 256284 (C.J.W.) and the Netherlands Organization for Scientific Research (NWO-VIDI, C.J.W., NWO-VICI, C.C.H.).

AUTHOR CONTRIBUTIONS

C.P.F. and C.J.W. designed the research. C.P.F. performed the experiments and analyzed the results. T.B. contributed to data in Figure 2H,I,K and S1F-G. L.S contributed to data in figure 4B,D,E and S2A-E. H.Y.H. performed local application experiments (Fig. 2M,N). P.B.H. provided the nanobody. C.P.F. and C.J.W. wrote the manuscript, with input from all other authors. C.J.W. coordinated and supervised the research.

COMPETING FINANCIAL INTERESTS

The authors declare no competing financial interests.

MATERIALS AND METHODS

Animals

All animal experiments were performed in compliance with the guidelines for the welfare of experimental animals issued by the Federal Government of The Netherlands. All animal experiments were approved by the Animal Ethical Review Committee (DEC) of Utrecht University.

Hippocampal slice cultures

Hippocampal slice cultures (400 µm thick) were prepared from postnatal day 5-7 of both male and female GAD65-GFP mice (Lopez-Bendito et al., 2004) as previously described (Müllner et al., 2015). In short, the hippocampi were dissected in ice-cold HEPES-GBSS (containing 1.5 mM $CaCl_2 \cdot 2H_2O$, 0.2 mM KH_2PO_4, 0.3 mM $MgSO_4 \cdot 7H_2O$, 5 mM KCl, 1 mM $MgCl_2 \cdot 6H_2O$, 137 mM NaCl, 0.85 mM Na_2HPO_4 and 12.5 mM HEPES) supplemented with 1 mM kynurenic acid and 25 mM glucose, and plated in a MEM-based medium (MEM supplemented with 25 % HBSS, 25 % horse serum, 30 mM glucose and 12.5 mM HEPES).

In GAD65-GFP mice, approximately 20% of the CA1 interneurons express GFP from early embryonic developmental stage into adulthood (Lopez-Bendito et al., 2004; Wierenga et al., 2010). The majority of GFP-labeled interneurons expresses reelin and VIP, while parvalbumin and somatostatin expression is nearly absent (Wierenga et al., 2010). For our study, the relatively low number of GFP-positive axons is crucial for proper analysis of individual boutons.

The slices were kept in culture for at least one week before the experiments (range 7-18 days in vitro) at 35 °C in 5 % CO_2. For live imaging experiments, slices were transferred to an imaging chamber, where they were continuously perfused with carbogenated artificial cerebrospinal fluid (ACSF; containing 126 mM NaCl, 3 mM KCl, 2.5 mM $CaCl_2$, 1.3 mM $MgCl_2$, 1.25 mM NaH_2PO_4, 26 mM $NaHCO_3$, 20 mM glucose and 1mM Trolox). The temperature of the chamber was maintained at 37 °C. Treatment and control experiments were conducted in slices from sister cultures.

Pharmacological treatments

The following drugs were used: 0.1/0.2 % DMSO, 1 nM Fc and Sema4D-Fc (amino acids 24-711) (both R&D Systems), 100 nM Latrunculin B (Santa Cruz Biotechnology), 200 nM Jasplakinolide (Tocris Bioscience) and 1 µM PHA-665752 (Sigma-Aldrich). We used the small molecule PHA-665752 (PHA), a specific MET inhibitor, to decrease endogenous phosphorylation of MET, without affecting MET expression or neuronal cell viability (Lim and Walikonis, 2008). We used 10 nM Fc or Sema4D for the local puffing experiments.

For treatments that were followed by immunostaining of inhibitory synapses, 1 nM Fc or Sema4D-Fc was added to the culturing medium and slices were left in the incubator for 2, 6 or 24 h before fixation.

Two-photon imaging

For acute treatments, drugs were added to the perfusion ACSF after a baseline period of 40 minutes (5 time

points) and we continued imaging for an additional 10 time points in the treatment period (total imaging period is 140 minutes). In longer treatments, we treated the slices for 6 hours after the baseline period (5 imaging time points) at the microscope and restarted imaging for 5 time points, for a total treatment period of 6 hours and 40 minutes (400 minutes). For activity blockade, 0.5 µM tetrodotoxin citrate (TTX; Tocris Bioscience) was added to the perfusion ACSF prior to the transfer of the slice to the imaging chamber. Time-lapse two-photon microscopy images were acquired on a Femtonics 2D two-photon laser-scanning microscope (Budapest, Hungary), with a Nikon CFI Apochromat 60X NIR water-immersion objective. GFP was excited using a laser beam tuned to 910 nm (Mai Tai HP, Spectra Physics). The 3D images (93.5 µm x 93.5 µm in xy, 1124 x 1124 pixels) consisted of 29-33 z stacks (0.5 µm step size in z). Small misalignments due to drift were manually compensated during the acquisition.

For the local treatment, we used HEPES-ACSF (containing 126 mM NaCl, 3 mM KCl, 2.5 mM CaCl2, 1.3 mM MgCl2, 1.25 mM NaH2PO4, 20 mM glucose, and 10 mM HEPES; pH 7.41) with 20 µM Alexa 568 (Invitrogen), in order to visualize the spread of the local puff. Sema4D or Fc was added to the HEPES-ACSF to a final concentration of 10 nM. The solution was loaded into a patch pipette (4-6 MOhm), and was locally applied to a GFP-labeled axon using a Picospritzer II (General Valve). Time-lapse two photon microscopy imaging was performed as described previously, except that a second laser (Spectra Physics) was used at 840 nm to visualize the area of the puff. The 3D images (51.3 µm x 51.3 µm in xy, 620 x 620 pixels) consisted of 18-22 z stacks (0.5 µm step size in z). After a baseline period of 20 minutes (5 TPs), the pipette was put into position before the stimulation. The stimulation consisted of 300 puffs of 20-50 ms at 2 Hz. The pipette was carefully retracted before continuing the time series for 10 additional time points (total imaging period of 70 minutes).

Two-photon image analysis

The analysis of inhibitory bouton dynamics was performed semi-automatically using ImageJ (US National Institute of Health) and Matlab-based software (Mathworks). The 3D coordinates of individual axons were selected at every time point by using the CellCounter plugin (Kurt De Vos, University of Sheffield, Academic Neurology). For each image, 1-5 stretches of axons (average length 78 µm with standard deviation 18 µm, with average of 31 boutons per axon with standard deviation 11; for local treatment experiments, average length 39 µm with standard deviation 8 µm, with average of 14 boutons per axon with standard deviation of 4) were selected for analysis.

A 3D intensity profile along the selected axons was constructed at each time point, and individual boutons were identified in a two-step process using custom-made Matlab software (Schuemann et al., 2013). In brief, an axon threshold was calculated to differentiate the axon from the background (2 standard deviations above mean intensity); subsequently, a local threshold (0.5 standard deviation above mean axon intensity) identified the boutons along the selected axon. Only boutons with at least 5 pixels above bouton threshold were included. Each image stack was visually examined and false positives and negatives were corrected manually. Only raw data was analyzed; images were median-filtered for illustration purposes only.

Boutons were classified as persistent when they were present during all time points, and non-persistent when they were absent during one or more time points during the imaging session. The average fraction of persistent and non-persistent boutons was calculated by normalization to the average number of boutons per axon. To bias our analysis towards synaptic events (Schuemann et al., 2013), we restricted our analysis to boutons that appeared for at least 2 time points at the same location during the imaging period. We verified that our main conclusions did not change when this restriction was released. Based on their presence during baseline and wash-in periods, we defined five subgroups of non-persistent boutons: new boutons (not present during baseline), lost boutons (not present during wash-in), stabilizing boutons (non-persistent during baseline, persistent during wash-in), destabilizing boutons (persistent during baseline, non-persistent during wash-in), and transient boutons (non-persistent in baseline and wash-in) (Fig. 1). Average fraction of each subgroup of boutons was normalized to the total average number of non-persistent (NP) boutons per axon. The duration of each bouton was defined as the number of time points present divided by the total number of time points per period. Bouton density was calculated as the average number of boutons at all time points divided by the 3D axon length.

Immunohistochemistry, confocal imaging and image analysis

For post hoc immunohistochemistry, organotypic hippocampal slices were fixed in 4 % (w/v) paraformaldehyde for

30 minutes at room temperature. Slices were rinsed in phosphate buffer and permeabilized with 0.5 % TritonX-100 in phosphate buffer for 15 minutes. Slices were blocked with 0.2 % TritonX-100, 10 % goat serum (ab7481, Abcam) in phosphate buffer for 60 minutes. Primary antibodies were applied overnight at 4°C in blocking solution. After washing, slices were incubated with secondary antibodies in blocking solution for 4h at room temperature. Slices were washed and mounted on slides in Vectashield mounting medium (Vector Labs).

The following primary and secondary antibodies were used: rabbit α-VGAT (1:1000; Synaptic Systems, 131 003), mouse α-gephyrin (1:1000; Synaptic Systems, 147 011), guinea pig α-VGLUT (1:400; Millipore, AB5905), rabbit α-Homer (1:1000; Synaptic Systems, 160 002), mouse α-myc (1:100; Oncogene Research Products, OP10), Alexa405-, Alexa-488 and Alexa-568 conjugated secondary antibodies (Invitrogen). For staining MET we used a previously described myc-tagged nanobody, which was shown to recognize MET with low nanomolar affinity (Heukers et al., 2014). We visualized the nanobody with an antibody against the C-terminal myc tag. We validated the nanobody staining in primary hippocampal cultures using a previously described immunostaining protocol (Esteves da Silva et al., 2015).

For immunostainings, high resolution confocal laser scanning microscopy was performed on a Zeiss LSM-700 system with a Plan-Apochromat 63x 1.4 NA oil immersion objective. Each image was a z-series of 11-35 images (0.3 µm z step size), each averaged 4 times. The imaging area in the CA1 region was 78 x 78 µm (1024 x 1024 pixels). The confocal settings were kept the same to compare fluorescence intensities between slices.

For the quantification of VGAT and gephyrin intensities per image, we determined per image the mean intensity of 3 randomly chosen areas of 10 x 10 µm of the average projection image from the 5 middle z-layers. For the cumulative plots individual values (per area) were used. Synaptic puncta size and number were determined using the PunctaAnalyzer plugin, and inhibitory synapses were defined as overlapping VGAT and gephyrin puncta. For determining co-localization of GFP-labeled boutons with synaptic marker VGAT or with MET, we manually inspected individual boutons through all z-sections. A bouton was only considered positive when at least one z stack of the bouton overlapped with VGAT or MET staining. The images were median-filtered only for illustration purposes.

Statistics

Data are represented as mean values ± standard error of the mean, unless stated otherwise. Statistical analysis was performed using GraphPad Prism software. Results from treatment and control experiments were compared using the Mann-Whitney U test (MW). The Chi-Square test (χ^2) was used for comparing fractions. For comparing multiple groups, we used the Kruskal-Wallis test (KW) followed by a posthoc Dunn's comparison test. We used a Two-Way ANOVA followed by a Sidak's multiple comparisons test (Two-Way ANOVA) to compare treatment effects at multiple time points. For the comparison of cumulative distributions, we used the Kolmogorov-Smirnov (KS) test. We have indicated the used tests in the figure legends. Differences between control and treatment were considered significant when $p < 0.05$ (*, $p < 0.05$; **, $p < 0.01$; ***, $p < 0.001$). In all figure legends and text, N indicates the number of independent experiments, and n indicates the number of axons/images analyzed.

REFERENCES

Bleckert, A., Photowala, H., and Alford, S. (2012). Dual pools of actin at presynaptic terminals. J. Neurophysiol. 107, 3479-3492.

Chen, S.X., Kim, A.N., Peters, A.J., and Komiyama, T. (2015). Subtype-specific plasticity of inhibitory circuits in motor cortex during motor learning. Nat. Neurosci. 18, 1109-1115.

Chia, P.H., Chen, B., Li, P., Rosen, M.K., and Shen, K. (2014). Local F-actin network links synapse formation and axon branching. Cell 156, 208-220.

Dobie, F.A., and Craig, A.M. (2011). Inhibitory synapse dynamics: coordinated presynaptic and postsynaptic mobility and the major contribution of recycled vesicles to new synapse formation. J. Neurosci. 31, 10481-10493.

Eagleson, K.L., Campbell, D.B., Thompson, B.L., Bergman, M.Y., and Levitt, P. (2011). The autism risk genes MET and PLAUR differentially impact cortical development. Autism Res. 4, 68-83.

Eagleson, K.L., Milner, T.A., Xie, Z., and Levitt, P. (2013). Synaptic and extrasynaptic location of the receptor tyrosine kinase met during postnatal development in the mouse neocortex and hippocampus. J. Comp. Neurol. 521, 3241-3259.

Esteves da Silva, M., Adrian, M., Schatzle, P., Lipka, J., Watanabe, T., Cho, S., Futai, K., Wierenga, C.J., Kapitein, L.C., and Hoogenraad, C.C. (2015). Positioning of AMPA Receptor-Containing Endosomes Regulates Synapse Architecture. Cell Rep. 13, 933-943.

Frias, C.P., and Wierenga, C.J. (2013). Activity-dependent adaptations in inhibitory axons. Front. Cell. Neurosci. 7, 219.

Froemke, R.C. (2015). Plasticity of cortical excitatory-inhibitory balance. Annu. Rev. Neurosci. 38, 195-219.

Froemke, R.C., Merzenich, M.M., and Schreiner, C.E. (2007). A synaptic memory trace for cortical receptive field plasticity. Nature 450, 425-429.

Fu, Y., Wu, X., Lu, J., and Huang, Z.J. (2012). Presynaptic GABA(B) Receptor Regulates Activity-Dependent Maturation and Patterning of Inhibitory Synapses through Dynamic Allocation of Synaptic Vesicles. Front. Cell. Neurosci. 6, 57.

Ganguly, A., Tang, Y., Wang, L., Ladt, K., Loi, J., Dargent, B., Leterrier, C., and Roy, S. (2015). A dynamic formin-dependent deep F-actin network in axons. J. Cell Biol. 210, 401-417.

Hensch, T.K. (2005). Critical period plasticity in local cortical circuits. Nat. Rev. Neurosci. 6, 877-888.

Heukers, R., Altintas, I., Raghoenath, S., De Zan, E., Pepermans, R., Roovers, R.C., Haselberg, R., Hennink, W.E., Schiffelers, R.M., Kok, R.J., et al. (2014). Targeting hepatocyte growth factor receptor (Met) positive tumor cells using internalizing nanobody-decorated albumin nanoparticles. Biomaterials 35, 601-610.

Honkura, N., Matsuzaki, M., Noguchi, J., Ellis-Davies, G.C., and Kasai, H. (2008). The subspine organization of actin fibers regulates the structure and plasticity of dendritic spines. Neuron 57, 719-729.

Judson, M.C., Bergman, M.Y., Campbell, D.B., Eagleson, K.L., and Levitt, P. (2009). Dynamic gene and protein expression patterns of the autism-associated met receptor tyrosine kinase in the developing mouse forebrain. J. Comp. Neurol. 513, 511-531.

Keck, T., Scheuss, V., Jacobsen, R.I., Wierenga, C.J., Eysel, U.T., Bonhoeffer, T., and Hubener, M. (2011). Loss of sensory input causes rapid structural changes of inhibitory neurons in adult mouse visual cortex. Neuron 71, 869-882.

Kuriu, T., Yanagawa, Y., and Konishi, S. (2012). Activity-dependent coordinated mobility of hippocampal inhibitory synapses visualized with presynaptic and postsynaptic tagged-molecular markers. Mol. Cell. Neurosci. 49, 184-195.

Kuzirian, M.S., Moore, A.R., Staudenmaier, E.K., Friedel, R.H., and Paradis, S. (2013). The class 4 semaphorin Sema4D promotes the rapid assembly of GABAergic synapses in rodent hippocampus. J. Neurosci. 33, 8961-8973.

Lim, C.S., and Walikonis, R.S. (2008). Hepatocyte growth factor and c-Met promote dendritic maturation during hippocampal neuron differentiation via the Akt pathway. Cell. Signal. 20, 825-835.

Lo, F.S., Erzurumlu, R.S., and Powell, E.M. (2016). Insulin-Independent GABAA Receptor-Mediated Response in the Barrel Cortex of Mice with Impaired Met Activity. Cellular signalling 36, 3691-3697.

Lopez-Bendito, G., Sturgess, K., Erdelyi, F., Szabo, G., Molnar, Z., and Paulsen, O. (2004). Preferential

origin and layer destination of GAD65-GFP cortical interneurons. Cereb. Cortex 14, 1122-1133.

Martins, G.J., Shahrokh, M., and Powell, E.M. (2011). Genetic disruption of Met signaling impairs GABAergic striatal development and cognition. Neuroscience 176, 199-209.

Müllner, F.E., Wierenga, C.J., and Bonhoeffer, T. (2015). Precision of Inhibition: Dendritic Inhibition by Individual GABAergic Synapses on Hippocampal Pyramidal Cells Is Confined in Space and Time. Neuron 87, 576-589.

Oh, W.C., Lutzu, S., Castillo, P.E., and Kwon, H.B. (2016). De novo synaptogenesis induced by GABA in the developing mouse cortex. Science 353, 1037-1040.

Oinuma, I., Ishikawa, Y., Katoh, H., and Negishi, M. (2004). The Semaphorin 4D receptor Plexin-B1 is a GTPase activating protein for R-Ras. Science 305, 862-865.

Paradis, S., Harrar, D.B., Lin, Y., Koon, A.C., Hauser, J.L., Griffith, E.C., Zhu, L., Brass, L.F., Chen, C., and Greenberg, M.E. (2007). An RNAi-based approach identifies molecules required for glutamatergic and GABAergic synapse development. Neuron 53, 217-232.

Peng, Y., Huentelman, M., Smith, C., and Qiu, S. (2013). MET receptor tyrosine kinase as an autism genetic risk factor. Int. Rev. Neurobiol. 113, 135-165.

Piccioli, Z.D., and Littleton, J.T. (2014). Retrograde BMP signaling modulates rapid activity-dependent synaptic growth via presynaptic LIM kinase regulation of cofilin. J. Neurosci. 34, 4371-4381.

Qiu, S., Lu, Z., and Levitt, P. (2014). MET receptor tyrosine kinase controls dendritic complexity, spine morphogenesis, and glutamatergic synapse maturation in the hippocampus. J. Neurosci. 34, 16166-16179.

Raissi, A.J., Staudenmaier, E.K., David, S., Hu, L., and Paradis, S. (2013). Sema4D localizes to synapses and regulates GABAergic synapse development as a membrane-bound molecule in the mammalian hippocampus. Mol. Cell. Neurosci. 57, 23-32.

Rex, C.S., Chen, L.Y., Sharma, A., Liu, J., Babayan, A.H., Gall, C.M., and Lynch, G. (2009). Different Rho GTPase-dependent signaling pathways initiate sequential steps in the consolidation of long-term potentiation. J. Cell Biol. 186, 85-97.

Sabo, S.L., Gomes, R.A., and McAllister, A.K. (2006). Formation of presynaptic terminals at predefined sites along axons. J. Neurosci. 26, 10813-10825.

Schuemann, A., Klawiter, A., Bonhoeffer, T., and Wierenga, C.J. (2013). Structural plasticity of GABAergic axons is regulated by network activity and GABAA receptor activation. Front. Neural Circuits 7, 113.

Siddiqui, T.J., and Craig, A.M. (2011). Synaptic organizing complexes. Curr. Opin. Neurobiol. 21, 132-143.

Staras, K. (2007). Share and share alike: trading of presynaptic elements between central synapses. Trends Neurosci. 30, 292-298.

Suarez, C., Carroll, R.T., Burke, T.A., Christensen, J.R., Bestul, A.J., Sees, J.A., James, M.L., Sirotkin, V., and Kovar, D.R. (2015). Profilin regulates F-actin network homeostasis by favoring formin over Arp2/3 complex. Dev. Cell 32, 43-53.

Sun, T., Krishnan, R., and Swiercz, J.M. (2012). Grb2 mediates semaphorin-4D-dependent RhoA inactivation. J. Cell Sci. 125, 3557-3567.

Sun, Y., and Bamji, S.X. (2011). beta-Pix modulates actin-mediated recruitment of synaptic vesicles to synapses. J. Neurosci. 31, 17123-17133.

Swiercz, J.M., Kuner, R., Behrens, J., and Offermanns, S. (2002). Plexin-B1 directly interacts with PDZ-RhoGEF/LARG to regulate RhoA and growth cone morphology. Neuron 35, 51-63.

Swiercz, J.M., Worzfeld, T., and Offermanns, S. (2008). ErbB-2 and met reciprocally regulate cellular signaling via plexin-B1. J. Biol. Chem. 283, 1893-1901.

Tasaka, G., Negishi, M., and Oinuma, I. (2012). Semaphorin 4D/Plexin-B1-mediated M-Ras GAP activity regulates actin-based dendrite remodeling through Lamellipodin. J. Neurosci. 32, 8293-8305.

Tyndall, S.J., and Walikonis, R.S. (2006). The receptor tyrosine kinase Met and its ligand hepatocyte growth factor are clustered at excitatory synapses and can enhance clustering of synaptic proteins. Cell Cycle 5, 1560-1568.

Villa, K.L., Berry, K.P., Subramanian, J., Cha, J.W., Chan Oh, W., Kwon, H.B., Kubota, Y., So, P.T., and Nedivi, E. (2016). Inhibitory Synapses Are Repeatedly Assembled and Removed at Persistent Sites In Vivo. Neuron 90, 662-664.

Vodrazka, P., Korostylev, A., Hirschberg, A., Swiercz, J.M., Worzfeld, T., Deng, S., Fazzari, P., Tamagnone, L., Offermanns, S., and Kuner, R. (2009). The semaphorin

4D-plexin-B signalling complex regulates dendritic and axonal complexity in developing neurons via diverse pathways. Eur. J. Neurosci. 30, 1193-1208.

Wierenga, C.J. (2016). Live imaging of inhibitory axons: Synapse formation as a dynamic trial-and-error process. Brain Res. Bull.

Wierenga, C.J., Becker, N., and Bonhoeffer, T. (2008). GABAergic synapses are formed without the involvement of dendritic protrusions. Nat. Neurosci. 11, 1044-1052.

Wierenga, C.J., Müllner, F.E., Rinke, I., Keck, T., Stein, V., and Bonhoeffer, T. (2010). Molecular and electrophysiological characterization of GFP-expressing CA1 interneurons in GAD65-GFP mice. PloS one 5, e15915.

Wu, Y.E., Huo, L., Maeder, C.I., Feng, W., and Shen, K. (2013). The balance between capture and dissociation of presynaptic proteins controls the spatial distribution of synapses. Neuron 78, 994-1011.

Xie, Z., Eagleson, K.L., Wu, H.H., and Levitt, P. (2016). Hepatocyte Growth Factor Modulates MET Receptor Tyrosine Kinase and beta-Catenin Functional Interactions to Enhance Synapse Formation. eNeuro 3.

SUPPLEMENTARY INFORMATION

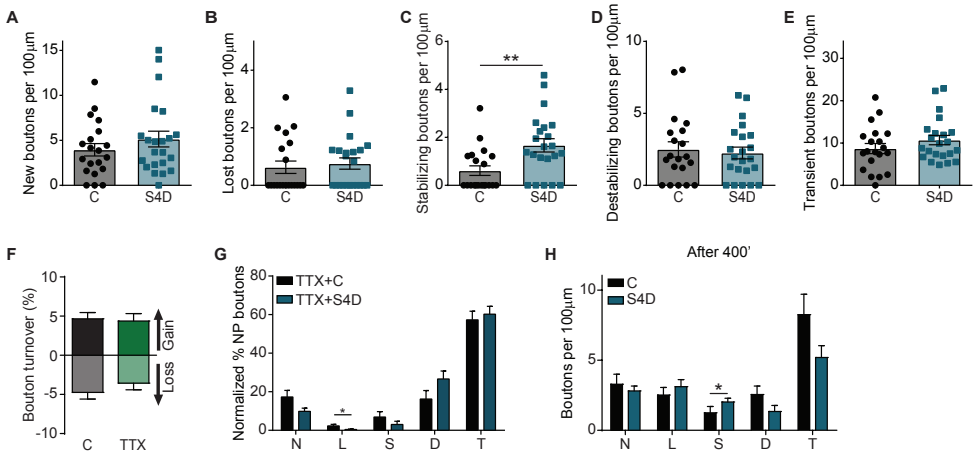

Figure S1. Effect of Sema4D treatment on inhibitory bouton dynamics. Related to Figure 2 and 3.
(A) Density of new boutons in axons treated with 1 nM Fc (C) and 1 nM Sema4D-Fc (S4D). $p = 0.41$ (MW).
(B-E) Same as in A, but for lost (B; $p = 0.61$), stabilizing (C), destabilizing (D; $p = 0.84$) and transient (E; $p = 0.34$). ** $p < 0.01$ (MW).
(F) Mean instantaneous bouton turnover (average of last 5 time points) in control (C) and TTX-treated slices. The instantaneous bouton gain (or loss) was defined as the fraction of boutons that were gained (or lost) between two consecutive time points (Schuemann et al., 2013).
(G) Average fraction of the five subgroups of non-persistent (NP) boutons (N – new; L – lost; S – stabilizing; D – destabilizing; T – transient) in C and S4D-treated axons in the presence of 0.5 µM TTX: N – new ($p = 0.08$); L – lost; S – stabilizing ($p = 0.23$); D – destabilizing ($p = 0.07$); T – transient ($p = 0.65$). * $p < 0.05$ (MW per subgroup).
(H) Density of non-persistent boutons (N – new; L – lost; S – stabilizing; D – destabilizing; T – transient) after treatment with 1 nM Fc (control; C) or 1 nM Sema4D-Fc (S4D) for 6 hours (400 minutes of total treatment). * $p < 0.05$ (MW per subgroup).
Data are represented as mean ± SEM. In A-E, data from 20 control axons (N=6) and 22 S4D-treated axons (N=5), in F from 17 control axons (N=4) and 17 TTX-treated axons (N=5), in G from 19 control axons (N=5) and 20 S4D-treated axons (N=5), and in H from 15 control axons (N=4) and 17 S4D-treated axons (N=4).

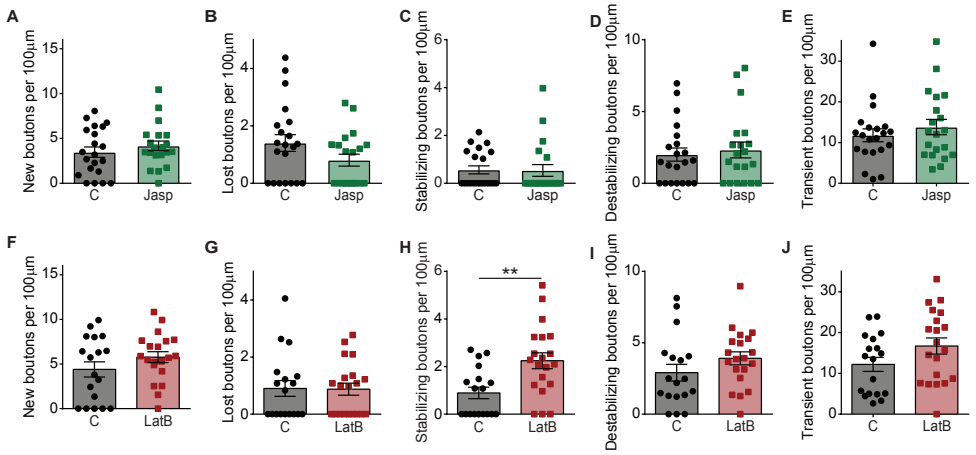

Figure S2. Effect of actin regulating drugs on inhibitory bouton dynamics. Related to Figure 4.
(A) Density of new boutons in control (C) and Jasplakinolide (Jasp; 200 nM)-treated slices. $p = 0.45$ (MW).
(B-E) Same as in A, but for lost (B; $p = 0.14$), stabilizing (C; $p = 0.55$), destabilizing (D; $p = 0.68$) and transient (E; $p = 0.58$).
(F-J) Same as in A-E, but for control (C) and LatrunculinB (LatB; 100 nM)-treated slices. For F, G, I and J, $p = 0.33$, 0.85, 0.11 and 0.08, respectively. ** $p < 0.01$ (MW).
Data are represented as mean ± SEM. Data from 21 control axons (N=6) and 20 Jasp-treated axons (N=5) in A-E, and from 18 control axons (N=5) and 20 LatB-treated axons (N=5) in F-J.

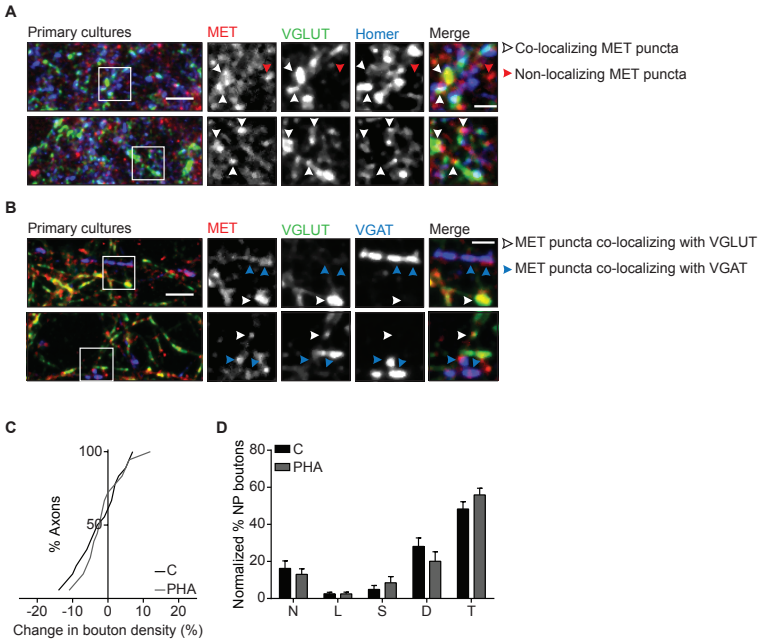

Figure S3. Enrichment of MET at synapses, and effects of MET inhibition on inhibitory bouton dynamics. Related to Figure 5.

(A) Images of primary cultures of hippocampal neurons immunostained for MET (red) and markers for excitatory synapses: presynaptic vesicular glutamate transporter (VGLUT; green) and postsynaptic Homer (blue). White arrows highlight MET puncta co-localizing with one or both markers. Red arrows indicate MET puncta that do not localize. Images are maximum intensity projections of 13 stacks. Scale bar 5 µm (overview) and 2 µm (zoom).

(B) Same as A, but neurons were stained with MET nanobody (red) and markers for excitatory presynapses (presynaptic VGLUT; green) and inhibitory presynapses (presynaptic vesicular GABA transporter VGAT; blue). White arrows indicate MET co-localizing with VGLUT and blue arrows indicate MET co-localizing with VGAT. Images are maximum intensity projections of 12 stacks. Scale bar 5 µm (overview) and 2 µm (zoom).

(C) Cumulative distribution of the change in mean bouton density during the wash-in period compared to baseline after wash-in of control (C) or 1 µM of PHA-665752 (PHA). ***p*** = 0.78 (MW).

(D) Average fraction of subgroups of non-persistent boutons in C and PHA-treated axons: N – new (p = 0.44); L – lost (p = 0.88); S – stabilizing (p = 0.51); D – destabilizing (p = 0.16); T – transient (p = 0.21).

Data are represented as mean ± SEM. In C-D, data from 18 control axons (N=4) and 18 PHA-treated axons (N=4).

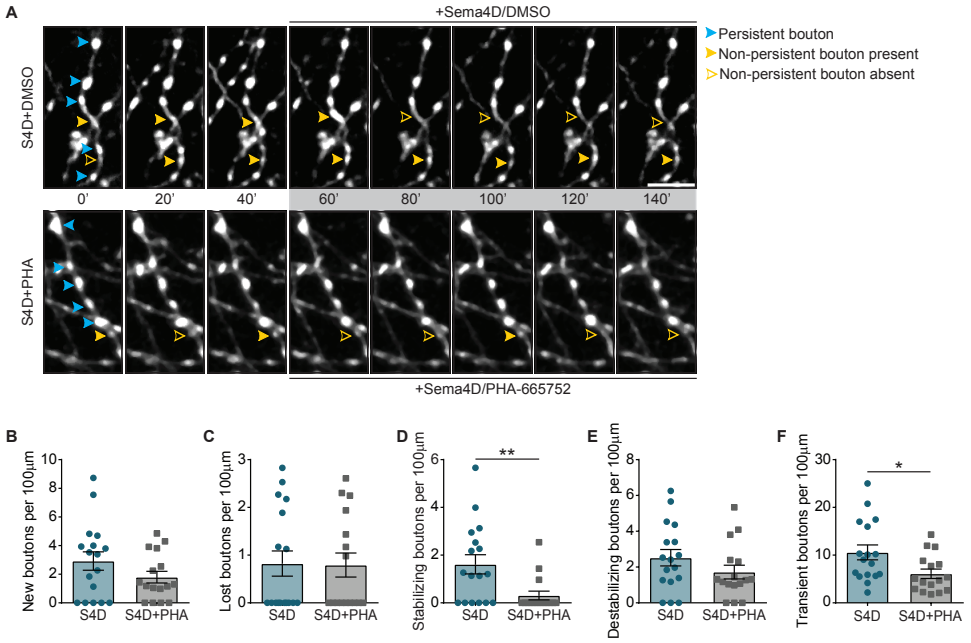

Figure S4. MET inhibition on Sema4D effect on inhibitory bouton dynamics. Related to Figure 5.
(A) Time-lapse two-photon images of GAD65-GFP-labeled axons in organotypic hippocampal slices during wash-in (grey box) of combination of 1 nM Sema4D and DMSO (S4D; upper panel) or combination of 1 nM Sema4D with 1 µM PHA-665752 (S4D+PHA; bottom panel). Images are maximum intensity projections of 15-16 z stacks. The images show persistent (blue arrowheads), and non-persistent boutons (yellow arrowheads). Filled arrowheads indicate that the bouton is present, and empty arrowheads indicate that the bouton is absent at that time point. Scale bar 5 µm.
(B) Density of new boutons in S4D and S4D+PHA-treated axons. $p = 0.34$ (MW).
(C-F) Same as B, but for lost (C; $p = 1$), stabilizing (D) destabilizing (E; $p = 0.14$) and transient (F) boutons. * $p < 0.05$, ** $p < 0.01$ (MW).
Data are represented as mean ± SEM. Data from 17 S4D-treated axons (N=4) and 16 S4D+PHA-treated axons (N=4) in B-F.

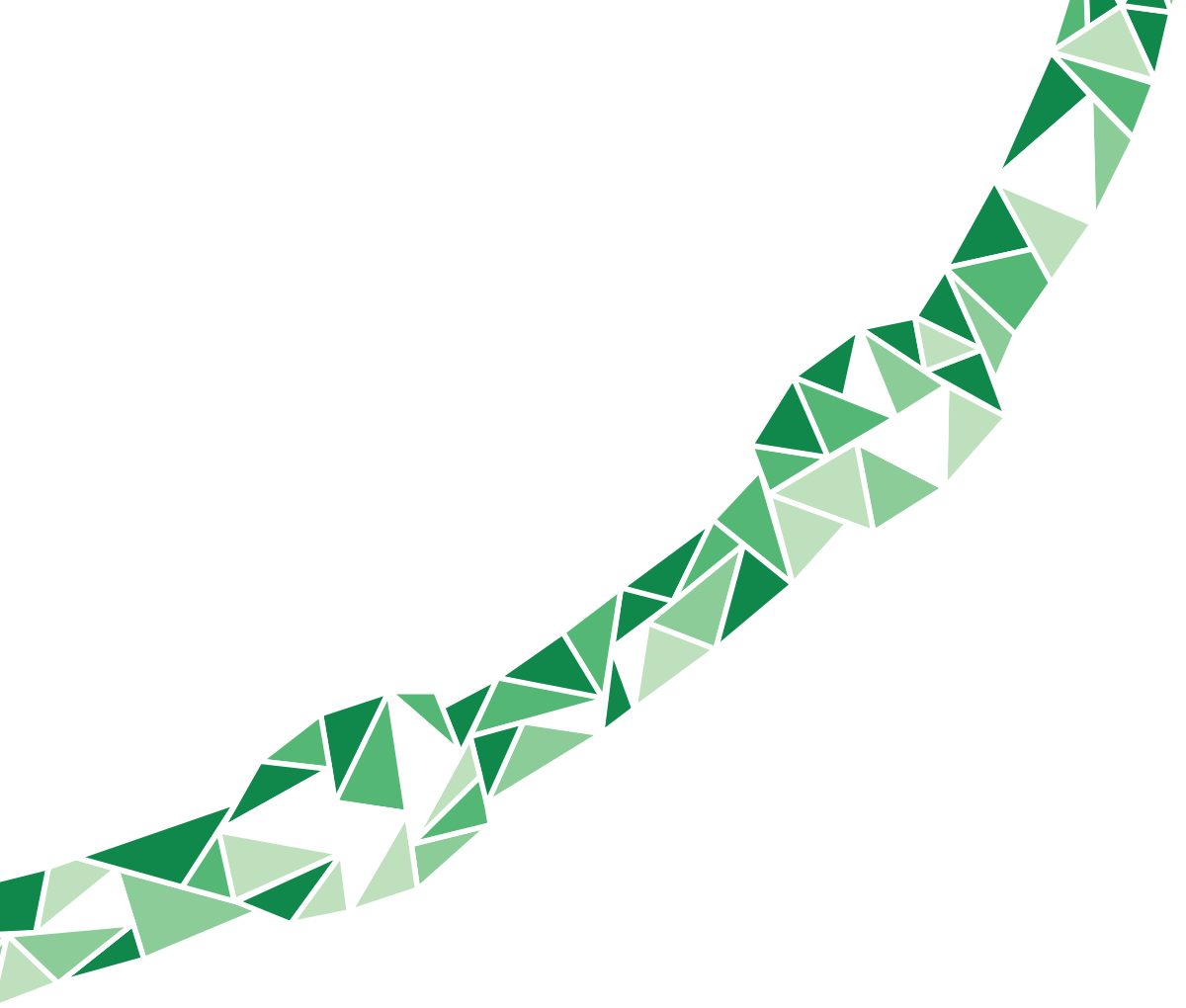

Cell Biology, Department Biology, Faculty of Science, Utrecht University, Utrecht, the Netherlands

Chapter 7

General Discussion

Cátia P. Frias

Understanding how neurons wire the brain and form functional connections has captured the attention of many neuroscientists around the world. The axon, the neuronal process specialized in transmitting electrochemical signals to other cells, extends considerably from the soma to reach its synaptic partners. The axon develops unique structural features important for its function, such as the presynaptic boutons where synaptic transmission occurs. In this thesis, we provided new insights into the development and growth of the axon (*chapters 3* and *4*), as well as into the dynamics of axonal presynaptic boutons (*chapters 2* and *6*). Moreover, we studied the interplay between motor proteins in synaptic maintenance and structure (*chapter 5*). Altogether, these results contribute to our knowledge on the mechanisms involved in axonal outgrowth and function, which may help us eventually to understand the etiology of neurodevelopmental disorders, such as autism. In this chapter, I further discuss some of the results of the thesis, put them into a broader context, and provide some future research questions and perspectives.

MOTOR PROTEINS KEEP SYNAPSES IN SHAPE

In neurons, the vast majority of proteins are synthesized in the cell body, and newly formed proteins have to be transported into the axon and dendrites. To assure that they reach the proper destination, proteins are carried in specific membranous organelles and protein complexes, and the transport is performed by motor proteins. The motor proteins fall into three superfamilies: kinesin (KIFs), dynein and myosin. Kinesins and dynein move in opposite directions along microtubules, while myosins bind to actin filaments. Besides driving the transport of cargo, motors can also control the dynamics of the underlying cytoskeleton. Several neurodevelopmental and neurological disorders have been linked to mutations in motor protein genes, highlighting the importance of motor-dependent processes in brain function (Franker and Hoogenraad, 2013; Hirokawa et al., 2010; Kneussel and Wagner, 2013). Therefore, it is essential to investigate the involvement of motor proteins in the development of neurons. In this thesis, we have identified motor proteins that may play a role in axon outgrowth and synaptic maintenance (*chapters 3* to *5*), by performing a targeted knockdown screen of motor proteins in cultured hippocampal neurons. From the data shown in these chapters, I further discuss three interesting findings. Firstly, I discuss a previously unrecognized role for KIF13A in dendritic development, followed by a potential role of postsynaptic KIF1A in excitatory synaptic maintenance, a kinesin mainly known for its role in presynaptic function. I finish this part by discussing a possible link between dynactin-6 (DCTN6) and MyosinIIb (MyoIIb), and how this interaction could be important in synapses.

KIF13A: an important dendritic motor?

KIF13A is a kinesin-3 family protein with roles in cytokinesis and in the transport of mannose-6-phosphate receptor, involved in the turnover of external soluble ligands, to the plasma membrane (Nakagawa et al., 2000; Sagona et al., 2010). In neurons, KIF13A is also required for the transport of the serotonin receptors to the plasma membrane (Zhou et al., 2013). In this thesis, we found that depletion of KIF13A led to significant reduction of dendritic processes (*chapter 4*) and the density of excitatory synapses (*chapter 5*). Our data suggest a previously undescribed role for KIF13A in the general development and maturation of dendritic, but not axonal, processes. Recently, KIF13A was shown to selectively drive the transport of cargo in the axon (Lipka et al., 2016) by using a truncated kinesin that lacks

the tail domain, which may have hindered KIF13A-based transport of dendritically-targeted cargo. In fact, the tail of KIF13A can interact with vesicles containing transferrin-receptor (Jenkins et al., 2012), suggesting that KIF13A may be capable of driving transport of cargo in dendrites. Therefore, expressing the full-length construct of KIF13A and evaluate where it is localized in hippocampal neurons may help us to understand the role of KIF13A in dendritic development and synaptic maintenance.

Several reports have established a link between KIF13A and the endosomal compartment. In fact, KIF13A has been shown to associate with recycling endosomes and control their positioning and morphogenesis (Delevoye et al., 2009; Delevoye et al., 2014). Intracellular α-amino-3-hydroxy-5-methyl-4-isoxazolepropionic acid receptors (AMPARs) are transported in recycling endosomes, and their removal from spines affects the excitatory postsynaptic architecture (Esteves da Silva et al., 2015). Therefore, one can speculate that depletion of KIF13A may affect the transport of AMPARs towards the postsynaptic density. It would be important to investigate if KIF13A mediates the transport of Rab11 in dendrites and spines, and if its depletion leads to changes on the postsynaptic structure. The fact that human KIF13A gene has been associated with schizophrenia (Jamain et al., 2001), a mental disorder associated with changes in synapses (Faludi and Mirnics, 2011), makes this protein an interesting target of future studies.

KIF1A: more than a presynaptic vesicle motor

Synapse formation and function relies on kinesin motors, and one of the kinesins involved in synapse formation is kinesin-3 protein KIF1A. Besides mediating the axonal transport of Rab3-positive synaptic vesicle precursors (Niwa et al., 2008; Wagner et al., 2009; Zhang et al., 2017), the presynaptic expression of KIF1A facilitates synapse formation in an experience-dependent manner (Kondo et al., 2012). In *chapter 5*, we found that postsynaptic KIF1A depletion reduces the density of excitatory synapses, suggesting for a dendritic role of this protein. Supporting this, KIF1A has been shown to mediate the transport of dendritic dense core vesicles and vesicles containing glutamate receptors (Lipka et al., 2016; Shin et al., 2003). Hence, the effects we observed upon depletion of KIF1A may be related to a defect in the targeting of proteins to the postsynaptic density. It would be interesting to investigate which cargo of KIF1A is required for the maintenance of excitatory synapses. Moreover, as KIF1A has been linked with synaptic plasticity (Kondo et al., 2012), it may be valuable to address if KIF1A transport is regulated in an activity-dependent manner. This could be addressed by following the vesicle movements of KIF1A into spines after chemical long-term potentiation in dissociated cultures, or by local uncaging of glutamate.

The regulation of kinesin motor activity is important to assure their proper functioning and localization. Several mechanisms control the motor activity of kinesin proteins, including autoinhibition (Verhey and Hammond, 2009). Recently, a new molecular mechanism has been described that involves kinesin binding protein (KBP). KBP was shown to bind to the motor domain of a subset of kinesins, inhibiting their microtubule binding activity (Kevenaar et al., 2016). From the KBP-regulated kinesins, only KIF1A and KIF15 may be important for the density of excitatory synapses in hippocampal neurons (*chapter 5*). It is possible to speculate that KBP activity may be important for the regulation of KIF1A and KIF15 transport in dendrites, similar to the regulation of KIF1A-mediated synaptic vesicle transport in the axon (Kevenaar et al., 2016). Loss of function and overexpression of KBP may help us to understand if regulation of KIF1A and KIF15 by KBP plays a role in synapse development and

maintenance in hippocampal neurons.

DCTN6: interaction with myosin?

It is remarkable that only one dynein motor is responsible for the minus-end directed cargo transport along microtubules, especially when compared to the myriad of kinesin motor proteins that perform different tasks. The cytoplasmic dynein motor is part of a massive complex that contains additional dynein subunits, which are important for several processes, including binding of dynein to cargo or determination of dynein processivity (Kikkawa, 2013; van den Berg and Hoogenraad, 2012). Dynein-related processes are highly dependent on dynactin, a multiprotein complex that is found from yeast to mammals (Schroer, 2004). The dynactin complex is composed of eleven different protein subunits, and some of these proteins are present in more than one copy per complex (Schroer, 2004). One of the dynactin proteins is called DCTN6, which has been shown to mediate the binding of the dynactin/dynein complex to both early and recycling endosomes (Yeh et al., 2012). When we depleted DCTN6 in mature hippocampal neurons, we found that the density of both excitatory and inhibitory synapses was reduced (*chapter 5*). It is plausible that the effects we observed may be due to a dynactin-independent function of DCTN6. Therefore, we also performed pull-down experiments combined with mass spectrometry analysis to identify possible links with synapses, and we found neurobeachin as one of our possible interactors. Drosophila mutants of neurobeachin exhibit abnormal synaptic architecture and transmission (Wise et al., 2015), suggesting for a role of neurobeachin in synapse function. Interestingly, neurobeachin has been shown to be involved in the targeting of inhibitory GABAA receptors to synapses (Farzana et al., 2016), and it can interact with excitatory postsynapse protein synapse-associated protein 102 (SAP102/Dlg3) (Lauks et al., 2012). The possible interaction of DCTN6 with neurobeachin may promote the proper trafficking and/or targeting of receptors to both excitatory and inhibitory postsynapse, or may be important for signaling pathways triggered by neurobeachin. It will be interesting to address if neurobeachin interacts with DCTN6 by performing pull-down experiments, and to map the interaction regions between the two proteins. Once this is achieved, it would be possible to use mutant neurobeachin that can no longer interact with DCTN6 or vice-versa, and determine if the trafficking and/or targeting of receptors towards postsynapses is dependent on the interaction between the two proteins.

Another possibility is that DCTN6 may be important for the maintenance of synaptic structure by regulating cytoskeleton dynamics. In *chapter 3*, by performing pull-down experiments followed by mass spectrometry analysis, we found that non-muscle myosin MyoIIb may interact with DCTN6. MyoIIb can translocate, crosslink and maintain tension on actin filaments (Vicente-Manzanares et al., 2009). MyoIIb-induced actin remodeling is involved in dendritic spine maturation, and determines the morphology, size and localization of postsynaptic density within the dendritic spine (Hodges et al., 2011; Ryu et al., 2006). MyoIIb motor activity also induces forces on actin filaments that promote actin polymerization, which is needed for the stabilization of synaptic plasticity (Rex et al., 2010). Therefore, I hypothesize that a potential interaction of MyoIIb and DCTN6 may be important for the maintenance of postsynaptic structures in both excitatory and inhibitory synapses under control or synaptic activation conditions. It will be interesting to address if MyoIIb indeed can interact with DCTN6 by performing pull-down experiments, and if they co-localize in excitatory and inhibitory postsynapses by performing overexpression and

immunocytochemistry experiments. Moreover, it would be interesting to address if DCTN6 may be required for the actin remodeling induced by synaptic activity.

ACTIN IS REQUIRED FOR PRESYNAPTIC BOUTON DYNAMICS

Actin filaments are present in all living organisms, and they are central for many cellular processes, from cell movement to intracellular trafficking (Pollard and Cooper, 2009). In neurons, actin is important for several neurodevelopmental processes, ranging from axon initiation and outgrowth to synapse formation and plasticity. Actin at axonal growth cones and at dendritic spines has intrigued of many neuroscientists throughout the years, while actin along the axonal shaft has remained less studied. However, recent live-imaging and super-resolution studies have uncovered a highly intricate architecture and dynamic behavior of axonal actin, leading to new models for the role of actin in axons (Roy, 2016).

Actin is highly enriched at presynaptic boutons (Wilhelm et al., 2014), and it is continuously assembled and disassembled under baseline conditions (Bleckert et al., 2012; Bourne et al., 2006; Colicos et al., 2001). During increased activity levels, actin can be recruited from the axonal shaft to presynaptic boutons (Colicos et al., 2001; Sankaranarayanan et al., 2003), suggesting that actin plays a role in activity-dependent circuit adaptation. However, studies addressing the role of actin remodeling on presynaptic bouton dynamics is sparse. In *chapter 6*, we showed that actin is involved in tuning inhibitory presynaptic bouton dynamics. More precisely, actin remodeling induced by nanomolar concentrations of LatrunculinB (LatB), an actin monomer sequestering drug, promoted the stabilization of inhibitory boutons without affecting bouton disassembly. In this way, our data suggested that actin remodeling is one of the first events during inhibitory synapse formation, in agreement with two recent findings in Drosophila (Piccioli and Littleton, 2014) and in C. elegans (Chia et al., 2014). Even though we show that both Sema4D and actin remodeling promote the stabilization of presynaptic boutons, we do not know which actin-interacting proteins or structures are involved in this process. I further discuss three possible, and not necessarily opposing, models involving (i) actin trails along the axon, (ii) transport and capture of synaptic vesicles, and (iii) actin structures at presynaptic boutons.

Actin trails along the axon

In *chapter 6*, we found that treatment with nanomolar doses of LatB promote the stabilization of inhibitory presynaptic boutons. The low doses of LatB used in our study presumably do not lead to the complete disassembly of actin structures (Bleckert et al., 2012; Ganguly et al., 2015; Honkura et al., 2008). However, we hypothesized that LatB treatment may affect axonal actin architectures, such as formin-dependent actin trails (Ganguly et al., 2015) or Arp2/3-dependent presynaptic clusters (Chia et al., 2014). Actin trails are dynamic actin filaments suggested to be a source of actin for presynaptic boutons or other axonal actin structures, such as actin rings (Ganguly et al., 2015). On the other hand, Arp2/3 complex has been shown to promote the formation of an actin patch at developing synapses, which is required for synapse assembly in C. elegans (Chia et al., 2014). Formin and Arp2/3 proteins have been shown to compete for the availability of actin monomers in fission yeast, maintaining the overall homeostasis of the actin cytoskeleton (Burke et al., 2014; Suarez et al., 2015). By limiting the availability of actin monomers, treatment with LatB may indirectly change the balance between formin- and Arp2/3-induced actin polymerization,

and thus regulate the subcellular actin cytoskeleton organization. In yeast, lowering the actin content in the cell prompts formin-induced actin polymerization, whereas increasing actin levels facilitates Arp2/3-induced actin polymerization (Burke et al., 2014). We speculate that LatB treatment may promote formins to induce the elongation of actin trails (Ganguly et al., 2015), which may contribute to the transport of actin into immature boutons. In this way, immature boutons may acquire a proper actin network for synaptic vesicle capture, further promoting their maturation to functional presynapses. Future studies will be required to unravel which axonal actin structures are involved in LatB-induced bouton stabilization. For example, inhibiting formin-dependent polymerization with small molecule SMIFH2 (Rizvi et al., 2009) may help us to understand if formins are required for the Sema4D-induced bouton stabilization.

Transport and capture of synaptic vesicles

At mature synaptic terminals, actin is thought to act as a barrier for the dispersion of regulatory proteins (Sankaranarayanan et al., 2003). Consequently, it is plausible to hypothesize that LatB treatment may contribute to weaken actin structures at mature terminals, promoting the exchange of synaptic vesicles between neighboring boutons. Future studies involving the use of FM dyes and fluorescence recovery after photobleaching, such as the ones performed by Darcy and colleagues (Darcy et al., 2006), may help us to address if local LatB treatment triggers the exchange of synaptic vesicles between boutons.

In cortical neurons, treatment with micromolar doses of LatB was shown to increase the pausing probability and the pausing duration of synaptic vesicles (Sabo et al., 2006). One may assume that increased pausing of synaptic vesicles may increase the likelihood of synaptic vesicle capture at immature inhibitory boutons. It will be important to address if these immature boutons acquire presynaptic proteins required for synaptic function, such as synapsin. In Drosophila, synapsin is one of the first proteins to arrive at immature boutons (Vasin et al., 2014). Therefore, it would be interesting to follow synapsin movement and accumulation into stabilized presynaptic boutons, as this would further sustain our claim that these boutons become functional presynapses within tens of minutes. We also showed in *chapter 6* that acquisition of presynaptic vesicles precedes the maturation of inhibitory postsynaptic sites following Sema4D treatment. As we suggest that both Sema4D and actin dynamics are cooperatively promoting the stabilization of inhibitory presynaptic boutons, future studies should address if LatB treatment also induces increases in the area of presynaptic clusters prior to the establishment of postsynaptic sites, similarly to Sema4D.

Actin structures at presynaptic boutons

Non-muscle myosin II proteins (MyoII) have been implied in the regulation of neurotransmitter release at excitatory presynaptic nerve terminals in different systems (Mochida et al., 1994; Peng et al., 2012; Seabrooke and Stewart, 2011). In inhibitory presynaptic boutons, the role of MyoII proteins has not been addressed so far. In *chapter 3*, we have focused on the role of one of the MyoII proteins, MyoIIb, in axon formation and we performed mass spectrometry experiments to identify possible MyoIIb interactors. These interactors may be important for MyoIIb function in hippocampal neurons, including the role in presynaptic boutons. One of the highest hits in our mass spectrometry analysis was MyoXVIIIa. MyoXVIIIa can form mixed bipolar filaments with MyoII proteins, and two roles for the mixed filaments have been proposed: (i) MyoXVIIIa may contribute to the attachment of MyoII/MyoXVIIIa filaments

to anchored structures, or (ii) the PDZ domains of MyoXVIIIa may contribute to the recruitment of specific proteins to the MyoII/MyoXVIIIa filaments (Billington et al., 2015). As several proteins at the active zone contain PDZ domains (Ackermann et al., 2015; Petzoldt et al., 2016; Sudhof, 2012), it is interesting to speculate that MyoII/MyoXVIIIa filaments may favor the localization of synaptic proteins to synapses. It will be important to address if MyoII and MyoXVIIIa are required for the stabilization of inhibitory boutons upon LatB treatment. This could be achieved by performing loss of function experiments using viral expression of knockdown constructs in inhibitory neurons, followed by treatment with LatB. MyoXVIIIa can also interact with β-pix (Hsu et al., 2010)), a Rac/Cdc42 guanine nucleotide exchange factor (GEF) involved in the regulation of actin dynamics. β-pix stimulates the polymerization of actin at presynaptic terminals, which was shown to be important for synaptic vesicle localization at presynaptic boutons of hippocampal neurons (Sun and Bamji, 2011). We showed that stabilized inhibitory boutons acquire synaptic vesicles in tens of minutes, suggesting that actin polymerization may take place at these locations. LatB treatment may induce changes on the actin cytoskeleton that may promote the activation of β-pix and its interaction with MyoXVIIIa. Addressing if these events are necessary for inhibitory bouton stabilization may be interesting in future studies.

CONCLUDING REMARKS

Our brain is an astonishingly complex organ composed of billions of neuronal cells. The complexity of the tasks executed by the brain depends on the intricate networks established between neurons. Neuronal networks are not static, and can undergo molecular and structural rearrangements that are critically involved in learning and memory formation. Uncovering how the cytoskeleton contributes to neurodevelopmental and plasticity processes has been a central question in Neuroscience. The results described in this thesis provide new mechanisms in the outgrowth of the axon and on the dynamics of synapses, opening new lines of research for the future. It is plausible to think that regulatory pathways activated early in development may be reused later in life, when plasticity-related processes occur. As discussed in this chapter, the different results described in this thesis are closely related to each other, and may improve our understanding on supposedly distinguished phenomena, such as axon outgrowth and presynaptic bouton dynamics. We live in exciting times with the development of novel tools and microscopy techniques that allow us to study the cytoskeleton in more detail and in more physiological situations. In fact, recent years have been successful in the observation of different actin structures in neuronal processes, but the large majority of these studies were performed in dissociated hippocampal neurons. Performing super-resolution or live-imaging studies in organotypic hippocampal cultures may provide insights on the role of such structures in a more physiological context. The ultimate goal would be to perform such studies in intact brain tissue, during experience-dependent circuit adaptation.

By studying the physiological phenomena underlying brain function and plasticity, we may become closer to understanding the pathophysiology of neurodevelopmental and neurological disorders. Many of these disorders have been associated with mutations in hundreds of genes that lead to defects in synapse development and function (Chen et al., 2014; Grant, 2012). One of such genes encodes the tyrosine-kinase receptor MET, and mutations in its promoter region have been associated with autism-spectrum disorder. Our

discovery of the involvement of MET in inhibitory bouton stabilization implies that defects on inhibitory connections may also underlie the etiology of autism spectrum disorders. Hence, the study of inhibitory plasticity in autism mouse models may help us to unravel to what extent local activity-dependent changes are required for the proper functioning of the brain.

REFERENCES

Ackermann, F., Waites, C.L., and Garner, C.C. (2015). Presynaptic active zones in invertebrates and vertebrates. EMBO Rep. 16, 923-938.

Billington, N., Beach, J.R., Heissler, S.M., Remmert, K., Guzik-Lendrum, S., Nagy, A., Takagi, Y., Shao, L., Li, D., Yang, Y., et al. (2015). Myosin 18A coassembles with nonmuscle myosin 2 to form mixed bipolar filaments. Curr. Biol. 25, 942-948.

Bleckert, A., Photowala, H., and Alford, S. (2012). Dual pools of actin at presynaptic terminals. J. Neurophysiol. 107, 3479-3492.

Bourne, J., Morgan, J.R., and Pieribone, V.A. (2006). Actin polymerization regulates clathrin coat maturation during early stages of synaptic vesicle recycling at lamprey synapses. J. Comp. Neurol. 497, 600-609.

Burke, T.A., Christensen, J.R., Barone, E., Suarez, C., Sirotkin, V., and Kovar, D.R. (2014). Homeostatic actin cytoskeleton networks are regulated by assembly factor competition for monomers. Curr. Biol. 24, 579-585.

Chen, J., Yu, S., Fu, Y., and Li, X. (2014). Synaptic proteins and receptors defects in autism spectrum disorders. Front. Cell. Neurosci. 8, 276.

Chia, P.H., Chen, B., Li, P., Rosen, M.K., and Shen, K. (2014). Local F-actin network links synapse formation and axon branching. Cell 156, 208-220.

Colicos, M.A., Collins, B.E., Sailor, M.J., and Goda, Y. (2001). Remodeling of synaptic actin induced by photoconductive stimulation. Cell 107, 605-616.

Darcy, K.J., Staras, K., Collinson, L.M., and Goda, Y. (2006). Constitutive sharing of recycling synaptic vesicles between presynaptic boutons. Nat. Neurosci. 9, 315-321.

Delevoye, C., Hurbain, I., Tenza, D., Sibarita, J.B., Uzan-Gafsou, S., Ohno, H., Geerts, W.J., Verkleij, A.J., Salamero, J., Marks, M.S., et al. (2009). AP-1 and KIF13A coordinate endosomal sorting and positioning during melanosome biogenesis. J. Cell Biol. 187, 247-264.

Delevoye, C., Miserey-Lenkei, S., Montagnac, G., Gilles-Marsens, F., Paul-Gilloteaux, P., Giordano, F., Waharte, F., Marks, M.S., Goud, B., and Raposo, G. (2014). Recycling endosome tubule morphogenesis from sorting endosomes requires the kinesin motor KIF13A. Cell Rep. 6, 445-454.

Esteves da Silva, M., Adrian, M., Schatzle, P., Lipka, J., Watanabe, T., Cho, S., Futai, K., Wierenga, C.J., Kapitein, L.C., and Hoogenraad, C.C. (2015). Positioning of AMPA Receptor-Containing Endosomes Regulates Synapse Architecture. Cell Rep. 13, 933-943.

Faludi, G., and Mirnics, K. (2011). Synaptic changes in the brain of subjects with schizophrenia. Int. J. Dev. Neurosci. 29, 305-309.

Farzana, F., Zalm, R., Chen, N., Li, K.W., Grant, S.G., Smit, A.B., Toonen, R.F., and Verhage, M. (2016). Neurobeachin Regulates Glutamate- and GABA-Receptor Targeting to Synapses via Distinct Pathways. Mol. Neurobiol. 53, 2112-2123.

Franker, M.A., and Hoogenraad, C.C. (2013). Microtubule-based transport - basic mechanisms, traffic rules and role in neurological pathogenesis. J. Cell Sci. 126, 2319-2329.

Ganguly, A., Tang, Y., Wang, L., Ladt, K., Loi, J., Dargent, B., Leterrier, C., and Roy, S. (2015). A dynamic formin-dependent deep F-actin network in axons. J. Cell Biol. 210, 401-417.

Grant, S.G. (2012). Synaptopathies: diseases of the synaptome. Curr. Opin. Neurobiol. 22, 522-529.

Hirokawa, N., Niwa, S., and Tanaka, Y. (2010). Molecular motors in neurons: transport mechanisms and roles in brain function, development, and disease. Neuron 68, 610-638.

Hodges, J.L., Newell-Litwa, K., Asmussen, H., Vicente-Manzanares, M., and Horwitz, A.R. (2011). Myosin IIb activity and phosphorylation status determines dendritic spine and post-synaptic density morphology. PloS one 6, e24149.

Honkura, N., Matsuzaki, M., Noguchi, J., Ellis-Davies, G.C., and Kasai, H. (2008). The subspine organization of actin fibers regulates the structure and plasticity of dendritic spines. Neuron 57, 719-729.

Hsu, R.M., Tsai, M.H., Hsieh, Y.J., Lyu, P.C., and Yu, J.S. (2010). Identification of MYO18A as a novel interacting partner of the PAK2/betaPIX/GIT1 complex and its potential function in modulating epithelial cell migration. Mo. Biol. Cell 21, 287-301.

Jamain, S., Quach, H., Fellous, M., and Bourgeron, T. (2001). Identification of the human KIF13A gene

homologous to Drosophila kinesin-73 and candidate for schizophrenia. Genomics 74, 36-44.

Jenkins, B., Decker, H., Bentley, M., Luisi, J., and Banker, G. (2012). A novel split kinesin assay identifies motor proteins that interact with distinct vesicle populations. J. Cell Biol. 198, 749-761.

Kevenaar, J.T., Bianchi, S., van Spronsen, M., Olieric, N., Lipka, J., Frias, C.P., Mikhaylova, M., Harterink, M., Keijzer, N., Wulf, P.S., et al. (2016). Kinesin-Binding Protein Controls Microtubule Dynamics and Cargo Trafficking by Regulating Kinesin Motor Activity. Curr. Biol. 26, 849-861.

Kikkawa, M. (2013). Big steps toward understanding dynein. J. Cell Biol. 202, 15-23.

Kneussel, M., and Wagner, W. (2013). Myosin motors at neuronal synapses: drivers of membrane transport and actin dynamics. Nat. Rev. Neurosci. 14, 233-247.

Kondo, M., Takei, Y., and Hirokawa, N. (2012). Motor protein KIF1A is essential for hippocampal synaptogenesis and learning enhancement in an enriched environment. Neuron 73, 743-757.

Lauks, J., Klemmer, P., Farzana, F., Karupothula, R., Zalm, R., Cooke, N.E., Li, K.W., Smit, A.B., Toonen, R., and Verhage, M. (2012). Synapse associated protein 102 (SAP102) binds the C-terminal part of the scaffolding protein neurobeachin. PloS one 7, e39420.

Lipka, J., Kapitein, L.C., Jaworski, J., and Hoogenraad, C.C. (2016). Microtubule-binding protein doublecortin-like kinase 1 (DCLK1) guides kinesin-3-mediated cargo transport to dendrites. EMBO J. 35, 302-318.

Mochida, S., Kobayashi, H., Matsuda, Y., Yuda, Y., Muramoto, K., and Nonomura, Y. (1994). Myosin II is involved in transmitter release at synapses formed between rat sympathetic neurons in culture. Neuron 13, 1131-1142.

Nakagawa, T., Setou, M., Seog, D., Ogasawara, K., Dohmae, N., Takio, K., and Hirokawa, N. (2000). A novel motor, KIF13A, transports mannose-6-phosphate receptor to plasma membrane through direct interaction with AP-1 complex. Cell 103, 569-581.

Niwa, S., Tanaka, Y., and Hirokawa, N. (2008). KIF1Bbeta- and KIF1A-mediated axonal transport of presynaptic regulator Rab3 occurs in a GTP-dependent manner through DENN/MADD. Nat. Cell Biol. 10, 1269-1279.

Peng, A., Rotman, Z., Deng, P.Y., and Klyachko, V.A. (2012). Differential motion dynamics of synaptic vesicles undergoing spontaneous and activity-evoked endocytosis. Neuron 73, 1108-1115.

Petzoldt, A.G., Lutzkendorf, J., and Sigrist, S.J. (2016). Mechanisms controlling assembly and plasticity of presynaptic active zone scaffolds. Curr. Opin. Neurobiol. 39, 69-76.

Piccioli, Z.D., and Littleton, J.T. (2014). Retrograde BMP signaling modulates rapid activity-dependent synaptic growth via presynaptic LIM kinase regulation of cofilin. J. Neurosci. 34, 4371-4381.

Pollard, T.D., and Cooper, J.A. (2009). Actin, a central player in cell shape and movement. Science 326, 1208-1212.

Rex, C.S., Gavin, C.F., Rubio, M.D., Kramar, E.A., Chen, L.Y., Jia, Y., Huganir, R.L., Muzyczka, N., Gall, C.M., Miller, C.A., et al. (2010). Myosin IIb regulates actin dynamics during synaptic plasticity and memory formation. Neuron 67, 603-617.

Rizvi, S.A., Neidt, E.M., Cui, J., Feiger, Z., Skau, C.T., Gardel, M.L., Kozmin, S.A., and Kovar, D.R. (2009). Identification and characterization of a small molecule inhibitor of formin-mediated actin assembly. Chem. Biol. 16, 1158-1168.

Roy, S. (2016). Waves, rings, and trails: The scenic landscape of axonal actin. J. Cell Biol. 212, 131-134.

Ryu, J., Liu, L., Wong, T.P., Wu, D.C., Burette, A., Weinberg, R., Wang, Y.T., and Sheng, M. (2006). A critical role for myosin IIb in dendritic spine morphology and synaptic function. Neuron 49, 175-182.

Sabo, S.L., Gomes, R.A., and McAllister, A.K. (2006). Formation of presynaptic terminals at predefined sites along axons. J. Neurosci. 26, 10813-10825.

Sagona, A.P., Nezis, I.P., Pedersen, N.M., Liestol, K., Poulton, J., Rusten, T.E., Skotheim, R.I., Raiborg, C., and Stenmark, H. (2010). PtdIns(3)P controls cytokinesis through KIF13A-mediated recruitment of FYVE-CENT to the midbody. Nat. Cell Biol. 12, 362-371.

Sankaranarayanan, S., Atluri, P.P., and Ryan, T.A. (2003). Actin has a molecular scaffolding, not propulsive, role in presynaptic function. Nat. Neurosci. 6, 127-135.

Schroer, T.A. (2004). Dynactin. Annu. Rev. Cell Dev. Biol. 20, 759-779.

Seabrooke, S., and Stewart, B.A. (2011). Synaptic transmission and plasticity are modulated by nonmuscle myosin II at the neuromuscular junction of Drosophila. J. Neurophysiol. 105, 1966-1976.

Shin, H., Wyszynski, M., Huh, K.H., Valtschanoff, J.G., Lee, J.R., Ko, J., Streuli, M., Weinberg, R.J., Sheng, M., and Kim, E. (2003). Association of the kinesin motor KIF1A with the multimodular protein liprin-alpha. J. Biol. Chem. 278, 11393-11401.

Suarez, C., Carroll, R.T., Burke, T.A., Christensen, J.R., Bestul, A.J., Sees, J.A., James, M.L., Sirotkin, V., and Kovar, D.R. (2015). Profilin regulates F-actin network homeostasis by favoring formin over Arp2/3 complex. Dev. Cell 32, 43-53.

Sudhof, T.C. (2012). The presynaptic active zone. Neuron 75, 11-25.

Sun, Y., and Bamji, S.X. (2011). beta-Pix modulates actin-mediated recruitment of synaptic vesicles to synapses. J. Neurosci. 31, 17123-17133.

van den Berg, R., and Hoogenraad, C.C. (2012). Molecular motors in cargo trafficking and synapse assembly. Adv. Exp. Med. Biol. 970, 173-196.

Vasin, A., Zueva, L., Torrez, C., Volfson, D., Littleton, J.T., and Bykhovskaia, M. (2014). Synapsin regulates activity-dependent outgrowth of synaptic boutons at the Drosophila neuromuscular junction. J. Neurosci. 34, 10554-10563.

Verhey, K.J., and Hammond, J.W. (2009). Traffic control: regulation of kinesin motors. Nat. Rev. Mol. Cell Biol. 10, 765-777.

Vicente-Manzanares, M., Ma, X., Adelstein, R.S., and Horwitz, A.R. (2009). Non-muscle myosin II takes centre stage in cell adhesion and migration. Nat. Rev. Mol. Cell Biol. 10, 778-790.

Wagner, O.I., Esposito, A., Kohler, B., Chen, C.W., Shen, C.P., Wu, G.H., Butkevich, E., Mandalapu, S., Wenzel, D., Wouters, F.S., et al. (2009). Synaptic scaffolding protein SYD-2 clusters and activates kinesin-3 UNC-104 in C. elegans. Proc. Natl. Acad. Sci. 106, 19605-19610.

Wilhelm, B.G., Mandad, S., Truckenbrodt, S., Krohnert, K., Schafer, C., Rammner, B., Koo, S.J., Classen, G.A., Krauss, M., Haucke, V., et al. (2014). Composition of isolated synaptic boutons reveals the amounts of vesicle trafficking proteins. Science 344, 1023-1028.

Wise, A., Tenezaca, L., Fernandez, R.W., Schatoff, E., Flores, J., Ueda, A., Zhong, X., Wu, C.F., Simon, A.F., and Venkatesh, T. (2015). Drosophila mutants of the autism candidate gene neurobeachin (rugose) exhibit neuro-developmental disorders, aberrant synaptic properties, altered locomotion, and impaired adult social behavior and activity patterns. J. Neurogen. 29, 135-143.

Yeh, T.Y., Quintyne, N.J., Scipioni, B.R., Eckley, D.M., and Schroer, T.A. (2012). Dynactin's pointed-end complex is a cargo-targeting module. Mol. Biol. Cell 23, 3827-3837.

Zhang, Y.V., Hannan, S.B., Kern, J.V., Stanchev, D.T., Koc, B., Jahn, T.R., and Rasse, T.M. (2017). The KIF1A homolog Unc-104 is important for spontaneous release, postsynaptic density maturation and perisynaptic scaffold organization. Sci. Rep. 7, 38172.

Zhou, R., Niwa, S., Guillaud, L., Tong, Y., and Hirokawa, N. (2013). A molecular motor, KIF13A, controls anxiety by transporting the serotonin type 1A receptor. Cell Rep. 3, 509-519.

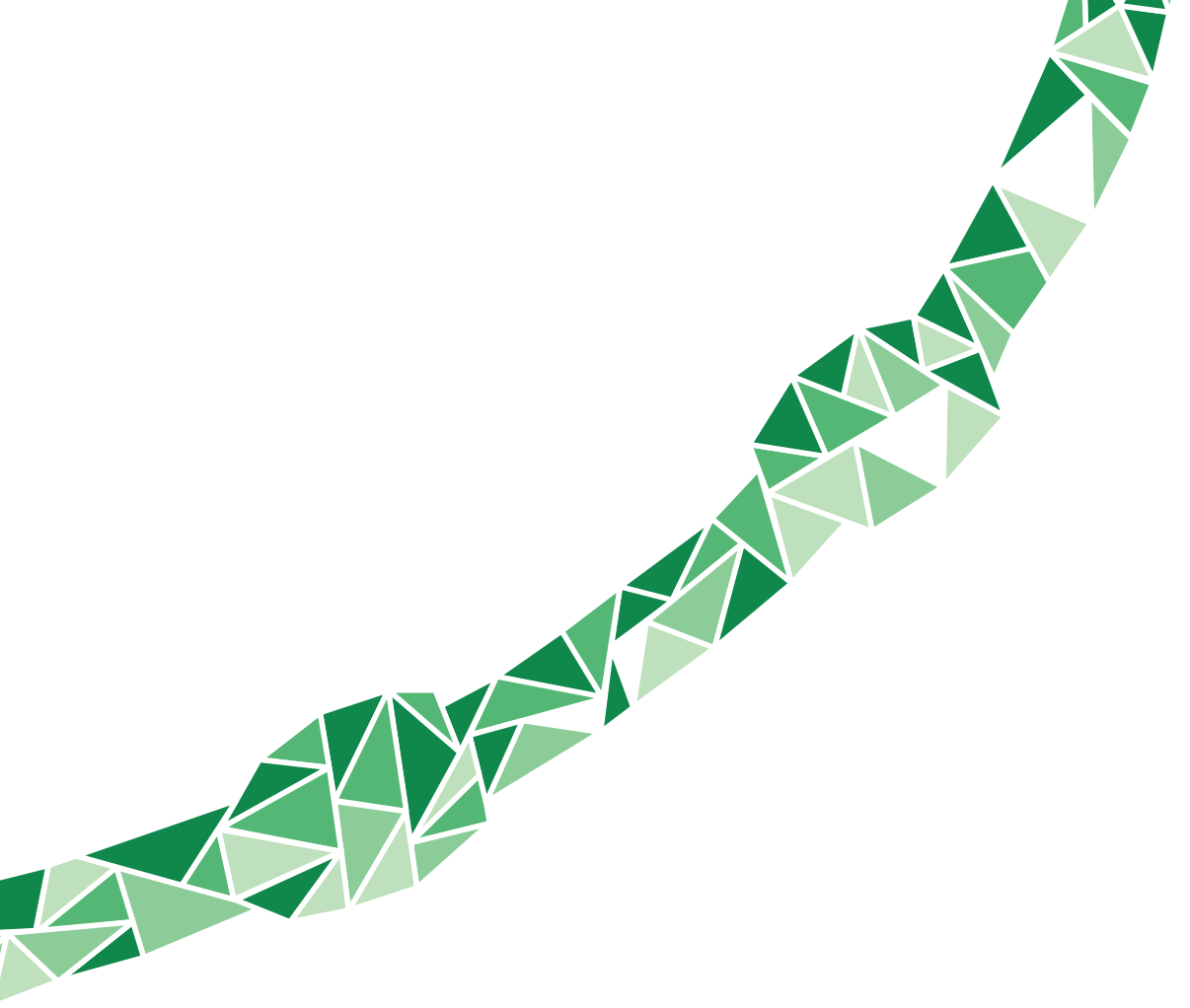

&

Addendum

SUMMARY

The brain is an astonishingly complex organ, central for many activities of the human body, such as movement and sensing. This organ is responsible for the translation of external information into coordinated and precise responses, being composed by billions of neurons. Neurons acquire an optimized structure for the reception and processing of information, with long protrusions extending from the neuronal cell body. These protrusions are morphologically and functionally different from each other, and are crucial for the establishment of a dynamic and intricate neuronal network. The axon is a long protrusion responsible for the transmission of electrochemical signals to other neurons, while dendrites receive these signals. The propagation of information from the axon of one neuron to the dendrite of another happens at specialized regions called synapses. When a signal travels along the axon and reaches the presynapse, it induces the fusion of synaptic vesicles with the plasma membrane in the presynaptic terminal, releasing neurotransmitters. These neurotransmitters can bind to receptors present at the postsynaptic membrane of the receiving neuron, generating a signal that can be transmitted to the next neuron. To ensure the accurate communication between neurons, synapses must be correctly assembled during development and supplied with specific proteins to the pre- and postsynaptic compartments. As most of the proteins are synthesized in the cell body, they need to be transported to the proper location by motor proteins, which use the underlying actin and microtubule cytoskeleton as rails. Interestingly, deficits in synapse formation and plasticity have been implicated in numerous neurodevelopmental, neuropsychiatric and neurodegenerative disorders, such as autism, schizophrenia or Alzheimer's disease. Therefore, studying the fundamental mechanisms of synapse formation and function may help us to better understand the processes that may underlie brain diseases.

The axon extends considerably from the soma to reach the appropriate synaptic partners, and the molecular mechanisms underlying this process have intrigued many neuroscientists. We can study axon development in a controlled environment by culturing neurons from rodent brains. In this system, the axon is formed within the first 24 hours after plating, and the factors that support axon development and outgrowth have to be delivered by motor proteins to the proper location. In *chapters 3* and *4*, we depleted different motor proteins from hippocampal neurons to study their role in the formation and extension of the axon. In *chapter 3*, we studied the role of myosin proteins, which walk along the actin cytoskeleton, in axon formation. We found that Myosin IIb is required for the establishment of the axon and that its depletion promotes changes in the microtubule cytoskeleton at the proximal part of the axon. In this way, we suggest that Myosin IIb may be required for the crosstalk between the actin and microtubule cytoskeletons during the early stages of axon development. In *chapter 4*, we focused on another superfamily of motor proteins, the kinesins, which walk along the microtubule rails. We found that several kinesin motor proteins are important for proper axon outgrowth. One of these kinesins was KIF19, which can trigger the breakdown of the microtubule rails in the cell. Besides the role on axonal growth, KIF19 is also important for the maintenance of distinct axon and dendritic compartments in hippocampal neurons.

The constant supply of synaptic proteins from and to the synapse is crucial for synaptic function. In *chapter 5*, we evaluated the contribution of each individual motor protein in the maintenance of both excitatory and inhibitory synapses. Dynein-interacting proteins promote transport along the microtubules in the opposite direction of kinesins,

and depletion of some of these proteins leads to changes in the density of both types of synapses. We also uncovered roles for dynein-interacting proteins in the maturation of postsynaptic specializations, in the surface level of excitatory neurotransmitter receptors and in the trafficking of membrane vesicles.

Chapters 2 and *6* are centered on the dynamics of presynapses along inhibitory axons. In *chapter 2*, we provide an overview of molecular mechanisms involved in the regulation of inhibitory presynaptic bouton dynamics. *Chapter 6* focuses on a new regulatory pathway of inhibitory synapse formation triggered the by the guidance protein Semaphorin4D (Sema4D). By treating hippocampal slices with Sema4D, we found that it promotes the stabilization of inhibitory presynaptic boutons. Moreover, Sema4D triggers a signaling pathway that requires the activation of MET, a protein previously shown to be reduced in the postmortem brains of autistic patients.

Altogether, this thesis describes fundamental mechanisms that support axon outgrowth and presynaptic function, providing new insights into how neurons wire the brain to establish a functional network. As many brain diseases are associated with deficits in synaptic transmission, the results described here may help us eventually to understand the etiology of neurodevelopmental and neurological disorders.

SAMENVATTING

Het brein is een indrukwekkend orgaan, dat ten grondslag ligt aan veel handelingen van het menselijk lichaam, zoals bewegen en waarnemen. Het brein, bestaande uit miljarden neuronen, is verantwoordelijk voor de vertaling van externe informatie naar gecoördineerde en nauwkeurige reacties. Neuronen ontwikkelen lange uitstulpingen uit het neuronale cellichaam en deze structuur is optimaal voor het ontvangen en verwerken van informatie. Deze uitstulpingen zijn qua vorm en functie verschillend van elkaar en zijn cruciaal voor het tot stand komen van een ingewikkeld en dynamisch neuronaal netwerk. Het axon is een lange uitstulping die verantwoordelijk is voor het zenden van elektrochemische signalen naar andere neuronen. Andere uitstulpingen, genaamd dendrieten, ontvangen deze signalen. Het zenden van informatie van het axon van het ene neuron naar de dendriet van het andere neuron vindt plaats op gespecialiseerde locaties genaamd synapsen. Wanneer een signaal door het axon reist en bij de presynaps uitkomt, activeert het de fusie van synaptische blaasjes met het plasmamembraan in het presynaptisch uiteinde, waarbij neurotransmitters vrijkomen. Deze neurotransmitters kunnen aan receptoren binden die zich aan de postsynaptische membraan van het ontvangende neuron bevinden. Hierbij wordt een signaal gegenereerd dat vervolgens naar een volgend neuron kan worden gestuurd. Om nauwkeurige communicatie tussen neuronen te waarborgen, moeten synapsen correct samengesteld worden tijdens de ontwikkeling en moeten zij van specifieke eiwitten worden voorzien voor de pre- en postsynaptische compartimenten. Omdat de meeste eiwitten in het cellichaam worden gemaakt, moeten deze vervolgens naar de juiste locatie worden getransporteerd door middel van motoreiwitten, die het onderliggende cytoskelet, bestaande uit actine en microtubuli, als rails gebruiken. Tekortkomingen in synapsformatie en plasticiteit zijn betrokken bij talrijke aandoeningen die te maken hebben met neuronale ontwikkeling, neuropsychiatrie en neurodegeneratie zoals autisme, schizofrenie of de ziekte van Alzheimer. Derhalve is het belangrijk om de fundamentele mechanismen van synapsformatie en -functie te bestuderen, wat ons kan helpen bij het beter begrijpen van de processen die tot hersenaandoeningen leiden.

Het axon strekt zich aanzienlijk uit vanuit het soma om de juiste synaptische partners te bereiken en de moleculaire mechanismen die hier ten grondslag aan liggen, zijn intrigerend geweest voor vele neurowetenschappers. We kunnen de ontwikkeling van het axon bestuderen in een gecontroleerde omgeving door neuronen van knaagdierhersens te kweken. In dit systeem wordt het eerste axon gevormd binnen de eerste 24 uur na uitplaten en de factoren die de ontwikkeling en de uitgroei van het axon ondersteunen, worden door motoreiwitten naar de juiste locatie gebracht. In *hoofdstuk 3* en *4* hebben we de hoeveelheid van verschillende motoreiwitten in hippocampale neuronen verminderd om de vorming en groei van het axon te bestuderen. In *hoofdstuk 3* hebben wij de rol van myosine-eiwitten, die over het actine-cytoskelet lopen, tijdens de vorming van het axon bestudeerd. Wij hebben gevonden dat myosine IIb nodig is voor de totstandkoming van het axon en dat de verminderde expressie veranderingen aan het microtubuli-cytoskelet in het deel van het axon dicht bij het cellichaam teweegbrengt. Wij concluderen dat myosine IIb mogelijk nodig is voor de interactie tussen de actine en de microtubuli van het cytoskelet tijdens de vroege stadia van de ontwikkeling van het axon. In *hoofdstuk 4* hebben we de nadruk gelegd op een andere superfamilie van motoreiwitten, de kinesines, die over rails bestaande uit microtubuli lopen. We hebben gevonden dat verschillende kinesinemotoren

belangrijk zijn voor de correcte groei van het axon. Één van deze kinesines was KIF19, die de afbraak van microtubuli in cellen in gang kan zetten. Naast de rol in axonale groei, is KIF19 ook belangrijk voor het onderhoud van specifieke axonale en dendritische compartimenten in hippocampale neuronen.

De constante toestroom van synaptische eiwitten van en naar de synaps is cruciaal voor het functioneren van de synaps. In *hoofdstuk 5* hebben we de bijdrage van elk individueel motoreiwit in het onderhouden van zowel excitatoire en inhibitoire synapsen geëvalueerd. Eiwitten die een interactie aangaan met dyneïne, stimuleren het transport over de microtubuli in de tegenovergestelde richting als kinesines en het verwijderen van enkele van deze eiwitten leidt tot veranderingen in de dichtheid van beide synapstypes. Bovendien hebben wij ontdekt dat eiwitten die interacteren met dyneïne een rol spelen in het volgroeien van postsynaptische specialisaties, in de hoeveelheid stimulerende neurotransmitters aan het oppervlak en in het transport van membraanblaasjes.

Hoofdstuk 2 en *6* zijn gecentreerd rondom de dynamiek van presynapsen langs inhibitoire axonen. In *hoofdstuk 2* hebben we een overzicht gegeven van de moleculaire mechanismen die betrokken zijn bij de regulatie van inhibitoire presynaptische boutondynamiek. *Hoofdstuk 6* richt zich op de nieuwe regulerende route in inhibitoire synapsvorming geïnitieerd door het gidseiwit Semaphorin4D (Sema4D). Door hippocampale plakken met Sema4D te behandelen, vonden we dat stabilisatie van inhibitoire presynaptische boutons wordt geïnitialiseerd. Bovendien initieert Sema4D een signaalroute die nodig is voor de activatie van MET, een eiwit dat in een verminderde hoeveelheid aanwezig was in post mortem brein van autismepatiënten.

Deze thesis beschrijft fundamentele mechanismen die de groei van het axon en de functie van de presynaps ondersteunen, wat bijdraagt aan nieuwe inzichten in hoe neuronen verbindingen maken om het brein te vormen als functioneel netwerk. Aangezien talrijke hersenaandoeningen geassocieerd zijn met tekorten in synaptische transmissie, zouden de resultaten die hier zijn beschreven uiteindelijk bij kunnen dragen aan het algemeen begrip van de etiologie van hersenontwikkelings- en neurologische aandoeningen.

SUMÁRIO

O cérebro é um órgão extremamente complexo, importante para muitas das actividades desempenhadas pelo corpo humano, tais como o movimento coordenado e os sentidos. Este órgão é responsável pela conversão de sinais exteriores em respostas precisas e coordenadas, sendo constituído por biliões de neurónios. Para a receção e processamento de informação, os neurónios adquirem uma morfologia única, estendendo longas protrusões originadas no corpo celular. Estas protrusões são morfológica e funcionalmente distintas, sendo importantes para o estabelecimento de uma rede neuronal dinâmica e intrincada. O axónio é a protrusão responsável pela transmissão de sinais eletroquímicos para o neurónio seguinte, enquanto as dendrites são estruturas especializadas na receção desses sinais. A passagem de informação do axónio de um neurónio para a dendrite de outro ocorre em regiões especializadas designadas sinapses. Quando um sinal viaja ao longo do axónio e atinge a pré-sinapse, ele desencadeia a fusão de vesículas sinápticas com a membrana plasmática do terminal pré-sináptico, induzindo a libertação de neurotransmissores. Estes neurotransmissores podem ligar-se a recetores localizados na membrana pós-sináptica do neurónio recetor, gerando um sinal que pode ser transmitido ao neurónio seguinte. De modo a assegurar uma comunicação precisa entre os neurónios, as sinapses têm de ser formadas corretamente durante o período de desenvolvimento e, continuamente, abastecidas com proteínas específicas dos compartimentos pré- e pós-sinápticos. A maioria das proteínas é sintetizada no corpo celular, tendo de ser transportadas para o seu destino final através da ação de proteínas motoras, que usam o citoesqueleto de actina ou de microtúbulos como auto-estradas celulares. Curiosamente, défices na formação e plasticidade das sinapses têm sido implicados em diversas doenças do neuro-desenvolvimento, neuropsiquiátricas e neurodegenerativas, como o autismo, a esquizofrenia ou a doença de Alzheimer. Deste modo, o estudo dos mecanismos que regulam a formação e função das sinapses pode ajudar-nos a compreender os processos que podem ser causativos de doenças cerebrais.

O axónio alonga-se desde o corpo celular para atingir os seus parceiros sinápticos e os mecanismos moleculares que despoletam este processo têm intrigado muitos neurocientistas. É possível estudar o desenvolvimento do axónio num ambiente controlado através da implementação de culturas de neurónios provenientes de cérebros de ratos e ratinhos. Neste sistema, o axónio forma-se nas primeiras 24 horas pós-cultura e os fatores que promovem o seu densenvolvimento e alongamento têm de ser transportados até ao local onde são necessários pelas proteínas motoras. Nos *capítulos 3* e *4*, nós removemos diferentes proteínas motoras para estudar a sua contribuição para a formação e o crescimento do axónio em neurónios de hipocampo. No *capítulo 3*, estudámos as miosinas, ou seja, as proteínas que caminham ao longo dos filamentos de actina. Este estudo mostrou que a Miosina IIb é necessária para a formação do axónio, e que a sua remoção origina modificações nos microtúbulos localizados na parte proximal do mesmo. Neste sentido, nós sugerimos que a Miosina IIb pode ser importante para a interação entre os filamentos de actina e microtúbulos durante os estadios iniciais do desenvolvimento axonal. No *capítulo 4,* focámo-nos noutra superfamília de proteínas motoras, as cinesinas, que se movem ao longo dos microtúbulos. Neste estudo descobrimos que diferentes cinesinas são importantes para uma extensão normal do axónio. Umas das cinesinas com efeito na arborização axonal foi a KIF19, uma cinesina capaz de promover a despolimerização dos microtúbulos na célula. Além do papel no crescimento axonal, a KIF19 é também importante para a manutenção dos

compartimentos axonal e dendrítico em neurónios do hipocampo.

O fluxo constante de proteínas sinápticas, de e para a sinapse, é indispensável para a função sináptica. No *capítulo 5*, avaliámos a contribuição de cada proteína motora na manutenção de sinapses excitatórias e inibitórias. As proteínas que interagem com a dineína promovem o transporte ao longo de microtúbulos na direção oposta das cinesinas. A diminuição da expressão destas proteínas induz alterações na densidade de ambos os tipos de sinapses. Neste estudo, também descobrimos que as proteínas interatoras da dineína têm funções na maturação de especializações pós-sinápticas, no nível superficial dos receptores de neurotransmissores excitatórios e no tráfego de vesículas membranares.

Os *capítulos 2* e *6* são centrados na dinâmica das pré-sinapses que se encontram ao longo de axónios inibitórios. No *capítulo 2*, nós proporcionamos uma visão geral dos mecanismos moleculares envolvidos na regulação da dinâmica dos botões pré-sinápticos inibitórios. O *capítulo 6* é focado no estudo de uma nova via de regulação de formação de sinapses inibitórias, desencadeada pela proteína sinalizadora Semaforina4D (Sema4D). Ao tratar as fatias de hipocampo com a Sema4D, descobrimos que esta proteína induz a estabilização dos botões pré-sinápticos inibitórios. Além disso, a Sema4D desencadeia uma via de sinalização que requer a ativação da proteína MET, cujos níveis estão reduzidos nos cérebros postmortem de pacientes autistas.

De um modo geral, esta tese descreve mecanismos fundamentais que suportam o crescimento axonal e a função pré-sináptica, dando novas perspetivas sobre a forma como os neurónios se conetam para formar uma rede funcional no cérebro. Considerando que muitas das doenças cerebrais estão correlacionadas com défices na transmissão sináptica, os resultados aqui descritos poderão, eventualmente, ajudar-nos a perceber a etiologia de doenças do neuro-desenvolvimento e neurológicas no futuro.

CURRICULUM VITAE

Cátia P. Frias was born on January 15th 1989 in Funchal, Madeira, Portugal. When she was 6 years old, she moved to the mainland, where she finished her high school education in 2006 at the Escola Secundária José Saramago in Mafra. In September of the same year, she started her Biology degree at the Faculty of Sciences from the University of Lisbon (FCUL). During the first two years, Cátia had general Biology courses and she chose the Genetics and Molecular specialization for her final year. She then enrolled in the Masters in Molecular Genetics and Biomedicine at the Faculty of Sciences and Technology from the New University of Lisbon (FCT-UNL) in September 2009. In September 2010, Cátia started her Masters research project at the Neuron-Glia Biology in Health and Disease group, led by Professor Dora Brites at the Research Institute for Medicines and Pharmaceutical Sciences – iMed.UL (Faculty of Pharmacy, University of Lisbon), with the daily supervision of Dr. Adelaide Fernandes. Her project aimed to evaluate if a neuroinflammatory stimulus mimicked by a transient incubation with pro-inflammatory cytokines could alter the progression of neuronal development. During this internship, she was also involved in a small side project to address the expression levels of surface receptors in 3 different hepatocarcinoma cell lines. She successfully defended her Master thesis in November 2011, and she finished her Masters with A-level grades (top 10% of all graduates). In June 2012, driven by her interest in fundamental research, Cátia joined the laboratories of Prof. Dr. Casper C. Hoogenraad and Dr. Corette J. Wierenga at the Cell Biology Division of Utrecht University as a Marie Curie Initial Training Network (ITN) fellow. During her time as a PhD student, Cátia participated in several workshops and courses, some provided by the NPlast network, and attended and presented her work in diverse national and international conferences. She was also involved in the organization of different meetings and she was engaged in training and supervising MSc and BSc students. During her PhD, Cátia studied the role of motor proteins in different neurodevelopmental processes and the molecular mechanisms underlying inhibitory presynaptic bouton dynamics. The results of her research are described in this thesis.

LIST OF PUBLICATIONS

Molecular pathway underlying bouton stabilization by Semaphorin4D during inhibitory synapse formation.
Cátia P. Frias, Tom Bresser, Lisa Scheefhals, Hai Yin Hu, Paul M. P. van Bergen en Henegouwen, Casper C. Hoogenraad, Corette J. Wierenga. In revision.

Three-step model for polarized sorting of KIF17 into dendrites.
Mariella A. Franker*, Marta Esteves da Silva*, Roderick P. Tas*, Elena Tortosa, Yujie Cao, Cátia P. Frias, Anne F. Jansen, Phebe S. Wulf, Lukas C. Kapitein, Casper C. Hoogenraad. Curr. Biol. (2016) 26(13): 1705-12. * *equal contribution*

Kinesin binding protein (KBP) controls microtubule dynamics and cargo trafficking by regulating kinesin motor activity.
Josta T. Kevenaar*, Sarah Bianchi*, Myrrhe van Spronsen*, Natacha Olieric, Joanna Lipka, Cátia P. Frias, Marina Mikhaylova, Martin Harterink, Nanda Keijzer, Phebe S. Wulf, Manuel Hilbert, Lukas C. Kapitein, Esther de Graaff, Anna Akhmanova, Michel O. Steinmetz, Casper C. Hoogenraad. Curr. Biol. (2016) 26(7): 849-61. * *equal contribution*

TRIM46 controls neuronal polarity and axon specification by driving the formation of parallel microtubule arrays.
Sam F. B. van Beuningen, Lena Will, Martin Harterink, Anaël Chazeau, Eljo Y. van Battum, Cátia P. Frias, Mariella A. Franker, Eugene A. Katrukha, Riccardo Stucchi, Karin Vocking, Ana T. Antunes, Lotte Slenders L, Sofia Doulkeridou, Peter Sillevis Smitt P, A. F. Maarten Altelaar, Jan A. Post, Anna Akhmanova, R. Jeroen Pasterkamp, Lukas C. Kapitein, Esther de Graaff, Casper C. Hoogenraad. Neuron (2015) 88(6):1208-26.

Activity-dependent adaptations in inhibitory axons
Cátia P. Frias, Corette J. Wierenga. Front. Cell. Neurosci. (2013) 7:219.

ACKNOWLEDGMENTS

Writing this part is going to be hard, but getting to this point also means I have made it this far. When one starts a journey, no matter of how much you plan or think things over, it is impossible to anticipate how the ride will be. I started this journey by moving to a different country, so I took Bette Davis' advice and I have fastened the seatbelt and prepared for a bumpy ride. When I started my PhD, I had many expectations and a naive idea that a PhD would be an acquisition of new and fancier knowledge. Well, now I see that a PhD is much more than that. A PhD is a constant fight within you, between excitement and frustration, between perseverance and disappointment. In fact, even though there were many bumps, hurdles, and disappointing moments, there were also many moments of joy, fulfilment and "Oh, it is working!". And I was fortunate to have the chance to meet people that allowed me to develop myself as scientist and as a person, and I hope I can demonstrate that in some words now.

Firstly, I would like to thank the two people that made all this possible, my promotor Casper and my co-promotor Corette. **Casper**, I am so thankful you gave me the opportunity to start this adventure! When I emailed you, I never expected that I would be applying for the NPlast position nor that I had a chance of getting it. During these last five years, you allowed me to grow scientifically, as you always gave me the freedom to think for myself. Your keen eye for detail and your openness to discuss the data would always lead to a new possible model at the end of our monthly meetings. No matter how depressing the results could be at the beginning of the meeting, I always left your office motivated to try harder and do more! I had the great chance of learning a lot from you in these meetings, but also at the different social events we were together, when you would always have many funny stories to share. I have always been impressed by your working capabilities and by how you manage to have time for all of us, besides all the responsibilities you have. I sincerely thank you for everything and I wish you all the best for your future.

Corette, when I first met you, you had recently moved to Utrecht to start your lab. I remember that you immediately tried to make me feel comfortable during the interview, by telling me some funny facts about your pregnancy. For almost a year, I was your only PhD student and look how your lab grew since then. I am so thankful for the atmosphere you create in the lab. At our meetings, I never felt afraid of saying my ideas out loud, and I never felt like there was no room to discuss things further with you (sometimes we could be talking about inhibitory synapses for a very long time). This comfort in saying what you think is one of the things I appreciated the most in being your PhD student, and I couldn't be happier to have had you as a teacher. I really appreciate your critical attitude towards science, your input throughout my PhD and everything you have taught me. The dealings of our paper were so frustrating at times, but I always knew you would have my back! Thank you for letting me develop as a scientist, for your "always question" attitude and most of all, for your support. I wish you all the best in the future, and I hope that the Wierenga group keeps on showing everyone at Cell Biology that "inhibitory boutons are very dynamic structures".

I would also like to thank the other group leaders of the Cell Biology department. **Anna**, your never-ending knowledge and your attention to detail make your input extremely valuable and pertinent. I was always amazed by your memory, and how you can easily recall any piece of data someone produced in the lab or the most obscure papers from the past. I

would like to thank you for all the input you gave throughout these years and for everything I learned from hearing you during the lab meetings. I wish you a very successful future and I hope that your lab continues with the great work on the cytoskeleton, as it has done until now. **Esther**, I always enjoyed having you around, as I knew you would always have a smile and a nice story to tell. You are a master around the lab, and you would always knew the answer to my questions. But more than that, I am impressed with your strong will and fighting spirit. I hope you get fully recovered soon and that you can make your wish of having dinner at De Librije a reality. But before that, I hope to see you and **Chris** happily enjoying my party! May your life be full of great, happy moments. **Lukas**, your creativity is displayed in any conversation one may have with you. I wish you the best and many successes for you and your diverse lab. **Paul**, it was great to share many lunch breaks with you, as you would always make those moments livelier with your stories. Thank you for helping with the MET part of the Sema4D story. Good luck with your research and your lab! **Sabrina**, you are probably one of the quietest Portuguese people I know. It was great having you around and to see you become a PI! Thank you for the kind words throughout the years, and I wish you a very successful time at Cell Bio! **Harold**, what a great addition to our department! In such a short time you managed to start your own lab, and I am sure the times ahead will be fruitful for you. Thank you for all the feedback and discussions on synapses! **Fons**, the Cell Biology department is not the same without you! Your light spirit always made everyone around you happier. It was special seeing your passion for teaching and to see how the students appreciate you. Enjoy your retirement, and keep on partying during the Limburgse Carnival! To the neighbors of the 5th floor, **Sander**, **Mike** and **Inge**, thank you for the great times during all the lab outings and borrels, and for your input during the seminars. All the best for your labs, and keep up the amazing work with the awesome nematodes.

To **Elly Hol**, **Gerard Borst**, **Jeroen Pasterkamp**, **Maarten Kole** and **Sander van den Heuvel**, thank you for being part of my committee and for assessing my thesis. I am looking forward to discuss my thesis with you. **Jeroen**, thank you for your input on the Sema4D story throughout all the NPlast meetings we had, as well during the submission process.

When I started my PhD, I was lucky enough to be placed in a room where only newcomers were sitting. My time at Cell Bio would not have been the same if I would have been sitting in a different office. **Marleen**, for a while you were the mystery PhD student that was on holidays to Surinam when I started, but once I met you, I realized "This is going to be an amazing office mate". Your energy, your kindness, your humor made my crazy lab days better. I truly appreciate the friendship we have developed, and it was an honor for me to be at your side at your PhD defense. I will never forget our duets and our talks. Thank you for being one of the warmest Dutch people I have ever met! I wish you all the best in the future, next to Michel and cutie Roxy! **Bas** (Basyyyy), the tall, hardstyle music-loving, squash, super-resolution guy! You always knew how to make the whole office laugh with your sense of humor. I remember when you first showed me what a State of Trance party was (that was a very long night, and I had so much fun!). Thank you for all the nice moments outside the lab and for helping me when I couldn't reach anything. I wish you good luck in your job and in your future. **Max**, you started almost at the same time as me, writing your Master's thesis about spines. Very early on you developed the high-pitched "Niceeeeeee" that truly showed your moments of triumph during imaging or analysis. We would always be in for adding a new cartoon regarding a scientist's life to our office door! I wish you all the best in San Francisco,

and all the best in your and Jasmijn's future. **Anaël**, you joined us in 2014 and you couldn't have been a better fit to our office. Your craziness and happiness were contagious, and our discussions about science were always so nice! Your (penguin) dance skills are awesome and we had so much fun together. I am the last one of us to leave O502, and I couldn't have wished for a better environment to work, discuss and laugh. Thank you all for all the moments in and outside the lab, and let's keep in touch! **Eliana**, the beautiful bride, you are very kind and you always want to learn more. I wish you all the best in your future, and I know you will have a bright one (everything always turns out fine). **Desiree**, it's very good to have you around! I really appreciate your *sangre latino* (see you at the next Fiesta Macumba)! Good luck with everything. **Mithila**, thank you for the scientific discussions and chats. You will do great in your Postdoc! **Marijn**, you are the most recent addition to the office, and I wish you all the luck in your PhD.

Throughout the years, a lab of two people is now an expanded, multinational lab! Wierengaatjes, what an awesome journey we had! **Hai Yin**, we worked a lot together, and had to deal with the struggles of not-working equipment or slice cultures. Always keep your sarcastic laughter when someone makes fun of your accent! :) Thank you for the help with the Sema4D story. I wish you a steady ending to your PhD, and I hope that you show everyone that local inhibition is awesome! But most of all, keep on being the strong little man you are. **René**, you joined the lab halfway through my PhD, and I never realized how much we needed a person like you. Not only you took a lot of weight of my shoulders, but you also made our atmosphere in the lab more colorful. Thank you for all the chats we had. I wish you the best in your new house and in your future. **Elske**, I was so happy when a girl joined the lab (it was a men's world)... Your kindness and calmness are exactly what the lab needs. I know you will master your PhD! Keep up the good work, and keep up the willingness to always do better. **Jian**, you joined the lab at a time that I was about to finish. Even though we didn't interact a lot at the beginning, I saw how nice of a person you are. I know things are hard at times, but I know with persistence things can be achieved. All the luck for your PhD. **Carlijn**, I hope you enjoy your time as a PhD student in this awesome lab. I will miss you guys!

Besides working in Corette's lab, I was also given the opportunity to work in Casper's lab, and there are many people that I would like to thank now. **Phebe** (Phebetje), I told you many times that you are the wheel that keeps the lab moving. The lab would be lost without you, and I do hope you feel valued enough. When I first met you, I was a bit scared of you and I didn't really know how to break the ice. That happened without me noticing, and we have become good friends ever since. Even though I am very thankful for all your help in the lab, I am more thankful for all the laughs and stories we have shared through the years. Keep on being the great person you are, and I hope the future brings you many pleasant surprises, Mama Wulf! **Bart**, your astonishingly dry humor, combined with your knowledge on any pop-culture subject, makes you the perfect company for the lunch breaks. I will always remember our quotes competitions ("I love the smell of bacteria in the morning"), our song likes and dislikes (The Stitches guy), and how you always made me smile. Thank you for everything, Bartje! **Gabi**, you are a very sweet woman and it is always fun to be around you! I wish you all the best in your future, and I hope we keep in touch (I will for sure keep on following your blog posts). **Martin**, I have always admired the passion you have for Science! You are always helpful, and you are never too busy to give your input. I am thankful for that, but also for all the good moments we shared (normally next to a glass of beer or wine). I

wish you a successful career and a happy life. **Amélie**, I really like your energy and spirit. Thank you for all the scientific discussions we had and for all the great moments outside the lab (including your amazing wedding). I hope your adventure in the US brings you much joy, and that you and your beautiful family have a life full of happiness. **Lena**, thank you for showing me how to stain slices! You are a very kind teacher, and I hope your career continues with many triumphs. **Olga**, your lively personality always brings joy to the lab and to the lunch breaks. It was great having you around and I wish you all the best in your next chapter in San Francisco! **Riccardo**, besides all your work with the mass spectrometry, I would like to thank you for always having time for a chat. You are a very kind person, and I really enjoyed all of our talks. I haven't forgotten the promise you made to me regarding my party... :) Good luck in finishing up! **Dieudonnée**, our neuron culture guru, I really like your awesome humor and taste for shoes! Thank you for all your hard work through these years with the neuron culture, and for all the help you gave when we had those horrible contaminations. I know you will do great with the finishing of your PhD! **Feline**, it is very special for me to see one of my Master's students becoming an independent researcher! Keep on being the motivated and proactive person you are. I had such a great time with you in Lisbon and Coimbra! Thank you for your hard work on the dynein story and for all the conversations and fun times. All the luck for your PhD. **Sybren**, the "always against you" man, the lunch breaks are never boring when you are around! Good luck with your PhD. **Yujie**, you are such a nice person! Never lose your smile. **Xingxiu**, **Ginny**, **Eitan** and **Jessica** good luck with your projects!

Casper's lab changed a lot throughout the years, and a lot of great people have left the lab by now. However, this doesn't mean that they are forgotten in any way. **Josta**, our friendship started to develop when we were organizing the Lab Outing and I was so flattered when you asked me to be your paranimf. Your organizational and social skills, associated with your happy and ready-to-dance personality made us having such great moments together throughout the years! I wish you all the best in your and Laurens' future! **Sam** (Sammy), even though we didn't really clicked at the beginning, we became friends and we have shared many nice moments in and outside the lab ever since. It is always fun having you around, and I am grateful for all the nice talks we had! May your future be as bright as you deserve. **Kah Wai**, you were one of the first people to leave Cell Bio and I remembered how weird it was not having you around. You always knew how to make me laugh and it is good to see how our friendship grew throughout the years. I wish you and your cute family the best in life! **Mariella**, you are such a sweet and kind person, and I am so happy to have you as a friend. You were always ready to tell me some motivational words when I needed them the most. I hope this new life with Suraj brings you many moments of joy and happiness. **Phil**, the German cloning master, your energy made everything in the lab more fun and fast. I learned a lot from you, especially when we were discussing slices and synapses. I wish you all the best for you and your family in Zürich. **Joanna**, you were the first person of the lab I worked with and I learned a lot from you. I wish you and Jan a happy life in San Francisco. **Elena** and **Petra**, you were great colleagues to have around! I would like to thank you for your work in the chapters 3 and 4 of this thesis and for all the discussions and talks throughout the years. Good luck in the States! **Marina**, from Postdoc to a PI in Hamburg! It was so good to see you grow like that, and I am thankful for all the help and funny moments we shared. I wish you all the best in the future. **Margriet**, the lunch breaks were livelier when you were around! I hope you have an amazing and successful life. **Laura**, **Marijn** and **Robert**, it was

nice to share some of my lab days with you! I wish you all the best in your life and career.

In 2014, I was part of the Lab Outing committee and I wasn't thinking that hard work would also lead to many great moments. We were lucky to have such a creative and enthusiastic group of people! **Vincent** and **Bram**, we formed the most creative, 90s-singing team (Go ViCaBra!), and being with you was guaranteed fun. **V**, I know this year was rough, but I know that after the storm there is calmness. I wish you all the luck in finishing up! **Bram**, all the best for you and your family. **Amol**, it was always good having you around, and we are finishing up almost at the same time. Good luck for your future! **Nora** and **Hanna**, I wish you the best.

At the 5th floor of the Kruyt building, there are many people with whom we share meetings, lunch breaks, chats at the coffee machine, lab outings, and they make the environment way more *gezellig*. **Eugene**, we have shared many moments outside the lab, between (karaoke) parties and laser-games. You are very valuable to Cell Bio, with your broad knowledge and kindness to help others. Thank you for all the fun moments and for all the chats. **Helma** and **Qingyang**, we had many fun conversations during our dinners at the Italian place, but must of all you were great colleagues to have around. To both of you, lots of happiness and success! **Ivar**, you were first in our office and you taught me how to count till ten in Dutch on my first weeks at Cell Bio. You are also defending soon, and I wish you all the luck for your future. **Anne**, **Roderick** and **Wilco**, thank you for all the conversations, lunch breaks and good moments together. Good luck with your (challenging) projects. **Ilya**, having candy at the office would always mean you would drop by for a short chat. Keep up on ruling the microscope facility and all the best. **Sofia** and **Rachid**, thanks for all the laughs throughout the years! **Nicky** and **Lisa**, the MacGillavry's girls, thank you for the lunch breaks and good luck with your PhDs! **Maud**, **York**, **Jingchao**, **Marjolein**, **Ankit**, **Chao**, **Chiung-Yi, Ben**, **Ruddi**, **Kai**, **Shasha**, **Fangrui**, **Raimond**, **Eric**, **Sara**, **Vida** and **Irati**, it was nice having you as colleagues! Thank you all for the good conversations we shared and I wish you all success in your life. Due to our neighbors from the Dev Bio department, I learned a lot about worms and asymmetric cell division throughout my PhD. **Suzanne**, **Lars**, **Julianne** and **Ruben**, thank you for all the chats and I wish you all good luck for the future (especially for those of you that still need to finish the PhD). **Janine** and **Helena**, you increased the Portuguese crew and it was nice meeting you. To all Dev Bio people, good luck with your projects!

I was given the opportunity to supervise 4 talented and smart Master's students, and I want to leave a word to them. **Renske**, you were my first student, and I really appreciate that you gave me the opportunity to learn how to be a supervisor. It was a tough start, but you developed so much during that year! Yours and **Feline**´s work contribute a lot for my chapter 5! :) **Tom**, a lot of times I would get pain in my neck from talking to you while we were standing! You may not have seen it at times, but I did appreciate having you as a student. **Lisa**, even though you knew I was finishing my PhD and I could be less available, you still took the chance of working together with me. Your work, together with Tom's work, helped in turning the Sema4D story into a nice piece of work! To all of you, thank you for the good science you have performed, for allowing me to learn how to be a supervisor, but most of all for the time together. I wish you all a bright future.

Halfway through my PhD, I got closer to a group of amazing and talented Master's students inhabiting the West student room. Westsiders, you are such a good, fun group of friends, and I am so happy I had the chance to meet you all better. Our party nights were

legendary! :) **Katerina**, **Maria**, **Rosanna**, **PJ** and **Robin**, thank you for the support, the spontaneous meetings, and the friendship. **Katerina**, **PJ** and **Robin**, you came back to Cell Bio for the PhD and I know you will do great! Good luck with your projects, and I wish you the best! **Maria**, even though life took you back to Greece, I know I can count on you whenever I need it. You are a very strong woman, and I hope the times ahead of you only bring you joy and happiness. **Rosanna**, lil'sis, keep on being the energetic person you are and I wish you all the best in your future!

The "tugas" of the 5th floor made my life in and outside the lab better, and I knew they would always have my back. It is funny how some people have the ability to change your life, and how they enter it not to leave anymore. We have lived many things, some better than others, but most importantly we have grown together. I can't imagine my life without your friendship, and I know we still have many things to live together. **Andrea**, we initially connected because of our common taste for movies and music. We could talk for hours about "There will be blood" or how great the music from Jeff Buckley is, but we developed a beautiful friendship that I hold dearly. I admire your strong will, your intelligence and your hard-working attitude. I know if there is something that may look impossible, you will find a way to make it work. I am glad to see you happy in your new adventure in sunny California, and you know I will always stick around to see the new chapters of your life. Obrigada por tudo, pimpolha! :) **Marta**, a nossa Martinha, I am so grateful to have met you! I still remember when you asked me to join the dancing lessons with you, and from then on you have become family to me. I have always admired your work ethics, your persistence and the way you always try to do more and better. I am extremely lucky to have you as a friend, and I am truly thankful for all the support you gave me throughout the years. I wish you the best life has to offer, and I am glad with how your life turned around in the last year. I will always be right there for you, whenever you need me.

The last words directed at people from the lab go to my paranymphs. Oh guys, how honored I am you accepted to be by my side on the last steps of this journey! **Dennis**, how far we have come since that interview of yours… Even though I didn't like you at the beginning, you are one of the people I hold more dearly from the lab. You are an intelligent, caring and talented guy and I am proud to be your friend. Just a piece of advice: caged glutamate is not good for your eyes, neither is MiliQ! ;) Thank you for all the support you gave me these last 2 years, and remember I will always be there for you, no matter where I end up. **Inês**, what can I say? Me and the other Portuguese girls were lucky you decided to come to Casper's lab. You are one of the most caring people I know, and your heart is gigantic. This chapter of my life is going to end with you by my side, and I couldn't have wished for anything better. Your friendship means a lot to me, and you are like the oldest sister I never had (we even dress the same way sometimes). Thank you for everything you do for me, and I do hope I show my appreciation to you! Always remember to put your well-being first, no matter how life may turn around. You deserve all the happiness in the world. And at every step of your way, you know I will be right there.

While becoming used to living in the Netherlands, I met several people that made my life outside the lab more fun. **Daniel**, it was amazing that you moved to the Netherlands, and that we became friends. I know that next to you, we will never have a boring meeting! Thank you for your friendship, and good luck with the PhD! **Roland**, I am so glad Inês met you and brought you to the crazy Portuguese family. I appreciate your calmness, your kindness, but most of all I appreciate your friendship and the nice words you always have for me. I wish

the Piekorz's an amazing life in Germany! Dancing made my crazy days better, and going to Touchée allowed me to meet some great people! **Elisa**, **Doenja**, **Vuza**, **Saskia** and **Serge**, your energy and personality helped me to deal with all the stress and frustration. Fromagies, may we keep on meeting for some dancing parties or for some stressful Jenga nights!

I was extremely lucky to be given the opportunity of being a Marie Curie ITN fellow. But more than that, I was lucky to meet a group of people that became my friends during our travels around Europe. All the times we were together there were many moments of happiness, laughter and friendship that a keep dearly in my memory. **Nplastists**, we are a crazy mixture of people that fit perfectly together and we have created something unique! Thank you for everything, thank you for all the moments we shared. I am proud of us, and I wish you all the best in your bright future. See you all soon! :)

Some of my college friends from Lisbon ended up in Utrecht, and this led to some memorable meetings together. Between mimosas, tons of food, pancakes (finally we had them) and games, we shared many stories, thoughts and laughter. **Ritinha** and **Caspar**, I wish you all the luck in your adventure in the city that never sleeps! **Ramalho** and **Ré**, you are such good people to have around. I wish you all the best in finishing your PhDs! **Andreia**, you are such a sweet girl and I really hope that things turn perfect for you. Keep your head high, girl! **Euclides**, the coolest man around, all the best in the future. Rock those worms of yours!

My dearest friends, the group that sticks together for more than a decade! Science and life created a physical distance between us, but that doesn't mean that our friendship gets weaker. On the contrary, when we are together, it is like nothing has changed. **Inês**, minha amora, I loved visiting you in Copenhagen and Malmö. You visited me at the right time in Utrecht, and you were that shoulder I needed. I wish you a happy life together with **Mário**, and many meetings in the future between the Netherlands, Denmark and Sweden! **João** (Djix), tio da sobrinha, you are an amazing person, a true friend. I hope the future only holds you nice surprises, as you well deserve. **João** (Teddyzãooo), I am so happy with how your life with **Elizabeth** is developing. I wish you all the happiness in the world for both of you. **Ricardo**, meu primogénito, keep on fighting for your dreams, whether they are in Iceland or anywhere else. **Inês**, good luck in finishing up your PhD! You can do this, girl! To all of you, you are part of the core, and I hope we meet each other very soon!

The trip to the Netherlands changed my life for the better. Even though I never thought I would fully integrate with the Dutch costumes, I see the Netherlands as my home now. And during the last 3 years, there are some people that made this even truer. **Dammans**, you welcomed me with your open arms and I feel like I have always been part of the family. All of our gatherings are always great and relaxed, and I really appreciate them! **Corinne** and **Harry**, your kindness and support mean a lot to me. I enjoy our travels and conversations a lot! **Marleen**, **Ron** and **Linde**, I wish you all the luck for the future. **Marleen**, I admire you and your hard work, and I am grateful for our talks about a scientist's life. **Linde**, jij bent de liefste! **Ellen** and **Bart**, I hope your life in Winschoten develops as you have dreamed. I hope the future brings you lots of joy and happiness.

À minha grande **família**, à base que me dá apoio em qualquer decisão que tome. Nós somos moldados pelas pessoas que nos rodeiam desde que somos pequenos, e vocês todos contribuíram para eu ser a pessoa que sou hoje. Não há palavras que possam descrever o quão importante é ter-vos aqui neste dia, a ver-me conquistar esta etapa. **Tiago** e **Tia Isabel**, vejo em vocês a força e a luta que tanto caracterizam a família Frias. Tia, estou tão

contente por vir conhecer as terras holandesas, e por a minha defesa ser importante para a tia. Primão, adorei o nosso encontro o ano passado, e quero que isto aconteça mais vezes, aqui ou em Londres. Tenho muito orgulho em ver a tua preserverança e a tua luta por uma vida melhor. Obrigada por virem e espero fazer esta vossa viagem valer a pena. **Carla** e **Andreia**, vocês nem sabiam que me iam visitar na altura mais determinante da minha vida. Vocês deram-me o apoio que eu precisava e fizeram-me lembrar que o mais importante é sentirmo-nos bem conosco próprios. No meio de muitas "Anacondas", parvoíces e gargalhadas, vimos e vivemos muitas coisas juntas, e sei que mais do que primas, somos conselheiras e confidentes. Obrigada por terem cá vindo, não uma, não duas mas três vezes! :) **Kikinha**, as nossas conversas semanais fazem-me tão bem, às vezes falamos de tanto que nem nos apercebemos que o tempo passa. Eu sei que esta minha vitória é sua também, e sinto todos os dias o quanto a Kika gosta de mim e o quanto orgulho tem em mim. Obrigada por tudo!

Avós, meus segundos pais, nenhum de vocês pode ver-me alcançar esta meta, mas sei que vocês estariam orgulhosos da vossa netinha. **Avó Zita** e **Avó Isabel**, tenho muitas saudades vossas! Obrigada por todo o amor que me deram em vida, eu lembro-me sempre de vocês. Sei que onde quer que estejam estão a ver-me com um sorriso nos lábios!

Aos meus **pais**, nem sei por onde começar... Sou uma sortuda por ter dois pais maravilhosos que me dão todo o apoio e liberdade para tomar as minhas próprias decisões. Sou quem sou porque vos tive como pais, e eu não podia estar mais orgulhosa de ser vossa filha. Vocês sempre lutaram pelo meu futuro, para que eu tivesse mais do que o que vocês tiveram, e olhem onde estamos hoje... :) **Papi**, você é a pessoa mais lutadora e escrupulosa que eu conheço! Você ensinou-me que nunca devemos parar de evoluir e que devemos enfrentar os nossos medos. **Mumy**, a sua bondade e sensibilidade fazem-na tão especial! A mãe pode não se aperceber, mas a sua garra e a sua persistência são inspiradoras! Obrigada por me mostrarem que os heróis são humanos, por serem como são, por serem o meu porto de abrigo. Esta tese é dedicada a vocês, porque sem vocês eu não estaria aqui. Adoro-vos!

Now it is time to thank the one that deserves more than words can describe. **Reinier**, you are the most amazing, caring and kind person I have ever met. Falling for you happened without me even noticing, and I couldn't be happier with how my life turned around. Many people spend a lifetime trying to find the right person, and I was lucky to find you right at Cell Bio! Thank you for all the love you give me, for making me feel special, for never letting me crash in the worst moments, for all the patience and support. This thesis is also yours! Amor, I am so grateful for our life together, and I cannot even wait for what the future is preparing for us. "And if you are in love, you are the lucky one". I surely am, amo-te imenso!

Hora est (atchiiimmm)!